University of Newcastle upon Tyne
School of Neuroscience

Assessment of Retinal Vascular Geometry in Normal and Diabetic Subjects

Submitted by:

Maged Selim Habib
MB BCH, MSc Ophth, FRCS Ophth, FRCOphth

Thesis submitted to the University of Newcastle upon Tyne in
candidature for the degree of Doctor of Medicine

2012

Author's Declaration

This Thesis is submitted to the degree of Doctor of Medicine in the University of Newcastle upon Tyne. The research detailed within was performed in the Department of Ophthalmology at Sunderland Eye Infirmary with collaboration of the Department of Computing and Informatics at Lincoln University under the supervision of Mr David H W Steel, Professor Andrew Hunter, and Mr Philip G Griffiths, in the period between September 2004 and February 2010 and it is my own work unless otherwise stated.

I hereby certify that none of the material offered in this thesis has been previously submitted by me for a degree or any other qualification at this or any other university.

Acknowledgements

Abstract

Diabetic retinopathy is the most common microvascular complication of diabetes mellitus and the leading cause of blindness in persons from age 20 to 74. The relative risk of blindness in persons with diabetes has been reported to be 5.2 times the risk of those without diabetes. The fundus abnormalities described in diabetic retinopathy result from structural damage to the microvasculature wall with subsequent leakage or as a result of retinal ischaemia with secondary overproduction of vascular growth factors. Several clinical and screening classifications schemes have been developed to categorize and quantify the severity of each of the retinopathic features based on the degree of retina involvement. The ultimate goals of these classification schemes have been to provide a system by which the natural history of the disease and the risk of progression of retinopathy and visual loss can be identified and the subsequent response to interventions can be evaluated to improve patient care.

The present strategies for dealing with diabetic retinopathy address retinopathy that is already established. However, recent studies - supported by computer based imaging analysis – have focused on changes in retinal vascular caliber and demonstrated various associations with increased risk of diabetes and predicted the onset of microvascular retinal complications. This suggests that other structural and geometrical parameters might also be utilised, which can provide more information regarding the retinal vascular network. Few studies have reported different changes in retinal vascular geometry with age, systemic hypertension and peripheral vascular diseases.

The objective of this thesis is to analyse the retinal vascular geometrical features in normal subjects and evaluate its role in diabetic subjects with different stages of diabetic retinopathy. For this purpose, a semi-manual vascular analysis technique is designed to measure and analyse the different retinal vascular geometrical parameters and ratios. The developed technique performance and precision is compared to other available manual and semi-manual vascular analysis techniques.

The various sources of variability in retinal geometrical measurements are then evaluated, including observer's measurement errors, variations in image capture, and potential short term changes in the subjects' vascular geometrical features.

The second step of this work is to perform a detailed analysis of the retinal vascular geometry in normal subjects, including the topographic distribution of different geometrical measurements across the fundus, the effect of different demographic and clinical factors, and the stability of measurements between both eyes.

The next step evaluates the retinal vascular geometry in diabetic subjects with different grades of diabetic retinopathy to determine any changes of geometrical features with advancement of retinopathic stages. The results demonstrate significant associations of changes in vascular structural and geometrical features with increased stages of diabetic retinopathy.

Finally, the predictive value of retinal vascular geometry analysis and its practical role on the individual level is analysed for a sample of subjects who progressed from no retinopathy to proliferative retinopathy as compared to a sample of subjects with no sign of progression. The preliminary results suggest that geometrical changes trend can be detected on the individual level with progression of diabetic retinopathy and those differences can be noted between progressors and non-progressors at baseline.

In conclusion, this thesis describes novel retinal vascular geometrical markers indicative of establishment of advancing diabetic retinopathy, together with a potential predictive role in determining risk of future progression to proliferative retinopathy.

Table of Contents

List of Tables

List of Figures

THESIS CHAPTERS

Chapter 1: Introduction to Diabetic Retinopathy

1.1 Overview

Diabetes mellitus is a major medical problem throughout the world with a rapidly rising prevalence. It causes an array of long-term systemic complications, which have considerable impact on both the patient and the society as it typically affects individuals in their most productive years. [1] Ophthalmic complications of diabetes are various and include corneal abnormalities, iris neovascularisation, cataracts and neuropathies. However, the most common and potentially most blinding of these complications is diabetic retinopathy. [2]

This chapter discusses the epidemiology of diabetic retinopathy in regards to the incidence and prevalence of the disease and the resulting visual impairment. The known risk factors will be described with evidence from different clinical studies. The exact mechanism by which diabetes causes retinopathy remains unclear, but the chapter will explain the several postulated theories that could govern the natural course and history of the disease. This will be followed by description of the different clinical features and the various clinical and screening classifications of diabetic retinopathy. The chapter will also highlight the known predictive models for proliferative diabetic retinopathy and the history and value of screening for diabetic retinopathy.

The discussion section will highlight the limitations of the current adopted classifications and the difficulty in diagnosing proliferative retinopathy, together with the frequently observed mismatch between retinal ischaemia and clinical retinopathic features in some patients. This would thus lead to the overall aim for this thesis to evaluate the role of retinal vascular geometrical changes in the diagnosis of advancing stages of diabetic retinopathy and the prediction of progression of the disease to proliferative retinopathy stages.

1.2 Introduction

Diabetic retinopathy is a chronic progressive sight threatening disease of the retinal microvasculature, associated with prolonged hyperglycaemia and other conditions linked to diabetes mellitus such as hypertension.

It is considered fundamentally the result of imbalance between retinal metabolism and vascular supply.

Impaired retinal vascular auto-regulation is a feature of progressive diabetic retinopathy. Diabetic retinopathy can be broadly classified into two principle stages; background retinopathy and sight threatening diabetic retinopathy which is further sub classified to either maculopathy - characterised by deterioration of retinal blood vessel integrity causing leakage into the retina and loss of blood vessels within the macular area, leading to visual impairment and possible blindness – or proliferative diabetic retinopathy associated with growth of retinal new vessels that can lead to blindness through intraocular haemorrhage and possible retinal detachment and scarring.

1.3 Epidemiology

Diabetes mellitus results in considerable morbidity and mortality, affecting about 180 million people worldwide.[3] Around 2-4 % of the UK population are known to have diabetes; of these 200,000 have type I and more than a million have type II diabetes.[4] Type II Diabetes is commoner in ethnic minority peoples and those who are socio-economically deprived.[5]

At any one time, 10 – 13% of people with diabetes will have sight-threatening retinopathy requiring medical follow up or treatment.

It is the commonest preventable cause of blindness in developed countries amongst the working age group, accounting for approximately 12% of all cases of blind registration in those < 65 years old. A recent report demonstrated that diabetic retinopathy accounts for 5.9% and 7.4% for full and partial blindness certification respectively in England and Wales. [6]

i.   Prevalence of diabetic retinopathy.

The prevalence of retinopathy of any severity in people with newly diagnosed diabetes is dependent upon the type of diabetes; the prevalence of retinopathy at diagnosis of type 1 diabetes is low ranging between 0 and 3% [7], while in type 2 diabetes, a higher proportion have an evidence of retinopathy at diagnosis (6.7 to 30.2%). [8, 9] An even higher prevalence was reported by the UK Prospective Diabetes Study **(UKPDS)** in newly diagnosed type 2 diabetics (39% in men and 35% in women). [10]

In general, population based studies from the UK showed a prevalence of retinopathy in 16.5% of diabetic patients identified through health district audits. [11]

In the Wisconsin Epidemiological Study of Diabetic Retinopathy **(WESDR)**: for patients with onset of diabetes before the age of 30 years, the prevalence of any retinopathy was 2% within 2 years of diagnosis of diabetes and 98% in those with disease duration >15 years. The prevalence of proliferative retinopathy was 0% in those within 5 years of diagnosis of diabetes, rising to 67% in those with disease duration >35 years. [12]

For patients with onset of diabetes after age 30 years, the prevalence of any retinopathy was 29% in those within 5 years of diagnosis and 78% in those with disease duration >15 years. The prevalence of proliferative retinopathy was 2% in those within 5 years of onset of diabetes, rising to 16% in those with disease duration > 15 years. [13]

ii.   Incidence of diabetic retinopathy

Two important studies provided data on the incidence of diabetic retinopathy:
In the WESDR, for patients with onset of diabetes before the age of 30 years, the incidence of any retinopathy developing for the first time over a 4-year and 10-year period was 59% and 90% respectively. The incidence of proliferative retinopathy over a 4-year and 10-year period was 11% and 30% respectively. [12]

For patients with onset of diabetes after the age of 30 years, the incidence of any retinopathy developing for the first time over a 4-year and 10-year period was 34 - 47% and 67 – 80% respectively. The incidence of proliferative over a 4-year and 10-year period was 2-7% and 10-23% respectively. [13]

Progression of retinopathy was more frequent in type 1 diabetes (41% over 4 years) and insulin dependent type 2 diabetes (34%) than non-insulin dependent diabetics. [14]

In the UKPDS, 22% of patients with no signs of any diabetic retinopathy at baseline developed retinopathy at 6 years, and in 29% of patients with baseline diabetic retinopathy, their retinopathy progressed 2 or more steps on the EDTRS scale after 6 years' disease duration. [15]

Recently, Klein et al described the 25-year cumulative progression and regression rates of diabetic retinopathy, macular oedema and clinically significant macular oedema in the WESDR. The 25-year cumulative rate of progression of diabetic retinopathy was 83%, progression to proliferative diabetic retinopathy was 42% and improvement of diabetic retinopathy was 18%. The lower risk of prevalent PDR in more recently diagnosed persons possibly reflects improvements in medical care over the study period. The 25-year cumulative incidence was 29% for macular oedema and 17% for clinically significant macular oedema. [16, 17]

iii. Prevalence of visual impairment

In the WESDR, no cases of legal blindness were found in persons aged < 25 years. The rate of legal blindness increased with age in both males and females, reaching a peak of 14% and 20% respectively in insulin-taking persons diagnosed with diabetes at age < 30 years at the age between 65 to 74 years. (Klein R: WESDR 1980-1982, unpublished data)

In the younger onset group, legal blindness first occurred in patients having diabetes for about 15 years or more, reaching 12% in patients with duration of diabetes more

than 30 years. However, in the older-onset group, rates of legal blindness were lower reaching only 7% in patients having diabetes for 20 to 24 years. [18]

Diabetic retinopathy was mostly responsible for legal blindness in 86% of younger-onset patients with severe sight impairment; this was less pronounced in the older onset patients. [18]

iv. Incidence of visual impairment

Analysis of the WESDR cohort re-examined 10 years after the baseline examination revealed a cumulative rate of legal blindness in 1.8% of younger onset diabetics as compared to 4% and 4.8% rates observed in older onset insulin dependent and non insulin dependent diabetics respectively. [19]

1.4 Risk factors

Several risk factors exist for the development and the progression of diabetic retinopathy, and for being registered as partially sight or blind.

1. Duration of diabetes

Duration of diabetes is considered as a reliable predictor of the presence of retinopathy, but the severity of the retinopathy is primarily influenced by other risk factors especially glycaemic control.

For younger-onset patients, both the frequency and the severity of retinopathy increased with increasing duration of diabetes. [12, 13] After diagnosis of diabetes, retinopathy was more frequent in the older-onset group compared with the younger-onset group. However, after 20 years or more of diabetes, fewer older-onset non-insulin dependent patients had any retinopathy (60% versus 99%) or proliferative retinopathy (5% versus 53%) than did younger-onset patients. [20]

In type 1 diabetes, the relationship between the duration of diabetes and the development of retinopathy has also been demonstrated in the Diabetes Control Complication Trial **(DCCT)** and other studies. [21, 22]

In the UKPDS study, the relationship between duration of diabetes and retinopathy in type 2 patients is not so clear, particularly since with continuing duration, there is continuing exposure to higher HbA1c values. [15]

The duration of diabetes is also an important risk factor for progression of retinopathy to sight-threatening eye disease in both types 1 and 2 diabetics. [23]

2. HbA1c and Glycaemic control

Chronic hyperglycaemia is considered the major risk factor in the development of diabetic retinopathy

In the WESDR, the glycosylated haemoglobin HbA1c level at baseline was found to be a significant predictor of the 4 and 10-year incidence of retinopathy, progression to proliferative retinopathy and incidence of macular oedema in the three diabetic groups studied; younger-onset diabetics, older-onset group taking insulin, and older-onset group not taking insulin. [24] These relationships were maintained after controlling for duration of diabetes, severity of retinopathy, and other risk factors measured at baseline.

The WESDR data also showed that the 4-year incidence and progression of retinopathy was greatest in the highest quartile of HbA1c. It is estimated that by reducing HbA1c from 11% to 9%, the rate of progression to proliferative disease would be halved. [25]

In the DCCT study, the rates of development of microvascular complications were evaluated in two groups of type 1 diabetics assigned either to strict (Mean HbA1c of 7.3%) or conventional (Mean HbA1c of 9.1%) glycaemic control over a mean follow-up period of 6.5 years.

For patients with no retinopathy at baseline, the strict control group showed a 76% reduction in the mean risk of developing retinopathy. In patients with mild retinopathy at baseline, tight control slowed the progression of retinopathy by 54% and reduced the likelihood of severe or proliferative retinopathy by 47%. [26]

The UKPDS similarly examined the effect of tight (Mean HbA1c of 7%) versus standard (Mean HbA1c of 7.9%) glycaemic control in newly diagnosed patients with type 2 diabetes. Compared with the conventional group, the risk reduction for progression of diabetic retinopathy – defined as two or more steps on the severity scale developed by the Early Treatment Diabetic Retinopathy Study **(EDTRS),** - over a 12-year period in the intensive group was 21%. In addition there was a 29% reduction in the need for retinal photocoagulation in the intensive group compared to the conventional group. [27, 28]

A meta-analysis of 16 published randomised clinical trials showed that the risk of retinopathy progression was insignificantly higher at 6 – 12 months of intensive glycaemic control. However, after > 2 years the risk was significantly lower. [29]

3. Hypertension

High blood pressure is a major independent risk factor in the development of retinopathy in both type 1 and type 2 diabetics.

In the WESDR, diastolic blood pressure was a significant predictor of the 14-year progression of diabetic retinopathy and incidence of PDR in patients with younger onset type 1 diabetics. After controlling of other risk factors, the relationship in between blood pressure and the incidence or progression of retinopathy remained. [30]

In the UKPDS, hypertensive patients were assigned to either tight control of blood pressure (144/82 mm Hg) or moderate control (152/87 mm Hg) over 9 years. The group assigned to tight blood pressure control experienced a 47% reduction in the risk of losing three lines of vision as compared to the group with standard blood pressure control. The effect was largely due to reduction in the incidence of macular

oedema. There was also a 34% reduction in the risk of progression of retinopathy status. [10]

Data from the EURODIAB Controlled Trial of Lisinopril in Insulin-Dependent Diabetics Mellitus **(EUCLID)** showed also a 50% reduction in the progression of retinopathy and reduced risk of blindness in non-hypertensive or mildly hypertensive patients in the Lisinopril treatment as compared to the placebo group. [31]

4. Nephropathy

Patients with diabetic nephropathy are more likely to have associated microvascular disease in the eye; with up to 96% of those with nephropathy also have retinopathy. [32] Patients with renal failure develop worsening of their retinopathy particularly affecting the macula, but are also at risk of PDR. [33]

In type II diabetes, microalbuminuria is an independent predictor of retinopathy. [34] In type 1 diabetics, the prevalence of proliferative retinopathy and blindness rose with increasing albuminuria, being 28% and 5.6% in those with microalbuminuria and 58% and 10.6% in those with macroalbuminuria, [35] while in type 2 diabetics, the prevalence of proliferative retinopathy was 5% and 12% with microalbuminuria and macroalbuminuria respectively. [36]

5.Age

Diabetic retinopathy is rare under the age of 10 years. Puberty with its attendant hormonal changes brings about accelerated changes in retinopathy status. The highest 4- year incidence in the WESDR was among patients aged 10-12 years at the baseline examination. [12]

6. Pregnancy

Diabetic retinopathy often gets worse during pregnancy. The Diabetes in early pregnancy study reported that the risk of progression is greatest in women with moderate to severe retinopathy at the start of pregnancy; 29% of subjects with

moderate retinopathy at baseline developed proliferative features, compared with 6.3% of those with minimal retinopathy at baseline. [37]

It was also reported that women with the highest glycosylated haemoglobin levels at the start of pregnancy and those who experienced rapid improvement in glycaemic control during pregnancy had the highest risk of progression of retinopathy status. [38]

7. Hyperlipidaemia

In the WESDR, higher total serum cholesterol was associated with higher prevalence of retinal hard exudates in both the younger and the older-onset groups taking insulin. [39] The EDTRS group reported that patients with persistently poor vision had higher blood cholesterol levels. The high levels of total cholesterol and LDL-cholesterol were associated with twice the number of retinal hard exudates compared with those with normal lipid levels, relating to the increased risk of losing vision, even after adjusting for macular oedema. [40]

1.5 Pathogenesis of diabetic retinopathy

There are multiple pathophysiological mechanisms in diabetic retinopathy that combine to produce its two defining features, both of which occur in the retinal vasculature.

First, increased vascular permeability resulting from the breakdown in the blood-retinal barrier, which in turn results in vascular leakage and accumulation of extracellular fluid. Second, the occlusion of capillary beds resulting in retinal ischaemia which leads eventually to the development of new vessels. These two pathological features coexist and are responsible for the visual problems associated with the development of diabetic retinopathy.

These pathological features are reflected at microscopic level by certain characteristic abnormalities commonly found with diabetic retinopathy: these are thickening of the capillary basement membrane, loss of capillary pericytes and loss of capillary endothelial cells.

Several biochemical mechanisms have been described which may independently, or in combination, produce these morphological and structural changes associated with diabetic retinopathy. [41]

1. The Polyol patway:

Glucose is metabolised through the polyol pathway when other pathways are saturated, thus it is mainly important in the presence of hyperglycaemia.
The pathway is modulated through aldose reductase, which converts glucose into sorbitol, this is in turn metabolized into fructose by sorbitol dehydrogenase at a slower rate. The net result is an accumulation of intracellular sorbitol, which leads to increased osmotic stress and can disrupt the cellular function. The increased aldose reductase mediates cellular damage also through reducing the levels of nicotinamide adenine dinucleotide phosphate (NADPH), thus impairing the free-radical scavenging ability. The polyol pathway also reduces the intracellular myoinositol levels, which is required for $Na^+/K^+ -$ ATPase activity and leads to impaired cell function. The sorbitol pathway is suggested to be present in the pericytes, but not the endothelial cells, and can thus account for the early preferential loss of capillary pericytes in diabetic microangiopathy. [42]

2. Activation of protein kinase C

Protein kinase C (PKC) is a widely distributed intracellular signal transducer for many cytokines and hormones acting upon the cell; it is an important mediator for various cell functions such as growth and differentiation, vascular permeability, DNA synthesis, basement membrane turnover and vascular smooth muscle contraction.

PKC is up-regulated by hyperglycaemia, and the increased activity – especially the PKC-ß isoform – has been implicated in the pathogenesis of different features of diabetic retinopathy;

- Basement membrane thickening, through increased synthesis of collagen and fibronectin.
- Retinal vasoconstriction, via inhibition of nitric oxide- mediated vasodilatation and increased endothelin expression, thus altering the retinal blood flow.
- Increased vascular permeability
- Increased production of vascular permeability factor (VPF) in response to high glucose levels.
- Increased endothelial surface expression of adhesion molecules, which increases the cellular adhesion to circulating platelets.
- Decreased Na^+/K^+ – ATPase activity. [43]

3. Non-enzymatic glycation of proteins

Glucose molecules are able to attach onto lysine residues of proteins, both extracellularly and intracellularly, the rate of which depends upon the circulating glucose concentration and the duration of exposure.

This process can affect proteins such as haemoglobin (producing glycosylated haemoglobin), cell membrane proteins, lens crystallins, plasma proteins and collagen. The products of this glycation process affect the cell functions, including regulation of free-radical mediated vascular damage and uptake of low-density lipoproteins.

Many cell types are affected including the pericytes, endothelial cells, and smooth muscle cells. This may lead to;

- Increased production of cytokines and surface adhesion molecules
- Increased vascular permeability and changes in cellular proliferation
- Up-regulation of extracellular matrix gene expression leading to increased production of basement membrane components.
- Toxicity to retinal capillary pericytes. [41]

4. Haemorheological factors

Various heamorheological factors are involved in the pathogenesis of diabetic retinopathy. These factors include the increased blood viscosity, increased platelet aggregation, increased leucocyte adhesion, and decreased red cell deformability. [44]

5. Abnormal retinal blood flow

The abnormal microvascular blood flow associated with diabetic microangiopathy in several tissues, including the retina, is attributed to a state of pseudo-hypoxia developing as a result of different mechanisms. First, the accumulation of retinal lactate that results from the metabolism of retinal glucose through the glycolytic pathway, can lead to an autoregulatory hyperperfusion. Secondly, a similar effect takes place via the polyol pathway with an imbalance in the ratio of NAD to NADH thus mimicking a hypoxic environment. The effect of the pseudo hypoxia is complicated by the true hypoxia, which develops in the presence of capillary occlusion. [45]

Increased retinal blood flow can inflict damage on the retinal vasculature through increased shear stress upon the vascular endothelium, thickening in basement membrane as an early compensatory mechanism, vascular stretching and break down of the blood-retinal layer.

6. Glucose-induced apoptosis

There is evidence that high circulating glucose concentration can lead to a paradoxical low pericyte glucose concentration, which can stimulate the pericytes to undergo apoptosis. Apoptosis of the endothelial cells has also been demonstrated in high glucose concentrations. [41]

7. Growth and angiogenic factors

The hypoxic environment that develops in diabetic retinopathy, following capillary closure, leads to the production of several angiogenic factors that leads in turn to the development of proliferative retinopathy. These factors include basic fibroblast growth factor (bFGF), Insulin-like growth factor 1 (IGF-1), transforming growth factor ß (TGFß), vascular endothelial growth factor (VEGF).

VEGF is now considered to be the most important growth factor implicated in the pathogenesis of diabetic retinopathy. The retinal VEGF activity is increased by the hyperglycaemia and hypoxia. The receptors of VEGF are present on the retinal endothelial cells and pigment cells. VEGF promotes vascular leakage and neovascularisation and is therefore involved in both of the principle features of diabetic retinopathy. [46]

1.6 Clinical features of diabetic retinopathy

The clinical features of diabetic retinopathy result from the pathological changes that occur within the retinal vasculature as previously described.

Diabetic retinopathy is generally classified into either non-proliferative or proliferative stages. Non-proliferative diabetic retinopathy (NPDR) includes all forms of retinopathy that precede the development of new vessels. It includes the background and preproliferative stages. Proliferative diabetic retinopathy (PDR) usually appears late in the disease, with the formation of new vessels. Diabetic maculopathy can be defined as any lesions of background retinopathy within the macular area.

The clinical features of diabetic retinopathy are:

1. Microaneurysms

These are considered the earliest clinically detectable lesions of diabetic retinopathy. They are not associated with any visible blood vessels, and represent localised dilatations or out-pouching of retinal capillaries at areas with relative weakness with pericyte loss.

They indicate a localised area in the microvascular circulation where the blood-retinal barrier is deficient and can thus be associated with abnormal vascular leakage. [47]

2. Haemorrhages

Haemorrhages can occur within the retina, where they remain confined by the retinal tissues and can be described as "dot and blot haemorrhages". They can also occur at the retinal surface and spread along the nerve retinal fibre layer forming "flame-shaped haemorrhages". The latter may suggest a coexistence of hypertensive vessel damage.

Haemorrhages occur from rupture of microaneurysms or other weak walled vascular abnormalities. They can appear early in diabetic retinopathy and increase in number with severity. Large dark blot haemorrhages suggest severe retinal ischaemia associated with arteriolar occlusion. [48]

3. Exudates

These are usually small collections of lipoprotein, which accumulates in the retina from abnormal vascular leakage, thus they are mostly found in the vicinity of microaneurysms. The number of exudates may paradoxically increase as the degree of extravascular fluid diminishes due to the precipitation of lipids and proteins.

4. Cotton wool spots (CWS)

Cotton wool spots appear as pale fluffy cream patches of variable sizes. They had been considered to signify adjacent areas of infarction of the nerve fibre layer. [49] The appearance is due to swollen nerve axons with the products of impaired axoplasmic transport 'damming up' bordering the infarcted zone. They represent an area of localised retinal ischaemia with the presence of arteriolar occlusion and have little predictive power for the subsequent development of proliferative retinopathy. [50]

5. Intraretinal microvascular abnormalities (IRMA)

They consist of vascular elements within the retina which branch with a pattern different from normal retinal vessels. IRMAs lie within the retina and therefore do not overlie retinal vessels or give rise to pre-retinal or vitreous haemorrhage. IRMA occurs adjacent to large areas of capillary bed non perfusion, branching into multiple hairpin-like loops. They might represent shunt vessels or intraretinal new vessels. [48]

6. Venous abnormalities

These abnormalities occur in the retinal veins in response to the hypoxic retinal environment.
- Venous dilatation can occur as an early sign and becomes more pronounced with further capillary shut down.
- Venous loops, where the vein deviates suddenly to form a loop
- Venous beading and reduplication of veins which are strong indicators of extensive capillary non-perfusion and hypoxia, its presence is a more powerful predictor of subsequent development of proliferative diabetic retinopathy than the presence of any other single abnormality. [51]

7. Neo-vascularisation

Widespread retinal ischaemia with closure of the capillary bed leads to newly formed blood vessels appearing on the retinal surface (NVE new vessels elsewhere) or overlying the optic disc (NVD disc new vessels).

NVD represents severe generalised ischaemia of the retina, whereas NVE is a response to a local ischaemia in the quadrant of the retina where they occur.
New vessels usually arise from a vein and have a haphazard growth pattern unlike the usual vascular pattern adopted by the normal retinal vessels radiating from the optic nerve head. These vessels extend in the plane between the retina and the posterior vitreous face.

1.7 Classification of diabetic retinopathy

There is a considerable overlap between the various available classifications. The differences between classifications relate mainly to the levels of retinopathy described and the terminology used.

1. Retinopathy

Diabetic retinopathy is classified according to the presence or absence of abnormal vessels as non-proliferative (background or preproliferative) retinopathy or proliferative retinopathy.

A) Non-proliferative diabetic retinopathy (NPDR)

In the International clinical diabetic retinopathy disease severity scale [52], NPDR is subdivided into
- Mild: microaneurysms only
- Moderate NPDR: more than microaneurysms but less than severe NPDR

- Severe NPDR: any of the following: extensive intra-retinal haemorrhages in each of 4 quadrants, definite venous beading in two or more quadrants, prominent IRMA in one or more quadrant.

The Airlie House grading system has initially used the following criteria to define the NPDR grades. [53]

- Mild NPDR: at least one microaneurysm
- Moderate NPDR: severe retinal haemorrhages in at least 1 quadrant or CWS, venous beading, or IRMA definitely present.
- Severe NPDR: severe retinal haemorrhages in 4 quadrants, or venous beading in 2 quadrants or extensive IRMA in one quadrant.
- Very severe NPDR: any two of the features of severe NPDR

This classification has then been modified into three grades to form the modified Airlie House classification [53];

- Mild NPDR: at least one microaneurysm
- Moderate NPDR: extensive intra-retinal haemorrhages and/or microaneurysms, and / or CWS, venous beading, or IRMA definitely present but not to the grade of severe NPDR
- Severe NPDR: CWS, venous beading and IRMA all present in at least 2 quadrants, or two of them present in at least 2 quadrants with intra-retinal haemorrhages and microaneurysms present in all quadrants, or IRMA present in each quadrant, being severe in at least one of them.

In the National Screening Committee (NSC) UK classification [54], NPDR is simply subdivided into

- R1: Mild NPDR: haemorrhages and microaneurysms only
- R2: Moderate to severe NPDR: Multiple deep dot and blot haemorrhages, any IRMA or any venous beading, looping or reduplication.

B) Proliferative diabetic retinopathy (PDR)

In the International clinical diabetic retinopathy disease severity scale, PDR is defined to have neovascularization and /or vitreous or pre-retinal haemorrhages. [52] In the NSC-UK [54] proliferative retinopathy is classified as:

(R3): Proliferative retinopathy, pre-retinal fibrosis +/- tractional retinal detachment, with new vessel formation NVD or NVE, fibrovascular proliferation, and pre-retinal or vitreous haemorrhage.

2. Diabetic Maculopathy

It is defined as any retinopathy lesion located within the macular area.

It can be classified to

a. Focal maculopathy: characterised by well-circumscribed leaking areas associated with complete or incomplete circinates of hard exudates, and often related to leaking microaneurysms.

b. Diffuse maculopathy: Generalised thickening of the central macula caused by widespread leakage from dilated capillaries in this area, it is often associated with cystic changes.

c. Ischaemic maculopathy: It is suspected in patients with unexplained visual loss in the presence of relatively normal looking macula. Blot haemorrhages in the paramacular region can be indicative of ischaemia.

d. Tractional maculopathy: It can be caused by vitreoretinal adhesions or by membrane formation either as epiretinal membranes or transretinal bands.

e. Mixed maculopathy: occurs with combined pathology particularly with diffuse oedema and ischaemia. Variable degrees of traction may also be involved.

Several large clinical trials have adopted different classifications for NPDR. The DCCT and the UKPDS used the classification provided by the International diabetic retinopathy severity scale, while the EDTRS used an additional classification of NPDR into mild, moderate, severe and very severe, based on standard fundus photographs set by the Airlie House grading system.

However, such classifications are rarely used clinically, as they are based on the "gold standard" 7-field 30º stereo-photography which is not undertaken in routine clinical practice.

Therefore for the purpose of this study, we have used diabetic retinopathy grading system developed for the EURODIAB IDDM Complications Study. This system is based on a two-field 45º retinal photography, and the diabetic retinopathy lesions are assessed against one or two more standard nasal and macular photographs for that lesion. In the study, each lesion was thus graded and given a numerical value. The detailed grading of the retinopathy lesions was used to calculate an overall retinopathy level per eye. The system proved to be accurate and repeatable as compared to the recognised gold standard system of 7-field stereo-retinal photography. [55] The use of this system, based on two-field 45º retinal photography, is also keeping with the two-field photography based UK diabetic retinopathy screening system.

The details and composition of the retinopathy levels of the EURODIAB system are described in table 1.1:

Level	Retinopathy Features
Level 0	No retinopathy
Level 1	**Minimal NPDR**: HMA= Grade 2-3 in 1 or 2 fields and /or HE = Grade 2-4 in 1 or 2 fields
Level 2	**Moderate NPDR** HMA = Grade 4 in only 1 field OR HMA = Grade 2 –3 in 1 or 2 fields PLUS: CWS = Grade 2-3 in 1 or 2 fields and/or IRMA = Grade 2 in 1 or 2 fields and /or VB = Grade 2 in 1 or 2 fields
Level 3	**Severe NPDR** HMA = Grade 4 in both fields OR HMA = Grade 2-4 in 1 or 2 fields PLUS CWS = Grade 4 in 1 or 2 fields and/or IRMA = Grade 3 in 1 or 2 fields and/or VB = Grade 3 in 1 or 2 fields
Level 4	**Photocoagulated** Scars of photocoagulation in any field
Level 5	**Proliferative** Any of New vessels (disc or elsewhere) Fibrous proliferations (disc or elsewhere) Pre-retinal haemorrhage Vitreous haemorrhage

Table 1.1: Allocated retinopathy levels and causative features HMA = Haemorrhages and microaneurysms, HE = Hard exudates, CWS = cotton wool spots, IRMA = Intra-retinal microaneurysms, VB = venous beading, NVE = new vessels elsewhere, NVD = new vessels disc. (Taken from Aldington et al 1995) [55]

1.8 Prediction of proliferative diabetic retinopathy

Previous studies have shown clearly that the presence of severe NPDR is predictive of subsequent neovascularisation; the Diabetic Retinopathy Study (DRS) reported that approximately 50% of eyes with severe NPDR progressed to proliferative diabetic retinopathy over a period of approximately 15 months. [56]

The EDTRS research group observed in detail the natural course of diabetic retinopathy in untreated eyes with mild to severe non-proliferative retinopathy. Gradings of baseline fundus photographs of these eyes were used to examine the power of various features and the combinations of these abnormalities to predict progression to proliferative retinopathy. [51] In their analysis, eyes with mild to severe NPDR were divided into 4 levels. (Level 35 [Mild NPDR], level 43 [Moderate NPDR], level 47 [Moderately severe NPDR], and level 53 [Severe NPDR]). The study results demonstrated that for each one level increase on the scale, the 1-year progression rate to PDR approximately doubles, increasing from 4.1% for level 35 to 12.2% for level 43, 26.0% for level 47, and 51.5% for level 53. Results after 3 and 5 years were similar. Further analysis of the relationship between the baseline severity of each retinopathy feature and the rate of progression to PDR was done. The 1-year progression rates to PDR increased fourfold or more with increasing severity of haemorrhages and/or microaneurysms, IRMAs and venous beading. They doubled with increasing severity of soft exudates. There appeared to be little or no relationship between severity of hard exudates and risk of PDR. The presence of venous beading was found to be the most powerful predictor of the subsequent development of PDR than any other abnormality. The baseline severity of other characteristics of the retinal veins –such as loops/reduplication, narrowing, sheathing-, arteriolar sheathing and arteriovenous nicking did not appear to have a strong relationship with the development of PDR. [51]

Although these described predictive values of the different diabetic retinopathy characteristic lesions are crucial for planning screening intervals, management, and follow up of eyes with NPDR, these characteristics are not always present before or at the time when pre retinal new vessels are first recognised. A possible explanation for this is the relatively transient nature of some of these lesions. Cotton wool spots

usually disappear within 6 to 12 months. Blot haemorrhages and IRMAs tend to disappear also after extensive capillary closure, with decrease in the number of small vascular branches producing a picture described as "featureless retina". [47]

1.9 Screening for diabetic retinopathy

Diabetic retinopathy is a disease, which fulfils all the necessary criteria to represent an excellent paradigm for screening as laid out in the principles for screening of human disease described by Wilson and Junger in 1968. [57] Those at risk form an identifiable population, it has a recognised disease pattern and laser treatment, when performed early, is effective in preventing loss of vision, particularly in proliferative disease. Advanced disease, when diagnosed late with well-established new vascularization and/or fibrovascular proliferations, is less amenable to treatment and much more costly, both economically and in terms of the patient's quality of life.

The National Screening Committee of the UK has recently recommended digital fundus photography as the preferred method for screening. The principles of the grading protocol set by the National Screening committee in the UK were to detect any retinopathy, detect the presence of sight threatening diabetic retinopathy, to allow precise quality assurance at all steps and to minimise false positive referrals to the hospital eye services. [58]

The evidence of effectiveness of screening is based on evidence of treatment efficacy, especially after early detection, and of cost effectiveness. [59]

A) Proliferative retinopathy

Several previous randomised controlled studies have shown that peripheral laser photocoagulation versus no treatment significantly reduced the risk of blindness after 2 or 3 years in patients with PDR with high- risk characteristics. [60, 61] (Eyes with high-risk characteristics have (1) NVD greater than one-half the disc area, (2) any NVD and vitreous haemorrhage, or (3) NVE greater than one-half the disc area and vitreous or pre-retinal haemorrhage).

The DRS found also that early versus deferred scatter argon laser treatment decreased the risk of severe visual loss at 5 years in patients with either preproliferative or proliferative retinopathy. [61] A subgroup analysis of the EDTRS found that the benefit was significant in people with type 2 diabetes and with severe preproliferative or early proliferative retinopathy without high risk characteristics. [62] The British Multicenter study [63] and the EDTRS [64] reported that panretinal scatter photocoagulation significantly reduced the risk of visual deterioration at 5 years in patients with preproliferative disease most of whom had maculopathy as compared to no treatment.

B) Maculopathy

The evidence of effectiveness of laser treatment for diabetic maculopathy has been established also by a number of randomised controlled studies. The EDTRS reported a significant reduction in moderate visual loss at 3 years in patients with macular oedema associated with mild to moderate retinopathy with macular laser treatment as compared to no treatment. [65] Subgroup analysis found that treatment was significantly more effective in eyes with clinically significant macular oedema, particularly in people in whom the center of the macula was involved or imminently threatened. [66]

Screening for diabetic retinopathy has been shown to be cost effective in health economic terms. To determine the impact of systemic population screening in Newcastle upon Tyne, the blindness prevalence in Newcastle health district was determined. It was reported that the rates for blindness and partial sight registration in the recent years, after the introduction of screening, were less than one third of those reported in surveys conducted prior to 1997, thus reducing the socio-economic impact on the surrounding community. [67]

1.10 Discussion

Diabetic retinopathy is in general considered the most common cause of blindness in the working age group. The UK leads the world in diabetic retinopathy screening. However, although digital photographic screening has proved to be effective at screening for diabetic maculopathy, the screening for and the prediction of PDR is problematical for several reasons.

1. The detection of retinal neovascularisation in PDR can be challenging. Disc and retinal new vessels can be difficult to detect especially on two-dimensional digital screening images as the new vessels can be blurred and out of focus, especially if they are elevated from the surface of the retina and attached to the posterior hyaloid face. This is compounded by the fact that patients with PDR often have poor pupil dilatation and/or cataractous changes that can further degrade the image quality.

   Small new vessels can also lie outside the two-field 45° screening photographs, an observation that has been noted by Aldington and colleagues, when comparing the two-field 45° photographs to the seven-field 30° gold standard photographs. As a result, these eyes can be assigned as non-proliferative rather than proliferative, and may subsequently go on to lose their vision with a vitreous haemorrhage. [55]

2. It is established, as previously discussed, that pan retinal photocoagulation for PDR is best applied at an early stage before visual loss occurs. Screening programmes therefore aim to detect people with PDR at the earliest stage, even if new vessels are not visible by referring patients with preproliferative retinopathy for further clinical examination and follow up by an ophthalmologist. However this also has its limitations. There is a debate regarding the optimum screening intervals for patients with different grades of diabetic retinopathy. Patients with no retinopathy particularly those with good control rarely develop sight threatening diabetic retinopathy STDR within a year. Although patients with severe NPDR have a high risk of developing new vessels, and 3 monthly review

is recommended, at least 50% will not progress during one year follow up. This means that for every ten patients with severe NPDR, up to fifty patient appointments will be needed each year with half of these detecting no change in retinopathy status. In general, the NSC currently recommend referral at the approximate level of moderate NPDR, which means many patients are referred and many appointments needed to follow these patients up.

3. The features of preproliferative diabetic retinopathy on their own can be hard to identify. IRMA lesions can be difficult to detect on retinal photographs and thus easily missed. Similarly, although venous beading is a reliable sign of retinal ischaemia, and strongly predictive for retinopathy progression, it can be very subtle and easily overlooked.

   Occasionally, patients can have only mild degrees of background retinopathy without significant intra-retinal haemorrhages, venous beading or IRMA, but still go on to develop new vessels with vitreous haemorrhages without actual warning signs of progression. This observation has been mainly noted in young Insulin dependent diabetics in particular, who can develop rapidly progressive PDR, from mild background retinopathy. Explanations that have been proposed to explain this include an assumption that these patients have gone through a phase when pre-proliferative signs were present but then faded before neovascularisation commences. [47] Other local factors such as the level of retinal non-perfusion and the presence or absence of significant arteriosclerotic changes are probably also influential in determining the rate of retinopathy progression and the need for laser treatment.

4. The phenomenon of "retinopathic momentum" was recognised in the DCCT and describes the relentless progression of retinopathy that occurs in these patients, despite treatment, once the retinopathy has reached a certain point. [68] "Retinopathic momentum" in proliferative retinopathy is probably related to the degree of underlying retinal ischaemia, which can be underestimated on photographic screening or clinical examination.

Similarly, but conversely patients with small NVE can occasionally not progress for several years without developing any problems

The assessment of retinal non-perfusion and new vessels detection can be aided by fluorescein angiography; however, this is an invasive technique with some degree of risk, hence, a non-invasive technique to assess the degree of retinal ischaemia would be ideal.

The various changes in blood flow discussed earlier suggest that the geometry of the retinal vascular network, which is designed to optimise flow, might be altered in different systemic vascular disorders. The details of these changes will be reviewed in the next chapter. These geometrical features include the relationship of vascular widths of the retinal vessels at vascular bifurcations, and the angles subtended by these vessels.

If the retinal vascular geometry was proven to be altered by retinal ischaemia in diabetes, then the measurements of these geometrical changes may provide an easy non-invasive way for assessing retinal ischaemia. Up until recently retinal blood vessels analysis has required detailed time consuming expert analysis by highly trained human observers using manual methods, thus large-scale analysis of retinal geometry for screening purposes has not been practical. However recent advances in computer-assisted analysis of retinal vessels have made studies investigating the retinal vasculature increasingly possible.

A number of researchers are working on automated analysis of digital screening images to aid the screening and grading processes. Sufficiently accurate automated detection would aid wider and more effective screening. To date, automated analysis has concentrated on the detection of retinal lesions characteristic of diabetic retinopathy such as microaneurysms, haemorrhage and exudates. There has been some recent work on the automated vascular segmentation and vessel width detection, and preliminary work on automated detection of venous beading. In the near future, automated retinal vascular geometrical analysis will be possible.

This project aims to assess retinal vascular geometry in patients with diabetic retinopathy and to analyse any changes that might be associated with the different grades of retinopathy. If it was shown that changes in retinal vascular geometry were altered in diabetic retinopathy, then automated retinal analysis of screening images in the future may aid in diabetic retinopathy classification and assist in predicting the possibility of retinopathy progression allowing more timely treatment.

Chapter 2: Retinal vascular geometry review

2.1 Overview

This chapter provides an overall review of the rationale for analysing the geometry of the retinal vascular network as a potential tool for diagnosing and predicting certain cerebral and systemic vascular diseases.

In the first section, anatomical considerations and relevant aspects on the embryological development of the retinal vessels are discussed. The basis behind geometrical and fractal methods of analysing vascular branching networks are also clarified.

This is followed by a discussion of the theoretical optimality principles that govern the vascular system. The extent that different normal vascular networks throughout the human body adhere and agree with these optimality principles with special emphasis on the retinal vascular network, is considered.

The next section reviews previous studies that have been performed for analysing various aspects of the geometry of the vascular networks in a variety of systemic vascular conditions.

The retinal vascular changes associated with the development and progression of diabetes are then explored, including previous work on differing features of diabetic retinopathy, retinal vessel width calibre and the fractal analysis of retinal vasculature.

This background is summarised and a hypothesis is presented on potential changes in the geometry of the retinal vascular network with diabetic retinopathy forming the basis of this thesis and the proposed plan for investigation.

2.2 Introduction

Branching patterns in nature have been associated with a wide variety of naturally occurring networks. These include river networks, trees, root systems and lightning bolts. These structures share a common feature of having a similar appearance when viewed at different magnifications; when the basic pattern is magnified, one can observe repeating levels of detail. These biological patterns are representative of the concept of "self-similarity", and objects that show self-similarity at different magnifications are called fractal objects. These fractals, found in nature, are called "random fractals", and their structure shows self-similarity only in a statistical sense. [69]

The human body contains diverse examples of biological branching trees that have been analysed as fractals; these include the branching of the bronchial tree, the branching of some cardiac muscle bundles, the branching of the His-Purkinje network, the small pulmonary arteries, the branching vascular system in the kidney and the heart, and the retinal circulation in the human eye.

Previous studies of patterns of vascular systems have raised various questions about ways to characterize blood vessel patterns, which parameters needed to be measured and whether there are theoretical models or optimisation principles that govern these patterns.

There are two approaches describing vascular systems,

Firstly, geometrical analysis of a vascular network can be used to measure the spatial properties of the vascular tree. This includes estimation of blood vessel diameters, lengths and branching angles. This can be combined with determination of blood flow velocities and other physiological blood flow measurements. These overall parameters are determined on a scale from the major arteries that provides the input to the capillary bed and to the veins that drain the tissues. The measured parameters can then be examined to assess how well they fit with theoretical optimisation models. [70-72]

Secondly, a newer approach has been adopted for studying vascular systems by using the fractal analysis to characterize the blood vessel patterns. If the vascular pattern is determined as being fractal "self-similar", the fractal dimension (D_f) can be measured which is a number that characterises the distribution of the branching vascular system in two-dimensional space. This is considered as a measure of the "roughness" of a fractal structure. [69]

This review will focus on the retinal vascular network. However, firstly the anatomy and embryological development of the retinal blood vessels will be discussed, which will allow the theories behind vascular changes that can take place in pathological vascular conditions, to be understood.

2.3 Anatomical Considerations

The retina has the highest oxygen requirement per unit weight for any tissue in the body and any alteration in circulation may result in functional impairment and tissue damage. It is supplied by two major blood vessel systems. The inner layers of nerve fibers and glial cells are supplied by the retinal circulation, which supplies the nutritive function for the inner two thirds of the retina.

The second circulatory system of the retina is the choroidal circulation which supplies the outer neural retinal layers and the retinal pigment epithelium, the choroidal circulation acts as both a nutritive and cooling system for the eye. The choroidal circulation is derived from two or three posterior ciliary arteries which are derived from the ophthalmic artery.

The retinal circulation is supplied by the central retinal artery and has one main collecting trunk, the central vein at the optic disc. The central retinal artery is derived from the ophthalmic artery which is a branch of the internal carotid artery. The central retinal artery enters the optic nerve 10mm behind the globe and appears at the optic disc where it branches into four main vessels, each supplying one quadrant of the retina. [73] Following bifurcation at the optic disc, the retinal artery and vein form extended branching patterns throughout the retina. The retinal arterial diameters

range between 40 – 160 μm. The branching patterns of the retinal circulation in the human retina are the subject of this review.

2.4 Embryological development of the Retinal Vascular System

Retinal vascularisation begins in the most superficial retinal layers at the optic nerve head and radiates outwards from this central point.

The human retina remains avascular until the fourth month of fetal development. [74] At the end of the four month period, vascular mesenchymal cells enter the nerve fiber layer, and spindle cells spread out towards the periphery of the retina. Vascular growth occurs outward from the disc. Retinal vascularisation proceeds via angiogenic sprouting from pre-existing vessels and it utilises different sources of endothelial cells, and (including) recruited circulating stem cells. Vascular growth occurs by two complementary mechanisms; vasculogenesis and angiogenesis.

Vasculogenesis is the development of a vasculature by differentiation and organisation of endothelial cells; it is the process by which the initial vascular tree forms from embryonic precursor cells. Angiogenesis is the formation of blood vessel from a pre-existing blood vessel by the migration and proliferation of differentiated endothelial cells. [69]

Various researchers have looked at different factors that could influence the retinal vascular development and patterns.

Previous studies have suggested that local oxygen tension has a large effect on retinal vascular development; it compensates for vascular insufficiency by the induction of angiogenesis. This was thought to be mediated by a hypoxia-inducible factor (HIF) complex – or an oxygen-sensitive molecule – that is activated in hypoxic cells and results in an increase in transcription of a broad range of genes and angiogenic growth factors such as the vascular endothelial growth factor (VEGF). [75] The idea that oxygen regulates blood vessel growth in the retina has received further evidence from the fact that pathological retinal angiogenesis takes place in several diseases that are characterised by retinal ischaemia. Moreover, experimentally lowering

inspired oxygen in neonatal kittens reduces the rate and density of retinal vascularisation. [76]

Other studies assessing the relative influence of genetic and environmental factors on the retinal vessels demonstrated that in normotensive adult twins, the retinal vessel diameters are governed predominantly by genetic factors accounting for 70% and 83% of the variance in arteries and veins diameters respectively. The remainder being attributable to unshared environmental factors. [77] These results supported earlier observations from the Beaver Dam Eye Study that showed that retinal vessel equivalents – such as the central retinal arteriole and venule equivalents and the arteriole-to-venule ratio – were more highly correlated between relatives than between unrelated individuals; these correlations were suggested as being the result of a number of shared genes. [78]

The most important function for the developed vascular architecture is to bring the circulatory system into close contact with a tissue to provide its nutritional supply. The vascular architecture thus develops in a certain manner to meet this function and ensure appropriate perfusion.

2.5 Optimal branching of the retinal vascular network

As previously described, the geometrical features of the retinal vascular network can be described in terms of various features such as branching angles and vascular branching diameters. From considerations of the design and function of the cardiovascular system, it is unlikely that the geometric features of this system are purely arbitrary. In fact, it has been suggested that the branching geometry of the retinal blood vessels is governed by various rules and principles resulting in optimal values for the angles and diameters which renders the network more efficient physiologically. [79]

The branching angles and the relationship of vessel diameters of vascular networks within the cardiovascular system – including the retinal blood vessels – were believed to be based theoretically on well defined physiological principles that govern the dynamics of fluid-conducting systems. Several investigators had

examined these principles, following the initial pioneering work by Murray in 1926. [70, 71]

Based on Poisseuille's equation, Murray postulated a law for connecting large to small vessels. He stated that for maximal efficiency in a circulation, the flow of blood in an arterial section should be proportional to the cube of the vessel diameter, and in a steady state the flow in the daughter branches must be equal to the flow in the parent vessel. Thus the cube of the radius of the parent vessel should equal the sum of the cubes of the radii of the daughter vessels $(d_0{}^3 = d_1{}^3 + d_2{}^3)$, where d_0, d_1 and d_2 represent the diameter of the parent vessel, the larger branch and the smaller branch respectively. In other words he predicted that an optimum vascular system must have its vessels connected in such a way that the flow is carried by a set of vessels whose radii cubed sum to a constant value. This leads to the definition of a parameter, the Junction exponent, (X) which satisfies $(d_0{}^x = d_1{}^x + d_2{}^x)$. [80] Murray's theory suggested that when $X = 3$, the vascular surface area available for metabolic exchange was maximised and power loses and intravascular volume was minimised. [70, 80]

Thus vascular networks, according to Murray's law, were predicted to have their flow rate, and vessel diameters related, with the total surface area tending to be greatest at the level of the smallest vessels to allow for maximal trans-mural exchange diffusion whilst flow velocity decreased. Importantly, the local vessel wall shear stress would remain constant. It was proposed that it was the vascular endothelium that coordinated this link between the branching diameters to maintain the unique constant low shear stress throughout the vascular network as reflected by the junction exponent. It was postulated that the changes in shear stress resulting from - or leading - to vascular endothelial dysfunction form the basis for diseased networks that would deviate from Murray's rules.

In a similar way, the theoretical optimal vascular branching angle between the two daughter vessels was estimated to be around 75 degrees.

Vascular networks were found to be comprised of both symmetrical bifurcations where the flow is equal in both daughter vessels and asymmetrical bifurcations

where the diameters and hence flow of both daughter branches were unequal. Two further expressions were postulated to describe the local branching geometry;

- The area ratio *(ß)*: defined as the sum of the cross sectional areas of the two daughter branches divided by the area of the parent. $(ß=d_1^2+d_2^2 \, / \, d_0^2)$
- The asymmetry ratio *(α)*: defined as the cross sectional area of the smaller branch divided by that of the larger $(α = d_2^2 \, / \, d_1^2)$ By definition, the value of this parameter should be between zero and one, being equal to one in the special case of a symmetrical bifurcation, thus $0 < α < 1$ [81]

Several investigators built on Murray's work, and described in detail certain optimality principles that govern vascular branching. In Zamir's studies, two of these principles proposed that the branching angles are optimised so that the lumen surface or the lumen volume of the vessels involved in the vascular junction is minimised, it then follows that the optimum branching angles are determined by the radii of the vessels involved. Another two principles proposed that the branching angles are in an optimum state when the pumping power required to drive the flow, or the drag force on the endothelial surface, is minimum, and thus as a consequence the optimum branching angles are dependent on the flow as well as the diameter of the vessels involved. [81]

There are various explanations that would favour and support these optimality principles; if the lumen surface of vascular junctions is minimised, then the corresponding amount of vascular tissue required for forming these junctions is also a minimised which may be considered a design advantage. Similarly, if the lumen volume of the vascular junctions is kept at minimum values, then the volume of blood contained in the vascular system will also be close to minimum; this decreases the amount of work exerted by the vascular system to pump the blood volume, and it also reduces the circulation time for oxygen and nutrients to be transmitted and delivered through the system.

The principle of achieving minimum power in cases of optimal vascular junctions is also supported by the fact that in such cases, the cardiac effort and rate of work will be close to minimum as the required power to pump the blood through the vascular

system is reduced. Finally, the principle of minimum drag is considered to be an important mechanical factor which is essential to facilitate the functional mechanisms of the vascular system. This drag factor reflects the shear force acting on the luminal tissue between the blood and the blood vessel wall. When this drag force is rendered to a minimum, the vascular junction is considered in a state of mechanical equilibrium whereby the other optimum principles can be applied on a local and individual basis. [72]

Zamir concluded that it was possible for an arterial junction to be in a state of very high degree of optimality if it fulfilled at least some and possibly all of these optimality principles.

Based on his previous four optimality principles, Zamir had calculated the predicted theoretical values for the total bifurcation angles in a vascular junction. He demonstrated that the total bifurcation angles values should lie within the range 75º to 102º - considering that the area ratio "*ß*" of the bifurcation is optimally equal to 1.26. [72]

It was noted that these principles and values applied in cases of symmetrical bifurcations and non symmetrical bifurcations, and the total bifurcation angle changes very little with changes in the degree of asymmetry. His results were thus keeping with Murray's earlier estimations. [81]

Moreover, certain qualitative features of the vascular network could be derived from the same optimality principles as follows; in the arterial system, when a blood vessel gives rise to a relatively small branch, the angle of that branch will be close to a right angle and the parent vessel will tend to continue almost unchanged in both size and direction. Further calculations predicted that in cases of arterial asymmetrical bifurcations, the larger branch would make a smaller angle with the direction of the parent artery than would the smaller branch. These features were not described for the venous system and whether the vascular venous system abides to the same optimality principles is not yet clear in literature. [72]

2.6 Previous studies on Normal Retinal Vascular Geometry

It is clear from the previous studies that the optimality principles described by Murray, Zamir and others were based solely on theoretical grounds generating optimal values and relationships for angles and diameters which would render a vascular network more efficient physiologically. Further experiments were thus conducted to determine the actual extent and power of these optimality principles in governing different networks within the cardiovascular system. Measurements of different vascular networks were made from normal healthy subjects with different techniques to assess the degree of optimality of its vascular junctions and compare their trends and values to the predicted optimum. [72, 79]

The degree of optimality of a vascular network shouldn't be estimated only as a mere difference between the measured and optimum branching angles and diameters values, but as the actual "cost" of that departure. The cost can be identified as the increase in value of the physiological entity which is minimised when the vascular bifurcations are considered optimum. These four entities as previously discussed are the pumping power required to drive the blood through the vascular junction, total endothelial drag forces, lumen surface, and lumen volume. [82]

Fanucci et al. examined the vascular geometry of different arterial junctions in normal healthy individuals; these included the carotid, aorto-renal, aorto-iliac, and femoral bifurcations. The results showed that for the branching vascular angles subtended by the larger and smaller daughter vessels with the parent vessel (θ_1 and θ_2 respectively), the majority of the measured data were within the optimal range or within only a 2% cost penalty, with an average of 6 – 13 % showing greater deviation. Their results, despite suffering a considerable amount of scatter, supported the theory that the branching vascular angles and diameters follow the theoretical optimality principles. Further work by Zamir et al. investigating human and rat cardiovascular systems, also showed a definite trend that was consistent with the optimum values, although again with some scatter. [82-84]

Interestingly, detailed analysis of both Fanucci's and Zamir's results revealed that the amount of data scatter for branching angles and vascular diameter ratios around

the theoretical curves were noted to be larger and less uniform for larger vascular branches as compared to smaller branches. The physiological peculiarities of the large vessels, as described below, were assumed to be responsible for such distribution. [85] A non-optimum vascular network features could mean that the flow conditions within that network were not ideal; however, it could also reflect that this vascular network had been governed by criteria other than those on which optimality is based. It was noted for example that the aorta and its major branches were under gross anatomical constraints and physiologically they not only had a blood conveying function, but also a storage role as well as a damping effect on the pulse pressure. As a consequence the aortic branching criteria might not be determined entirely by the known physiological optimality criteria, and actually its branching angles and diameters were not thus classified to be optimum. In contrast, the human retinal vascular network had been found to demonstrate a relatively high degree of optimality in terms of its branching characteristics which suggests that retinal vessels are under less physiological or anatomical constraints, thus free to branch optimally. [82] Nevertheless, potential anatomical constraints are considered in the retina, with the major superior and inferior temporal arcades form a semi-elliptical path to enclose the macular area and radiate in the direction of the temples. [86]

In their study, Zamir and his co-workers derived some quantitative information on the branching angles and relative vascular diameters of 59 arterial bifurcations of a healthy human male with normal vision, and compared it to theoretical results. [87] The measurements were taken from handmade drawings of magnified red-free retinal photographs.

They described the arterial bifurcations in terms of:

(1) The vascular diameters of the parent, and the larger and smaller branches as d_0, d_1 and d_2 respectively.

(2) The bifurcating angles which the larger and smaller branches make with the direction of the parent vessel as *"$\theta 1$"* and *"θ_2"* respectively.

(3) They also used the non-dimensional parameters as the area ratio *"β"* and the asymmetry ratio *"α"*.

The theoretical curves as well as the experimental data results were expressed by curves representing the relationships between the branching angles or the vessel diameters ratios and the asymmetry ratio α following the four optimal principles. On each curve, an optimum region was plotted which is bound by several curves, each dictated by one optimality principle. [87]

Zamir's results in general demonstrated a qualitative tendency towards the optimum curves. Quantitatively, for the bifurcating angles θ_1 and θ_2 and the total bifurcating angle "θ" ($\theta = \theta_1 + \theta_2$), an average of 47% of data points fell within the optimum region +/- 10 % deviation from optimum curve. Similarly, for the relationships between the diameters ratios of larger branch or smaller branch to the parent vessel (d_1/d_0) and (d_2/d_0) respectively and the asymmetry ratio, 64% of the actual data fell within the same region range. Zamir's results suffered from the limitation of measuring techniques available at that time, and this was compounded by the image quality with faint and fuzzy images of some vessels. Furthermore, there was uncertainty in vessel diameter' measurements owing to the curved and non uniform vessel walls found in some bifurcation regions, all resulting in reading errors that might have added to the data scatter. One other possible reason for the noted scatter could have been that some arterial bifurcations might not lie perfectly planar within the retinal tissues and hence generating a distorted view of the bifurcation that would consequently affect its measurements. Despite these limitations, their data on the retinal arterial vascular system appeared to support Murray's law and the fact that these bifurcations were governed by the theoretical optimality principles.

Similar supportive data was obtained from a further comparative study of retinal arterial bifurcations in human and rhesus monkey eyes. Measurements were taken from the central area around the optic disc and fovea of red-free retinal photography of the human eye and from fluorescein angiogram of the monkey eye. [83] The results from both the human and the monkey arterial bifurcations gave reasonable support to the theoretical principles governing arterial branching in the cardiovascular system, though the results were still associated with a fair amount of biological scatter. The results still indicated that the governing principles proposed by the theoretical models are the same as those that govern their data.

However, the relatively small sample size used for these studies together with the lack of information about retinal venous vascular bifurcations left this area of research open for further studies and analysis.

Increasing interest in the analysis of retinal vascular networks and possible implications in the pathogenesis of systemic diseases, together with the rapid development of imaging analysis techniques, has lead to further quantitative studies being carried out to assess the optimality of different retinal vascular geometrical features in normal and disease conditions.

Stanton and colleagues reported in their study a mean (+/- SEM) junction exponent of 2.65 (+/- 0.18) and a mean (+/- SEM) bifurcation angle of 84 +/- 3° of arteriolar bifurcations in fluorescein angiograms of 13 normotensive subjects aged 30-80. The measurements were performed by means of operator-directed image analysis software. [88] Geometrical analysis of retinal vasculature from red-free fundus photographs of six normotensives by King et al agreed broadly with Stanton's results reporting a mean total bifurcation angle of 78.4 +/- 4°. [89]

In a later study by Chapman et al., using an operator directed edge detection programme on digital retinal photographs of 6 normotensive subjects aged 26-50, the mean junction exponent and bifurcation angles of the arteriolar junctions were 3.87 and 79.9° respectively. [90] In a further study by the same group comparing the retinal vascular geometrical features in normal subjects and subjects with peripheral vascular disease, their normal data on arterial bifurcations of 8 normotensives had a mean bifurcating angle of 79 +/- 11°. [91]

In an experiment by Martinez-Perez et al. comparing normotensive and hypertensive subjects, a novel semi-automated technique was described to measure the geometrical and topographic features of the arterial retinal vascular network. Their results from normal data presented a median junction exponent and total bifurcating angle of 2.07 and 84.50° respectively. [92]

2.7 Previous studies on alterations in retinal vascular geometry

The studies described in the previous section quantitatively assessed the degree of optimality of the retinal vascular bifurcations in normal subjects using a variety of different measurement techniques available at the time. Other studies have also looked at the influence of different factors such as age or systemic vascular disease on these bifurcations, and are discussed in this section.

2.7.1   Age

In their study, Stanton et al reported a decline in bifurcation angle with age, however, the rate of decline was greater among normotensive as compared to hypertensive subjects, similarly Stanton's results showed significant reduction in the junction exponent value beyond 3 with age progression. [88]

2.7.2   Low birth weight

There had been an increasing interest in early life influences on the pathogenesis of cardiovascular disease, owing to the excess of ischaemic heart disease that has been observed amongst families with increased rates of stillbirth and infant mortality. [93] This has lead to a hypothesis suggesting that a reduced birth weight might be associated with persistent abnormalities in the vasculature, independent of influences related to hypertension, age or other peripheral vascular disease.

In a cohort cross-sectional study, Chapman et al reported significantly narrower bifurcation angles in members of low-birth-weight groups than in higher-birth-weight groups. There was however no significant association between blood pressure and the bifurcation angles. Chapman et al also found no association between junction exponents and either birth weight or blood pressure.

His results speculated that a presumed impairment in the vascular network development might accompany the impairment of foetal growth as manifested in relatively low birth weights. This could result in life-long alteration in the vascular

architecture that might explain the higher than normal cardiovascular risk in adulthood. [94]

2.7.3 Peripheral vascular disease (PVD)

In a study by the Atherosclerosis Risk in Communities (ARIC) group, generalised arteriolar narrowing was reported to be associated with the presence of carotid plaques, while arteriovenous nicking was associated with markers of inflammation and vascular endothelial dysfunction. [95]

Chapman et al investigated whether a relationship existed between symptomatic peripheral vascular disease and the vascular diameters at retinal arterial bifurcations. Their results showed significant deviation of the junction exponent from the optimum values in normotensive subjects with peripheral vascular disease. No difference in bifurcation angles were noted between the age and blood pressure matched groups with and without PVD. It was suggested that the results reflected the presence of abnormal endothelial function of the retinal microvasculature in subjects with PVD, which could be mediated through a variety of metabolic and heamodynamic abnormalities observed in these patients. [91]

This study also supported previous work that was done to assess the importance of endothelial function in the maintenance of optimum geometrical and topographic network features. In his experiment on 6 healthy volunteers, Chapman et al demonstrated a significant alteration in junction exponents associated with the inhibition of endothelial nitric oxide (NO) after injection of N^G mono-methyl-L-arginine (L-NMMA) - a competitive inhibitor of NO synthetase. It was argued that the altered junction exponent might have reflected the adverse consequences of dysfunctional endothelium on circulatory energy costs and shear stress, thus supporting the theoretical model set by Murray as previously discussed. [96]

This interesting relationship between endothelial shear stress and vascular bifurcations was highlighted by Ingebrigtsen et al in a study on cerebral vessels. Using a new technique to analyse vascular geometrical features from three-dimensional reconstructions of rotational digital subtraction angiography images of

cerebral vessels, the geometrical optimality at arterial bifurcations without saccular aneurysms were compared to those with angiographic evidence of aneurysms. The results showed a significant difference with respect to the mean observed arterial bifurcating angles of the middle cerebral artery, distal internal carotid artery and basilar artery; the angles were larger in bifurcations with aneurysms compared to those with no lesions [(70+/-23) versus (52+/-21) for larger branch bifurcating angle θ_1 respectively] and [(96+/-23) versus (79+/-20) for smaller branch bifurcating angle θ_2 respectively]. The mean junction exponents and vessel radii were not significantly different between the groups. In multivariate regression analysis of the data, the measured bifurcating angles acted as independent significant predictors for the presence of an aneurysm. Since saccular aneurysms were known to arise at areas where the vessel wall is exposed to maximum impact of hemodynamic shear stress, the authors concluded that their results could support the hypothesis that only a small increase in shear stress – which could be caused by the unfavourable bifurcation geometry – might be sufficient to initiate aneurysm formation once a disruption of the internal elastic lamina has occurred. [97]

2.7.4 Hypertension

Several studies have investigated the effect of hypertension on the retinal vascular tree. Previous work had focused mainly on qualitative description of target organ damage such as haemorrhages, exudates and arteriolar-venular crossing phenomena. Interest then developed into the quantitative assessment of retinal vascular geometrical features in hypertension to ascertain their diagnostic and prognostic value for disease.

Stanton et al reported in a retrospective observational study that bifurcation angles were more acute in hypertensive age matched group as compared to a normotensive group. (74 +/- 3° as compared to 84 +/- 3° respectively) as measured from fluorescein angiograms. Junction exponents were similar for both groups. The results implied that disadvantageous branching geometry in human retinal vasculature occurred secondary to increased power costs of blood transport and uneven distribution of the shear forces throughout the vascular tree resulting from hypertension. [88]

The results were supported by King et al in a study using red free retinal images of six normotensive and six hypertensive subjects. The bifurcation angles were reported to be narrower amongst the hypertensive group as compared to the normotensive group. (68 +/- 2º versus 78 +/- 4º respectively p= 0.05). [89]

In a later study, Chapman et al, utilising digitalised retinal photographs, demonstrated a slight decrease in the mean junction exponent in age matched hypertensive group as compared to normotensive subjects [3.12(2.77-3.48) as compared to 3.87(3.14-4.59) respectively]. Mean bifurcation angles did not differ significantly between both groups. [75.6º (67.3-83.9º) in hypertensives verses 79.7º (74.9-84.5º) in normotensives]. [90]

Breathing 100% O2 resulted in vasoconstriction of retinal arterioles and narrowing of the bifurcation angles and this appeared to be of greater magnitude in normotensive than in hypertensive subjects. Similarly, breathing 5% CO_2 resulted in vasodilatation in normotensive subjects but not in the hypertensive group. [90] Interestingly, despite the noted changes in vessel diameters in normotensive subjects following breathing of the different gas mixtures, there were no significant changes in junction exponent. The results appeared to support the concept that in the acute response to vasoactive stimuli, the need to maintain constant shear stress in retinal vessels would lead to strict adherence to the optimality principles. This was in contrast to deviations from theoretical optimums noted in junction exponent with advancing age owing to the chronic dysfunctional endothelium. The authors also suggested that the reduced vascular reactivity that was noted in the hypertensive group could reflect structural changes in the retinal microvasculature with high blood pressure or possible impaired endothelial function.

In a pilot study comparing the geometrical and topological properties in red-free fundus images of ten age and gender matched normotensive and hypertensive subjects, Martinez-Perez et al did not find any significant difference in the arterial branching angles between the two groups. [92] The results were therefore not in agreement with the conclusions of the previous studies by Stanton et al, and King et al. [88, 89] This was attributed to the difference in the measurement techniques and sample sizes used, and larger studies were recommended.

2.8 Predictive value of retinal vascular geometry analysis

Several studies have established the predictive value of a variety of retinal microcirculatory abnormalities such as microaneurysms, arteriolar-venular nicking, and focal and generalized arteriolar narrowing for future cardiovascular events. [98-100] In a recent study, Witt et al examined the predictive value of different dimensionless retinal vascular geometrical features in terms of ischaemic heart disease and stroke mortalities using data from the Beaver Dam Eye Study cohort, using a semi-automated method for analysis of digitalised red free retinal images. The examined parameters included the arteriolar and venular length: diameter ratio (LDR), tortuosity, bifurcation optimality ratio, and bifurcation angle. The optimality ratio was calculated as the mean daughter vessels diameter divided by the parent vessel diameter multiplied by a correction factor. For a theoretically optimum bifurcation, the optimality ratio was found to be 0.79, and the optimality deviance is defined as the absolute difference from this value. [101]

The study results revealed that the quantitative retinal microvascular features measured at baseline were associated with incident IHD and stroke; subjects with incident IHD had impaired bifurcation optimality reflected in an increased optimality ratio, whereas the arterial tortuosity was significantly reduced, independent of known cardiovascular risk factors. Stroke subjects had increased arteriolar length-diameter ratio LDR – evidence of increased arteriolar narrowing – although this was dependent on blood pressure. Arteriolar and venular bifurcation angles were not found to be associated with IHD or stroke death in that study. These results suggest and highlight the importance of retinal microvascular evaluation as a useful non-invasive predictor tool for target organ damage and cardiovascular risk; however a perfect correlation of structural microvascular changes in the retina with coronary or cerebral microvascular disease could not be found.

2.9 The relationship between retinal and cerebral vessels

The retinal and cerebral microvasculatures share many morphological and physiological properties. Embryologically, the retina is an extension of the diencephalon, and both organs share a similar pattern of vascularization during development. [102] The inner retinal and cerebral microcirculations share certain anatomical features owing to their similar functions acting as endothelial barriers. The mechanical barrier is attributed mainly to the tight junctional intercellular complexes between the endothelial cells of both the cerebral and the retinal vasculature. These barriers act as dynamic interfaces owing to the presence of a specific carrier-mediated transport protein. [103, 104]

Both the retinal and cerebral circulations have local process of control (autoregulation) in place to maintain a constant blood flow and delivery of nutrients against a broad range of external factors. [105] This is mediated by the vascular smooth muscles of both the retinal and cerebral arterioles.

As the retinal vasculature is devoid of autonomic innervation beyond the lamina cribrosa, the retinal circulation is not under any neurogenic control, however, some neurogenic input is applied to the choroidal circulation and vasoconstriction of the choroidal vessels occurs via sympathetic stimulation. Likewise, no autonomic innervation exists in the cerebral vessels beyond the pial vessels; however, there is evidence of cholinergic pathway to the frontoparietal cortical microvasculature that can induce vasodilatation and results in increase of the cortical blood flow. [106]

2.10 Retinal microvascular signs in cognitive decline and dementia

It has been shown that the assessment of the cerebral vasculature is an important sign in determining an individual's risk of particular cerebrovascular diseases such as vascular dementia. [107] However, the techniques used to detect these changes are often expensive and available only in specialised centers. Retinal digital image analysis may indirectly provide such information owing to the morphological and physiological similarities mentioned above.

Several studies have examined the presence of retinal microvascular changes in patients with cognitive impairment. Kwa et al demonstrated that retinal arteriolar narrowing and the presence of retinal exudates correlated with MRI signs of cerebral white-matter lesions. In addition, the presence of lacunar infarcts highly correlated with retinal exudation.[108] In the Atherosclerosis Risk in Communities Study (ARIC), Wong et al showed that the presence of retinal microaneurysms, haemorrhages and exudates was independently associated with a small decrease in cognitive function. [109]

These results suggest that vascular permeability might play an important role in cerebrovascular damage leading to the cognitive decline, as microanuerysms and haemorrhages were highly and more consistently associated with the cognitive impairment rather than the arteriolar narrowing. [109]

In the recent population-based Cardiovascular health study, Baker et al described the association of retinal microvascular signs with cognitive function and dementia among individuals 65 years of age or older. The retinal signs examined included retinopathy signs (microaneurysms, haemorrhages, cotton wool spots, hard exudates, macular oedema, intraretinal microvascular abnormalities, venous beading, new vessels at disc or elsewhere, and vitreous haemorrhage), arteriovenous nicking, focal arteriolar narrowing, and arteriolar and venular caliber. The results of this cross sectional study demonstrated that individuals with retinopathy signs had impaired cognitive function, and in persons with hypertension, retinopathy signs and focal arteriolar narrowing were associated with dementia. Their results were consistent with the hypothesis that in persons with hypertension, a larger proportion of dementia is related to microvascular disease than in persons without hypertension. [110]

A common deficiency of the studies discussed above is that they used subjective observer-driven techniques to assess retinal microvascular abnormalities.

Using a more objective semi-automated technique Patton et al has studied recently the association of different retinal vascular geometrical parameters with cognitive ability in an elderly population. The measured vascular parameters included the

central retinal artery (CRAE) and vein equivalents (CRVE), and the arteriovenous ratio (AVR) of the six largest arterioles and venules within a circular zone 0.5 and 1 disc diameter from the optic disc edge. The median angle of first five arteriolar bifurcations and the median branching coefficient (BC) were also estimated. The branching coefficient was described as an alternative way of expressing Murray's laws of optimality [70, 71] *[BC = (D_1^2 + D_2^2)/ D_0^2]* where D_0 is the width of the parent vessel, and D_1 and D_2 are the widths of the two branching child vessels. It was shown that the (BC) should approximate 1.26 to achieve minimal work across the retinal vasculature. Their results showed that deviation of the BC from optimality was significantly associated with general cognitive ability and verbal fluency, whereas deviation of arteriolar bifurcations angle from optimality was significantly associated with logical memory. CRAE, CRVE and AVR did not contribute significantly to any cognitive test scores. [111] The (BC) formula was shown to be equivalent – yet slightly superior to the fixed theoretical area ratio β previously described. [112]

2.11 Retinal vascular changes with Diabetes

As described in this chapter, it has become obvious that the rapid advances in digital retinal photography and image analysis have allowed precise definition and characterisation of subtle retinal vascular changes in large populations with different systemic vascular diseases.

Several studies over the years have explored the relationships of these vascular signs with the development and progression of the diabetes together with their predictive and prognostic values.

The vascular changes identified in diabetes as well as pre-diabetes were categorised by Nguyen et al into 3 different categories: Classic retinal vascular changes such as diabetic retinopathy, isolated retinopathy signs (microaneurysms, haemorrhages and cotton wool spots), changes in retinal vascular calibre. [113] These will now be discussed in detail.

1. The incidence and prevalence of diabetic retinopathy with diabetes had been well defined over the past 30 years. The two major risk factors of diabetic retinopathy are hyperglycaemia (as confirmed by two main clinical trials, the DCCT in patients with type I diabetes, and the UKPDS in patients with type II diabetes) [26, 28] and hypertension (as confirmed by the UKPDS) demonstrating that blood pressure lowering agents reduced the risk of retinopathy independent of the glycaemic levels). [10] Hyperlipidemia had been noted recently to be a possible third major risk factor as supported by data evidence from the Fenofibrate Intervention and Event Lowering in Diabetes FIELD study. [114]

2. Isolated retinopathy: Prospective studies data have demonstrated that 10% of individuals 40 years and older without diabetes may develop isolated retinopathy signs (such as microaneurysms, haemorrhages and cotton wool spots) within 5 years. [115, 116] These isolated retinopathy signs could be transient. [117] The pathophysiology of these isolated retinopathy signs in non-diabetics and non hypertensives are not well understood. They have been associated with increasing age [118], elevated blood pressure [119], and glucose intolerance. [120] It has been speculated that these isolated retinopathy signs might represent early microvascular damage from a combination of risk factors reflecting an underlying process leading to clinical diabetes or hypertension. However, data from large population based studies including the ARIC and Beaver Dam studies has suggested that isolated retinopathy signs are not necessarily markers of future diabetes risk, except in certain circumstances; in the Beaver Dam study among persons aged less than 65 years, at baseline isolated retinopathy was associated with an increased 15-year incidence of diabetes. (OR 3.68, 95% CI 1.23-10.96). [121] Similarly, in the ARIC study, among participants with family history of diabetes, isolated retinopathy signs were also associated with increased 3-year risk of diabetes (OR 2.3, 95% CI 1.0-5.3). [122]

3. Changes in retinal vascular calibre: Prospective data from the ARIC and the Beaver Dam population-based cohorts demonstrated an association between smaller retinal arterio-venous ratio AVR and incident diabetes. [123, 124] (In the ARIC, OR 1.71, 95% CI 1.13-2.57 while the Beaver Dam study reported OR 1.53, 95% CI 1.03-2.27). This had been recently explained to be by reflecting wider retinal

venular calibre rather than narrower arteriolar calibre. The retinal venular widening might result from increased blood flow associated with hyperglycaemia and retinal hypoxia thus reflecting the early microvascular changes that occur in the development of diabetes. The venular dilatation could be related to endothelial dysfunction in turn resulting from increased production of nitric oxide secondary to high levels of cytokines reported to be associated with impaired glucose metabolism and diabetes. [125, 126]

Moreover, recent analysis of the prospective data from these cohort studies had suggested that the changes in retinal vascular calibre might predict the development of type 2 diabetes [123, 124] as well as impaired fasting glucose. [127]

2.12 Changes in retinal vascular architecture with Diabetes

The geometrical and architectural patterns of the retinal vascular network in diabetes have not been described in the medical literature; nevertheless the evidence of vascular endothelium dysfunction and altered heamodynamic flow occurring with diabetes is fully established. As previously discussed, architectural changes in retinal microvasculature has been associated with hypertension, such as increase in the retinal arteriolar length-to-diameter ratio [89], increased venular tortuosity [128], and reduced branching angle at the arteriolar bifurcations. [88]

In accordance with the previous described data concerning altered retinal vascular geometrical features associated with vascular endothelial dysfunction, it seems logical to foresee certain changes in the vascular architecture that could be associated with the occurrence and progression of diabetes.

In a retrospective analytical study, Avakian et al investigated the effectiveness of region based fractal analysis as a potential tool for objective quantitative evaluation of vascular changes that might take place with vascular retinal diseases including diabetes. [129]

As discussed earlier in this chapter, fractal analysis is a method for studying the fractal geometry of certain complex spatial patterns of different networks including the retinal vascular network whereby the spatial pattern remains constant despite change of scale or magnification. The fractal dimension (D_f) of the branching vascular tree is a measure of altered pattern or branching density.

In their study, Avakian et al described the space filling density of the superficial retinal arterial and venous trees in the posterior fundus of normal subjects and patients with non-proliferative diabetic retinopathy. Measurements were made from linearized images by means of the fractal dimension (D_f) and confirmed by grid intersection (P_v). Only vessels >/ 50 µm were included. Their analysis revealed that the space-filling density of the superficial retinal vascular tree across the posterior pole was equivalent in the NPDR and normal retina; however regional-based fractal analysis suggested that the mean +/- SD vessel density was significantly reduced in the NPDR macular area relative to the normal macula. (1.41 +/- 0.02 versus 1.46 +/- 0.02 respectively, p= 0.008). In contrast, the differences between vessel density in the normal and NPDR paramacular regions were not strongly significant. (1.37 +/- 0.02 versus 1.40 +/- 0.02 respectively, p = 0.168). The decreased vessel density in the NPDR macula correlated well with previous reported results of decreased perifoveal capillary density in NPDR. [130, 131] The decreased vessel density in the maculae of diabetic patients might have resulted from non-perfusion, drop out and/or narrowing of vessels.

The fact that the fractal analysis results in this study could not differentiate between the normal and diabetic vascular networks across the entire retina whilst the regional based analysis revealed significant differences supported a concept suggested by Masters. [69] In his review, Masters suggested that the global analysis of the retinal circulation could miss early changes in the microvascular system associated with early disease, and recommended that local region-based analysis of the retinal vascular network should be used in future to identify early changes.

2.13 The relationship between retinal vascular geometry and vascular density

A study by Woldenberg and Horsfield in 1986 suggested that arterial branching geometry was influenced by optimality principles as well as the needs of a space filling branching pattern. [132] The bifurcation angle, the junction exponent and the length-diameter relationship appeared to be related to and have an effect on the vessel density. Kiani and Hudetz had demonstrated in a computer simulation experiment that vessel density in a microvascular network consistently decreased as the mean bifurcation angle between the daughters' vessels narrowed. [133] This trend was also noted by Stanton et al in a study of hypertensive subjects, although it failed to reach statistical significance. [88] However, the same study reported a statistically significant relationship between the median bifurcation junction exponent and the arterial microvascular density, the latter being calculated as the total number of perfused arterial blood vessel segments in a retinal fluorescein angiography image per square millimetre.

Stanton explained that such a relationship between the vascular junction exponent and the vessel density could be theoretically explained. A larger junction exponent value reflects a smaller difference in diameter between the parent and daughter arterioles. Thus with greater exponent values, a network would need a greater number of bifurcations between feeding arterioles and capillaries and were therefore likely to be associated with larger numbers of micro-vessel segments. [88] On the other hand, the more acute bifurcations and reduced junction exponent levels found in older and hypertensive vascular networks might reflect an altered space-filling branching pattern and reduced microvascular density.

Another geometrical parameter that could influence vascular spacing and density is the distance between bifurcations – the micro-vessel segment length. King et al compared retinal arteriolar segment lengths (expressed as a dimensionless length: diameter L:D ratio) in red free retinal images of six normotensive and six hypertensive subjects. Their results demonstrated that L:D ratio was more than

double in hypertensive as compared to normotensive subjects. (47.3 +/- 3.4 versus 22.6 +/- 1.4, p = 0.00003). [89]

Further studies confirmed this relationship between L:D ratio and microvascular density. In their study, Martinez-Perez et al reported a larger L:D ratio for hypertensives as compared to normotensive subjects (26.00 versus 14.91 respectively, p <0.001). Their results reflected the vascular network "rarefaction" associated with hypertension. [92]

The results were further supported by the findings of a recent study comparing changes in retinal vascular topology with essential and malignant hypertension utilizing the semi-automated multiscale image analysis programme used by Martinez-Perez, Hughes et al found that the mean arteriolar L:D ratio was significantly increased in essential hypertensive and malignant hypertensive patients as compared to normotensive subjects. (29.6 +/- 8 versus 33.4 +/- 9.9 versus 20.7 +/- 5.1 respectively, p<0.01). [128]

It is clear from this review of published studies that analysis of the geometry of the retinal vasculature could offer non-invasive assessment of early changes in the vasculature which were otherwise not detectable on routine clinical examination. This might allow early detection of retinal ischaemia associated with diabetes or hypertension in the absence of other clinically detectable retinopathic features, or act as an independent marker of advancing stages of retinopathy. It might also help the monitoring of progression of diabetic retinopathy. However, the conclusions of these studies and the described associations of vascular changes are based on large populations' studies. It is still unclear whether these alterations in vascular measurements are sufficiently precise to differentiate between patients or identify risk at an individual person level. [113] Furthermore, despite the present availability of large published data on the associations and risk predictions of retinal vascular changes with different vascular diseases or cerebral changes, there is a lack of age, gender and blood pressure specific normative data of retinal vascular geometry that could be used as a reference for future studies.

Based on this review, the following facts can be summarised;

1. There is evidence of retinal vascular geometry alterations with hypertension and other systemic conditions associated with abnormal vascular development, probably secondary to abnormal vascular endothelium which could be either developmental or acquired. [88, 90]

2. There is evidence for an association between dysfunctional vascular endothelium and abnormal shear stress and abnormal retinal vascular geometry. Moreover, an association between retinal micro-vascular abnormalities in diabetes and dysfunctional vascular endothelium and altered shear stress is also established. [96, 125, 126]

3. There are studies showing that patients with diabetic retinopathy can have abnormal topographic features such as rarefaction reflected by a decrease in retinal vascular density as measured by fractal analysis. [129]

4. There is published data on the association of altered vascular density with changes in other vascular geometrical patterns such as the vascular bifurcation angle, the junction exponent, and the length-diameter ratio. [88, 92, 128]

We thus hypothesize that alterations in retinal vascular geometry measured at retinal vascular bifurcations may occur before or with known features of diabetic retinopathy. These changes could potentially act as a sensitive marker to the development of diabetic retinopathy and retinal ischaemia and predict and mirror progression of diabetic retinopathy before other clinically visible signs.

To evaluate this proposed theory, this thesis includes the following:

1. Development of a robust, repeatable and precise technique for measurement of retinal vascular widths and bifurcation angles.

2. Evaluation of the various sources of measurement variability such as the intra-observer and inter-observer variability, together with assessment of the effect of the inevitable variability in image-capturing techniques on the consistency of the obtained measurements. The stability of the different geometrical measurements within a short period of time on an individual basis would also be estimated, together with the effect of acute changes in blood glucose and systemic blood pressure on the obtained measurements. The performance of the developed technique in estimating different architectural and geometrical parameters would be compared to that of other available techniques.

3. Evaluation of normative retinal vascular geometrical data obtained from normal volunteers as measured with the developed technique.

4. A cross-sectional comparative assessment of retinal vascular bifurcation geometry as collected from age matched diabetic subjects with different grades of diabetic retinopathy.

5. A longitudinal assessment of alterations in retinal vascular geometrical measurements over time associated with or without progression of diabetic retinopathy in subjects followed up over a number of years, to assess the diagnostic and predictive value of geometrical analysis of the retinal vascular network on an individual basis.

Chapter 3: Assessment of Retinal Vascular Geometry: Methods and Materials

3.1 Overview

In this chapter, detailed description of the vascular bifurcations is given as an important geometrical feature. The different parameters that can be extracted and estimated for each bifurcation to assess the state of the vascular network are discussed. The chapter provides a background to the previous techniques used for vessel width measurement and estimation of bifurcating angles. The limitations of these techniques are presented thus stimulating the motivation for developing a new measurement technique that could address these limitations. The development of the custom-designed semi-manual technique used for the thesis will be described in detail. This will be followed by discussing the methods and materials used for the study, and the recruitment process for normal and diabetic subjects for certain experiments within this project. The inclusion and exclusion criteria will be also described together with the different clinical and photographic procedures that were performed for these volunteers, and the clinical data collected for analysis.

3.2 Background

As previously discussed, diabetic retinopathy remains a common complication of diabetes and a leading cause of blindness and visual impairment. Although diabetic retinopathy cannot be cured, the progression of the disease can be slowed or even halted if it is detected early and treatment is given. Diabetic retinopathy thus represents an excellent paradigm for screening.

Current classification and grading protocol systems are largely based on the identification of the results of microvascular malfunction, such as microaneurysms, round or blot haemorrhages, exudates, and disc or retinal new vessels, rather than the changes occurring in the retinal vessels themselves. Furthermore a number of recent studies have shown that alterations in retinal vessel diameter may predict progression of the diabetic retinopathy and that retinal vessel diameter may change after successful photocoagulation treatment for macular oedema or proliferative retinopathy.

However, earlier studies analysing local vascular changes in blood vessels had noted that a narrowed vessel could be the result of a thickened arteriosclerotic wall encroaching upon the lumen, or it could represent a mere constriction ("Spasm"). It was thus difficult to distinguish organic from functional variations in caliber. It seemed that it was impossible to differentiate early stages of "arteriosclerosis" from systemic vascular disease "such as hypertension and diabetes" by evaluating – as a sole parameter – calibre changes of retinal vessels. [134]

This in turn has lead to the development of more scientific interest in studying other geometrical and topographic parameters of the retinal vascular network, such as the bifurcation angles, the relationship between parent and daughter vessel widths, and the branching patterns in relation to vascular diameters in individual angles. Alterations of these geometrical parameters were associated with age, systemic hypertension and peripheral vascular diseases, together with other conditions of vascular stress such as retinopathy of prematurity. The details of these studies were discussed previously. Other studies used fractal characteristics of the retinal vascular

network as a diagnostic scheme to develop quantitative indexes of diabetes as reflected by the vascular density.

Based on the findings and results of these studies, together with the known relationship between vessel density and retinal bifurcation geometry as summarised by bifurcating angles and vessel widths ratios, the theory for this project was established. There was thus a need to develop a reliable, precise and repeatable measurement technique that could allow us to assess and estimate the different retinal geometrical features accurately from the retinal images of normal and diabetic subjects to evaluate our theory.

The goal for the developed technique was to be robust in detecting bifurcation geometry features such as the bifurcating angles and correctly measuring vascular widths allowing the various relationships between the branching angles and the diameter relative ratios at individual bifurcations to be determined. The technique should be able to deal with bifurcations of different configurations, contrast and sizes. It should be able to overcome distractions present in a retinal image such as haemorrhages, exudates and provides consistent and reliable results.

3.3 Objectives

1. To review the previously published manual and semi-manual approaches for vessel width detection and estimation of bifurcating angles as a background to the custom–designed technique developed for this thesis.
2. To describe the computer-assisted semi-manual measurement technique developed for evaluating the different parameters of retinal vascular bifurcation geometry, and the methods for analysis.
3. To describe the inclusion and exclusion criteria for subjects and images included for this project, the photographic techniques and the relevant corresponding clinical data collected.

3.4 What is a vascular bifurcation?

A vascular bifurcation can be defined as a branching site at which a single stream of blood divides into two separate streams. These two branches may vary considerably in size and direction but the site is defined as a bifurcation in all cases. [85] Thus whether the parent vessel divides into two comparable daughter branches (symmetrical branching), or one branch is more larger than the other (asymmetrical branching), or whether the parent vessel appears to continue unchanged after giving off a small side branch, the site is defined to be a bifurcation in all cases.
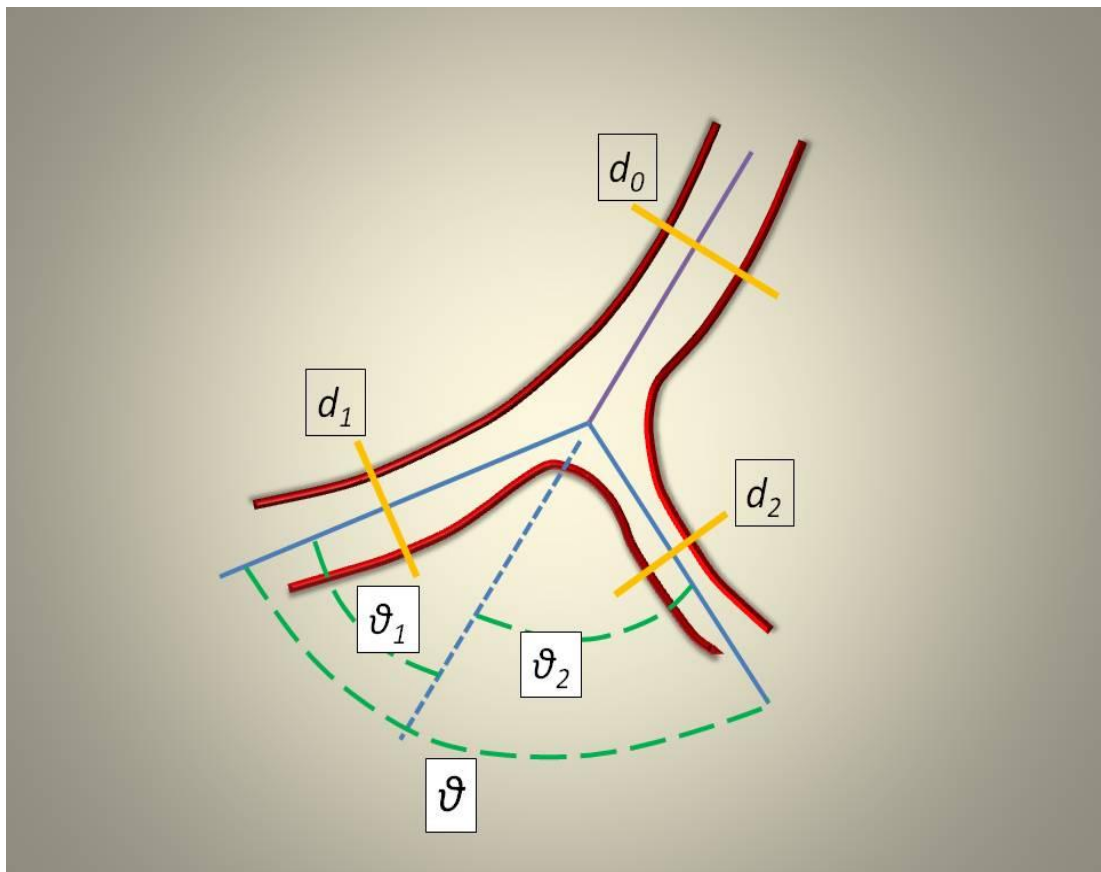
Figure 3.1: Diagram of geometrical features within a normal vascular bifurcation in which (d_0), (d_1) and (d_2) represent the diameters of the parent, first and second daughter vessels respectively. $(\theta 1)$ and $(\theta 2)$ represent the angle subtended by the first and second daughter vessels with the projection of the parent vessel axis respectively. (θ) represents the bifurcating angle between the two daughter vessels where $(\theta 1 + \theta 2 = \theta)$.

3.5 Previous techniques for vessel width detection and bifurcating angle estimation

The definitions and previous methods used for the measurement and estimation of vascular widths and bifurcating angles will be discussed in this section.

3.5.1   Retinal vascular width

The effect of the retinal vessel structure on the apparent and actual vessel width, together with its relation to the true blood column width was evaluated by several studies. This relationship was highlighted in a study by Brinchmann-Hansen and Heier in 1986, in which the effect of density changes in the vessel wall on the apparent size of the blood column was explained. [134]

When the retina is illuminated for imaging or viewing, the light emitted from a fundus camera or ophthalmoscope is reflected back by the pigment epithelium and / or the choriocapillary layer. Blood vessels absorb some of the reflected light. When an image of a blood vessel is viewed from point (C), the apparent width of the vessel is believed to be the width of the streaming column of erythrocytes viewed perpendicular to the flow direction point (P). The surrounding plasma zone and the vessel wall are transparent. Fig 3.2
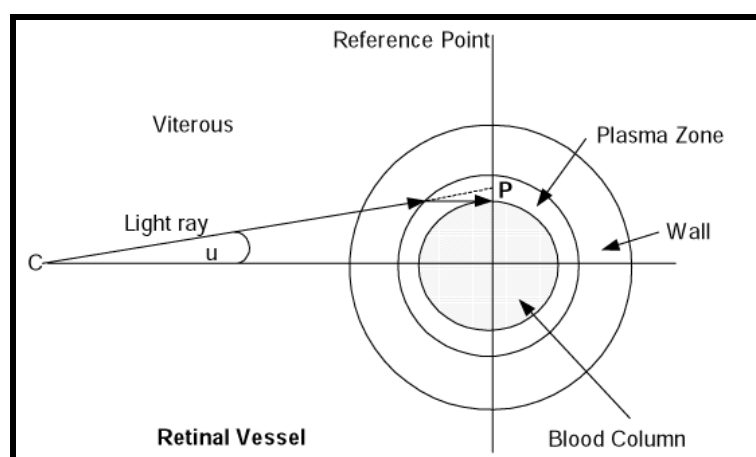
Figure 3.2 The apparent and true vessel width of the blood column *(based on Brinchmann-Hansen O, Heier H. Acta Ophthalmolog Suppl. 1986;179:29-32)*

Variations in the thickness of the vessel wall and the index of refraction have negligible influence on the apparent width of the blood column. However, due to the measured indices of refraction in the plasma and vitreous, it is accepted that within wide physiological limits the apparent width of the blood column is proportional to the true width.

Looking at the retinal blood vessel as a vascular cross-section, the overall transmittance through a vessel including the blood column and wall resembles a Gaussian curve. Finding the point that the blood column meets the wall on that curve is extremely difficult and has inspired many measurement algorithms, which will be discussed further in the next section. Some blood vessels (typically arteries) also include a light streak known as a light reflex that runs down the central length of the blood vessel. The light reflex is understood to run across the surface of the plasma zone and blood column and is believed to be generated mainly from the intravascular column of erythrocytes and the rough reflecting surface generated by various smooth membranes of the vessel wall with different refractive indices. Light reflexes are more common in younger retinas due to their increased reflective surfaces. However, arteriosclerosis can also affect the appearance of the light reflex by changing the reflective index of the vessel wall, thus increasing the observed intensity. [134]

Early attempts for obtaining measurements have been made both directly using ophthalmoscopy and indirectly using fundus photographs. Direct methods that require direct ophthalmoscopic observations suffered obvious major inaccuracies and subjective bias. Non-standardized illumination, low magnification and low resolving power contributed to poor precision.

3.5.1.1 Manual Techniques for vessel width detection

Further developments in retinal imaging and image processing have resulted in better techniques to assess retinal vascular changes. With digital imaging, the green channel (the monochrome image obtained by screening through a green filter) is used to enhance the contrast of the retinal vessels against the retinal pigment epithelium. Images can be then magnified and viewed with high-resolution monitors. Automatic contrast enhancement and sharpening of the images help to identify the vascular

network. Several methods can then be used to measure vessel widths; the observer can determine the vessel edge by locating the points using a mouse driven cursor at the point where the vessel becomes uniformly darker than the adjacent retinal pigment epithelium. The distance between the two identified points can be measured and used to estimate the vessel width. As an alternative method Hubbard and co-workers applied a circle with its center on one edge of the vessel and its circumference touching the opposite edge, thus the radius of the circle representing the perpendicular width. [135]

These methods appear to be relatively accurate with larger vessels near the optic disc with better defined vessel walls but are less consistent for smaller or hazy vessels, as they are still dependent on visual appraisal of determination of vessel widths, thus suffer from the restricted ability of human eye in discriminating different grey intensity levels in photographic films.

3.5.1.2 Semi-manual Techniques for vessel width detection (Intensity profiles methods)

Further research aimed at developing rather more objective measures in which the photographic films were converted into "intensity" profiles. Transverse cross-sectional lines are positioned across segments of interest on retinal vessels, which are then presented in a graphical form and the width and the intensity profiles of both the blood column and the its central light streak can be analysed. [134] The conceptual basis for such modelling is the differential behaviour of light propagation through vessels and the reflectance off the vessel wall compared to its local background of retinal pigment epithelium.
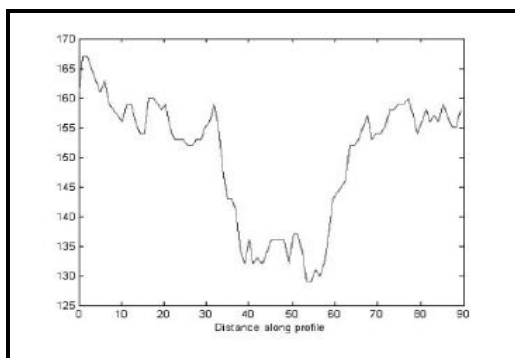
Figure 3.3 Sample vessel profile

Several previous authors had described different semi-automated or semi-manual algorithms for measuring vascular diameters by utilising these graphic cross sectional profiles.

A. Full Width Half Maximum Technique

Brinchmann-Hansen and Engvold have developed their algorithm called "Full Width Half Maximum" (FWHM) to measure vascular width. In their approach, the vessel width is determined by the calibre of the vessel and by the "roughness" of the reflecting surface in question, whereas the intensity is a function of surface reflectivity. The width of the light streak is taken to be the full width at half maximum intensity. [136]

The approach calculates a "half height point" on the left and right sides of the initial estimated mid-point of the profile. On each side, the minimum and maximum intensity levels are calculated and the "half height point" is located where the profile crosses the midpoint in intensity between the minimum and the maximum. The FWHM estimate of the profile width is the distance measured between these half heights points.
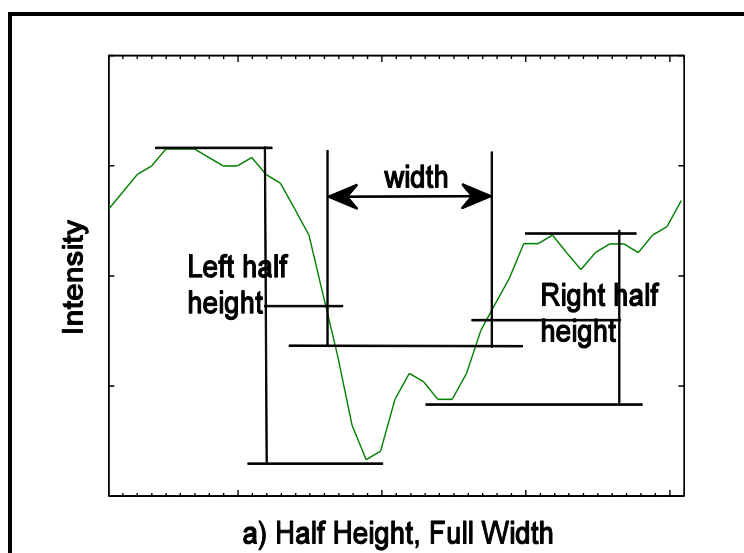
Figure 3.4 Full Width Half Maximum Technique

B. Gregson's Rectangular Technique

In an alternative approach, Gregson et al described their method for estimating vessels width by utilising "a rectangular profile" of a fixed height that is fitted to the profile data. The height is fixed to the difference between the minimum and maximum intensity values in the profile. The width of the rectangular profile is adjusted until the area under the rectangular profile is equal to the area under the profile data. [137]
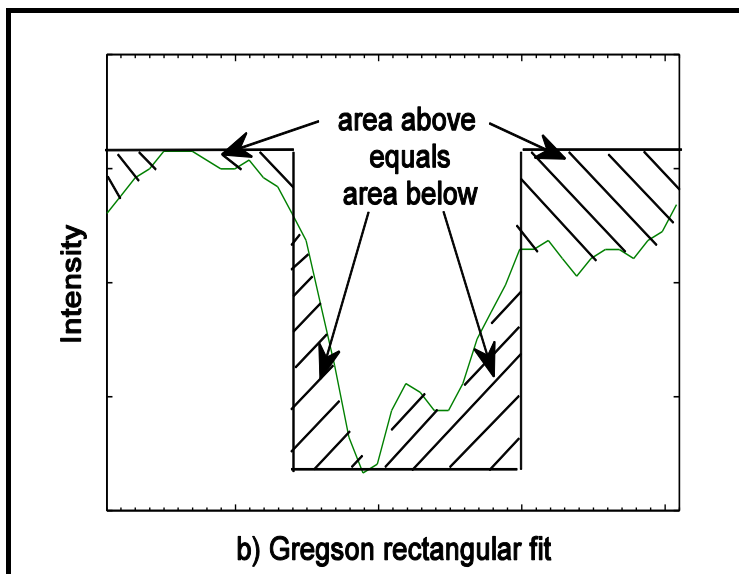
Figure 3.5 Gregson's Rectangle Technique

C. Kick Points Technique

Rassam et al later developed a sophisticated technique to calculate vascular widths based on the "Kick points".

The "Kick points" are defined as two distinct skew points that can be observed on the slopes of the transmittance profiles near the base. Kick points occur where the vessel wall meets the most lateral extent of the blood content; the horizontal distance between the kick points indicates the blood column width. This approach appeared to be more accurate in estimating the vessel width as compared to finding the width at

half height. However the kick points were not easily identified in all cases. To observe the kick points, the photographs must be of high resolution and well focused. The shape of the intensity curves change with focusing which render it difficult to identify the kick points but has no effect on the degree of separation between the points. [138]
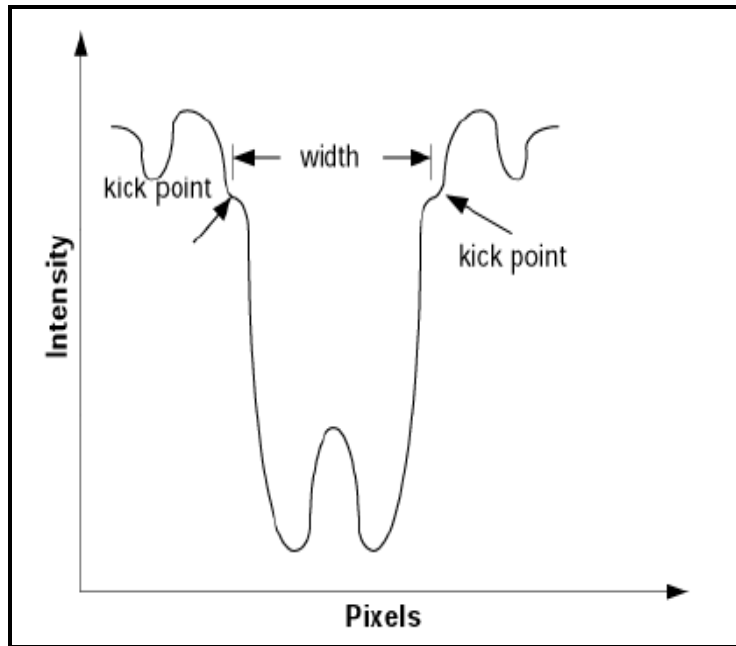
Figure 3.6 Kick points technique

3.5.1.3 Semi-automated methods for vessel width detection

A. Cross-Sectional Techniques using the Gaussian profiles

Other computer algorithms have been described for semi-automated measurement of retinal vessels width.

Some of these methods are based on fitting of "Gaussian models" (a profile of predefined curve) to the intensity cross section of the vessel, to determine a set of parameters characterising the vessel. This includes work done by Zhou et al [139], Gao et al [140], and Chapman et al [141], who developed and adjusted their algorithms to improve the technique performance on vessels with light reflexes. The majority of these approaches use a one cross sectional profile to measure the vascular diameter.
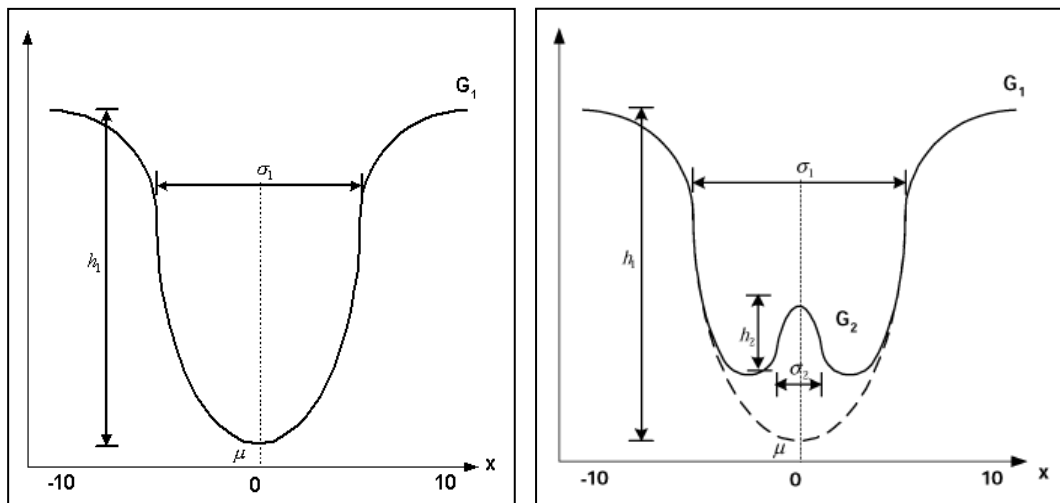
Figure 3.7 Cross sectional profile of a Gaussian model without and with light reflex (G_1) for the Gaussian profile (G_2) for the light reflex Gaussian profile. (h_1 and σ_1 represent height and width of the profile)

B. Two-dimensional techniques using the Gaussian profiles.

In contrast, Gaussian profile "match filters" form a two dimensional profile that can perform better in cases with poorly defined vascular edges but are limited to set sizes. To overcome this problem, Lowell et al introduced a two dimensional model with a Gaussian profile which is optimised to best fit the observed vessel within a rectangular region of interest. This allows the vessel width calculation to the sub-pixel accuracy and the smoothing introduced by the two dimensional nature of the profile improves this accuracy. [142]
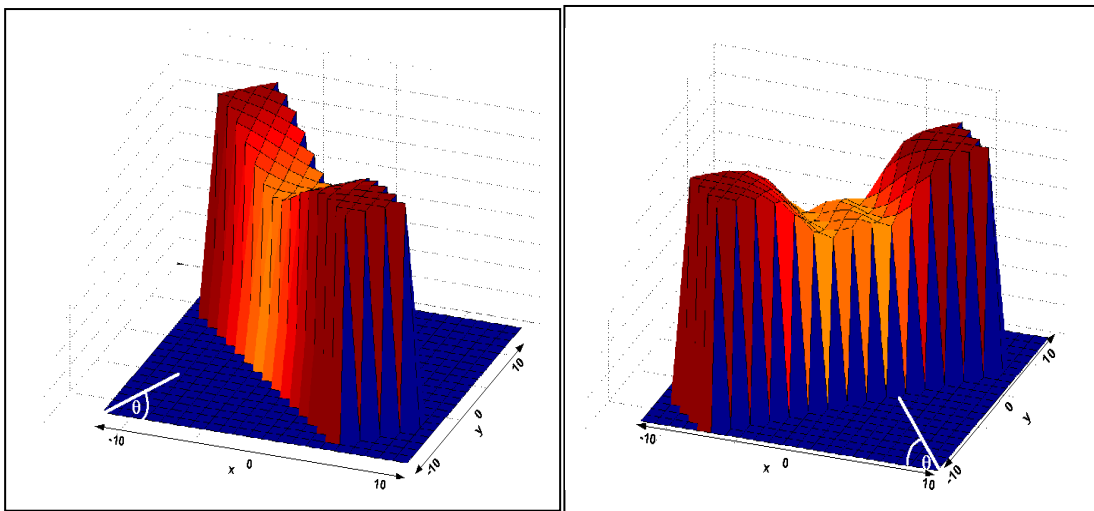
Figure 3.8: Two dimensional representation of a Gaussian profile without and with light reflex.

C. Width detection by sliding window filters

Chapman et al described another algorithm using the Sliding Linear Regression Filter (SLRF) measurements. The identification of the vessel edge positions was made by means of linear regression within a sliding window filter. The method is based upon the fitting of a line by linear regression – relating image intensity gradient against distance along a vessel cross-section – within a window of points. The window is

progressively moved by a single point at a time across the entire cross section of interest. [141]
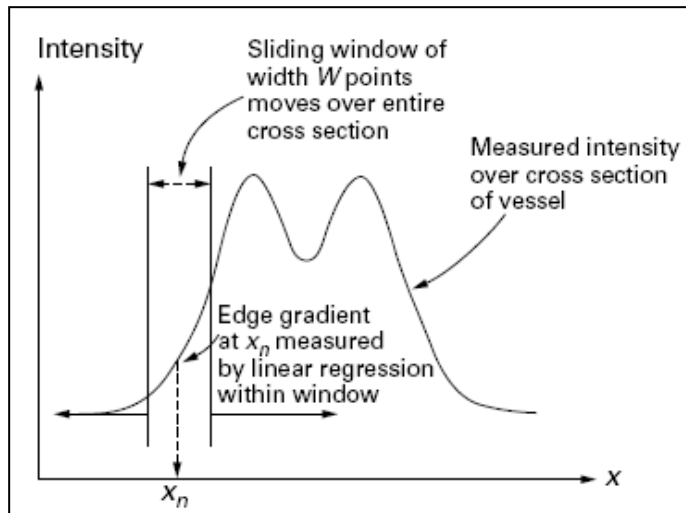
Figure 3.9 Sliding Linear Regression filter Technique

All the previous described techniques – apart from the Gaussian profile match filters and Lowell et al two dimensional Gaussian profile model – are based upon measurement of vessel width along a cross section of the vessel manually selected by the operator to lie normal to the vessel axis. This would lead to a limited amount of information in the intensity cross-section, and therefore would be expected to be susceptible to image intensity noise and imperfections in the image acquisition process such as the effect of pixel density.

At this step, there are two known main sources of uncertainty; firstly the local variations of the width along the retinal arterial and venous vessels, which can potentially alter the estimated width measurement, should different points along the vessel wall be selected by the observer at 2 different occasions. Secondly, the intra-observer repeatability in subjectively defining any given measurement point along the vessel wall.

In addition to above mentioned different manual, semi-manual or semi-automated algorithms for vascular width estimation, there have been many described

approaches in literature for automated vessel segmentation in retinal images in the past – as a prerequisite for development of fully automated methods for vessel width detection. These techniques used different combinations of edge detection or matched filter methods with artificial neural networks and different tracking methods for vessel extraction. The details of these methods are beyond the scope of this work.

None of these models are individually fully adequate for all applications as most of them appear to perform better mainly with higher resolution fundus images, and further refinements and work is needed to be done on handling noisy retinal images and the varied appearance of the vascular network. Overall combinations of these modelling ideas are considered the best approach at this stage for vessel segmentation. Of course the more sophisticated models are associated with higher computational demands and costs. To date, fully automated methods for vessel width detection have not been established, more work in this area is underway to develop and validate such techniques.

3.5.2   Bifurcation angles

An apex of a vascular bifurcation is a very special site from the point of view of local haemodynamics and due to the very large number of arterial bifurcations in the cardiovascular system, the site is also considered an important structural unit from the functional anatomy point of view of the system. [143]

On reviewing literature on previous work done to describe the vascular bifurcation geometrical features, there appear to have two ways of identifying the bifurcation apparent apex and the angles exerted between the two daughter vessels.

1. In the first method, the center-line of each vessel in the vicinity of the junction is constructed. Straight lines are then fitted through these, and these straight lines are then regarded as the longitudinal axes of the vessels. Where the center-line is curved, the tangent line to the curves is traced to represent the vessel. The meeting point for the progression of the three lines describes

the apex. The angles made by the larger and smaller daughters with the apparent continuation of the parent vessel represent θ_1 and θ_2 respectively. The sum $\theta_1 + \theta_2 = \theta$ (Total bifurcation angle) (Figure 3.10 A)

2. In the second method, the centrelines of the three vessels are identified in the same way, and the straight lines are fitted, yet the three lines do not necessarily meet in a single point to create the bifurcation apex. Instead, the daughters' central lines meet the parent centreline at different points and the angles at these points are used to calculate the bifurcation angle in the same way. (Figure 3.10 B)
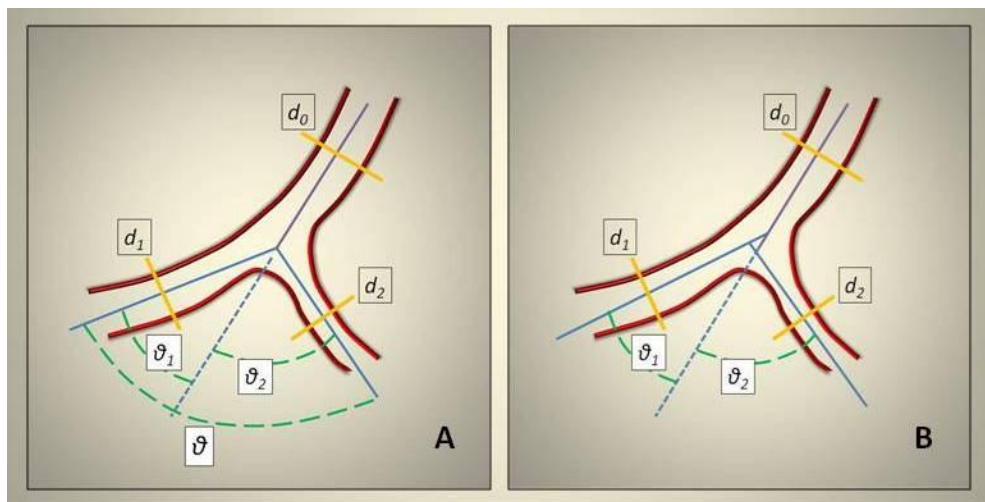
Figure 3.10 Methods for defining the bifurcating angle (A) With or (B) Without a common apex point

Previous studies and theories were based on the first model where
$\theta = \theta_1 + \theta_2$, in which θ is the total bifurcating angle and θ_1 , θ_2 are the angles subtended by the larger and the smaller daughter vessel with the projection of the parent vessel respectively. However in the second model it is obvious that the mathematical equation would not correlate with the geometrical illustration as shown where the bifurcating angle between the two daughters θ would not be equal to $\theta_1 + \theta_2$. This might affect detailed analysis of variable geometrical indices of a vascular tree to describe its geometrical characteristics; we have thus adopted the first model for this project.

Methods adopted for retinal vascular geometrical analysis has not changed greatly over the past decade. Previous attempts using these techniques to quantitatively analyse retinal bifurcations had focused mainly on larger vessels, and evaluate proximal bifurcations where the blood columns are more obvious and the vessel walls are better defined.

Earlier manual measurement techniques of branching angles depended upon drawing the center lines of the vessels near the junction and then using a simple protractor to read the angles between them. [87]

Subsequently, the measurements techniques have been performed mainly semi-manually where the vessel diameters were measured close to the bifurcation and the angles between straight lines fitted by eye, and calculations done by means of commercially available software. [88, 94]

Martinez-Perez et al described a semi-automated method to measure and quantify the geometrical properties of the retinal vascular tree. The algorithm is based on vessel segmentation for detection of the vessel tree and identifying significant points in the vascular tree as bifurcation, crossing points and terminal points. For each identified vascular segment, three different angles were measured: the total angle, the head angle and a tail angle. The total angle of a branch was computed along the total length of the segment line while the head and tail angles were calculated over a distance of five times the radius of a particular bifurcation point *(r)* where *r* is the radius of the maximum circle centered on that point that fits inside the boundary of the bifurcation. [92]
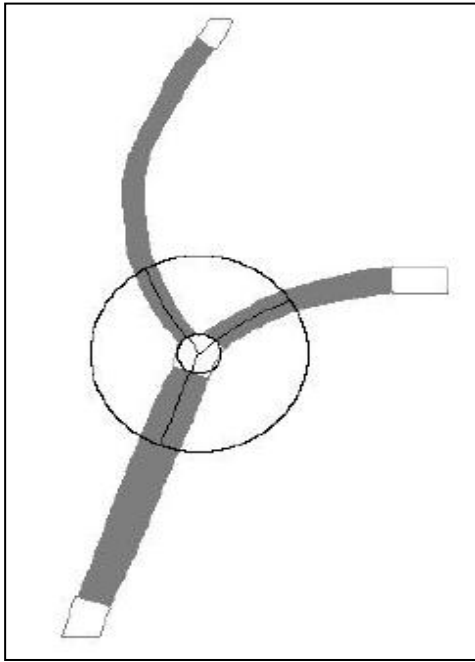
Figure 3.11 The head and tail bifurcating angles are defined and measured within a distance of 5 times the radius defined in the bifurcation point.

The authors reported difference in bifurcation angles values when their algorithm measurements were compared to a manual technique. This was attributed to the obvious variability in measurement techniques, in particular the definition of what represent the actual angle at a bifurcation.

In this thesis, we wanted to ensure that we measure the true bifurcation angle as closely as possible to its apex, mainly to record or estimate the very first deflection of the blood vessels at the bifurcation, rather than a surrogate albeit repeatable measures. Our aim was to design a reliable and accurate operator driven, computer assisted **semi-manual** technique for assessment of retinal vascular bifurcation geometry with topographic location of the bifurcation in relation to the optic disc.

3.6 Development of semi-manual Rectangle mark-up Technique

The image analysis algorithm used was designed using the MATLAB software package (MATLAB version 7. 0.1, MathWorks Inc. Massachusetts, USA). The computerised tool for semi-manual vascular analysis was written and introduced by the Lincoln School of Computer Science, University of Lincoln. UK under supervision of Professor Andrew Hunter.[144] Image analysis took place in two steps; labelling and marking of retinal bifurcations.

3.6.1 Labelling of retinal bifurcations

The analysed retinal images were presented within the MATLAB system. The images could be viewed in either full coloured mode, red free or contrast enhanced mode with the facility to toggle between the three viewing modes. The red free retinal images provided better viewing of the retinal vascular network with enhancement of vessel edge detection, which could be accentuated, further with the contrast enhanced images, by applying a subtraction technique to improve the edge detection.

The operator selected clear and / or relatively evaluable arterial and venous bifurcations in each image, where the vessels at the vicinity of the junction were not grossly masked by any distracters such as dense haemorrhages or exudates plaques. Vascular bifurcations lying in the area within a half-disc diameter from the optic disc margin were excluded, as first order arterioles or venules are considered to be measured some distance away from the disc, where these vessels become unambiguously arteriolar and venular rather than arterial or venous thus all selected bifurcations would respond uniformly to physiological vascular heamodynamic changes that occur with the cardiac cycle. [135] Following selection, the type of bifurcation (arteriolar or venular) was manually identified.

The system displayed a list of the nominated bifurcations; each bifurcation was defined by its vertical and horizontal pixel location. Once the process was completed, the labelled image was saved to be ready for marking in the next step.
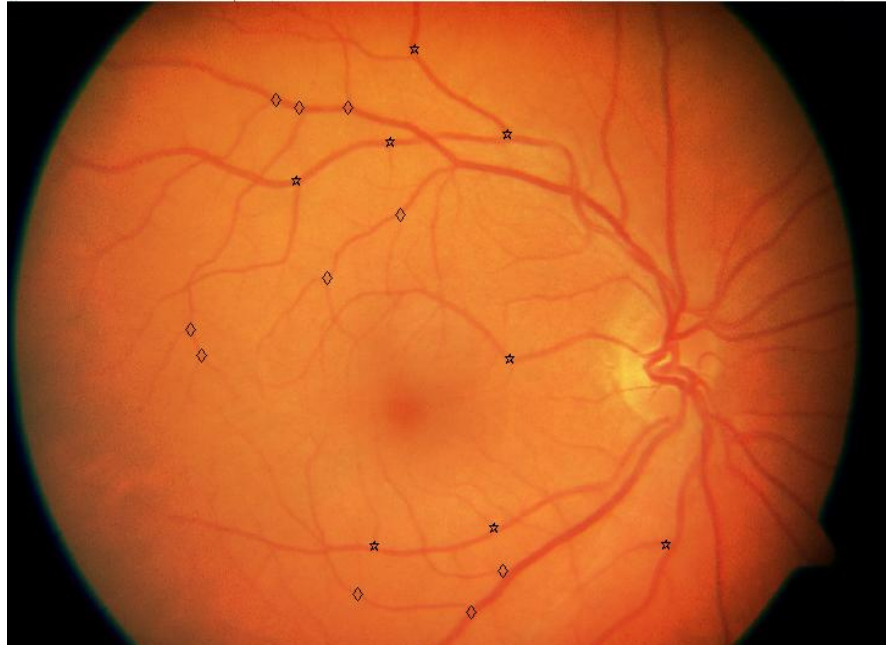
Figure 3.12 Labelled retinal fundus image. * denotes arteriolar bifurcations and ◊ denotes venular bifurcations

3.6.2 Marking labelled retinal bifurcations

The objective of this next step was to measure the bifurcation angle and diameters of the vascular segments around the bifurcation to determine its various geometrical parameters.

The marking technique used to measure these parameters went through a number of changes and modifications until we developed a methodology that was robust enough to measure all bifurcations despite widely varying contrast and size.

The initial marking step was to identify the optic disc location and size. Four points were placed by the operator with a mouse-driven curser at the superior, inferior, nasal, and temporal poles of the optic disc margin. The algorithm connected the 4 points to create an ellipse that would generally fit over the optic disc margin. The mean of the vertical and horizontal ellipse diameters determine the average optic disc diameter in pixels. This information was used later to determine the degree of

eccentricity of the marked bifurcations in terms of their distance from the optic disc center in units of disc diameters.

3.6.2.1 First version of the marking algorithm

In this version, the diameter of the parent vessel was calculated as the linear distance between two opposite points placed by the operator, judged to correspond to opposite edges of the vessel in a plane perpendicular to its axis at the point where the vessel wall appeared parallel.

The apex of the bifurcation was defined as the center of a circle that would maximum-fit inside the boundaries of the bifurcation, the radius of which was provisionally estimated by the predetermined parent vessel diameter. Finer adjustment could be done to change the circle size to best-fit inside the bifurcation vicinity.

Three points were then placed along the circle circumference corresponding to the midpoint of the parent and the daughter vessels – a point where an imaginary longitudinal central line running along the axis of each vessel meets the circle circumference. (Vessels' mid-points)

The system connected the apex with the 3 vessel midpoints. The total bifurcation angle (θ) was measured between the 2 daughter vessels. ($\theta 1$) and ($\theta 2$) representing the angle formed between the extension along the direction of the parent vessel and the largest and smallest vessel respectively.
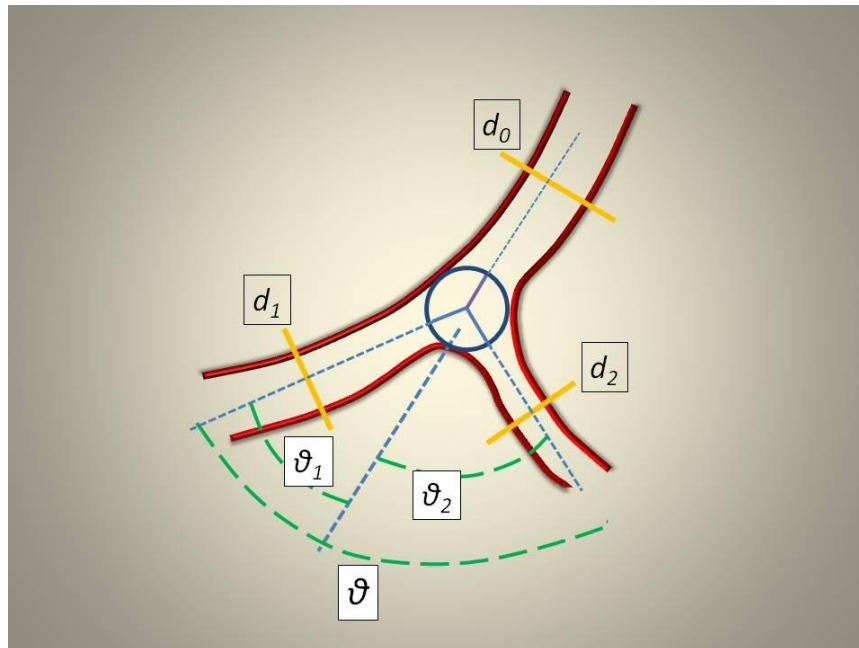
Figure 3.13 First version for identification of bifurcation apex

This marking technique was assessed for a sample of 100 bifurcations. The analysis revealed considerable flaws that affected the accuracy and reliability of our measurements;

1. Although the initial angle measurements acquired with this technique appeared to be accurately representable of the actual visible vascular bifurcating angles, this did not prove to be true in several cases. In a variety of conditions, the actual apex of the bifurcation (the junction point) did not coincide with geometrical apex as defined by the centre of the best fit circle within the boundaries of the bifurcation. This applied to cases as when the parent vessel's ostium (the region where the vessel lumen opens into the junction vicinity) at the junction did not lie perpendicular to the axis of the vessel, thus the junction point appeared to be deviated to one side rather than being in the center of the bifurcation.

In other cases where the bifurcating angle was considerably acute, the junction point tends to recede backwards – towards the parent vessel ostium to produce an angle that corresponds with the apparent vessels axes. In these cases, the angle produced with the junction point at the center of the best-fit

circle appeared noticeably wider and / or altered from the actual bifurcating angle.

Furthermore, in cases of small bifurcations where the best-fit circle is very narrow, it proved to be hard to identify the correct selected location for the vessels' mid-points especially with the zooming and magnification used with this application.

2. As mentioned above, the calculation for the bifurcating angle measured with this technique is based on the straight lines connecting the apex with the 3 vessels' mid-points placed at the circumference of the best-fit circle. The distance between these points is the radius of the best-fit circle which is in turn a factor of the parent vessel diameter.

   Owing to the relative close proximity between the 4 points, inevitable intra-observer and / or inter-observer variation in defining the vessel mid-points were noted. It became obvious that even inadvertent clicking on adjacent pixels along the circumference could result in large drifts in the orientation of the resultant straight lines, and consequently in the estimated angles. This effect could be compounded if this variation in defining the apex and vessel mid-points occurred more than once in the same bifurcation.

3. Furthermore, the described technique did not address the inherent problems in identifying the vessel width diameter through two points corresponding to the opposite vessel edges, especially in vascular segments with non-uniform width, together with the considerable uncertainty of the orientation of these points in relation to the longitudinal axis of the vessel segment.

Based on the above observations and inconsistent results obtained with the existing algorithm, a modified technique was designed that addressed the above-mentioned problems.

The main feature in the modified technique was that it was designed to give more flexibility in defining the junction point of a bifurcation, and to extend the distance between the junction points and the vessels' mid-points in an attempt to reduce the magnified error resulting from the observer variability in defining the vessel mid-points. The modified version overcame also the abovementioned problems with vascular width estimation.

3.6.2.2 Second Version of the Marking algorithm

The pre-labelled images are presented within the MATLAB application as before, with a list of the nominated vascular bifurcations. Bifurcations chosen for marking are viewed in a zoomed up mode (with each image pixel represented as a 16 x 16 square). Thus providing greater granularity available than at the original image resolution which allows the bifurcation to be more precisely defined.

1. Estimation of Bifurcating angle:

1. The diameter of the parent vessel is roughly calculated as the linear distance between two points placed at the vessel' opposite edges, in a plane perpendicular to its axis as before

2. The provisional location of the bifurcation apex point is defined by placing an intersection point by the operator within the vicinity of the bifurcation.

3. The parent and the daughter vessels' mid-points are identified by clicking at a point along an imaginary center line for each vessel running along its longitudinal axis.

4. The intersection point is joined by the system with the three vessel mid-points to form a "Y" shaped model, each of its arms measures three times the predetermined parent vessel diameter.

5. The location of any of the four points can be moved or adjusted at any stage, until the arms of the "Y" figure coincide with the central longitudinal axis of the parent and daughter vessels, and parallel to the vessel wall edges, or the tangent to central line in case of curved vessels. This is irrespective to the position of the junction point in relation to the geographical center within the bifurcation junction. In all conditions, the length of the "Y" model arms is unaltered.

Once the ideal position is achieved, the points' position is saved to the system and used for calculation of the bifurcating angles.

It is worth-mentioning that the parent vessel diameter roughly estimated at this stage is utilised only for determining the arms' length of the "Y" model.
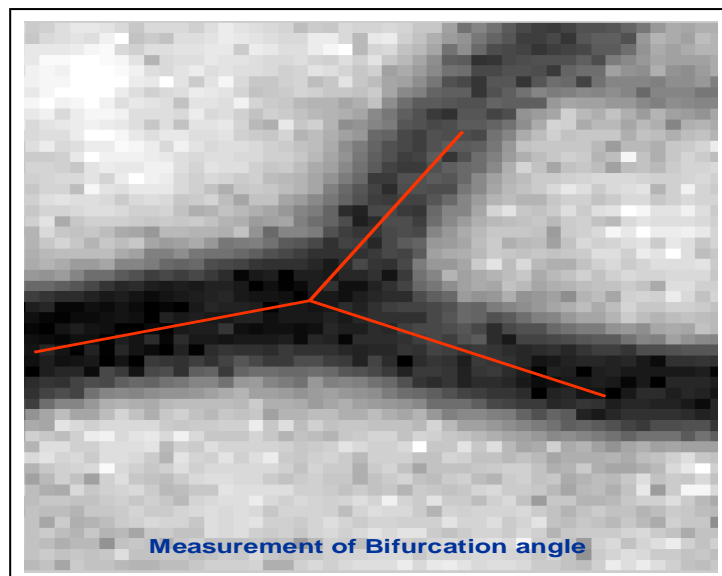
Figure 3.14 Second version for identification of bifurcation apex

2. Determination of blood vessel diameters

Unlike the previously mentioned manual and semi-manual techniques for vessel width determination which relied on the positioning of only two points along the opposite vessel edges on a line normal to the axis of the vessel, the developed new technique involved the observer aligning a rectangle over each vascular segment. The rectangle width determines the diameter of the vessel.

1. For each of the parent and two daughter vessels, a segment which appears fairly uniform in thickness is selected where the vessel course runs relatively straight. The vessel segments are selected at approximately uniform distance - equivalent to the provisional predetermined parent vessel diameter in the previous step - from the bifurcation point for each individual vascular bifurcation wherever possible. Segments had to be chosen distal to and excluding its ostium region as it approaches the bifurcation where the vessel walls tend to flare as it enters the vicinity of the junction.

2. Two points are placed by the operator along the axis of the center-line of the selected segment to determine the orientation of the rectangle's longitudinal axis. A third point is placed at one of the vessel segment lateral boundaries to define its edge where the pixels appear uniformly darker than its immediate surroundings.

3. The algorithm uses the information regarding the three points' locations to construct an aligned rectangle; the width of which is calculated in pixels as double the distance between the lateral boundary point and the central-line predetermined by the two midpoints. The rectangle's length is oriented along the axis of the two center points and calculated as twice the estimated width.

4. The observer may then click to either side of the rectangle to adapt its width and can click around its corners to adjust its direction. This process of adjusting the rectangle parameters can be repeated until the observer is satisfied with the rectangle alignment and width overlying the selected segment. The rectangle would always maintain the length: width ratio at all times.
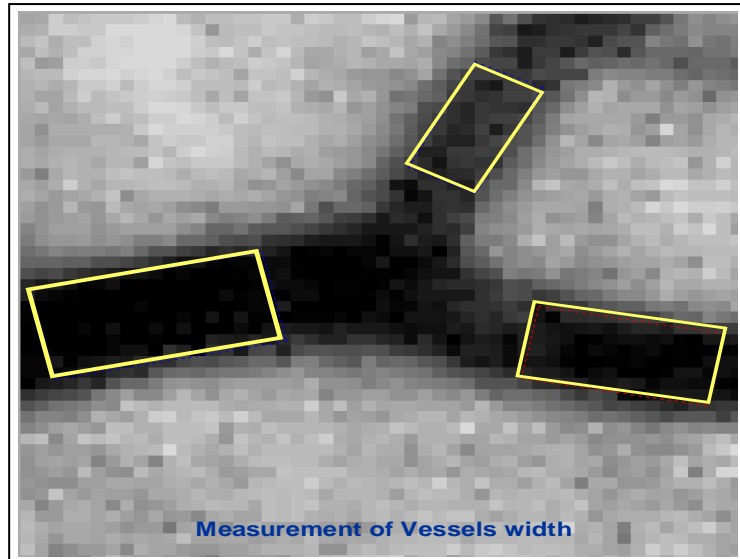
Figure 3.15 Second version for identification of vessel width

This novel operator-directed image analysis for vessel width detection utilises a computer assisted semi-manual technique that still relies on subjective visual appraisal of where the widths were to be taken by selecting pixels of different grey intensity levels from its surrounding RPE background. The advantage of using a fitted rectangle for width detection is to average out and "smooth" the estimated vessel width across a "region" of the selected vessel rather than at a single point. This in turn helps to reduce the errors resulting from locating individual pixels only at opposite vessel edges as described with other previous techniques. Accurate orientation of the rectangle' longitudinal axis also ensures that the estimated vessel width is obtained at a precise perpendicular to the vessel axis at this region. Other semi-manual or semi-automated previously described methods that suffered from problems with plane orientation of the cross sectional profiles can be used by taking advantage of the rectangle orientation.
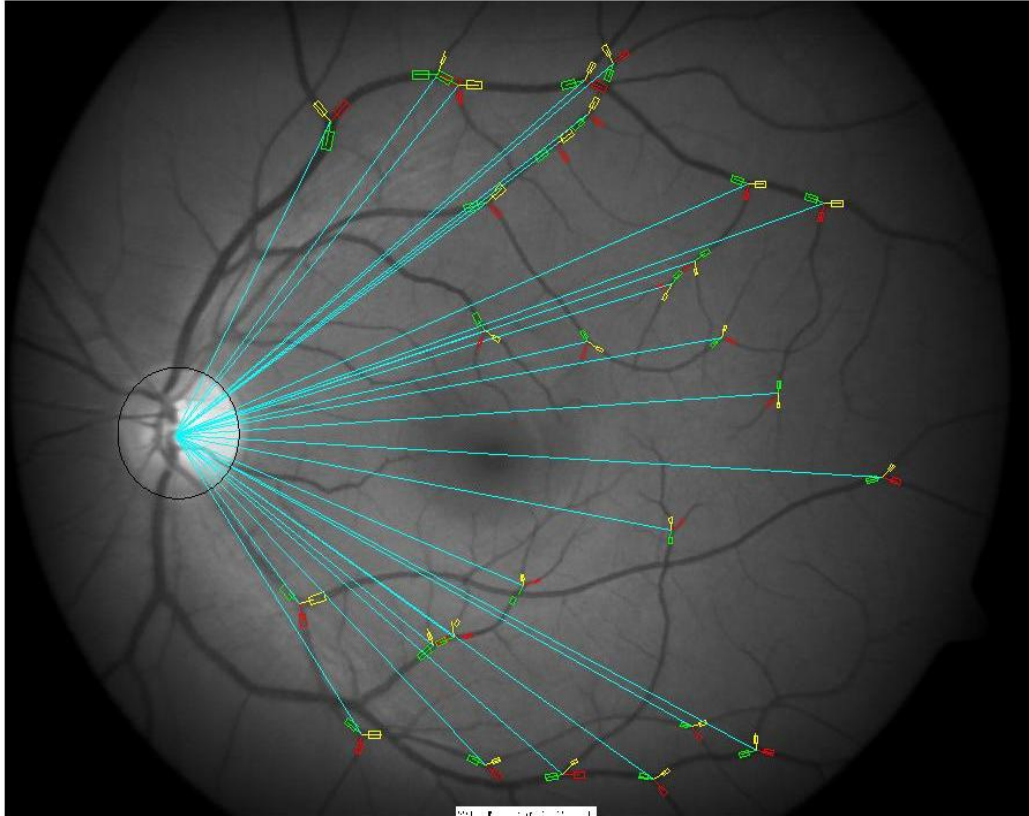
Figure 3.16 An example of a marked image with labelled and marked selected bifurcations, vascular segments are colour coded for each bifurcation, and distance from optic disc center is measured.

3.6.3 Geometrical Indices

For each analysed bifurcation, the following architectural and geometrical parameters were extracted and estimated.

1. Absolute width measurements for the parent vessel segment, the larger branch and the smaller branch vessel segments as denoted by d_0, d_1 and d_2 respectively.

2. Relative diameter ratios: λ_1 and λ_2 are the diameter of the larger and smaller vessel segment respectively divided by the diameter of the parent segment at a bifurcation. [145]

3. The bifurcation index (λ): it is also called the degree of asymmetry. The value of λ is determined by dividing the diameter of the smaller child d_2, by the

diameter of the larger child d_1, so the value of λ is greater than 0 and less or equal 1.0 [81] ($\lambda = d_2 / d_1$)

4. Asymmetry Ratio (α): The cross sectional area of the minor daughter divided by that of the major. $\alpha = d_2{}^2 / d_1{}^2$. The bifurcation index λ and the asymmetry ratio α are measurements of the degree of bifurcation asymmetry. The bifurcation is set to be symmetrical if its λ or α equal unity, which means that the radii of the branch segments are equivalent. If these factors are less than unity, then the bifurcation is asymmetric, severe asymmetry holds when these factors approach a zero value. Thus ($0 < \alpha$ or $\lambda < 1$)

5. Area Ratio (β): The sum of cross sectional areas of the two daughter branches divided by that of the parent vessel. [81] $\beta = d_1{}^2 + d_2{}^2 / d_0{}^2$

6. Junction Exponent (χ): The exponent χ relating the parent and daughter vessel diameters. [70, 71] ($d_1{}^x + d_2{}^x = d_0{}^x$)

7. Bifurcating angles θ_1, θ_2 are the angles subtended by the larger and smaller vessel segments respectively with the direction of the parent vessel. The total bifurcating θ is the angle between the two child vessel segments. ($\theta = \theta_1 + \theta_2$)

8. The optimality parameter (ρ): this parameter was developed by Chapman et al in an attempt to overcome the sensitivity and inaccuracies associated with calculating the junction exponent. This parameter intends to get a measure of how much the pattern of vessel widths at any junction deviate from the optimum junctional exponent of 3. $\rho = [\, d_0{}^3 - (d_1{}^3 + d_2{}^3) \,]^{1/3} / d_0$ [91] this new calculation was reported to be less prone to small errors in vessel measurement than the junction exponent. It could also be calculated for circumstances where d_2 or $d_1 > d_0$ [146]

As presented above, for the purpose of this study, we have analysed a variety of architectural and geometrical parameters to describe the retinal vascular network. These parameters were measured in either absolute values such as pixels and degrees, or relative (non-dimensional) features as well as ratio estimates. The absolute vessel width measurements were thus influenced by the size and resolution of the images utilised for the study, and thus absolute width results in this study could only be applicable to fundus images with comparable properties and resolution. Such limitation could – to a lesser extent – be considered for the angular measurements. Conversely, relative diameter ratios and area ratios' results are not affected by image resolution.

Other architectural features such as vessel tortuosity and length / diameter ratio were not analysed for the study due to the limitation of the designed semi-manual algorithm. Optimality deviance, as previously described by Witt et al [101] was not calculated for this thesis. Optimality deviance was estimated as a measure of the extent of deviation of measured optimality ratio (derived from the β area ratio) from the theoretically predicted optimum value of 0.79 (calculated as 1/1.26 theoretical optimal β area value). Optimality deviance was defined as the absolute difference from this value. However, in his previous work, Zamir demonstrated that actually the theoretical value of β area ratio ranges from 1 in the case of highly non-symmetrical bifurcations to 1.26 in the case of symmetrical bifurcations. [81] It was thus considered inapplicable to use the optimal deviance parameter - with its current definition as a difference from a fixed value of 0.79 - in our study as we included a wide variety of symmetrical and asymmetrical bifurcations in our analysis.

3.7 Subjects recruitment and clinical procedures

The thesis was carried out in accordance with the Declaration of Helsinki (1989) of the World Medical Association. The protocols were approved by local Sunderland Research Committee (Reference Number: SLREC 1129) and all recruited subjects gave written informed consent.

The retinal fundus images utilised for geometrical analysis for the different experiments within this thesis were collated from two main sources:

1. The retinal images database of diabetic subjects from the Sunderland Eye Infirmary, and the screening retinal images database from the South of the Tyne and Wear (SOTW) diabetic retinopathy screening service.

2. The retinal images of recruited normal and diabetic subjects who participated in the normality and repeatability studies for this thesis.

3.7.1 Retinal images of diabetic subjects

Retinal images of diabetic subjects were utilised for the diabetic cross-sectional and prospective longitudinal studies. Images of diabetic subjects with different grades of diabetic retinopathy were randomly selected from the image database at the Sunderland eye infirmary and from the screening images database at the South of the Tyne and Wear diabetic retinopathy screening service. Retinal images of diabetic subjects with no clinically detectable diabetic retinopathy, minimal non proliferative, severe non proliferative and proliferative diabetic retinopathy were considered for inclusion for the study. Random sampling within each group occurred through generating a sequence of random digits utilising a net-based research randomiser programme. The retinal images collected from both the hospital and the screening service database were captured using similar camera systems and followed the same photographic technique described below. Retinal images with any evidence of concurrent vascular disease such as retinal arterial or venous occlusion, previous pan retinal laser treatment, or optic nerve disease including glaucomatous cupping were

then excluded. All images included for the study were made anonymous and then coded following a designed coding system which was established and secured by the study group. The images were saved in a password protected hospital computer system with restricted access to the study team only.

3.7.2 Study Subjects

The recruited subjects were male and female normal and diabetic volunteers aged 25 – 65 years. The diabetic patients were attending the diabetic retinopathy clinic at Sunderland Eye Infirmary as part of their clinical care, while the normal subjects were either patient's relatives who showed interest in taking part in the study or members of the staff at the Sunderland Eye Infirmary.

Recruitment of the study subjects occurred through wall mounted posters displayed in out-patient clinics, reception and patient's waiting areas at Sunderland Eye Infirmary. The posters described the main aim for the study and invited volunteers for participation; this was approved by the local Sunderland Research and Development department. Interested subjects were then given a patients' information leaflet that detailed the aims and objectives of the study, together with description of the imaging procedures and clinical checks needed. The subject's rights for choosing to participate or not, and the confirmation of anonymous status of the included retinal images were also stated. (See appendix) A contact telephone number of the principle investigator was provided for further enquiries. Subjects who read the information leaflet and agreed to take part in the study gave a formal written consent.

3.7.2.1 Recruited Diabetic Subjects

Type I or II diabetic patients with different grades of diabetic retinopathy with no previous pan retinal laser photocoagulation treatment were recruited.

The exclusion criteria were:

1. Previous pan retinal photocoagulation or extensive focal laser treatment. This was decided to rule out any possible confounding factor for laser treatment on

the retinal ischaemic state and thus any potential effect on the local geometrical features of the vascular network.

2. Refractive error beyond sphere equivalent of + / - 3 in either eye. Previous studies reported reduction in the central retinal artery blood flow in myopic eyes, and retinal blood flow had been found to be inversely proportional to axial length in a glaucomatous population.[147] Such change in blood flow could in part influence the retinal vascular geometry. Furthermore, Patton et al demonstrated that increased ocular axial length was associated with narrowing of the arteriolar and venular diameters; however such association was not noted for junction exponent estimates or bifurcating angles measurements. [148] However, it is worth noting that in this study, central arteriolar bifurcations around the optic disc were utilised for analysis following Hubbard's technique [135] yet it is still not clear whether the effect of increased axial length or myopia could be exaggerated for relatively peripheral bifurcations near the edge of the 50° retinal fundus image. For this reason, we opted to include retinal images for subjects with low to moderate myopia and hypermetropia only in an attempt to reduce the potential effects of this confounding factor on the geometrical analysis. [149] We acknowledge that the subject's refraction could be also influenced by corneal factors, and could thus be less accurate than axial length measurements to define myopia, [148] however this was chosen owing to the limited resources available for this study and the more likely availability of information on refractive measurements in the clinical notes for the thesis experiment sections where retrospective collection of clinical data were performed.

3. Concurrent ocular pathology – including cataract, glaucoma, corneal opacities, small pupil or any other retinal and optic nerve head pathology. This was important to ensure that any confounding factors that could potentially degrade the image quality were excluded. In addition, subjects with evidence of ocular hypertension or glaucomatous damage were excluded to rule out the effect of increased intraocular pressure on the retinal vessels as suggested in recent reports. [150, 151]

4. Associated uncontrolled systemic hypertension with documented blood pressure measures of more than 140 / 90 repeatedly recorded within the previous 12 months.

3.7.2.2 Recruited Normal subjects

The group consisted of an equivalent number of age matched non-diabetic volunteers with no prior history of hypertension from among the patients' relatives and staff at the Sunderland Eye Infirmary. These subjects completed a self-assessed health questionnaire. History of smoking was also documented. The subjects in this group formed the control group for subsequent diabetic studies. Geometrical data from the retinal image analysis of these subjects constituted the normative data which was used for benchmarking further results of the diabetic studies.

3.7.3 Clinical Procedures

The diabetic subjects and healthy normal controls who participated in the repeatability study were invited for two visits, two to three weeks apart.
During each visit, the blood pressure and heart rate were recorded for all volunteers together with random blood sugar levels for the diabetic subjects. The body mass index BMI was also recorded for the normal healthy volunteers who were recruited for the normality study.

3.7.3.1 Blood pressure measurement:

Systolic and diastolic blood pressure and heart rate were measured for all the normal and diabetic subjects in the right arm with the subject seated using an automated Blood pressure monitor Ormon 711 Automatic IS (Tokyo, Japan) The average of three consecutive measurements were taken after 15 minutes rest with at least 1-minute interval between the readings before installation of dilating drops.

3.7.3.2 Random blood sugar level measurement

The diabetic patients' random blood sugar levels were checked using Accu – Chek advantage (Mannheim, Germany) machine during each visit. The results were saved in an entry sheet for future analysis.

3.7.3.3 Body mass index (BMI) calculation

Normal healthy volunteers had their body mass index calculated after checking their weight in kilograms and height in metres. This was performed to assess the effect of BMI on the distribution of the normative data. The BMI was defined as the individual's body weight divided by the square of their height. It was then categorised into three groups; underweight for BMI < 18.5, normal weight for BMI 18.5 – 24.9, overweight for BMI 25 – 29.9, and obese for BMI > 30.

3.7.4 Photographic methods

Mydriatic retinal photography was performed for all recruited subjects following a standardised protocol for the study. Mydriasis was induced using Tropicamide 1% and Phenylepherine 2.5% eye drops.

Fifty degrees nasal and temporal retinal images were captured for each eye by an experienced ophthalmic medical photographer using a Zeiss FF 450 Plus fundus camera fitted with a JVC KY-F70B 3CCD digital camera with a resolution of 1360 X 1024 pixels.

The temporal retinal images were positioned such that the fovea was at the center of the image and the optic disc lay at the nasal end of the horizontal meridian of the field of view. Nasal retinal images were positioned such that the optic disc was positioned one to two disc diameters in from the temporal edge of the field, on the horizontal meridian. (Figure 3.17)
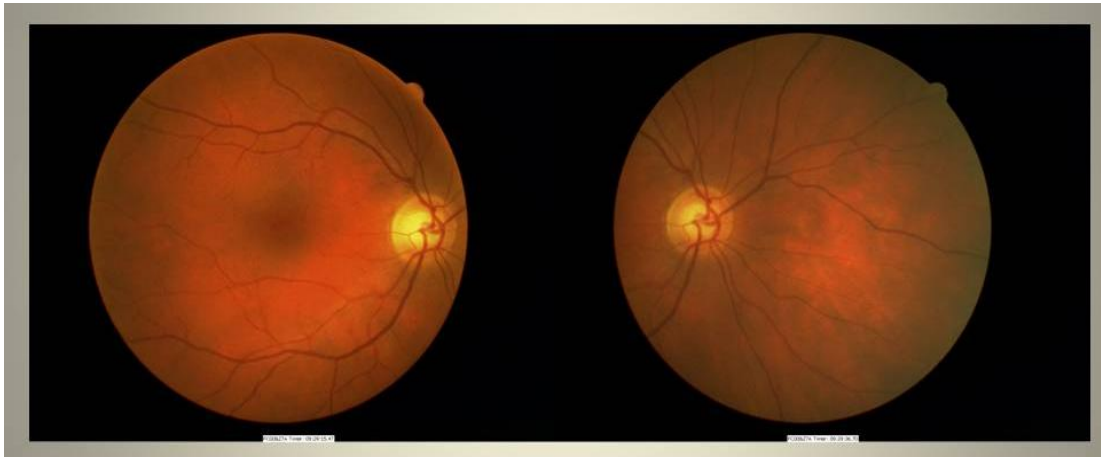
Figure 3.17: An example of temporal and nasal retinal images as set by the study photographic protocol.

During the first visit, the invited subjects were initially seated in a dimly lit room for 15 minutes, after which the clinical tests were performed and then the mydriatic drops were installed. The subjects waited for further 15 minutes to achieve maximum papillary dilatation. Three sets of retinal images were then captured for each subject ten minutes apart. Each set of retinal images consisted of nasal and temporal field images for each eye. In some cases, more than one attempt was needed to capture a clear fundus image with good contrast and field centralisation. Caution was taken to avoid excessive repeated attempts of flash photography for each set to avoid blanching of the retinal pigment epithelial cells and reduce any potential effect of the bright camera light on the retinal vascular diameters. The subjects were seated in the dimly lit room during the 10-minute intervals. They were then invited to return back in two to three weeks time for one further set of retinal images following the same protocol.

During the second visit, mydriatic drops were installed and subjects were seated for 15-minutes before capturing the set of retinal images. One set of temporal and nasal retinal images was captured for each eye.

All saved retinal images were made anonymous and coded following the study's coding system. The code allowed to link retinal images of different sets for the same patient, and thus to be grouped together for data analysis, such facility was pivotal

for the repeatability studies. The images were stored in a password-protected computer with restricted access.

3.7.5 Image quality assessment

All retinal images considered for inclusion for this thesis studies were assessed for combined field position and image quality according to a modified system derived from the definition of acceptable image quality guidelines set by the National Screening grading and quality assurance subcommittee for diabetic retinopathy. Retinal images were considered of good quality when the centre of fovea is less than 1 disc diameter from the center of the image in a temporal retinal image, or the optic disc at 1 to 2 disc diameters from the edge of the image in a nasal retinal image, with retinal vessels clearly visible across > 90% of the image in both cases. Only images with an overall "good" quality scores were included for the study. [152]

3.7.6 Diabetic Retinopathy grading

All fundus images were graded for diabetic retinopathy using the developed system of 45° field grading standards for the assessment of diabetic retinopathy for the EURODIAB IDDM complications study based on the principles of the Modified Airline House classification scheme as described by Aldington and his co-workers [55] in which different diabetic lesions were assessed against one or more standard photographs for the lesion. Subsequently, detailed grading for each lesion type was used to calculate an overall retinopathy level for each retinal image. A combinatorial overall severity level for each eye was produced after assessing the nasal and temporal field images' severity levels. The eye was assigned to the higher severity level. [55]

All retinal images used for this thesis were graded by an experienced diabetic retinopathy secondary grader, who had no access to any demographic or clinical data regarding the patient. All retinopathy grading were tabulated and saved for future analysis.

3.7.7 Data Collection

The demographic and clinical data of all selected subjects and images were retrieved from the clinical hospital notes. After linking this data with the relevant fundus image, no identifiable data was kept to ensure patient anonymity

Collected data included age, sex, type and duration of diabetes and methods of treatment, history of systemic hypertension and / or hypercholesterolemia. The history of associated vascular diseases was also recorded, this included history of ischaemic heart disease, cerebral vascular diseases (transient ischaemic attacks and vascular strokes), peripheral vascular disease including history of claudication, peripheral neuropathy, nephropathy and proteinuria, and history of foot ulcers. History of current or previous smoking was also checked, and classified into: never smoker, current smoker, and ex-smoker which was defined as smoking more than one or more cigarettes per day for one year or more.

3.8 Conclusion

This chapter presented a background of the previously described manual and semi-manual techniques used for retinal vascular analysis. The process of development of our custom built technique was demonstrated, the aim of this technique is to overcome the defects and shortcomings of the other techniques, and to achieve a comparable level of reliability and precision. The recruitment procedure and included subjects were also described. In the next chapter, the performance of the developed technique is evaluated with regards to its precision, and the repeatability of the geometrical measurements utilising this technique is assessed.

Chapter 4: Assessment of Reliability of Retinal Vascular Geometrical Measurements and Technique Performance

4.1 Overview

In the previous chapter, we described the development process of a custom-designed semi-manual measurement technique for retinal image vascular analysis. The next important step was to assess the variability of measurements obtained by this developed technique and to evaluate its performance against the other established semi-manual measurement techniques. In this chapter, we describe the identified potential sources of variability in determining the vascular measurements, related to either the observer or the photographic technique or to variations in the individual retinal vascular parameters over a short period of time. In the various chapter sections, we examine each source of variability and analyse its results. The performance of the developed technique is also compared to that of the other semi-manual techniques to determine the effect of the adopted modifications in the measurement technique as previously described on the precision of the acquired measurements. The outcome of this study establishes the range of variability in our technique's measurements, and consequently determines the minimum detectable differences between different cohorts of analysed images that can be detected and that can possibly differentiate normal from pathological retinal vascular networks.

4.2 Introduction

Digital imaging technology, image processing and computer algorithms for analysis of the retinal vascular network are rapidly evolving. The development of these systems offers an important diagnostic tool that could be used in large-scale screening programmes.

As discussed in chapter 2, changes in the retinal vascular diameters have been found to be associated with ageing, and with various systemic vascular conditions such as hypertension and atherosclerosis. [88, 91] In addition quantitative measurements of retinal vascular topography have been used recently to understand the relationship between the retinal microvasculature and other cerebral and systemic vascular diseases. [101, 153] However changes in blood vessel diameters were found to be very small, thus accurate and reproducible objective methods of measurements are vital if meaningful data are to be collected.

Several previous studies have thus been conducted to identify the sources of variability and the levels of accuracy of the available techniques for vascular measurements used in these studies. Similarly, this study was set to identify and evaluate the impact of different sources of variability that could potentially have an effect on the reliability and accuracy of the different structural and geometrical measurements and estimates obtained with the developed semi-manual technique utilised for this thesis. These variations could be related to the observer's performance with the measurement technique or related to inevitable variations in the photographic procedure, or it could be related to actual variations in the individual's retinal vascular geometrical features over short period of time.

Furthermore, it was important to compare the performance of the developed technique against the other established manual and semi-manual vascular measurement techniques to assess whether the adopted changes in vascular width estimation in our technique - as previously described – has led to more precise vascular measurements. The outcome of this study would determine the range of our measurement error and variability, and thus consequently would set to identify the

minimum differences that could be appreciated between normal and pathological retinal vascular networks when analysed with the developed technique.

4.3 Objectives

The objectives of this study were:

1. To evaluate the potential aspects of variability and repeatability that could affect the retinal geometrical measurements obtained with the custom-designed computer-assisted semi-manual rectangle-method technique used in this study.

2. To assess the performance of the used semi-manual rectangle method technique in comparison to the other available techniques.

1). Variability and Repeatability of measurements.

We investigated two potential determinants of variability:

A) **Observer variability**: This study was designed to evaluate variations in measurements between different analyses of the same retinal photograph.

    I-   **Intra-observer variability**: To assess the variability of measurements of repeated analyses by the same observer

    II-   **Inter-observer variability**: To assess the variability of measurements in between different observers.

B) **Individual variability**: This study was designed to estimate the variability of measurements between analyses of repeated retinal photographs for an individual.

    I-   **Intra-visit study**: To assess the variability of measurements obtained from three retinal photographs taken for the same individual ten minutes apart in a single visit. Any detected

variability could reflect inevitable variability of the photography process that can have an impact on the retinal vascular measurements.

II-   **Inter-visit study**: To evaluate the variations in the retinal geometrical measurements between retinal photographs of the same patient captured two to three weeks apart, to assess the impact of short-term changes in blood pressure, or blood glucose level over this period on the stability of these measurements.

2). Assessment of the semi-manual rectangle-method Technique performance

The precision of the performance of the custom-designed semi-manual technique used in this thesis was measured in relation to other semi-manual techniques for vessel width detection used in other studies, namely the "Kick points" technique, "Full width Half Maximum algorithm", "Gregson's" technique, "Single Gaussian algorithm" and the "Two Dimensional Gaussian model" techniques. This was designed to compare our developed technique, which depends on subjective assessment of the vascular width along a short distance of the vessel segment, relying on discriminating between different grades of the grey intensity across the vessel edges in the retinal images, to the other techniques that rely on the computer-generated intensity profiles, which represent the grey-level profile across the vessel diameter compared to its local background at a particular point.

4.4 Subjects and methods

Data analysed for this study was obtained from retinal photographs of the recruited age-matched normal and diabetic volunteers who participated in the repeatability study. The normal subjects were self-assessed healthy individuals while the diabetic subjects - with different stages of diabetic retinopathy - were recruited from the diabetic clinic at Sunderland Eye Infirmary. Details of inclusion and exclusion criteria together with the recruitment procedure are described chapter 3.

The 50 degrees mydriatic nasal and temporal retinal photographs used for this part of the project were captured according to the protocol set for the study by an

experienced ophthalmic medical photographer as previously described in detail in section 3.7.4.

4.4.1 The Observer Variability Study

Nasal and temporal retinal image sets of 4 eyes of 4 different participants (2 normal and 2 diabetic subjects) (one eye per participant) were randomly selected for this study, a total of 8 images. The first observer labelled the images, in which 10-20 clearly identifiable arteriolar and venular bifurcations were selected across the whole image, excluding the vascular bifurcations lying within half-disc diameter of the optic disc margin. Extra care was taken to ensure that the nominated bifurcations are evenly spread across the retinal image, peripheral versus proximal and superior versus inferior in relation to the image horizontal raphé, thus bifurcations of different sizes and with a wide range of contrast are included for analysis. Bifurcations that were masked by crossing over vessels, haemorrhages and / or large exudates were excluded, especially if the edges of one of the vessels at the vicinity of the bifurcation could not be identified.

The first observer marked the nominated bifurcations in the labelled images three times over a period of two months. Details of the marking procedure are described in section 3.2.2. The labelled images were not marked in any particular order and the observer was masked of his own previous results. In a separate setting, a second observer then marked the same selected bifurcations in the labelled retinal images once. Both observers were masked of each other's results. The resultant architectural and geometrical measurements and estimates as calculated by the computer system were tabulated, in which the corresponding results of the three assessments by the first observer and that of the second observer for each particular bifurcation were linked together to facilitate comparative analysis at group as well as bifurcation level.

4.4.2 The Individual Variability Study

For this section, we selected 8 eyes of 8 subjects from our recruited volunteers' data set. (Two normal and 6 diabetic participants, with different grades of diabetic retinopathy). (One eye per participant) The 4 sets of nasal and temporal retinal images captured for each eye over the 2 study visits (three in the first visit and one in the second visit) were included, thus a total of 64 images were analysed. The images were labelled as previously described, to nominate 10 - 20 arteriolar and venular bifurcations in each image. Care was taken to include a wide range of vascular bifurcations of different calibres, evenly spread across the image and with different levels of contrast.

For each set of nasal or temporal images of each eye, the same bifurcations were selected across the 4 images (A, B, and C in first visit and D in second visit), a custom-designed computer tool was written that helped the observer links the corresponding bifurcations over the 4 images, and thus the marking results for each bifurcation were displayed together to facilitate further analysis of variation within and between visits. This step was crucial at that stage to make sure that "like for like" comparisons were made.

All the labelled images were marked once by a single observer. The images were presented to the observer in a random order, to lessen any bias that can occur whilst marking influenced by previous experience of marking corresponding bifurcations within the same set of retinal images. The observer was masked of any relevant subject's clinical data or the formal diabetic retinopathy staging.

The systemic blood pressure of all subjects and the blood glucose levels recorded for the included diabetic subjects at the two visits were tabulated. The difference in mean blood pressure and the difference in the recorded random blood glucose levels between the two visits were calculated for further sub-analysis of the results.

4.4.3 The Technique Comparison Study

For this experiment, we selected 5 temporal fundus images, one image representing each of the different populations groups that are subsequently studied in this thesis, namely: Normal subjects, Diabetic subjects with no retinopathy, subjects with mild Non-proliferative diabetic retinopathy, subjects with severe non-proliferative diabetic retinopathy, and subjects with proliferative diabetic retinopathy.

In each image, ten to twenty identifiable vascular bifurcations were labelled. These nominated bifurcations were then marked by the semi-manual rectangle tool designed for this study by a single observer - who undertook the image analysis and vascular marking for the rest of the thesis. Furthermore, the observer then placed 2 points, one on each side of the vessel edge - in the same vicinity where the rectangle was previously drawn - drawing a line that traverses the vessel axis. The orientation of this line can be altered and adapted by changing the position of one of the points, till the line appeared to be perpendicular to the vessel longitudinal axis at that point. Care was taken to place the 2 points further away from the vessel edge thus creating a line significantly wider than the predicted vessel diameter, thus a distance of at least half of the vessel diameter on either side of the vessel edge was included. This resulted in easier visualisation and appreciation of the line orientation in the vicinity of the vessel in question, and allowed fine adjustments of the line orientation by subtle alterations of the points' position. The cross-sectional line was then converted and presented graphically as an intensity profile of the blood column width. The intensity profile was then used to estimate the vascular segment width by utilising the different previously described semi-manual techniques. (Figure 4.1) All vascular measurements and markings were performed by the same observer while the data were extracted and analysed by the same computer group.
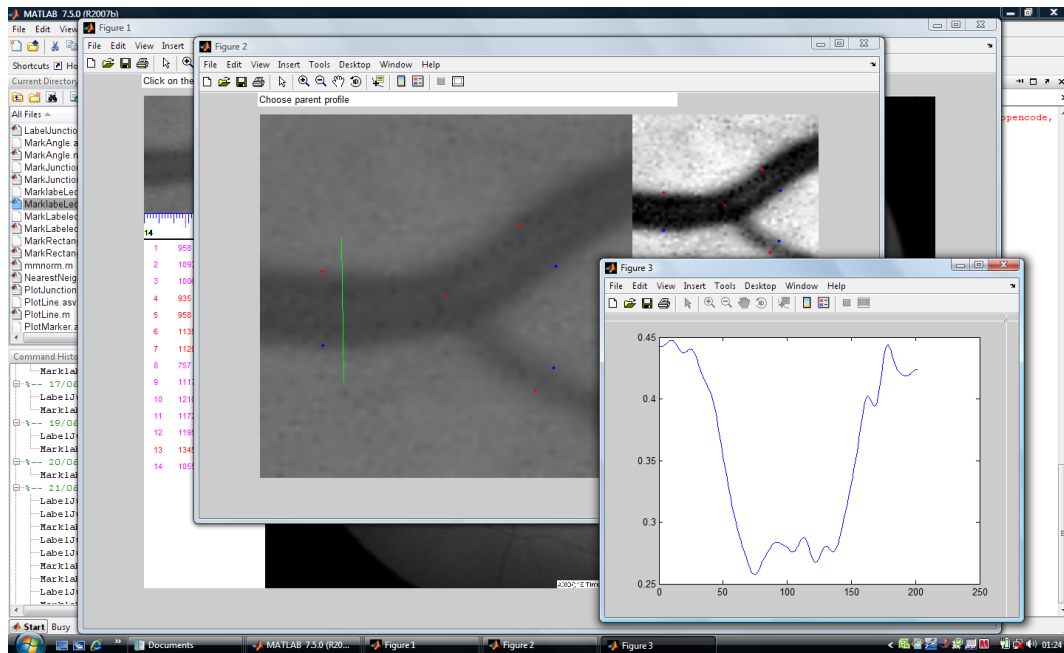
Figure 4.1 Creation of the intensity profile for determination of vascular width using semi-manual measurement techniques.

Initially, the position of the kick points on the intensity profile was determined by the same observer to define the vessel width using these points. (See Figure 3.6) The kick points were defined as the slant points at the vessel profile, marking the edge of the blood column. Similarly, the vessel width was then estimated as the distance between the mid-points at the half height of intensity around the center of the profile using the Full Width Half Maximum technique FWHM (see Figure 3.4), or as the width of a rectangle fitted inside the profile using Gregson's rectangle technique (See Figure 3.5). The vessel width was also estimated from the intensity profile by utilising a designed computer tool – developed by the collaborative computer department at Lincoln University - which would fit a single Gaussian filter (See Figure 3.7), and then applying a two-dimensional Gaussian model, both to determine the vessel diameter (See Figure 3.8). The details of these techniques were described in Chapter 3. All the results of vascular measurements for the different techniques were extracted by the computer team at a later stage, thus avoiding any potential bias by the observer that could have occurred at the marking phase.

The measurements derived from the different techniques for each vessel width were then tabulated and the different ratios and parameters were calculated accordingly for each technique for further comparison.

4.5 Statistical analysis

Simple descriptive analysis of the overall data was presented in the form of box plots and summary tables including the following values (Minimum, maximum, median, 1st Quartile, 3rd Quartile, and means).

4.5.1 Observer variability study

1. Intra-observer study

For the intra-observer study, we used the one way analysis of variance to assess the intra-observer repeatability. This was expressed as the estimation of the "within-subject standard deviation" (SW). The difference between the subject's measurements and the true value would be expected to be less than 1.96 SW for 95% of observations as per Bland and Altman. [154] The variability of the measurements obtained by the same observer was also expressed as the "Coefficient of Variation", defined as the ratio between the standard deviation and the mean values.

As for using the "within-subject standard deviation" as an index of measuring the repeatability error, we had to ensure that the subject standard deviation was independent of the subject mean. We tested this relationship by using the Kendall Tau coefficient. Under the circumstances where a relationship was found (defined as having a p value <0.05), logarithmic transformation of the data was plotted to remove the association. In most cases, this was successful in resolving any association, and thus both variables were rendered independent. Standard deviation of the logarithmic scale was then calculated. The resultant standard deviation was then ant-logged to produce a dimensionless ratio (Geometric standard deviation). The repeatability measure is then expressed as the estimated "Coefficient of variation". [155]

Further sub-analysis of each parameter by characteristics (Normal versus Diabetics), (Arteries versus Veins), (position in relation to the image horizontal raphe), (large versus small bifurcations) was done by comparing scatter plots of the standard

deviation against the mean. If any obvious difference between the plots was noted, further analysis was done.

2. Inter-observer study

For the Inter-observer variability, a Bland-Altman assessment was used to assess the level of agreement between the two observers utilising the Medcalc statistical software version 12.2.1.0. The assessments were made between the first measurements performed by Observer 1 and those performed by Observer 2.

Bland-Altman graphs were plotted, the arithmetic mean, standard deviation and the 95% upper and lower limits of agreement were determined. Data was presented for the arteriolar and venular bifurcations.

4.5.2 Individual Variability study

1. Intra-visit study

The variability of measurements obtained from images captured 10 minutes apart in the same visit was evaluated using the one way analysis of variance. This was expressed as the values of the "within-subject standard deviation SW" as described previously together with the coefficient of variation. For logarithmic transformed data, the geometrical standard deviation was calculated and the estimated Coefficient of variation ratio was presented. [154, 155]

The association between standard deviation and subject mean was assessed using the Kendal tau coefficient. The clinical and statistical cut off point for transformation was set for a K tau value > 0.2 and p value < 0.05

Further sub-analysis of each parameter by characteristic was done by comparing the scatter plots of standard deviations versus subject means, in relation to size, type, and position of the bifurcation and comparisons between normal and diabetic subjects, if

any obvious difference is noted, then the within subject standard deviation was calculated to compare the subgroups of data.

2. Inter-visit study

The agreement of measurements between the first image captured in the first visit and the image captured in the second visit 2 weeks later was evaluated using the Bland-Altman assessment method. The arithmetic mean, standard deviation and 95% upper and lower limits of agreement were shown. Data were plotted for the normal and diabetic subjects.

Sub-analysis of the results was done to evaluate the effect of short term changes in systemic blood pressure between the visits on the variability of measurements, and the effect of change in blood glucose levels in diabetics. The data was subdivided into high versus low blood pressure changes, as well as into high versus low blood glucose changes. The one sample T test was performed to assess the differences between the two visits for each subcategory and the mean difference values, standard deviation, 95% confidence interval were calculated.

4.5.3 Technique comparison experiment

On evaluating technique performance, we wished to assess the accuracy and precision of the techniques. Accuracy is defined as a measurement of the agreement between the estimates of a value and the "true" value. Precision defines the strength of agreement between replicate measurements. It described how close multiple values are to each other.

In the absence of the ground truth for the actual vessel width for bench-marking, it was not possible to evaluate the "accuracy" of the compared techniques; we thus opted to rather assess the "precision" of the compared techniques as a measure of performance.

Precision is usually described in terms of standard deviation and percentage coefficient of variation. However to provide further assessment on the precision of performance, we selected the different vascular ratios and parameters with known or predicted theoretical values and ranges. The degree of precision of the different techniques was then evaluated as the range and extent of departure of the estimated calculations from these predicted theoretical values, together with the standard deviation and coefficient of variation. The selected parameters were; β ratio (predicted value = 1.26), Junction exponent χ (predicted value = 3), optimality parameter ρ (predicted value = -0.01 +/- 0.54). [91]

Another indication of the precision of the technique performance was to estimate the number (and percentages) of "failures" - events encountered by each technique in measuring the vessel width and calculating the different ratios and parameters. Such "failures" could happen for different reasons such as pathology, central light reflex, blurred vessel edges or corrupted edges, where the vessel diameter wasn't identifiable.

4.6 Results

4.6.1 Observer variability study

Eight images were analysed for this study. Nasal and temporal sets of four eyes of four different subjects. Two left and two right eyes. Two subjects were diabetics and two were normal. A total of 117 bifurcations were nominated and analysed. (41 arteriolar bifurcations and 76 venular bifurcations). 67 bifurcations were situated above the image horizontal raphe while 50 bifurcations were below.

The range of values obtained for each parameter in the 3 measurements by the first observer compared to the measurements of the second observer are summarised in Table 4.1. The parameters were divided to

a. Absolute width measurements of the parent, larger and smaller branch vessel segments in pixels. (d_0, d_1 and d_2 respectively)

b. The total bifurcating angle, together with the branching angles of the larger and the smaller vessel segments in degrees (θ, θ_1 and θ_2 respectively)

c. Architectural and geometrical ratios (α, β, λ, λ_1, λ_2, χ, and ρ)

For each parameter, the minimum, maximum, median, 1st quartile, 3rd quartile, and the mean were calculated as in Table 4.1

	Observer 1			observer 2
	1st measure	2nd measure	3rd measure	
Parent vessel d$_0$				
Min	3.42	3.58	3.54	3.41
Max	15.87	15.75	15.69	17.02
Median	7.04	7.27	7.02	8.17
1st quartile	5.74	5.76	5.64	6.96
3rd quartile	9.16	9.39	9.16	10.15
Mean	7.65	7.72	7.61	8.74
Child 1 vessel d$_1$				
Min	3.09	3.09	2.77	3.15
Max	12.56	13.18	12.95	15.08
Median	6.56	6.47	6.37	7.56
1st quartile	4.85	4.82	4.88	5.78
3rd quartile	8.42	8.41	8.26	9.08
Mean	6.81	6.93	6.78	7.83
Child 2 vessel d$_2$				
Min	2.16	2.26	2.39	2.83
Max	10.41	10.10	10.32	11.90
Median	4.52	4.76	4.63	5.85
1st quartile	3.86	3.90	3.77	4.74
3rd quartile	5.95	6.12	6.12	7.25
Mean	5.00	5.17	5.04	6.14
Theta angle θ				
Min	42.01	44.13	42.31	47.40
Max	125.85	122.47	128.70	117.68
Median	80.73	81.06	81.20	83.02
1st quartile	69.58	69.58	70.26	74.99
3rd quartile	90.46	90.85	90.89	90.58
Mean	80.55	80.43	80.85	82.07

Theta 1 angle θ_1				
Min	2.98	0.81	1.48	1.45
Max	83.72	79.25	86.18	83.39
Median	24.11	23.48	24.12	23.55
1st quartile	15.29	15.20	15.93	16.29
3rd quartile	34.44	34.32	33.78	31.31
Mean	26.45	26.26	26.65	25.80
Theta 2 angle θ_2				
Min	6.40	7.15	5.17	4.31
Max	95.17	102.22	110.61	112.91
Median	52.04	52.17	52.46	57.56
1st quartile	41.23	39.36	39.74	42.62
3rd quartile	69.20	68.41	68.07	67.35
Mean	54.11	54.17	54.20	56.27
Lambda λ				
Min	0.38	0.35	0.33	0.40
Max	0.99	1.29	1.33	1.19
Median	0.78	0.79	0.78	0.81
1st quartile	0.67	0.68	0.67	0.70
3rd quartile	0.88	0.89	0.88	0.92
Mean	0.76	0.78	0.77	0.81
Lambda 1 λ_1				
Min	0.64	0.54	0.59	0.68
Max	1.13	1.11	1.11	1.17
Median	0.90	0.92	0.88	0.89
1st quartile	0.81	0.82	0.82	0.84
3rd quartile	0.95	0.97	0.95	0.95
Mean	0.89	0.90	0.89	0.89
Lambda 2 λ_2				
Min	0.33	0.34	0.29	0.34
Max	0.90	1.03	1.01	0.97
Median	0.68	0.70	0.68	0.72
1st quartile	0.59	0.62	0.60	0.64
3rd quartile	0.74	0.76	0.75	0.81
Mean	0.67	0.69	0.68	0.72

Alpha α				
Min	0.14	0.12	0.11	0.16
Max	0.98	1.66	1.76	1.42
Median	0.61	0.62	0.61	0.66
1st quartile	0.45	0.46	0.45	0.49
3rd quartile	0.78	0.80	0.77	0.85
Mean	0.60	0.64	0.63	0.68
Beta β				
Min	0.70	0.62	0.67	0.85
Max	1.82	1.98	1.99	2.08
Median	1.26	1.28	1.27	1.32
1st quartile	1.08	1.14	1.10	1.19
3rd quartile	1.42	1.47	1.41	1.45
Mean	1.25	1.30	1.27	1.33
Junction exponent χ				
Min	1.29	1.19	1.26	1.48
Max	11.78	13.88	9.20	22.80
Median	2.86	2.99	2.89	3.64
1st quartile	2.21	2.29	2.27	2.66
3rd quartile	4.00	4.27	3.80	4.82
Mean	3.44	3.62	3.28	4.20
Optimality parameter ρ				
Min	-0.93	-1.00	-1.01	-1.06
Max	0.83	0.87	0.85	0.74
Median	-0.23	-0.45	-0.32	-0.48
1st quartile	-0.62	-0.68	-0.61	-0.64
3rd quartile	0.56	0.48	0.53	0.40
Mean	-0.06	-0.16	-0.08	-0.24

Table 4.1: The descriptive statistical data for the different geometrical parameters as measured by Observer 1(measure 1, 2, and 3) and Observer 2 (measure 4)

The data were also displayed as box plots showing the same parameters. (Figure 4.2)
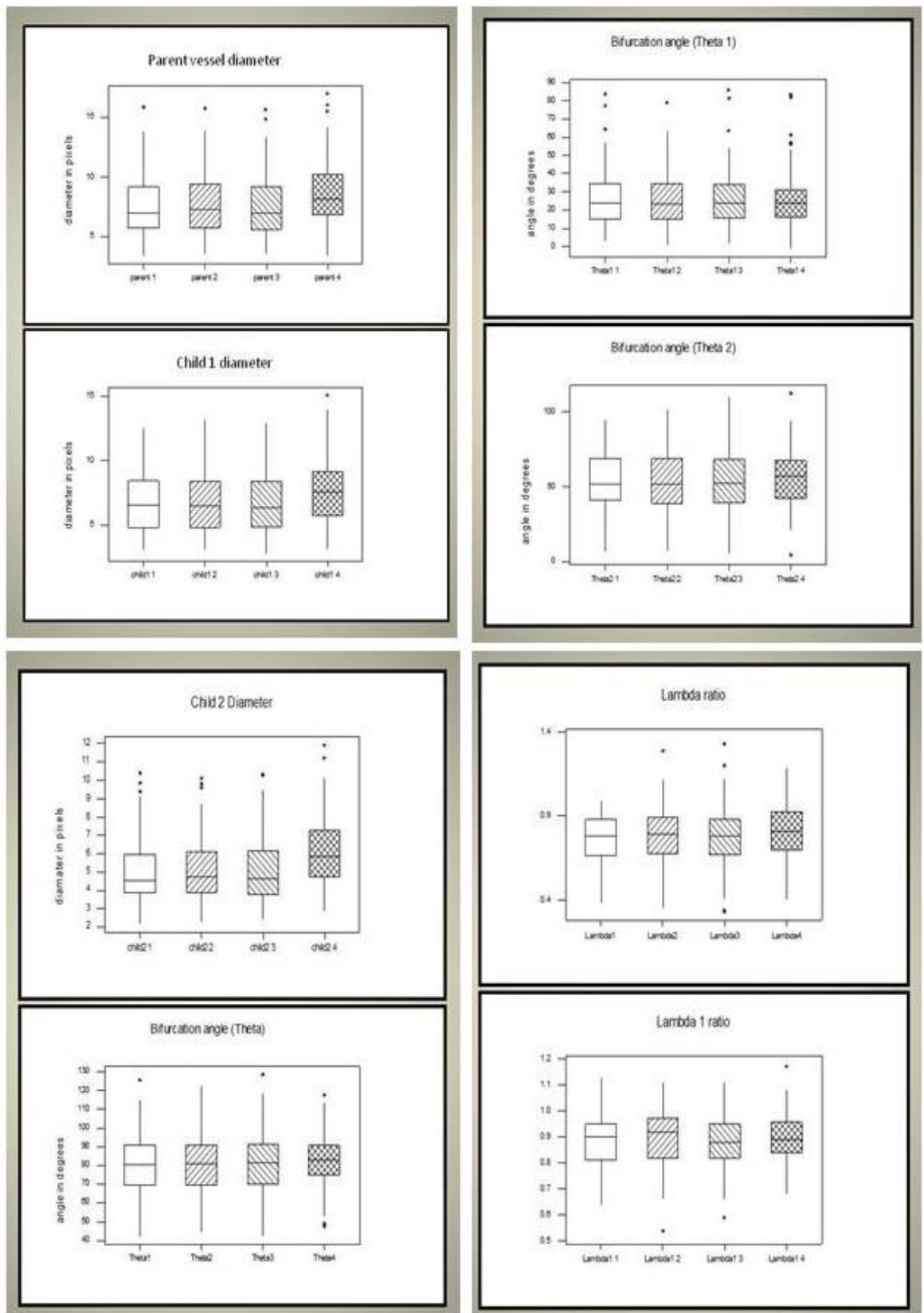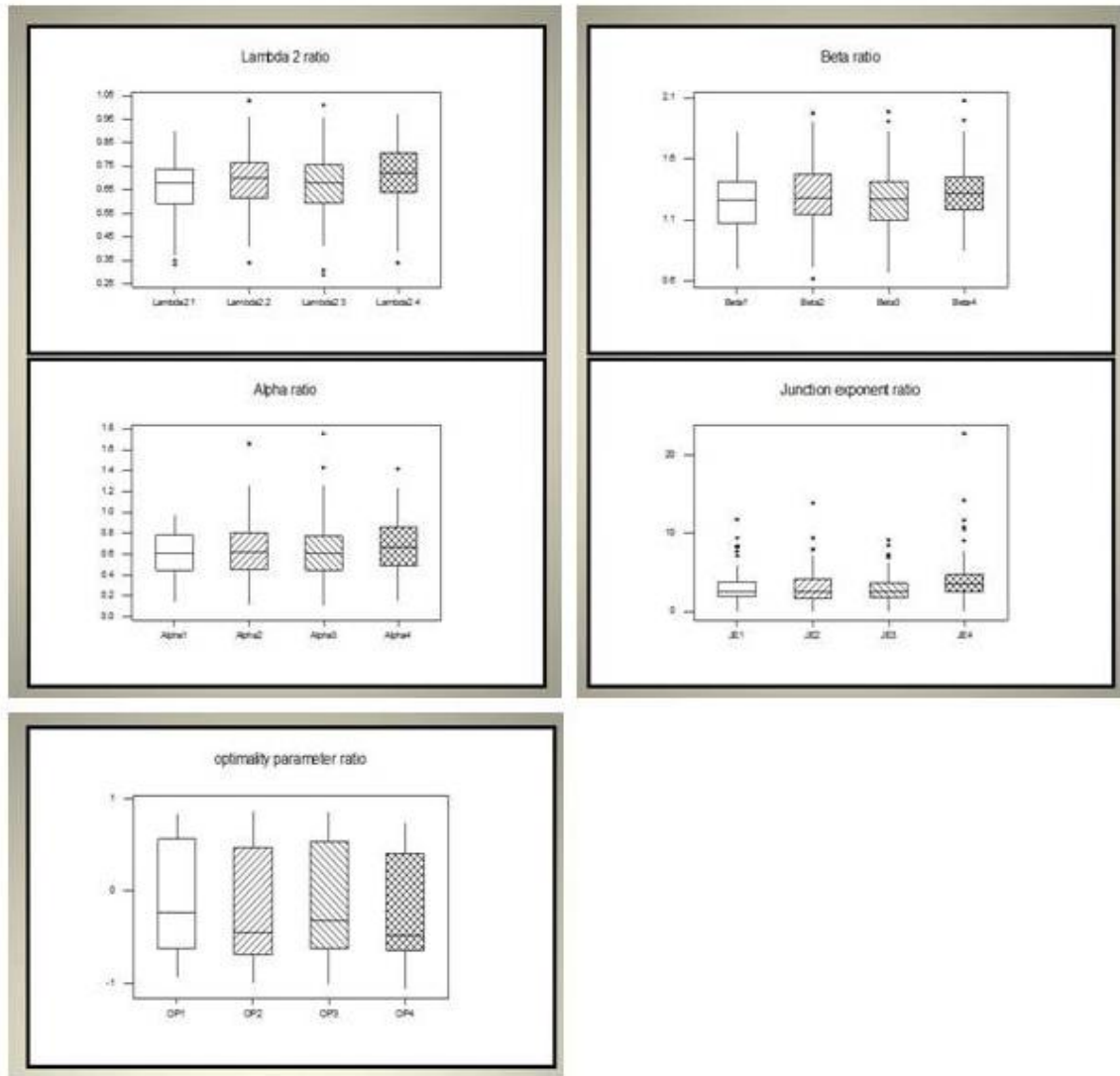
Figure 4.2: Box plots of the different geometrical parameters for repeated measurements by observer 1 (measures 1, 2, and 3) and by observer 2 (measure 4)

On evaluating the box plots, there seemed to be an overall overlap of the ranges of measurements and medians for all the parameters within the first observer's 3 measurements and between both observers. However, there was also a persistent trend of recording larger measurements in the absolute widths parameters (parent width, child 1 width, child 2 width) as estimated by the second observer as compared to the first observer's measurements. This trend was noted to be less obvious when comparing the ratios parameters' estimates. There was no evidence of any fixed trend when comparing the angle measurements within and across both observers. These variations and trends were then evaluated and quantified as follows.

1. Intra-observer variability

The associations of the standard deviation and mean values were evaluated with the Kendal Tau test for all parameters, a statistically significant association was noted for child1 vessel diameter d_1, λ, λ_2, α and β ratios, thus logarithmic transformation was performed and the values were rendered independent, and one way analysis of variance was performed for the logarithmic data for these parameters.

The results of the one way analysis of variance for the intra-observer variability for the different parameters are summarised in table 4. 2 (a) and (b)

	Within-subject SD (SW)	Percent Coefficient of variation
Parent width d_0	0.3511	3.8%
Child 2width d_2	0.3395	5.5%
θ angle	2.361	2.4%
θ_1 angle	1.772	5.6%
θ_2 angle	2.224	3.4%
λ_1	0.0469	4.6%
Junction exponent χ	1.178	23%
Optimality parameter ρ	0.3312	--

Table 4.2a

[Note: the coefficient of variation for the optimality could not be calculated as the mean is close to zero, and the data include (+ve) and (-ve) values]

	Geometric Standard deviation	Coefficient of Variation
Child 1 width d_1	1.0512	5.10%
λ	1.0725	7.25%
λ_2	1.0618	6.10%
α	1.0387	3.87%
β	1.0941	9.40%

Table 4.2b

Table 4.2:
Table 4.2a: Intra-observer variability: Within-subject standard deviation, in units of the original data for the parameters with untransformed data, together with the coefficient of variation.

Table 4.2b Intra-observer variability: Geometric standard deviation ratio for the logarithmic transformed data and its expression as coefficient of variation ratio.

Sub-analysis of the data showed no obvious difference in the scatter of the variability for any of the measurements and ratio estimations in relation to the size or type of the vascular bifurcation (arteriole versus venule), position of bifurcation (superior versus inferior to the horizontal raphe), and between diabetic and normal subjects. Moreover there was also no relationship detected between the variability of measurements and the distance of the bifurcation from the disc (as calculated by the disc ratio = distance of bifurcation to disc center in pixels / diameter of disc in pixels). An example of this relationship is presented below for the measurements of the larger child vascular segment diameter (Child 1) in figures 4.3 and 4.4
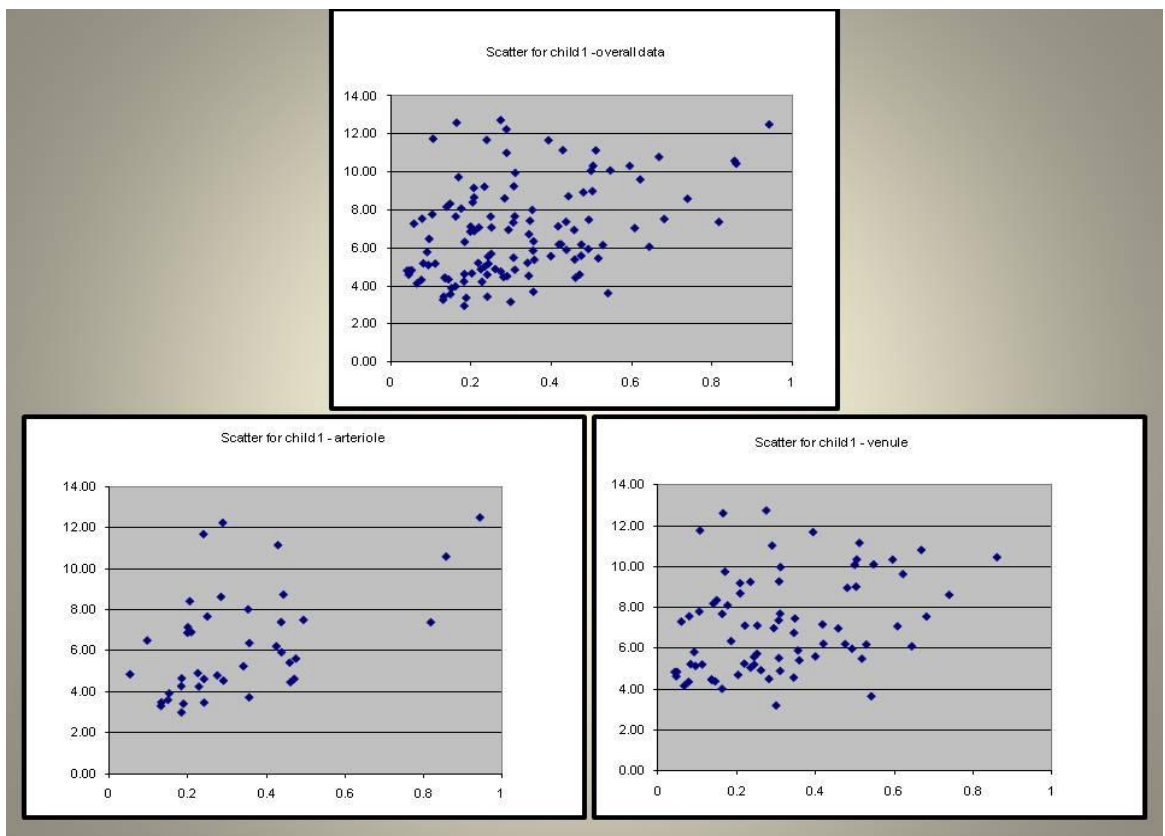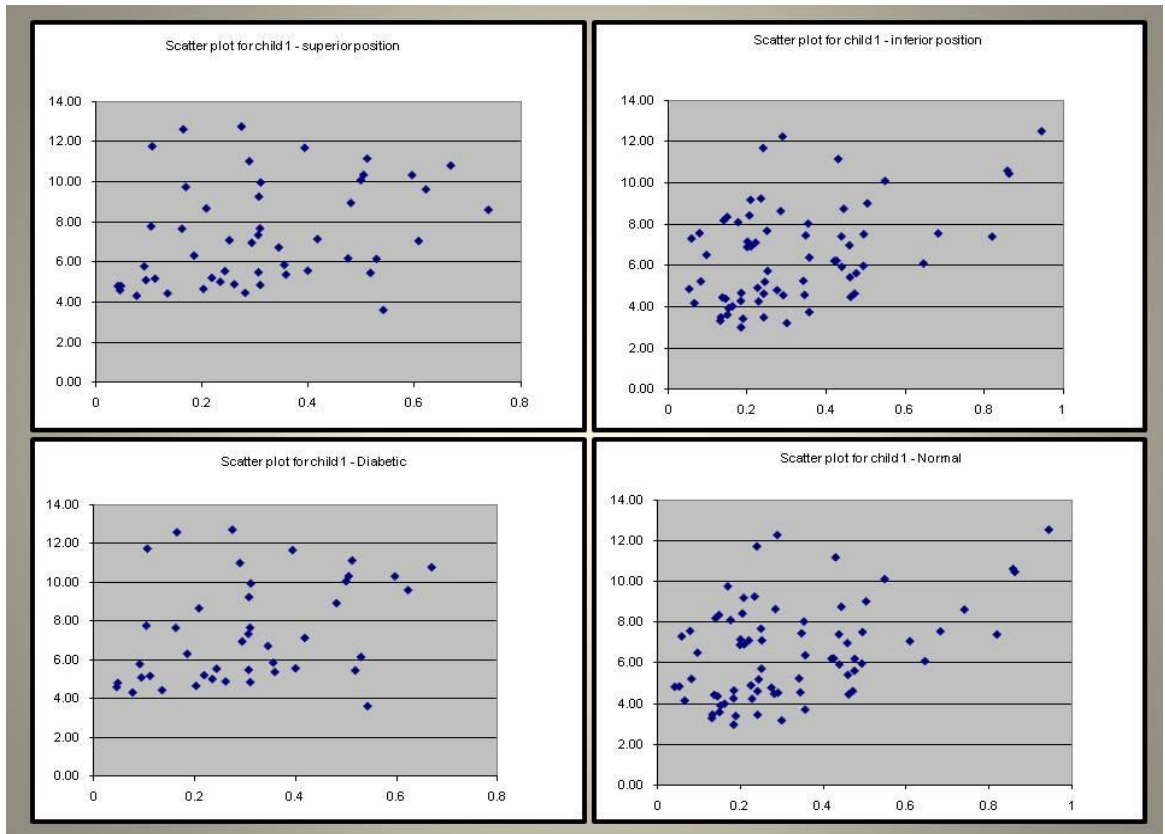
Figure 4.3: An example of scatter plots for Child 1 vessel diameter measurements demonstrating the relationship between the standard deviation and mean measurements for the intra-observer variability, in relation to the size, type, and position of the bifurcation and between normal and diabetic subjects.
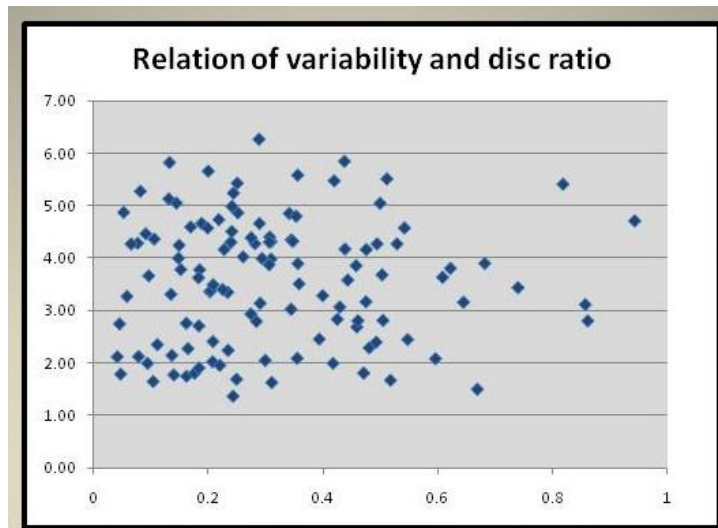
Figure 4.4: An example of the relationship between the standard deviation of measurements and the disc ratio for Child 1 vessel diameter

2. Inter-observer variability

The summary of the results for the Bland-Altman analysis between first measurements obtained by Observer 1 and measurements obtained by Observer 2 is displayed in table 4.3, demonstrating the arithmetic mean, standard deviation, and the 95% limits of agreement for the analysed parameters.

INTER-OBSERVER AGREEMENT				
			95% Limits of Agreement	
	Mean	St Deviation	Upper	Lower
Parent d_0	-1.08	1.04	0.95	-3.1
Child 1 d_1	-1.01	1.11	1.15	-3.2
Child 2 d_2	-1.13	1.03	0.88	-3.2
Theta θ	-1.51	8.12	14.4	-17.4
Theta 1 θ_1	0.61	7.73	15.8	-14.5
Theta 2 θ_2	-2.15	8.12	13.8	-18.1
Alpha α	-0.08	0.21	0.33	-0.49
Beta β	-0.08	0.24	0.39	-0.55
Lambda λ	-0.05	0.12	0.21	-0.31
Lambda 1 λ_1	-0.01	0.08	0.17	-0.18
Lambda 2 λ_2	-0.05	0.11	0.16	-0.26
Junction exponent χ	-1.01	2.86	4.71	-6.59
Optimality parameter ρ	0.18	0.62	1.41	-1.05

Table 4.3: Results of the Bland-Altman analysis for the inter-observer agreement for the architectural and geometrical parameters

Examples of the Bland-Altman plots for the inter-observer agreement regarding absolute vessel width measurements, angular measurements, and architectural ratio estimates are presented in figures 4.5 – 4.7 respectively.
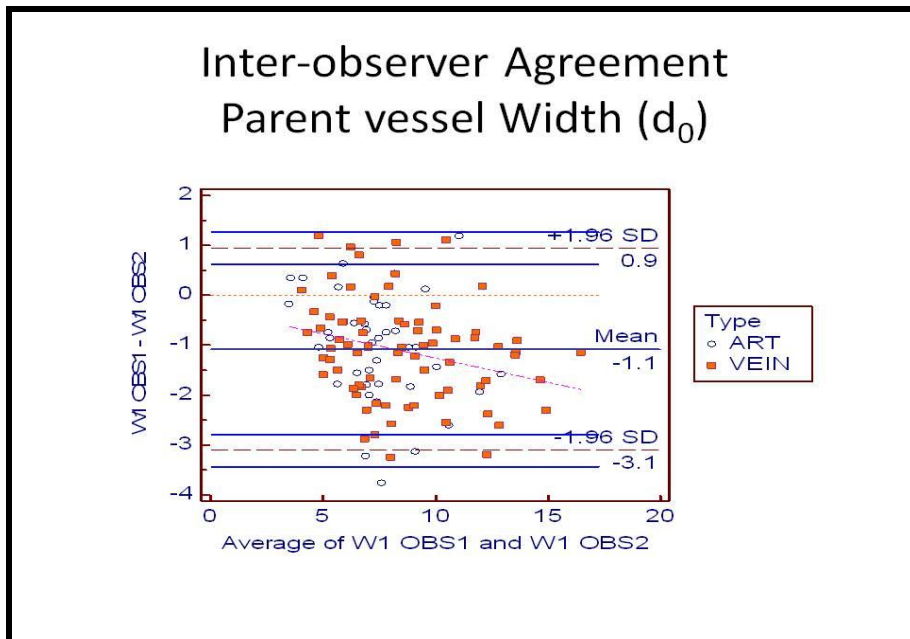
Figure 4.5: An example of Bland-Altman plot for inter-observer agreement for absolute vessel width measurements (Parent vessel width) for arteriolar and venular vascular segments. Observer 1 (OBS1), Observer 2 (OBS2), vessel width (W1)
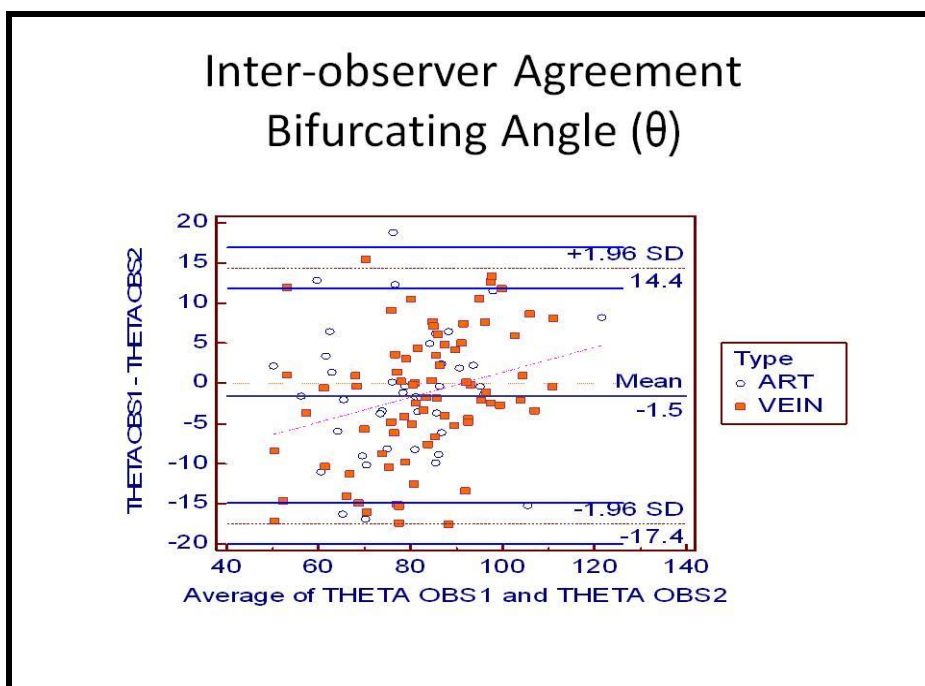
Figure 4.6: An example of Bland-Altman plot for inter-observer agreement for angular measurements (Total bifurcating angle) for arteriolar and venular vascular segments. Observer 1 (OBS1), Observer 2 (OBS2), Bifurcating angle (Theta θ)
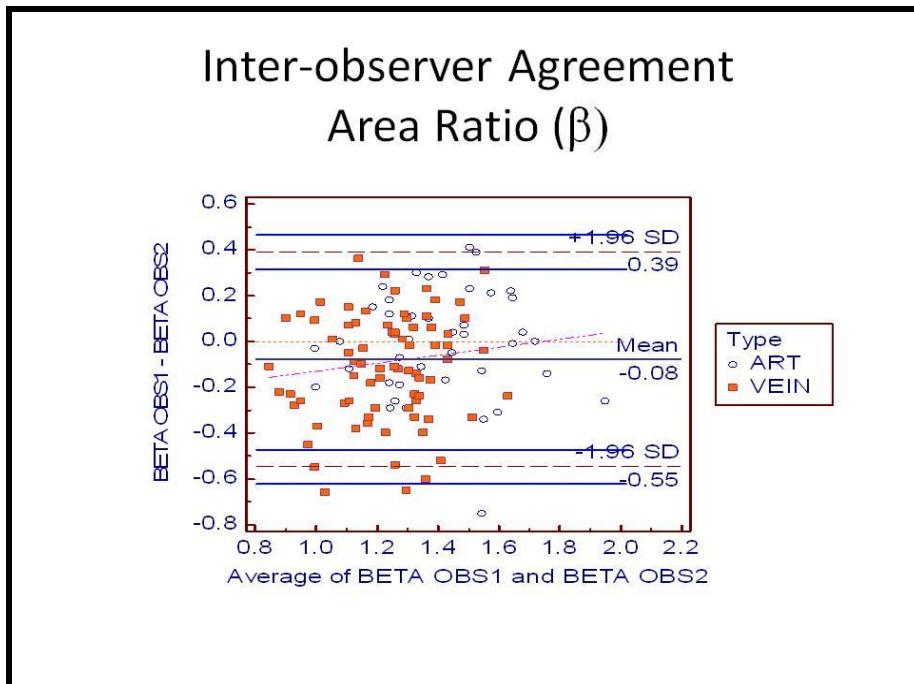
Figure 4.7: An example of Bland-Altman plot for inter-observer agreement for ratio estimates (Area Ratio β) for arteriolar and venular vascular segments. Observer 1 (OBS1), Observer 2 (OBS2), Area Ratio (Beta β)

As presented in table 4.7 and figures 4.5 – 4.7, the results indicated that there was a wide 95% limit of agreement noted between both observers for absolute vessel width measurements, with observer 2 measurements consistently recorded as higher than those of observer 1, resulting in a relatively large mean difference. This appeared true for the arteriolar and the venular segments. The Bland-Altman plot in figure 4.5 suggested also that the inter-observer differences were more obvious in larger vascular segments rather than small segments. This bias was less noted for relative diameter ratios and other geometrical ratio estimates. However, large standard deviation and wide 95% limit of agreement was also evident for the junction exponent estimates, which echoed its poor intra-observer repeatability. Concerning the angular measurements, there was no obvious systematic bias noted between both observers, however the wide limits of agreement would be considered clinically significant if comparisons are made between measurements obtained by different observers. These limitations might reflect the semi manual nature of the technique and thus the inevitable individual difference in defining the vascular edge and interpreting angular changes. No differences in the results were noted between arteriolar and venular vascular bifurcations.

4.6.2 Individual variability study

Eight eyes of 8 subjects were analysed for this study. Four right and four left eyes were included. Two subjects were normal healthy volunteers while four subjects were diabetics with different stages of diabetic retinopathy. Four sets of nasal and temporal retinal images captured over the two visits were analysed for each eye, thus a total of 64 images were analysed. The 8 eyes included a total of 119 bifurcations which were labelled and marked four times. Fifty seven arteriolar bifurcations and 62 venular bifurcations were analysed. Fifty nine bifurcations were situated above the horizontal raphe while 60 bifurcations were below it.

The results of this study assessed the variability of measurements across images captured in a same visit within 10 minutes of each other (Intra-visit variability), and images captured 2 weeks apart (Inter-visit variability)

Table 4.4 summarises the descriptive statistical values obtained for the different parameters as measured in the 4 images (Images 1, 2, 3 captured in visit 1 and image 4 captured 2 weeks later). The values summarised are the minimum, maximum, median, 1st quartile, 3rd quartile and mean values for each parameter.

	Visit 1			Visit 2
	1st measure	2nd measure	3rd measure	
Parent vessel d_0				
Min	3.51	4.39	3.26	3.42
Max	13.18	13.00	13.57	14.90
Median	7.49	7.51	7.13	7.53
1st quartile	5.74	6.00	5.80	6.20
3rd quartile	8.80	8.72	8.69	8.69
Mean	7.56	7.61	7.54	7.66
Child 1 vessel d_1				
Min	2.99	3.27	2.70	2.95
Max	12.32	11.41	11.99	11.80
Median	6.64	6.27	6.13	6.47
1st quartile	5.45	5.28	5.17	5.23
3rd quartile	7.93	7.66	7.90	8.00
Mean	6.78	6.64	6.59	6.72
Child 2 vessel d_2				
Min	2.52	2.71	2.57	2.80
Max	11.16	9.90	10.77	10.78
Median	4.76	4.75	4.60	4.84
1st quartile	3.85	4.15	3.99	4.05
3rd quartile	5.99	6.18	5.78	5.94
Mean	5.10	5.26	5.10	5.25
Theta angle θ				
Min	46.83	43.00	43.88	45.83
Max	133.64	135.16	129.16	130.51
Median	79.49	78.89	78.50	79.98
1st quartile	68.96	67.08	68.10	67.41
3rd quartile	86.95	88.98	89.78	89.82
Mean	79.26	79.23	79.08	79.33
Theta 1 angle θ_1				
Min	0.54	-0.13	0.41	-1.25
Max	85.02	88.90	88.03	82.13
Median	21.16	21.24	20.94	23.00
1st quartile	12.83	12.50	12.22	11.99
3rd quartile	34.01	35.79	34.79	36.57
Mean	25.02	26.28	25.57	25.65
Theta 2 angle θ_2				
Min	11.99	11.07	10.00	10.25
Max	113.91	111.06	110.66	106.39
Median	53.89	53.53	55.49	51.41
1st quartile	39.84	35.76	37.86	39.33
3rd quartile	67.11	66.80	68.30	65.92
Mean	54.24	52.96	53.52	53.68

Lambda λ				
Min	0.37	0.34	0.33	0.34
Max	0.99	2.12	2.64	2.36
Median	0.77	0.83	0.78	0.79
1st quartile	0.67	0.66	0.63	0.66
3rd quartile	0.89	0.94	0.92	0.93
Mean	0.77	0.83	0.81	0.82
Lambda 1 λ_1				
Min	0.69	0.47	0.38	0.42
Max	1.10	1.14	1.12	1.07
Median	0.90	0.88	0.90	0.90
1st quartile	0.85	0.84	0.83	0.82
3rd quartile	0.96	0.94	0.95	0.94
Mean	0.90	0.88	0.88	0.88
Lambda 2 λ_2				
Min	0.34	0.30	0.34	0.34
Max	1.00	1.00	1.03	0.99
Median	0.68	0.71	0.68	0.72
1st quartile	0.61	0.59	0.60	0.59
3rd quartile	0.79	0.82	0.80	0.82
Mean	0.69	0.71	0.69	0.70
Alpha α				
Min	0.13	0.11	0.11	0.12
Max	0.99	4.49	6.98	5.55
Median	0.59	0.68	0.60	0.63
1st quartile	0.45	0.43	0.40	0.43
3rd quartile	0.79	0.89	0.85	0.87
Mean	0.61	0.75	0.74	0.73
Beta β				
Min	0.77	0.71	0.76	0.77
Max	2.04	2.09	1.91	2.08
Median	1.29	1.27	1.24	1.24
1st quartile	1.13	1.16	1.16	1.12
3rd quartile	1.44	1.44	1.45	1.49
Mean	1.30	1.31	1.29	1.30
Junction exponent χ				
Min	1.36	1.25	1.43	1.43
Max	24.38	19.20	12.15	15.22
Median	3.08	3.34	3.04	3.12
1st quartile	2.49	2.57	2.61	2.47
3rd quartile	4.53	4.38	4.34	4.82
Mean	4.26	3.95	3.83	4.10

Optimality parameter ρ				
Min	-1.02	-1.05	-0.95	-1.04
Max	0.76	0.80	0.81	0.80
Median	-0.36	-0.43	-0.33	-0.31
1st quartile	-0.62	-0.61	-0.63	-0.67
3rd quartile	0.46	0.44	0.43	0.44
Mean	-0.15	-0.18	-0.12	-0.14

Table 4.4: The descriptive statistical data for the different geometrical parameters as measured in Visit 1 (measure 1, 2, and 3) and Visit 2

The data are displayed then in the form of box plots to evaluate whether any obvious variation trend could be noted between the visits as shown in figure 4.8
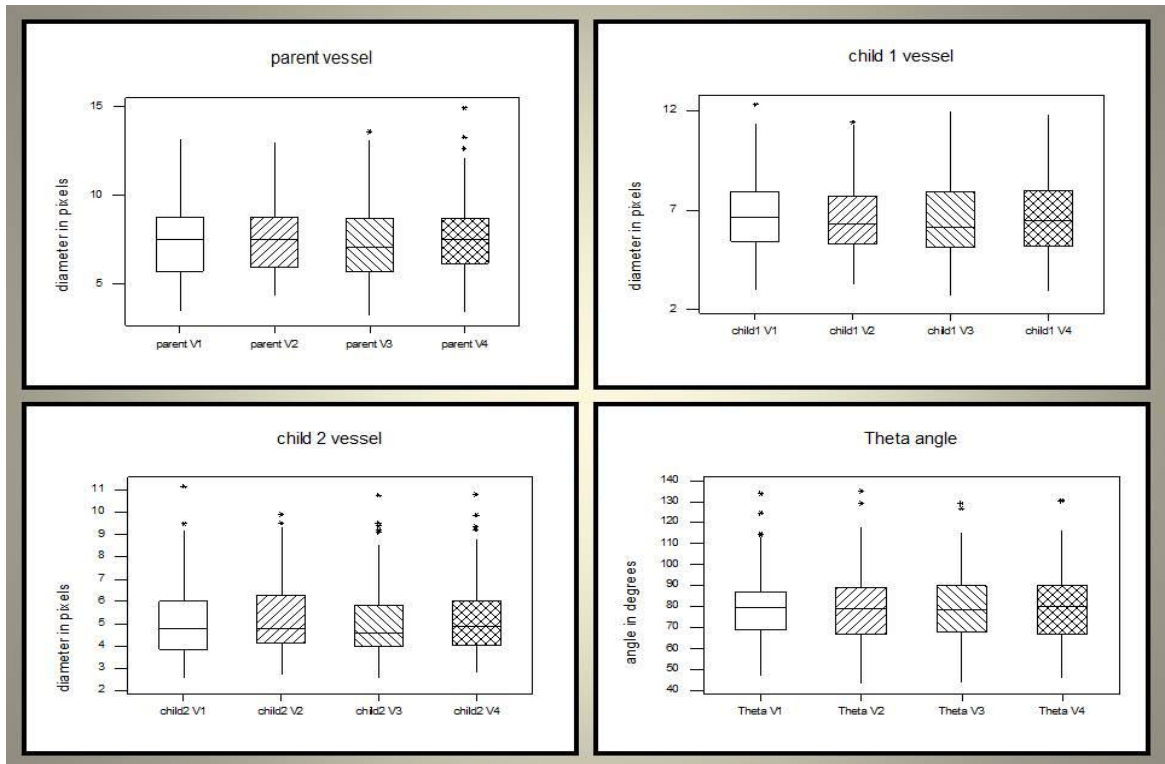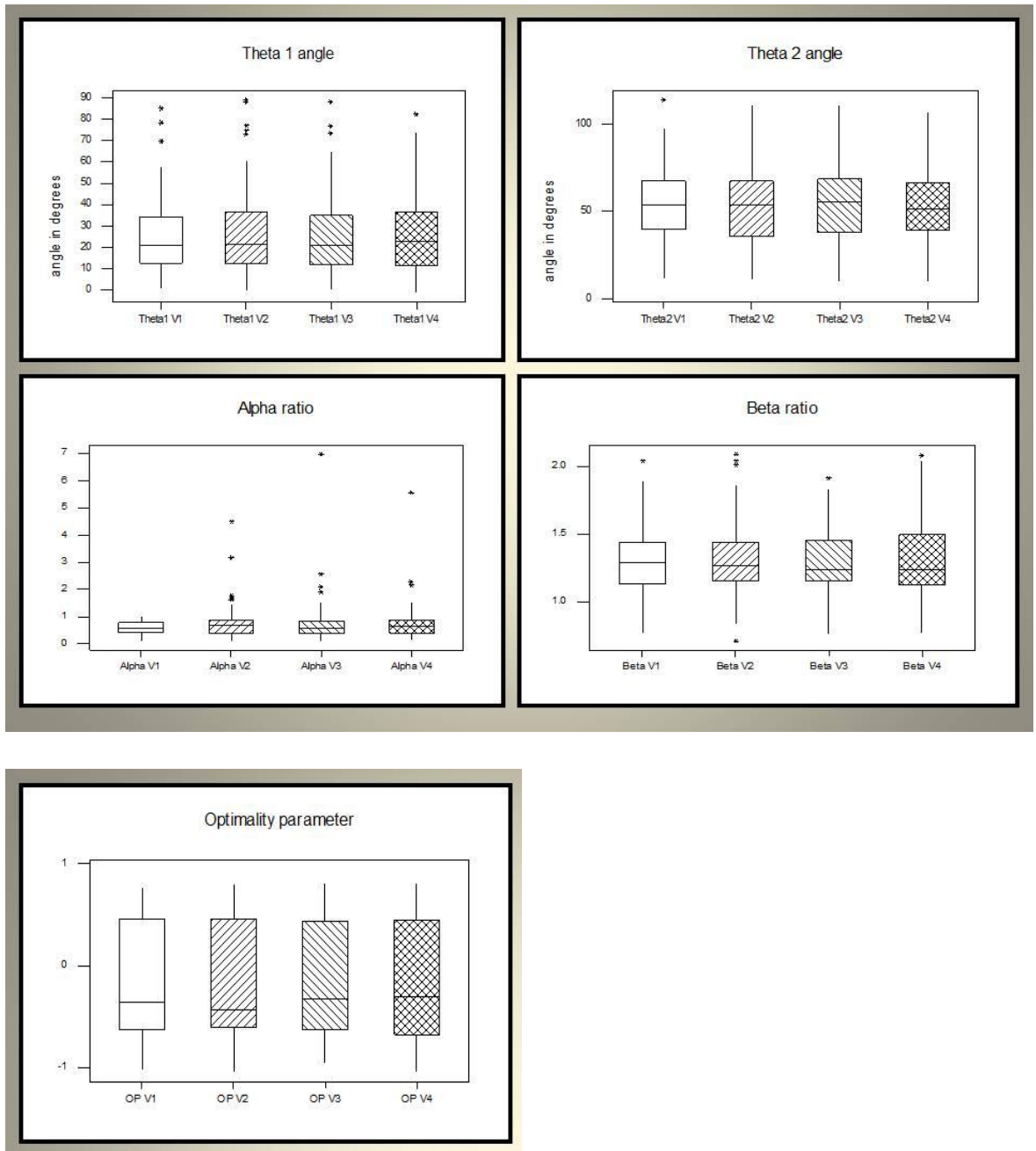
Figure 4.8: Box plots demonstrating the descriptive statistical data for the different geometrical measurements and estimates obtained during the first and second visit.

On evaluating the different data values and the box plots, there was no obvious systematic trend noted in the measurements variability in-between the visits, especially when assessing the variability within the first 3 images as compared to the fourth image. The range of measurements and medians appeared to be overlapping for all parameters across the images regardless of which visit. It did not seem that the

longer time interval between images captured at different visits had contributed to any extra source of variability in measurements.

1. Intra-visit Study

The intra-visit variability of measurements obtained from the first 3 images captured at the same visit was then quantified by using the one way analysis of variance and the within subject standard deviation and was calculated, together with the coefficient of variation. In cases of logarithmic transformation, the geometric standard deviation was calculated and the coefficient of variation was estimated.

The Kendal Tau coefficient was performed to evaluate the association between the variables (subject's standard deviation and mean) for all the parameters. Clinical and statistical significant associations were found in 5 parameters; α, β, λ, θ_1 angle, and χ in which both the K Tau and p values exceeded our set thresholds.

Logarithmic transformation of data was thus performed for these parameters; this resulted in removing the association for α, β, and λ, and the one way analysis of variance was calculated for the logarithmic transformed data. However, this did not remove the association for θ_1 angle, and χ, thus one way analysis of variance could not be performed. Table 4.5 summarizes the results of the one way analysis of variance and the coefficient of variation for the intra-visit measurements.

	Within-subject SD (SW)	Coefficient of variation
Parent width d_0	0.55308	6.14%
Child 1 width d_1	0.5862	7.00%
Child 2 width d_2	0.577	8.90%
Theta angle θ	4.553	4.10%
Theta 2 angle θ_2	4.353	5.40%
Lambda 1 λ_1	0.063	6.10%
Lambda 2 λ_2	0.066	8.30%
Optimality parameter ρ	0.4089	- - - -
Theta 1 angle θ_1	- - - -	9.10%
Junction exponent χ	- - - -	34%

	Geometric Standard deviation	Coefficient of variation
Alpha α	1.059	5.90%
Beta β	1.0142	1.40%
Lambda λ	1.127	12.70%

Table 4.5

Table 4.5a: Intra-visit variability: The within-subject standard deviation, in units of the original data, for the parameters with untransformed data, together with the coefficient of variation.

Table 4.5b: Intra-visit variability: The coefficient of variation calculated for the logarithmic transformed data

Further sub-analysis for each parameter was performed to ascertain the effect of the vascular bifurcation type, and position on the resulting relationships, as well as comparing diabetic to normal subjects. Comparison of the resultant scatter plots for each subcategory for all the parameters showed no obvious difference in the distribution of data.

2. Inter-visit study

Bland-Altman analysis was used to assess the agreement of vascular width and angular measurements and ratio estimates obtained from Image 1 captured in the first visit and Image 4 captured in the second visit two weeks later. The summary of the

mean difference, standard deviation and the 95% limit of agreement for the analysed parameters are displayed in table 4.6.

INTER- VISIT AGREEMENT				
			95% Limits of Agreement	
	Mean	St Deviation	Upper	Lower
Parent d_0	0.00	0.81	1.61	-1.59
Child 1 d_1	0.06	0.77	1.57	-1.46
Child 2 d_2	0.00	0.79	1.51	-1.61
Theta θ	0.13	6.53	12.9	-12.7
Theta 1 θ_1	-0.21	3.98	7.59	-8.01
Theta 2 θ_2	0.34	6.75	13.7	-12.9
Alpha α	-0.05	0.21	0.36	-0.47
Beta β	-0.01	0.25	0.48	-0.51
Lambda λ	-0.02	0.12	0.21	-0.27
Lambda 1 λ_1	0.01	0.08	0.17	-0.15
Lambda 2 λ_2	-0.01	0.11	0.19	-0.23
Junction exponent χ	-0.11	3.77	7.32	-7.46
Optimality parameter ρ	0.03	0.61	1.21	-1.15

Table 4.6: Results of the Bland-Altman analysis for the inter-visit agreement for the architectural and geometrical parameters

Examples of the Bland-Altman plots for the inter-visit agreement regarding absolute vessel width measurements, angular measurements, and architectural ratio estimates are presented in figures 4.9 – 4.11 respectively. The data were subdivided into normal and diabetic subjects.
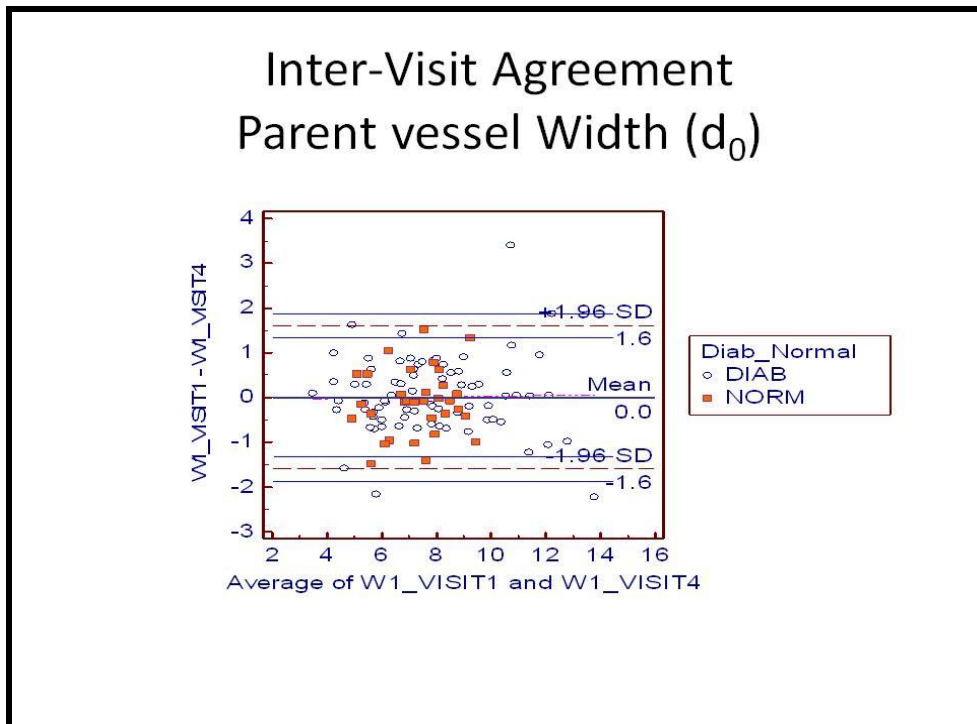
Figure 4.9: An example of Bland-Altman plot for inter-visit agreement for absolute vessel width measurements (Parent vessel width d0) for vascular segments of diabetic and normal subjects. Diabetic (DIAB), Normal (NORM), vessel width (W1)
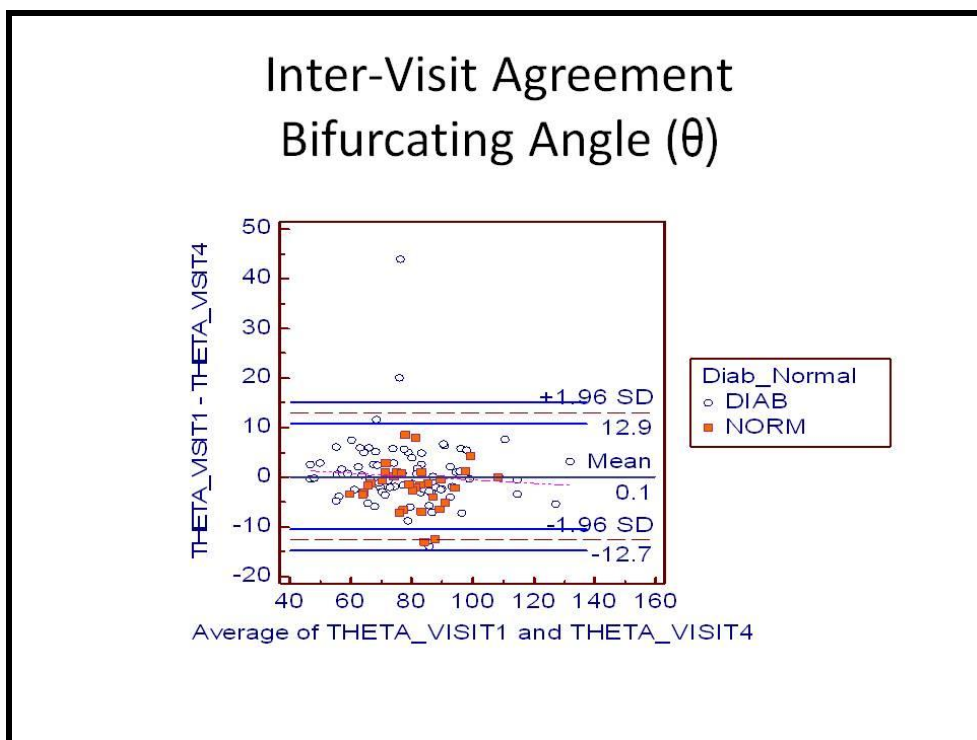
Figure 4.10: An example of Bland-Altman plot for inter-visit agreement for angular measurements (Total bifurcating angle) for vascular segments of diabetic and normal subjects. Diabetic (DIAB), Normal (NORM), Bifurcating angle (Theta θ)
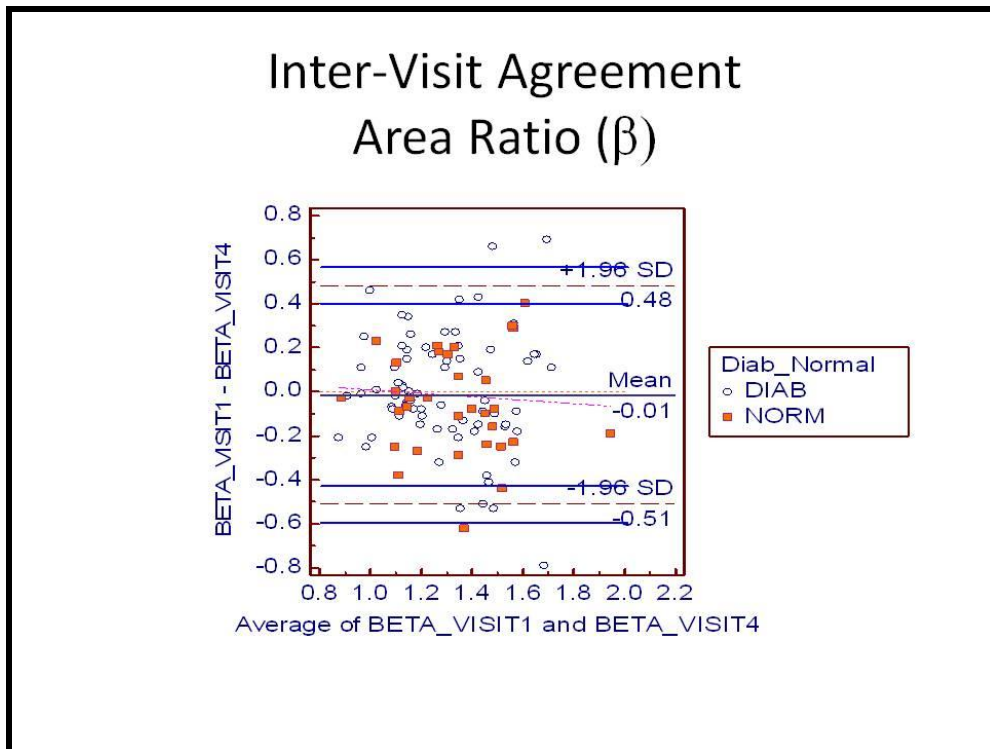
Figure 4.11: An example of Bland-Altman plot for inter-visit agreement for ratio estimates (Area Ratio β) for vascular segments of diabetic and normal subjects. Diabetic (DIAB), Normal (NORM), Area Ratio (Beta β)

The results of the Bland-Altman assessment presented in table 4.6 and figures 4.9 – 4.11 showed no consistent trends of difference for the absolute width measurements, angular measurements or ratio estimates calculated for parameters analysed from the two images captured 2 weeks apart. The standard deviations were moderately higher than those calculated for the intra-visit study for most of the analysed parameters. Wide 95% limits of agreement were noted, similar to those reported for the inter-observer study, yet with no clear bias to any side in relation to the mean difference. There was also no obvious difference in the results between the normal and diabetic subjects. In general, it was valid to conclude that the time-gap of two weeks between visits did not add a clear component of variability to this found across images captured in close succession at the same visit.

The data were then sub-analyzed to detect whether short-term changes in systemic blood pressure or blood glucose levels in diabetics would influence the results.

A) Blood pressure changes

The inter-visit data for the different geometrical measurements and estimates in the normal and diabetic subjects were divided into two categories; high mean blood pressure change, and low mean blood pressure change. An arbitrary cut point of mean blood pressure change of 20 mmHg was used to categorize the data, based on the median value of blood pressure change in our data.

The mean difference values, 95% confidence interval and the p values for the T test were calculated for both categories as shown in table 4.7

A. Low mean blood pressure change

	Mean Difference	95% Confidence Interval		p value
Parent d_0	-0.05	-0.15	0.18	0.802
Child 1 d_1	0.02	-0.14	0.18	0.857
Child 2 d_2	-0.12	-0.29	0.05	0.314
Theta θ	-0.23	-1.27	0.81	0.879
Theta 1 θ_1	-0.4	-1.21	0.41	0.724
Theta 2 θ_2	0.17	-0.94	1.27	0.85
Alpha α	-0.06	-0.11	-0.02	0.04
Beta β	-0.05	-0.1	0.00	0.384
Lambda λ	-0.03	-0.06	0.00	0.0633
Lambda 1 λ_1	0.00	-0.02	0.01	0.3312
Lambda 2 λ_2	-0.03	-0.05	0.00	0.161
Junction exponent χ	-0.46	-1.18	0.25	0.7235
Optimality parameter ρ	0.1	-0.02	0.22	0.468

B. High mean blood pressure change

	Mean Difference	95% Confidence Interval		p value
Parent d_0	-0.05	-0.4	0.31	0.803
Child 1 d_1	0.19	-0.13	0.5	0.89
Child 2 d_2	0.21	-0.08	0.07	0.8009
Theta θ	1.48	-2.67	5.63	0.797
Theta 1 θ_1	0.45	-1.23	2.14	0.9699
Theta 2 θ_2	1.03	-3.23	5.29	0.854
Alpha α	-0.01	-0.08	0.07	0.8363
Beta β	0.11	0.01	0.2	0.189
Lambda λ	0.00	-0.05	0.04	0.908
Lambda 1 λ_1	0.04	-0.01	0.08	0.1133
Lambda 2 λ_2	0.03	0.00	0.06	0.535
Junction exponent χ	0.57	-0.66	1.79	0.507
Optimality parameter ρ	-0.23	-0.47	0.01	0.179

Table 4.7: The results of the T test for the different geometrical parameters showing the mean difference, 95% confidence interval and p-values for the low blood pressure change (4.7 a) and the high blood pressure change (4.7b) categories.

B) Blood glucose changes

Similarly, the inter-visit data for the diabetic subjects were then subdivided into 2 categories according to the extent of change in the blood glucose levels recorded at the two visits. An arbitrary cut point of blood glucose change of 10 mmol was used to categorize the data, based on the median value of blood glucose change in our data. The mean difference values, 95% confidence interval and the p values for the T test was calculated for both categories as follows in table 4.8

A. Low blood glucose change

	Mean Difference	95% Confidence Interval		p value
Parent d_0	0.09	-0.13	0.31	0.905
Child 1 d_1	0.1	-0.09	0.29	0.8944
Child 2 d_2	-0.06	-0.29	0.16	0.6095
Theta θ	0.76	-0.56	2.07	0.917
Theta 1 θ_1	-0.67	-1.65	0.31	0.9792
Theta 2 θ_2	1.42	0.27	2.58	0.9079
Alpha α	-0.06	-0.12	-0.01	0.128
Beta β	-0.04	-0.11	0.02	0.619
Lambda λ	-0.03	-0.07	0.00	0.2353
Lambda 1 λ_1	0.00	-0.02	0.02	0.4771
Lambda 2 λ_2	-0.03	-0.06	0.01	0.405
Junction exponent χ	-0.3	-1.33	0.73	0.8363
Optimality parameter ρ	0.06	-0.1	0.22	0.9869

B. High blood glucose change

	Mean Difference	95% Confidence Interval		p value
Parent d_0	-0.08	-0.43	0.28	0.4433
Child 1 d_1	0.16	-0.16	0.48	0.8879
Child 2 d_2	0.24	-0.04	0.51	0.6266
Theta θ	1.52	-1.24	4.27	0.6617
Theta 1 θ_1	0.46	-1.26	2.18	0.875
Theta 2 θ_2	1.06	-3.3	5.42	0.8068
Alpha α	0.01	-0.06	0.08	0.8461
Beta β	0.12	0.02	0.21	0.105
Lambda λ	0.01	-0.04	0.05	0.8019
Lambda 1 λ_1	0.03	-0.01	0.08	0.099
Lambda 2 λ_2	0.04	0.01	0.07	0.3184
Junction exponent χ	0.62	-0.63	1.88	0.2412
Optimality parameter ρ	-0.27	-0.5	-0.04	0.0916

Table 4.8: The results of the T test for the different geometrical parameters showing the mean difference, 95% confidence interval and p-values for the low blood glucose change (4.8a) and the high blood glucose change (4.8b) categories.

The results of the sub-analyzed data demonstrated no obvious effect of the blood pressure or blood glucose short term changes in diabetics on the overall results. None of the parameters' results showed any statistically significant systematic variability between the two visits, this was reflected by the T test high p values. However, on reviewing the data, there was a striking observation of an increased range of difference of the bifurcation angle measurements between the 2 visits – as reflected by a wide 95% confidence interval – noted only with high mean blood pressure and high blood glucose changes as compared to the corresponding low change categories. The rest of the vessel width measurements and ratios estimates did not show a similar trend.

<u>4.6.3 Technique comparison study</u>

Table 4.9 summarizes the descriptive statistical values for the beta ratio, junction exponent and the optimality parameter when estimated by the developed semi-manual technique as well as the other different previously described semi-manual techniques, together with the Coefficient of variation and the number (percentage) of failure events. Note that the coefficient of variation could not be calculated for the optimality parameter as the mean values near zero and variables contain positive and negative values.

	Beta ratio β								
	Mean	95% Confidence Interval		Std Deviation	Min	Max	1st Quartile	3rd Quartile	Coefficient of variation	N* Missed data (%)
Rectangle technique	1.31	1.26	1.35	0.21	0.9	2.01	1.16	1.42	16.40%	0 (0%)
Kick Points	1.41	1.28	1.52	0.57	0.47	3.57	1.00	1.76	40.51%	0 (0%)
FWHM	2.05	1.64	2.45	1.71	0.28	11.43	1.26	2.01	83.74%	18 (20%)
Gregson	2.23	2.09	2.36	0.64	1.44	4.10	1.74	2.56	28.85%	0 (0%)
Single Gaussian	1.82	1.69	1.93	0.58	0.79	4.64	1.47	2.00	31.70%	0 (0%)
Two Dimensional Gaussian	1.75	1.57	1.93	0.77	0.43	4.47	1.21	2.13	43.24%	17 (19.5%)
	Junction Exponent ratio χ								
Rectangle technique	3.76	3.35	4.17	1.95	1.72	13.86	2.57	4.28	50.91%	2 (2.9%)
Kick Points	3.58	2.64	4.52	3.70	0.95	20.97	1.69	4.08	103%	28 (32.18%)
FWHM	4.60	2.98	6.05	4.54	0.66	24.95	2.30	5.35	98.76%	53 (60.91%)
Gregson	6.92	4.93	8.90	4.30	2.83	17.25	3.66	8.79	62.13%	65 (74.71%)
Single Gaussian	6.61	4.71	8.51	5.39	1.48	25.69	2.53	9.21	81.48%	51 (58.62%)
Two Dimensional Gaussian	4.80	3.42	6.17	4.33	0.9	19.87	2.07	6.26	90.34%	49 (56.32%)
	Optimality parameter ratio ρ								
Rectangle technique	-0.15	-0.26	0.03	0.54	-1.01	0.71	-0.59	0.45	- - - - -	0 (0%)
Kick Points	-0.18	-0.34	-0.01	0.78	-1.56	0.91	-0.89	0.65	- - - - -	0 (0%)
FWHM	-0.56	-0.76	-0.35	0.89	-3.15	0.96	-0.99	0.35	- - - - -	13 (14.94%)
Gregson	-1.04	-1.12	-0.97	0.35	-1.70	0.34	-1.26	-0.86	- - - - -	0 (0%)
Single Gaussian	-0.74	-0.86	-0.63	0.54	-1.84	0.79	-1.00	-0.70	- - - - -	0 (0%)
Two Dimensional Gaussian	-0.56	-0.73	-0.38	0.76	-1.88	0.93	-1.09	0.22	- - - -	17 (19.54%)

Table 4.9: Descriptive statistical data and the Standard deviation and coefficient of variation for the Beta ratio, junction exponent, and the optimality parameter as measured by the different semi-manual techniques.

The results demonstrated that the custom-designed rectangular technique seemed more precise when estimating the different parameters, with reference to the predicted theoretical values, when compared with the other techniques. This was reflected by mean values closer to theoretical values, narrower ranges of measurements, with lower standard deviation, together with lower coefficient of variation as estimated for "β" and "χ".

The kick-points technique performance was the closest to that of the custom-designed rectangle technique; however it still suffered from higher coefficient of variation as compared to the developed rectangle technique. As for the other techniques; FWHM, single Gaussian, Two-dimension Gaussian, and Gregson, their performance suffered from poor precision with the calculated estimations deviating further away from theoretical predictions with much higher standard deviations, wider ranges of measures, and much higher coefficients of variation. This could be related to the relatively low level of image resolution utilised for this study as compared to results from high-resolution scanned images reported elsewhere, together with the fact that in our study, vascular segments of different sizes were analysed unlike previous studies which focused on large vascular segments in a concentric zone around the optic disc. The optimality parameter coefficient of variation could not be calculated; however the designed rectangle technique still achieved a relatively low standard deviation and narrower range of estimations as compared to the other techniques.

The performance of the custom-designed semi-manual technique was consistent when assessed in different vascular type and size and position in relation to the image horizontal raphe and the distance from the optic disc, as confounding factors for vessel edge clarity and definition. No relationship was found when the differences in geometrical estimations for the analysed vascular bifurcations between the developed technique and any other semi-annual technique were plotted against their optic disc ratio – defined as the distance of the bifurcation from the optic disc divided by the mean optic disc diameter.

Furthermore, the "Full width Half Maximum" technique, and the "Two dimensional Gaussian" technique registered a significant number of "failure events" for

estimating Beta and optimality parameter as compared to the other techniques. There was a higher percentage of "failure events" for estimating the junction exponent parameter by all the other different techniques as compared to our custom designed technique. Failure of estimating the junction exponent parameter could be due to either: (1) Estimating a child vessel diameter to be slightly larger than the parent vessel diameter. (2) Failure all together to measure one or more of the 3 vessel diameters around the bifurcation.

The first possibility is a well recognised observation noted before by previous researchers that might reflect the different orientations of the vascular segments in relation to the surface of the retina thus producing this effect when viewed in a two-dimensional image. [87] The latter could happen for different reasons such as the presence of pathological distractions at the vicinity of the vessel (eg: haemorrhages, exudates.), central light reflex, image background noise, blurred vessels.

On analysing the cause of "failures" on estimating the junction exponent by the different techniques, inaccurate estimation of child vessel diameter as compared to parent vessel diameter was responsible for an average of 70%, as compared to 30 % complete failures to estimate a vessel width diameter

4.7 Discussion

Over the recent years, several studies have been conducted to evaluate retinal vascular changes associated with systemic vascular diseases. For example, the Atherosclerosis Risk in Communities study have reported that reduced arteriovenous ratio AVR, as quantified from retinal photography, is independently associated with current and past blood pressure levels [156], with a variety of markers for inflammation and endothelial dysfunction, and with incident clinical stroke. [98]

The reliability and repeatability of assessment of these microvascular abnormalities by retinal photography were previously assessed and had shown retinal photography to be a useful tool in epidemiological research investigating the microvascular contribution to cardiovascular disease. [157] The main findings of Couper's et al

study focused on evaluating the variability of estimations of the central retinal arteriolar equivalent, central retinal venous equivalent and the arteriovenous ratio. The results demonstrated, as expected, that the variability in the individual variability study (single individual, repeat photographs) tended to be higher than in the grader variability study (single photograph, repeat grading), and that the intra-grader reliability was consistently better than the inter-grader reliability.

Similarly, more interest had evolved to evaluate further dimensionless features of the retinal vascular geometry and their associations with systemic vascular disease including hypertension, and other conditions such as increasing age [88], peripheral vascular disease and low birth weight. [90, 91, 94] In addition, further studies have been conducted and various research groups have been exploring the role of these geometrical changes in retinal vascular bifurcations as independent indicators and / or predictors of systemic and cerebral vascular diseases.

Such dimensionless entities that had been used include bifurcation angles, junction exponents, optimality parameter, and different area ratios, together with other features such as length: diameter ratios and fractal dimensions. The use of these dimensionless features nullified the necessity of correcting for any of the camera or ocular magnification factors when attempting to compare vascular measurements between different subjects from fundal photographs. [146] However, the reliability of measuring and estimating these features and parameters has yet to be determined accurately in the literature in a similar way to the central retinal arterial and venous equivalents previously investigated in Couper's et al work.

This study was thus conducted to evaluate the impact of different aspects of grader and individual variability on retinal vascular geometrical measurements as estimated by our computer-assisted semi-manual technique. The precision of performance of the used technique for obtaining and calculating these different parameters was also compared to those of the other available semi-manual techniques used for vessel width measurements.

This step was important in our research project for future interpretation of the results of further experiments comparing fundus images in disease states. The results,

determining the range of variations in our measurements and the background "noise", would enable us to estimate the minimum detectable yet clinically significant difference that could be appreciated between images of different patients' groups with different grades of diabetic retinopathy that would not be simply attributed to mere variability in measurements.

The observer variability study results reflected factors relating to the observers experience in understanding and defining the vessel edge, and the ability of the custom-designed used technique to determine them, and calculate the vessel width, bifurcating angle, and other vascular ratios and parameters in a precise fashion with the given image resolution.

The individual variability study results accounted for inevitable involuntary eye movements and changes in camera alignment and other image capturing variability, as well as changes that could occur in the retinal vascular network over a short period of time. Nevertheless, the variations in the individual study involved also the observer study variability as both components could not be segregated.

Another source of potential variability in the measurements of retinal vascular diameters that has been previously examined is the effect of the pulse cycle. Previous research has shown that retinal vessel diameters change at different points in the pulse cycle. Venular diameters were found to be smallest in early systole, and increasing to a maximum level in early diastole. The arteriolar diameter peaked slightly earlier. [158] However, Knudtson and co-workers found that the variations across photographic images within the same point in the pulse cycle were generally too wide to detect differences across pulse cycle. They concluded that the main sources of individual and grader variability reduce any effect the pulse point may have on the retinal vessel diameters when using their own methodology. [159] In this study, the retinal photographs were taken at random points in the pulse cycle, thus although variability from the pulse cycle might have existed – however small to be detected using an observer driven semi-manual technique as previously suggested [160] – it occurred at random in the same way in all the study participants with or without disease, and thus it would not bias any possible relationships assessed substantially. The fact that our study utilised dimensionless features of the retinal

vascular geometry, and that large arterial and venous bifurcations around the optic disc were excluded from our analysis makes it unlikely that pulse cycle variation would have a significant effect on our results.

It is worth mentioning here that the retinal images used for the variability studies were all selected to be of at least "good quality" guided by the standards set by the National Screening grading and quality assurance subcommittee for diabetic retinopathy. [152] Images with poor quality secondary to cataract or other media opacity were excluded. This was decided in an attempt to rule out other confounding factors relating to image quality that would affect the technique reliability allowing us to solely evaluate the observer and individual variability factors. We thus acknowledge that the reliability results presented here are based on such selected quality and such results might be degraded further if the developed semi-manual technique is used for blurred images with low contrast or different resolution or other altered image properties. On the other hand, we believe that the retinal images with "good" quality utilised for these studies reflected real-life situation being of the same resolution and properties as those captured routinely in most of the diabetic-screening settings without any specific image alterations specially set for the study purpose. Images of "poor" or "inadequate" field or contrast standards secondary to dense cataract or other media opacities are generally rejected anyway from the screening process and deemed unassessible and patients are routinely referred for clinical assessment.

Observer variability results

1. Intra-observer variability

The results of the intra-observer study showed a coefficient of variation in absolute vessel width measurements - as estimated by our developed semi-manual technique - ranging from 3.8 % and 5.5 %, this compared favourably with results previously published by Newsom and his co-workers, who reported an intra-observer coefficient of variation of 6 % to 34 % in vessel width measurements by an observer driven technique utilising the Full Width Half Maximum algorithm. [160] In practical terms, our results reflected an average "within-subject standard deviation" of less than half a pixel, for vessel width measurement, in all the analysed vascular bifurcations of

different sizes, which could be considered acceptable considering the resolution of fundus images used for this study.

The intra-observer coefficient of variation for angle measurements ranged from 2.4 % to 5.6 %, reflecting also a within-subject standard deviation of average 2 degrees only. Similar results were also shown for the other ratios and parameters estimations with coefficient of variation values ranging from 3.8% to 9.4%, to our knowledge, there are no similar published data available on other techniques for comparison. However, our results revealed a high coefficient of variation reaching 23% and relatively wider range of measurements noted in the junction exponent estimations.

In a similar work done by our computer scientist collaborators, using a novel automated technique to analyse retinal geometrical features, [161] it was found that there was a noticeable discrepancy between published data on junction exponent and actual measurements obtained with their data set. They reported that the junction exponent values were greater than 10 for approximately less than 4% of cases and greater than 5 for less than 21% of cases. (Unpublished data). Analysis of the results showed that the junction exponent values suffered from over-sensitivity and wide scatter. This was further clarified by a mathematical investigation which demonstrated that in vascular bifurcations, an error of vessel width measurement of less than one pixel in only one vascular segment can shift the junction exponent values from the optimum theoretical value of 3 to a value of 1 as shown in table 4.10

Junction exponent = 3				Junction exponent = 1		
D0	d1	d2		d0	D1	d2
1.26	1	1		2	1	1
2.08	2	1		3	2	1
3.04	3	1		4	3	1
4.02	4	1		5	4	1
5.01	5	1		6	5	1

Table 4.10: A mathematical experiment to demonstrate the over-sensitivity of junction exponent calculations

This over-sensitivity of the junction exponent calculations to minor variation in vessel width estimations might explain our wide range of measurements and high variability and make it a less than ideal value for investigational studies.

2. Inter-observer variability

We then assessed the agreement between graders by comparing the measurements and estimations obtained from the first image analysis by the first observer with those obtained from the second observer's image analysis. The results of the Bland-Altman assessment suggested that there was a notable clinically significant difference between graders in estimating vessel width. This was also noted, yet in a lesser extent, for relative diameters and ratio estimates. There was no obvious similar trend regarding angular measurements. These results were in agreement with previous reports of subjective observer variation in defining the width of the blood column, with some observers tending to over-estimate the width, by including the shadowing effect around the vessel edge. This variation can exist in larger vessels where this shadowing effect is exaggerated as well as in small vessels.

The large calculated standard deviations and wide 95% limits of agreement noted for the inter-observer variability study could be considered clinically significant if measurements obtained by different observers utilising the adopted semi-manual technique are compared. Such fact constitutes a considerable limitation to applying the designed technique in clinical setting where measurements would be obtained and analysed by different users. This reflects the inevitable variation in observer input in semi-manual techniques and highlights the need for development of fully automated vascular analysis software packages that would overcome this hurdle in retinal vascular analysis. It is worth noting that for the rest of the thesis experiments, only one observer analysed the retinal images, thus the inter-observer variability was not taken into account for further analysis and thus the large inter-observer variability would not reflect on, or discredit further results presented in this thesis to answer the research hypothesis.

Individual variability

1. Intra-visit variability

The variability of measurements obtained from images captured on the same day as analysed by the same observer were then assessed. Our results showed that there was a considerable increase in the coefficient of variation of measurements across images as compared to the intra-observer variation. Nevertheless, the coefficient of variation of absolute vessel width measurements in our study ranged from 6.1% to 8.9%, which compared favourably to the coefficient of variation range of 5.0% to 29.9% for measurements obtained from images taken at different times by the observer-driven method as reported by Newsom and his co-workers. [160] Similarly, the coefficient of variation for the bifurcation angles measurements, and ratios estimations – excluding the junction exponent – ranged from 1.4% to 12.7%. In terms of units of the original data, the within-subject standard deviation for vessel width measurements averaged around half a pixel, and for the bifurcating angles estimations, the average within-subject standard deviation was 4 degrees.

Again, the poor reliability of junction exponent estimates was reflected by a rather high coefficient of variation reaching 34%. Considering the high intra-observer and intra-visit coefficient of variation calculated for the junction exponent, it was deemed of poor reliability, and thus of questionable significance in further analysis. We have included the results of junction exponent analysis in the rest of the study for completion of data analysis and to compare with other published data; nevertheless, caution was taken in interpreting its subsequent results based on the results presented here.

2. Inter-visit variability

We concluded this section of the study for evaluating individual variations of the retinal vascular features over time by assessing the agreement of measurements and estimates of the different retinal geometrical parameters between images captured

two weeks apart. We also examined the effect of short term changes in mean systemic blood pressure and blood glucose levels over the period of two weeks on the variability of measurements. Our results showed no obvious trend or bias for the mean differences values between the two visits in relation to absolute vessel widths, angular measurements or relative widths and ratio estimates. The standard deviations were comparable – yet slightly higher – to the intra-visit within-subject standard deviations. The wide 95% limits of agreement reflected merely the measurement variations from different captured images as previously reported to be the main source of variability. The results noted from the Bland-Altman plots revealed no evidence of difference in the measurements agreement levels between normal and diabetic subjects as noted by the spread of measurements around the arithmetic mean difference values.

However, it was of interest to note the increase in range of variability of the bifurcating angles measurements between the 2 visits in subjects with high blood pressure or high blood glucose changes as reflected by the wide 95% confidence interval as calculated by the T test. The exact cause behind this observation is difficult to interpret, yet it might reflect a certain feature of vascular network stress as a consequence of the altered blood flow in the retinal vessels resulting from these acute changes in blood pressure and / or blood glucose levels. [162]

In an experimental study on small arterioles in a striated cremaster muscle, Frame and Sareluis presented interesting unexpected findings of changes in the bifurcating angles with changes in blood flow between rest and maximal dilatation. These changes were estimated to be as high as +/- 50 degrees at any junction. They speculated that these changes might reflect angle participation in the regulation of flow distribution. [163] In their study, they thus demonstrated that the bifurcation geometry was not anatomically invariant (ie: fixed and unable to change), but can change significantly with changes in flow.

We acknowledge that there is a difference in the vessel wall structure and vascular orientation between the retinal vascular network and striated muscle arterioles; however, we may speculate that our findings might reflect a similar geometrical change in the retinal vascular bifurcations as a response to blood flow changes. In the

study by Frame and Sarelius, the overall mean angle values at rest were not different from the mean angle during maximal dilatation, this was explained by the fact there was an equal likelihood for angle increase or decrease at each position, an observation that could also be applied to our data and explain the low mean difference found in the high blood pressure and blood glucose change subgroups despite the wide 95% confidence interval. These results would need further exploration and in-depth analysis to confirm this observation due to its implications on further retinal vascular geometrical studies.

The overall results of the variability study showed that the main sources of measurements variation were across-images as well as within observers. The intra-visit and inter-visit variability was in keeping with the results of previous studies [159], and could reflect subtle changes in angles of the captured retinal images that came along with changes in eye positioning each time a photograph was taken. These limitations of the current photographic technology would outweigh the accuracy and precision of different technique measurements. Photographic techniques allowing automated alignment of sequence of retinal images might help reduce this source of variability. The inter-observer variability demonstrated here constitutes a significant practical limitation for the application of the semi-manual technique in clinical practice where retinal architectural and geometrical data are collated by multiple users and would thus preclude sensitive comparisons to be made and results to be verified.

Technique comparison

In this section, we compared the precision of the performance of our custom designed semi-manual technique to other used semi-manual and observer assisted techniques. The results showed that the designed technique performance was comparable and actually more precise than the other techniques as reflected by the lower standard deviation values, tighter confidence intervals and lower coefficient of variations for the examined parameters. This might reflect the fact that all other measuring vessel width techniques relied on measuring the direct distance between two points defined by an observer. The observer then estimates the vessel width from the developed intensity cross sectional profiles through identifying the kick points or

155

placing a rectangle centred on these profiles, or identifying the width at half height of the profile. These techniques suffered from certain problems:

1. These methods depend on measuring the direct distance between two points defined by the observer. The judgement of these corresponding points along the vessel edge would reflect the width at that particular point only and might suffer inaccuracies especially with hazy or tortuous vessels.

2. The placement of these points should also be accurately oriented to create a perpendicular profile to the vessel longitudinal axis to reflect the true width at that point. Inaccuracies of definite orientation of these two points could lead to faulty over-estimating of the vessel width.

3. These methods would then rely on defining the vessel width from the developed cross sectional intensity profile, which could suffer markedly with the given image resolution and contrast of the examined vessel

In our experiment, we noted that, with the given image resolution for this study, it was difficult to define the position of the kick points from the developed intensity profile to accurately define the vessel width, even in fairly high contrast and clear vessels as shown in the examples below. This might have adversely affected the precision of the other techniques performances. (Figure 4.7)
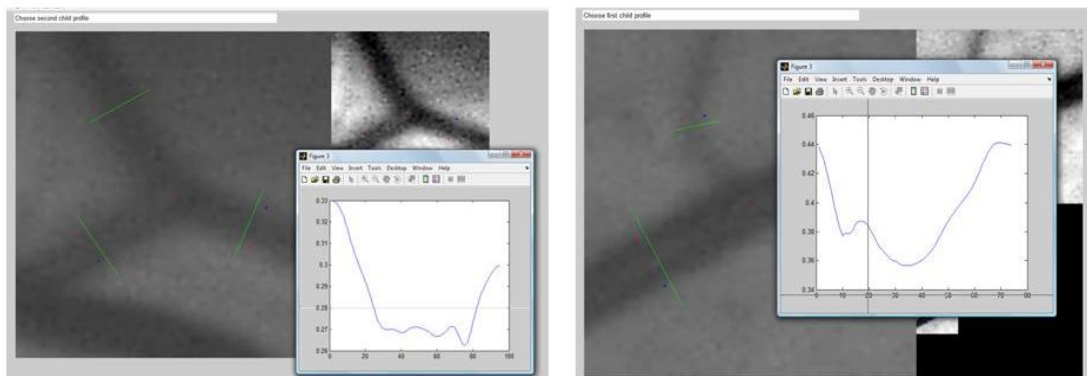
Figure 4.12: Examples of vessel intensity profiles generated with the available image resolution with poor definition of the kick points.

On the other hand, the developed technique depended on placing a rectangle over a vessel segment, which made adaptation of the rectangle direction to the segment direction easier, and solved one of the main difficulties of orientation for manual width measurements. At the same time, the observer judgement on the correct edge was not made just at a particular point but along a short continuous distance which made width measurements more robust and less affected by blurring and low contrast edge.

4.8 Conclusion

In this chapter, we examined the precision of performance of our developed technique, and evaluated the potential sources of variability in our measurements and geometrical parameter estimations. The overall results demonstrated that the geometrical parameter measurements were reproducible and the variations found compared favourably to those reported in other studies. The technique could thus be reliably used for further analysis of similar population cohorts for the research purpose to identify any differences in retinal vascular geometrical features between normal and diabetic subjects, with considerations to be made for the technique to be utilised by a single observer for the rest of the study to minimise the potential sources of variability.

Chapter 5: Assessment of Retinal Vascular Geometry in Normal Subjects

5.1 Overview

In the previous chapter, we established the observer and individual sources of variability associated with our custom developed semi-manual measurement technique and the repeatability of the different architectural and geometrical measurements obtained utilising this technique. The precision of the technique's performance as compared to other semi-manual measurement techniques was also determined. The results were deemed satisfactory for the technique to be used for further assessment of the different retinal vascular geometrical parameters in cohorts of normal and diabetic subjects. In this chapter, we evaluate the range and distribution of the vascular geometrical parameters measurements and estimations in a cohort of healthy normal volunteer subjects, and the degree of optimality of these measurements as compared to theoretical predictions.

The results of this study constitute a valuable comprehensive normative data which would act as a benchmark reference set for further analysis of retinal vascular geometry in similar population cohorts of diabetic subjects in this thesis, and also for any future similar work on geometrical analysis of the retinal vascular network in other systemic vascular diseases.

5.2 Introduction

The retinal vasculature has the advantage of being easily viewed directly and noninvasively, thus offering a unique and easily accessible "window" to study the health and disease of the human microcirculation in vivo. [113]

Novel advances in retinal photographic techniques and in image analysis have now allowed detailed objectives measurement of the retinal vascular changes. In particular, recent developments in quantitative measurement of retinal vascular calibre have greatly increased the knowledge of the clinical significance and influence of systemic, environmental and genetic factors on the retinal vasculature. [78, 164] Moreover many recent studies have been published associating the changes in retinal vascular calibre measurements with systemic vascular diseases such as diabetes [165, 166] and hypertension [156, 167, 168], and cardiovascular outcomes such as stroke [98, 169] and coronary heart disease. [99]

Similarly, new computer-assisted tools and methods allowed the measurement of other architectural changes in the retinal microvasculature. As previously discussed, for example hypertension had been associated with reduced branching angle at arteriolar bifurcations, and reduced microvascular density. [88, 128] Some of the retinal vascular geometrical changes had also been associated with increased cardiovascular risk. For example, the Beaver Dam study demonstrated that suboptimal arteriolar bifurcation and decreased arteriolar tortuosity were associated with coronary heart mortality. [101]

The measurements of these early changes in the retinal vascular calibre and architecture – not detectable on routine clinical examination – might thus allow the identification of individuals with or at risk of diabetes and hypertension and their subsequent complications; however there are certain issues that should be addressed before retinal vascular analysis can be utilized in clinical practice.

One of these main issues is the lack of normative reference data for the vascular measurements to be implemented in clinical settings; despite a large published data on the associations and risk prediction of retinal vascular measurements in different

population-based studies, there is a lack of age, body size and blood pressure-specific normative data. [113] There is also limited understanding and analysis of changes in the retinal venular geometry, as most of previous studies have focused mainly on the retinal arteriolar changes. [170]

This study was thus conducted in an attempt to provide a normative reference data for retinal arteriolar and venular vascular geometrical measurements in healthy adults, using our custom-designed semi-manual technique. This data was essential to establish age matched control data to compare with the cohorts of diabetic subjects with different grades of diabetic retinopathy to be analysed for this project. Moreover the resulting normative data would also be helpful in providing a benchmark for further future studies evaluating the associations or predictive values of the retinal geometrical architecture changes with different systemic vascular diseases using the same tool.

The study evaluated also the topographic distribution of the various retinal vascular architectural and geometrical measurements in a normal population. This was set to map any differences in these measurements across the retina in normative states to set a bench mark against which the spread of retinal vascular measurements in diabetics can be compared. Previous studies have suggested that there is certain topographic distribution of diabetic retinopathy lesions across the retina that might reflect certain risk factors for retinopathy progression that should be considered in future automated quantification of diabetic retinopathy. [171] Such regional differences in the distribution of diabetic retinopathy lesions could be related to corresponding regional differences in the adaptive mechanisms of retinal vasculature to increased blood pressure and increased metabolism in diabetes together with differences in retinal vascular diameters. [172]

5.3 Objectives

The objectives of this study were

1. To describe the distribution of retinal vascular geometrical measurements, and their associations with age, body mass index and smoking history in a cohort of healthy adult volunteers.

2. To assess the degree of consistency of the measured normative data with the optimal values – which render the vascular network efficient physiologically – as calculated on theoretical grounds as previously discussed.

3. To compare the retinal vascular geometrical measurements between both eyes in a sample of healthy adults to assess the inter-eye stability of measurements.

5.4 Subjects and methods

The study was approved by the local Sunderland NHS Trust medical ethics committee and followed the tenets of the Declaration of Helsinki, including informed consent.

The participants of this study were healthy non-diabetic, non-hypertensive volunteers who were invited to take part in the research project. The invitation process took place through wall-mounted posters describing the purpose and objectives of the research project. The approved patient information leaflet designed for the project, together with the consent form was provided to volunteers willing to take part in the study. They were mainly relatives of patients attending the Sunderland Eye Infirmary or members of the staff. All subjects in self-assessed good health were invited.

Exclusion criteria included any concurrent ocular pathology that would adversely affect the image quality or could possibly alter the retinal vascular architecture, such as corneal opacities, small pupils, cataract or other retinal and / or optic nerve pathology. Subjects with known refractive error beyond sphere equivalent of +/- 3 dioptres were also excluded, in an attempt to reduce any possible increased effect of the altered peripheral retinal curvature associated with high refractive errors on viewing peripheral vascular bifurcations, as well as rule out any detrimental association of altered retinal blood flow with myopia that might confound our results on the different geometrical parameters as previously discussed.

The blood pressure and body mass index (defined as weight in kilograms divided by height in square meters) were obtained for all participants following the study protocol previously described. Smoking history was recorded. Smoking was categorized as being non smoker, current smoker or ex-smoker. Positive ex-smoker history was defined by smoking one or more cigarette per day for as long as one year.

Dilated 50 degrees nasal and temporal retinal photographs were obtained for both eyes for all subjects using a Zeiss FF 450 Plus fundus camera fitted with a JVC KY-F70B 3CCD digital camera with a resolution of 1360 X 1024 pixels. Details of the study photographic protocol were described previously.

The nasal and temporal retinal images sets of one eye per subject were randomly selected for 20 recruited volunteers to be analysed. In addition, the retinal images of both eyes were analysed for a randomly selected sample of 5 normal subjects for the inter-eye comparison.

In the selected group of images, all identifiable arteriolar and venular bifurcations across the image were labelled and measured. Bifurcations lying within a circular zone of 1 disc diameter around the optic disc were excluded. Care was taken to include a wide spread of bifurcations across the whole image field, above and below the horizontal raphe and central as well as peripheral bifurcations. The details of the labelling and marking custom-designed computer algorithm were described in the methodology chapter.

The geometrical measurements extracted from each bifurcation were described in terms of

1. Absolute vessel width measurements in pixels (parent vessel width, larger child (child 1) vessel width, and smaller child (child 2) vessel width). The diameters of the parent vessel, larger child branch, and the smaller child branch were expressed as d_0, d_1, and d_2 respectively.

2. Bifurcating angles in degrees (θ, θ_1, θ_2): The bifurcation angle (θ) is the angle between the two children vessels, while angle θ_1 is the angle between the first (larger) child segment and the parent direction, and angle θ_2 is the angle between the second (smaller) child and the parent direction.

3. Relative diameter ratios, such as (λ, λ_1 and λ_2) and area ratio (β), the asymmetry ratio (α), the junction exponent (χ), and the optimality parameter (ρ).

The use of the absolute vessel widths could be complicated by the fact of variable ocular magnification effects; however the standardised photography technique adopted for all the study subjects tended to reduce this effect. These problems were also overcome by expressing the bifurcation diameters in terms of relative as well as actual measurements, which were independent of magnification effects and allowed for comparison of retinal vascular changes between individuals. [148]

- The diameter ratios, (Lambda 1 and Lambda 2) λ_1 and λ_2 are the diameters of the child 1 and child 2 divided by the diameter of the parent segment respectively. $\lambda_1 = d_1 / d_0$, $\lambda_2 = d_2 / d_0$.
- The bifurcation index (Lambda) λ is determined by dividing the diameter of the smaller child d_2 by the diameter of the larger child d_1 so the value of λ is greater than 0 and less or equal 1 ($\lambda = d_2 / d_1$)
- The asymmetry ratio α is the cross-sectional area of the smaller branch divided by that of the larger. The value of α is greater than 0 and less or equal 1. ($\alpha = d_2^2 / d_1^2$).

- The area ratio β (the expansion factor), is the sum of the cross-sectional areas of the two branches divided by that of the parent segment at a bifurcation. $\beta = (d_1^2 + d_2^2)/d_0^2$

- The junction exponent; the exponent χ relating the parent and daughter diameter vessels as follows: $(d_1^x + d_2^x) = d_0^x$

- The optimality parameter ρ; in which $\rho = [d_0^3 - (d_1^3 + d_2^3]^{1/3} / d_0$.

The range of measurements of these different geometrical parameters was calculated for the selected healthy volunteers. These values were compared between both eyes in a sample of subjects. The degree of optimality of the retinal vascular networks in the cohort of healthy volunteers was evaluated by assessing the adherence of their geometrical measurements to the theoretical predicted optimum values.

5.5 Statistical analysis

Descriptive statistical analysis is initially presented for the overall data, and the arterial and venous subcategories. Values presented were the mean, minimum, maximum, 1st and 3rd quartiles, standard deviation and the 95% confidence interval range. Unpaired two sample T test was then used to assess the difference of geometrical measurements between different subcategories such as arteriolar versus venular bifurcations, superior versus inferior, and nasal versus temporal bifurcations. The unpaired two sample T test was also used to compare the various geometrical measurements and estimates between right and left eyes for a sample of subjects. The mean difference, 95% confidence interval of the difference and the p value were presented in the results. P values of 0.05 or less were considered statistically significant for the t test results. Multiple regression analysis calculations were made to assess the effect of continuous variables such as age, BMI, and optic disc ratio on the results. Regression plots were used to demonstrate any relationships. A p-value of 0.05 or less was also considered significant for the regression analysis.

5.6 Results

1. Descriptive analysis of the distribution of the geometrical vascular parameters in normal subjects

The nasal and temporal retinal images sets of 20 eyes of 20 normal subjects (Five males and 15 females) were analysed for this study. The mean age was 48.4 years (SD = 11.1), (range 31-65yrs). Ten right and 10 left eyes were assessed. A total of 542 retinal vascular bifurcations were nominated and analysed. Two hundred and thirty bifurcations were arterial while 312 were venous.

The range of measurements and estimates were calculated for the overall data of all the parameters. The analysed parameters included the absolute vessel width measurements, bifurcating angles estimates, relative diameter ratios and other geometrical ratios as previously described. For each parameter, the mean, minimum, maximum, 1st and 3rd quartiles, standard deviation and 95% confidence interval were calculated. The data were then subdivided into arteriolar and venular bifurcations and descriptive statistical measurements were calculated for all parameters of each category as above and shown in table 5.1

OVERALL DATA	MEAN	MINIMUM	MAXIMUM	STD DEVIATION	95% CONFIDENCE INTERVAL		1ST QUARTILE	3RD QUARTILE
PARENT WIDTH d_0	8.06	3.47	14.83	2.34	7.86	8.25	6.14	9.80
CHILD 1 WIDTH d_1	7.25	3.05	14.18	2.26	7.05	7.44	5.37	8.73
CHILD 2 WIDTH d_2	5.22	2.43	12.31	1.57	5.09	5.35	4.06	6.18
ALPHA α	0.58	0.09	1.00	0.23	0.56	0.60	0.40	0.77
BETA β	1.27	0.66	2.32	0.21	1.25	1.28	1.13	1.40
LAMBDA λ	0.75	0.29	1.00	0.16	0.73	0.76	0.64	0.88
LAMBDA 1 λ_1	0.90	0.64	1.10	0.08	0.89	0.90	0.85	0.95
LAMBDA 2 λ_2	0.66	0.29	1.05	0.13	0.65	0.67	0.58	0.75
THETA ANGLE θ	77.19	38.32	132.46	15.50	75.88	78.49	66.25	87.74
THETA 1 ANGLE θ_1	24.57	0.04	71.66	21.08	22.80	26.35	12.16	33.31
THETA 2 ANGLE θ_2	53.40	8.00	106.99	19.68	51.74	55.05	39.35	67.36
JUNCTION EXPONENT χ	3.69	1.24	18.92	2.11	3.51	3.87	2.48	4.20
OPTIMALITY PARAMETER ρ	-0.11	-1.15	0.89	0.54	-0.15	-0.06	-0.58	0.45

ARTERIOLES								
	MEAN	MINIMUM	MAXIMUM	STD DEVIATION	95% CONFIDENCE INTERVAL		1ST QUARTILE	3RD QUARTILE
PARENT WIDTH d_0	7.45	3.54	13.54	1.75	7.23	7.67	6.14	8.53
CHILD 1 WIDTH d_1	6.76	3.10	14.18	1.73	6.54	6.98	5.47	7.97
CHILD 2 WIDTH d_2	5.25	2.50	12.31	1.58	5.08	5.47	4.07	6.24
ALPHA α	0.64	0.11	1.00	0.21	0.61	0.67	0.49	0.82
BETA β	1.37	0.80	2.32	0.21	1.32	1.37	1.20	1.45
LAMBDA λ	0.79	0.33	1.00	0.14	0.77	0.81	0.70	0.90
LAMBDA 1 λ_1	0.91	0.72	1.10	0.07	0.90	0.92	0.86	0.95
LAMBDA 2 λ_2	0.71	0.32	1.05	0.11	0.69	0.72	0.62	0.79
THETA ANGLE θ	75.34	38.32	128.85	15.90	73.28	77.40	62.47	86.30
THETA 1 ANGLE θ_1	24.83	0.40	71.66	15.34	22.85	26.81	12.35	35.31
THETA 2 ANGLE θ_2	50.63	8.38	98.64	19.77	48.07	53.18	37.68	62.76
JUNCTION EXPONENT χ	4.16	1.48	17.47	2.16	3.88	4.44	2.77	4.75
OPTIMALITY PARAMETER ρ	-0.28	-1.15	0.78	0.51	-0.35	-0.22	-0.65	0.28

VENULES								
	MEAN	MINIMUM	MAXIMUM	STD DEVIATION	95% CONFIDENCE INTERVAL		1ST QUARTILE	3RD QUARTILE
PARENT WIDTH d_0	8.50	3.47	14.83	2.60	8.22	8.79	6.18	10.63
CHILD 1 WIDTH d_1	7.60	3.05	13.85	2.51	7.32	7.88	5.31	9.62
CHILD 2 WIDTH d_2	5.18	2.43	11.28	1.57	5.00	5.35	4.03	6.08
ALPHA α	0.54	0.09	0.99	0.23	0.52	0.57	0.34	0.72
BETA β	1.21	0.66	1.86	0.18	1.19	1.23	1.08	1.32
LAMBDA λ	0.72	0.29	1.00	0.171	0.70	0.73	0.59	0.85
LAMBDA 1 λ_1	0.89	0.64	1.06	0.08	0.88	0.90	0.84	0.94
LAMBDA 2 λ_2	0.63	0.29	0.96	0.129	0.61	0.64	0.54	0.72
THETA ANGLE θ	78.54	39.52	132.46	15.08	76.87	80.21	68.10	88.5
THETA 1 ANGLE θ_1	24.39	0.04	70.83	24.46	21.69	27.09	11.74	31.7
THETA 2 ANGLE θ_2	55.42	8.00	106.89	19.38	53.29	57.56	40.41	68.9
JUNCTION EXPONENT χ	3.35	1.24	18.92	2.01	3.13	3.58	2.32	3.63
OPTIMALITY PARAMETER ρ	0.02	-0.93	0.85	0.52	-0.04	0.08	-0.49	0.50

Table 5.1: Descriptive geometrical measurements for the overall normal vascular bifurcations, and the arteriolar and venular subgroups.

The geometrical parameters collated from the arteriolar and venular bifurcations subgroups were then compared. The overall data was also subdivided into nasal and temporal, superior and inferior subgroups to assess the distribution of measurements across the fundus of the normal subjects.

The unpaired two sample T Test was then used to identify whether there were statistical differences in the spread of measurements between the subgroups. The mean difference, 95% confidence interval and the p values are presented for each parameter in each test as shown in tables 5.2, 5.3 and 5.4

Two sample T test arterioles versus venules				
	mean difference	95% Confidence Interval		P value
PARENT VESSEL WIDTH	-1.05	-1.42	-0.69	0.000
CHILD 1 VESSEL WIDTH	-0.84	-1.20	-0.48	0.000
CHILD 2 VESSEL WIDTH	0.09	-0.17	0.365	0.490
ALPHA	0.099	0.06	0.137	0.000
BETA	0.134	0.098	0.168	0.000
LAMBDA	0.073	0.046	0.097	0.000
LAMBDA 1	0.020	0.004	0.029	0.014
LAMBDA 2	0.081	0.059	0.101	0.000
THETA ANGLE	-3.20	-5.90	-0.54	0.018
THETA 1 ANGLE	0.40	-2.90	3.80	0.800
THETA 2 ANGLE	-4.80	-8.10	-1.40	0.005
JUNCTION EXPONENT	0.81	0.44	1.18	0.000
OPTIMALITY PARAMETER	-0.30	-0.39	-0.21	0.000

Table 5.2: Results of the unpaired T test comparing arteriolar versus venular geometrical data in healthy subjects

Two sample T test nasal versus temporal				
	mean difference	**95% Confidence Interval**		**P value**
PARENT VESSEL WIDTH	-0.41	-0.81	0.00	0.048
CHILD 1 VESSEL WIDTH	-0.36	-0.75	0.02	0.066
CHILD 2 VESSEL WIDTH	-0.54	-0.8	-0.277	0.000
ALPHA	-0.048	-0.09	-0.006	0.024
BETA	-0.03	-0.068	0.008	0.120
LAMBDA	-0.035	-0.065	-0.006	0.019
LAMBDA 1	0.002	-0.019	0.016	0.760
LAMBDA 2	-0.029	-0.053	-0.005	0.015
THETA ANGLE	-1.70	-4.50	1.21	0.260
THETA 1 ANGLE	-0.90	-4.20	2.40	0.600
THETA 2 ANGLE	-2.00	-5.70	1.78	0.300
JUNCTION EXPONENT	-0.27	-0.64	0.09	0.150
OPTIMALITY PARAMETER	0.066	-0.031	0.163	0.180

Table 5.3: Results of the unpaired T test comparing nasal versus temporal geometrical data in healthy subjects

Two sample T test superior versus inferior				
	mean difference	**95% Confidence Interval**		**P value**
PARENT VESSEL WIDTH	-0.05	-0.45	0.35	0.810
CHILD 1 VESSEL WIDTH	0.33	-0.31	0.46	0.720
CHILD 2 VESSEL WIDTH	-0.11	-0.38	0.158	0.420
ALPHA	-0.012	-0.052	0.028	0.550
BETA	0.014	-0.022	0.05	0.440
LAMBDA	-0.01	-0.038	0.017	0.470
LAMBDA 1	0.009	-0.004	0.022	0.190
LAMBDA 2	-0.004	-0.025	0.018	0.750
THETA ANGLE	0.50	-2.13	3.13	0.710
THETA 1 ANGLE	-3.30	-6.67	0.20	0.065
THETA 2 ANGLE	2.60	-0.80	5.90	0.130
JUNCTION EXPONENT	-0.04	-0.41	0.32	0.810
OPTIMALITY PARAMETER	-0.03	-0.127	0.056	0.440

Table 5.4: Results of the unpaired T test comparing superior versus inferior geometrical data in healthy subjects

On analysing the results comparing the arteriolar and venular measurements, there was an overall statistically significant difference noted in most of the absolute width measurements, angular estimates and the other geometrical ratios. These results suggested that, in healthy normal subjects, venular vascular bifurcations were generally larger than the arteriolar counterparts. The venular vascular network exhibited also wider bifurcating angles as compared to the arteriolar network. There was an apparent difference in the relationship of the vascular segments widths at the vicinity of the bifurcations between the two subgroups leading to a significant difference in the asymmetry and area ratios as well as the junction exponent estimates, with the arteriolar system showing a tendency towards higher values as compared to the venular network.

On comparing the nasal and temporal bifurcations, the results of the unpaired two sample T test demonstrated a statistically significant difference of the absolute vessel width and relative diameter ratio of the parent and smaller child vessels, with the temporal vessels being wider than their corresponding nasal vessels. Such a difference was not noted for the larger child vessel segment. This was also reflected in a difference in the asymmetry ratio (α) between these subgroups which was statistically significant. The rest of the geometrical ratio parameters and bifurcating angular estimates revealed no clear trends or statistical significant differences.

Similarly, the results of analysis of the superior versus inferior vascular bifurcations subcategories showed no statistical difference in any of the measurements and estimations of the examined geometrical parameters, thus suggesting no fixed trend in the distribution of these geometrical features across the horizontal raphe in the retinal vascular network of normal subjects.

The distribution of the different geometrical measurements across the retina in relation to their proximity to the optic disc was evaluated using the liner regression analysis and regression plots comparing each of the parameters as a factor of the optic disc ratio.

The results showed a statistically significant inverse relationship of all the absolute vessel widths for the parent and child vessels to the optic disc ratio. (R-sq = 7, 6.1,

and 9.2 for d_0, d_1, and d_2 respectively) (p = 0.000). These results reflect the distribution of the larger retinal vessels around the optic disc with the gradual decrease in width with sequential branching towards the retinal periphery.

There was no similar relationship detected for the bifurcating angle estimates against the optic disc ratio (R-sq= 0.0, p = 0.630), in addition, no trends or relationships could be noted for the relative diameter ratios (R-sq= 0.2, 0.0, and 0.4 for λ, λ_1, and λ_2 respectively) (p= 0.200) or the other geometrical ratios' estimates. An example of the regression plots for the different geometrical parameters is shown in figure 5.1
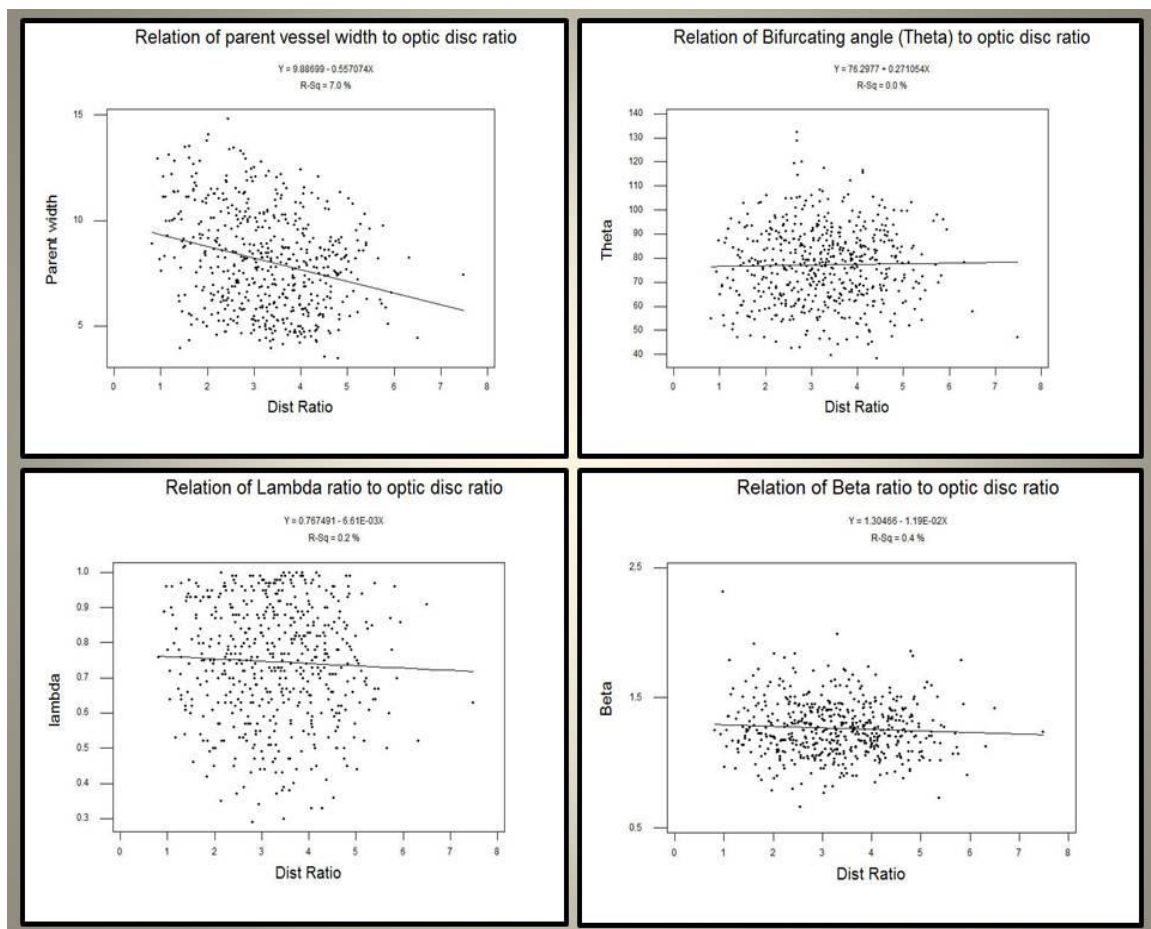
Figure 5.1: Examples of Regression plots for absolute vessel widths (Parent vessel), angular measurements (Θ angle), relative diameter ratios (Lambda ratio), and geometrical ratios (Beta ratio) in relation to optic disc ratio.

We then evaluated the relationship of the different recorded and calculated geometrical measurements with certain identified variables such as age, body mass index, and smoking history.

The unpaired T test was used to assess the effect of smoking history on the geometrical parameters in normal healthy subjects by comparing current smokers to non smokers as shown in table 5.5

Two sample T test current smoking versus non-smoking				
	mean difference	95% Confidence Interval		p value
PARENT VESSEL WIDTH	0.42	-0.12	0.96	0.120
CHILD 1 VESSEL WIDTH	0.46	-0.08	0.99	0.092
CHILD 2 VESSEL WIDTH	0.16	-0.20	0.51	0.380
ALPHA	-0.01	-0.07	0.4	0.620
BETA	0.01	-0.04	0.05	0.950
LAMBDA	-0.01	-0.05	0.03	0.480
LAMBDA 1	0.01	-0.02	0.02	0.520
LAMBDA 2	-0.01	-0.04	0.02	0.480
THETA ANGLE	-2.10	-5.20	0.90	0.170
THETA 1 ANGLE	-0.90	-4.11	2.33	0.590
THETA 2 ANGLE	-1.30	-5.40	2.80	0.530
JUNCTION EXPONENT	-0.27	-0.64	0.12	0.170
OPTIMALITY PARAMETER	0.03	-0.08	0.15	0.510

Table 5.5: Results of the unpaired T test comparing the geometrical data in smokers versus non-smokers healthy subjects

The results of the T test showed no significant difference between the two subgroups for any of the analysed geometrical parameters. A similar result was also found when non-smokers were compared to the ex-smokers subgroup.

Multiple regression analysis was then used to examine the effect of age and BMI on the different geometrical parameters. For each parameter analysed, the **(F ratio)** determine the existence of linear relationship between the measurements and "combined" effect of the two variables (age and BMI) and the p value for

significance. The **(T ratio)** demonstrate whether any of the variables has an influence on the measurements over and above the other variable and the p value denotes the significance. The spread of the results is shown in table 5.6

RESULTS OF MULTIPLE REGRESSION ANALYSIS			
		AGE	BMI
	Combined F Ratio (p value)	T Ratio (p value)	T Ratio (p value)
PARENT VESSEL WIDTH	1.87 (0.156)	-1.56 (0.249)	1.43 (0.153)
CHILD 1 VESSEL WIDTH	2.20 (0.111)	-1.23 (0.221)	1.58 (0.114)
CHILD 2 VESSEL WIDTH	1.11 (0.329)	-1.44 (0.150)	-0.52 (0.602)
ALPHA	2.59 (0.076)	0.82 (0.410)	-2.03 (0.043)
BETA	0.55 (0.575)	0.01 (0.996)	-1.05 (0.295)
LAMBDA	2.67 (0.070)	0.61 (0.545)	-2.61 (0.031)
LAMBDA 1	0.67 (0.551)	-0.60 (0.547)	0.93 (0.353)
LAMBDA 2	2.42 (0.090)	0.36 (0.720)	-2.13 (0.034)
THETA ANGLE	0.49 (0.614)	-0.99 (0.324)	-0.15 (0.878)
THETA 1 ANGLE	0.94 (0.393)	1.36 (0.174)	0.26 (0.797)
THETA 2 ANGLE	1.69 (0.185)	-1.84 (0.067)	-0.31 (0.760)
JUNCTION EXPONENT	2.06 (0.129)	0.24 (0.809)	-1.98 (0.048)
OPTIMALITY PARAMETER	0.11 (0.894)	-0.46 (0.647)	0.07 (0.943)

Table 5.6: The results of the multiple regression analysis demonstrating the effect of age and BMI on the geometrical measurements in healthy normal subjects.

The results of the multiple regression analysis showed no obvious combined or separate effect of age and BMI on most of the geometrical features, apart from a weakly significant effect of BMI on the α, λ, λ_2, and junction exponent χ ratios. Linear regression plots were observed for these relationships, and a very low R-sq was noted in each case, thus the clinical significance of such relationships could be ignored.

2. Assessment of degree of consistency of our normative measured data with theoretical and optimal values.

In this section, we evaluated the degree of optimality of our data results as compared to the published theoretical calculated optimal values and relationships.

- An arterial junction was defined to be highly optimal when the area ratio β measured between 1.15 and 1.4, and the total bifurcating angle is between 75º and 102º, with the four optimality principles being closest to their predictions. The area ratio Beta also equals 1.26 in symmetrical bifurcations. [72, 81]

In this study, the total bifurcating angle (θ) ranged between 75º and 102º in 52% of overall cases. (45% in arteriolar bifurcations and 56% in venular bifurcations), (47% in proximal bifurcations and 53.5% in distal bifurcations)

Furthermore, the area ratio β values of 1.15 to 1.4 occurred in 48% of the overall data. (44% in arteriolar bifurcations and 49% in venular bifurcations), (45% in proximal bifurcations and 48% in distal bifurcations).

As previously shown in table 5.1, the mean value of β ratio was 1.27 in the overall cases of this study, however this value deviated from the theoretical calculated value when the data were sub classified to arteriolar and venular bifurcations with the mean beta value estimated as 1.37 and 1.21 respectively. It is noteworthy that in our study, symmetrical and asymmetrical bifurcations were included, and no segregation was done for analysis. This might explain the discrepancy of our collective results from the calculated theoretical value.

- Theoretically, the branching angle of the smaller child vessel (θ_2) is always greater than that subtended by the larger child vessel (θ_1) and the maximum value of (θ_2) is 90º. [72]

In this study, the described relationship was true in 82.7% of the overall data. (81.4% in arteriolar bifurcations and 83.8% in venular bifurcations), (80% in proximal

bifurcations and 84.5% in distal bifurcations). The (θ_2) branching angle values in our results reached 106.9º, and in total the (θ_2) angle measured more than 90º in 2.9% of the overall bifurcations. (3.4% in arteriolar versus 2.5% in venular bifurcations, and 4% in proximal versus 2.1% in distal bifurcations)

- Theoretically, at a junction, the parent vessel segment width should be greater than the first child segment width, which in turn should be greater than the second child segment width, thus in theory the values of the asymmetric ratio α, and the relative vessel diameter ratios λ , λ_1 and λ_2 should all be less or equal 1

Our results showed alpha values to be always equal or less than 1. In cases of the diameter ratios λ, λ_1, and λ_2 the resulting values exceeded the value of 1 in some cases of the overall data and in the subcategories with varied percentages as follows

Percentage of cases with values exceeding 1					
	Overall	**Arteriolar**	**Venular**	**Proximal**	**Distal**
Lambda	1.10%	2.10%	0.31%	0.45%	0.00%
Lambda 1	5.50%	7.80%	4.10%	5.45%	5.90%
Lambda 2	0.10%	0.40%	0.00%	0.45%	0.00%

- In an optimal branching condition, the junction exponent χ should be equal to 3

In this study, our results demonstrated an overall mean junction exponent χ of 3.69, the means of the arteriolar and venular bifurcations subcategories were 4.16 and 3.35 respectively. It was also estimated as 3.82 for proximal bifurcations as compared to 3.60 for the distal bifurcations.

As we discussed in the previous chapter, the junction exponent estimates suffered from being vulnerable to minor changes in vessel width calculations. Indeed, this was also noted in the normative data presented here. The junction exponent was 0 for 6.4% of the overall results (8.2% in arteriolar bifurcations and 5.4% in venular bifurcations), (6.3% in proximal bifurcations and 7.3% in distal bifurcations). The junction exponent values also measured more than 5 in 14% of the overall cases. (20% in arteriolar bifurcations versus 9.7% in venular bifurcations), (17% in proximal bifurcations as compared to 12.2% in distal bifurcations)

- Based on theoretical calculations, the relationships of the different parameters in arterial bifurcations against the asymmetry ratio α had been plotted. The resultant theoretical predicted curves were governed by the optimality principles of minimisation of lumen surface, lumen volume, pumping power and endothelial drag. [87]

Our arteriolar normative results demonstrated a qualitative tendency towards the theoretical curves, however with a considerable amount of variability in certain parameters. This could be explained in part by the expected normal biological scatter. The theoretical predictions and our normative data are presented in terms of "β, λ_1, λ_2, θ, θ_1, θ_2" features as a function of "α" as shown in figure 5.2 – 5.7
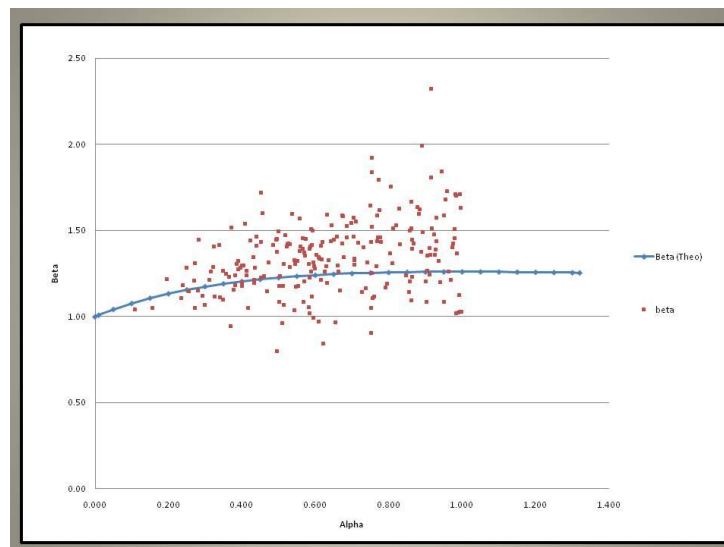
Figure 5.2: Measurements of β in relation to α. The solid curve line is based on theoretical results, while the scatter points represent our arteriolar normative data results.
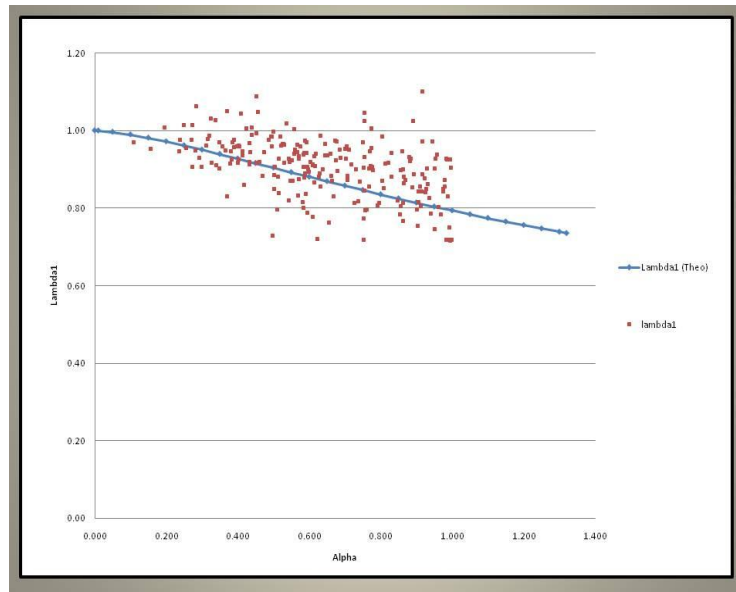
Figure 5.3: Measurements of λ_1 in relation to α. The solid curve line is based on theoretical results, while the scatter points represent our arteriolar normative data results.
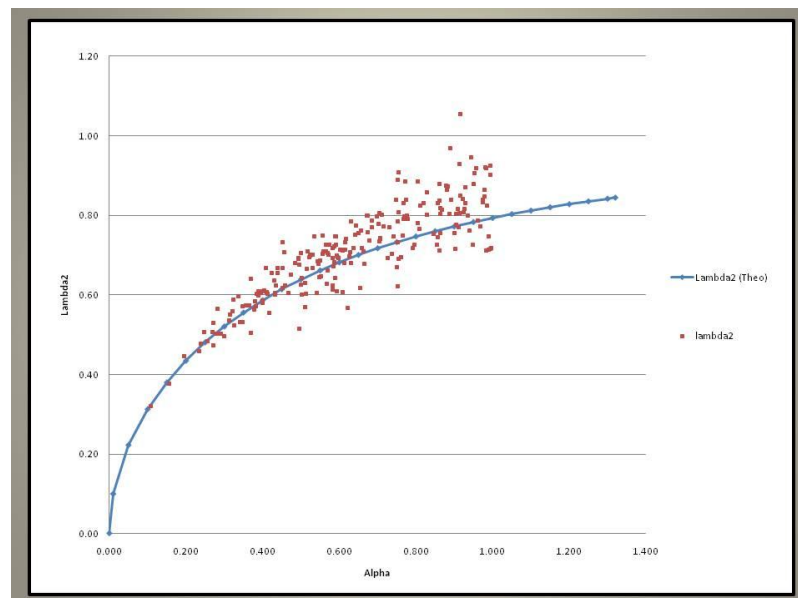
Figure 5.4: Measurements of λ_2 in relation to α. The solid curve line is based on theoretical results, while the scatter points represent our arteriolar normative data results.
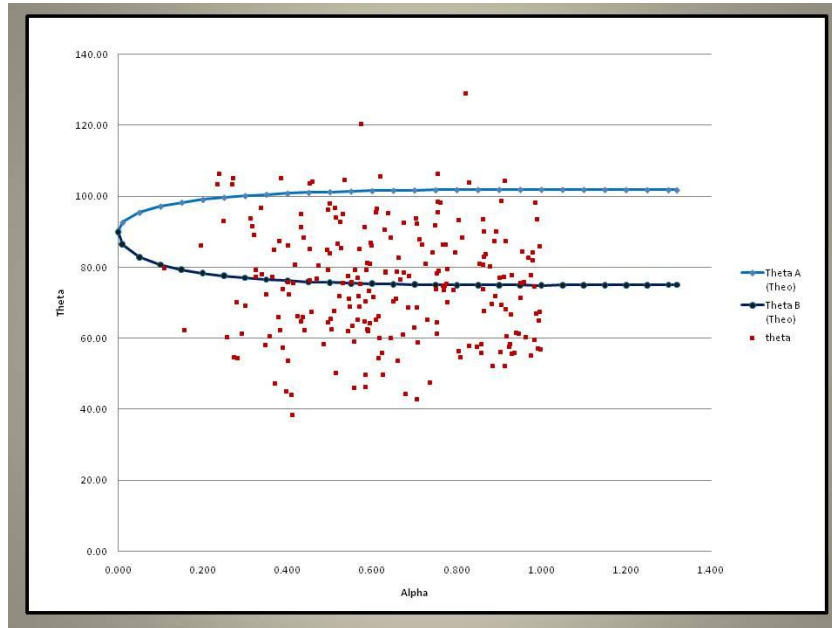
Figure 5.5: Measurements of θ in relation to α. The solid curve line is based on theoretical predictions based on condition of minimum lumen surface and drag and minimum lumen volume and pumping power, while the scatter points represent our arteriolar normative data results.
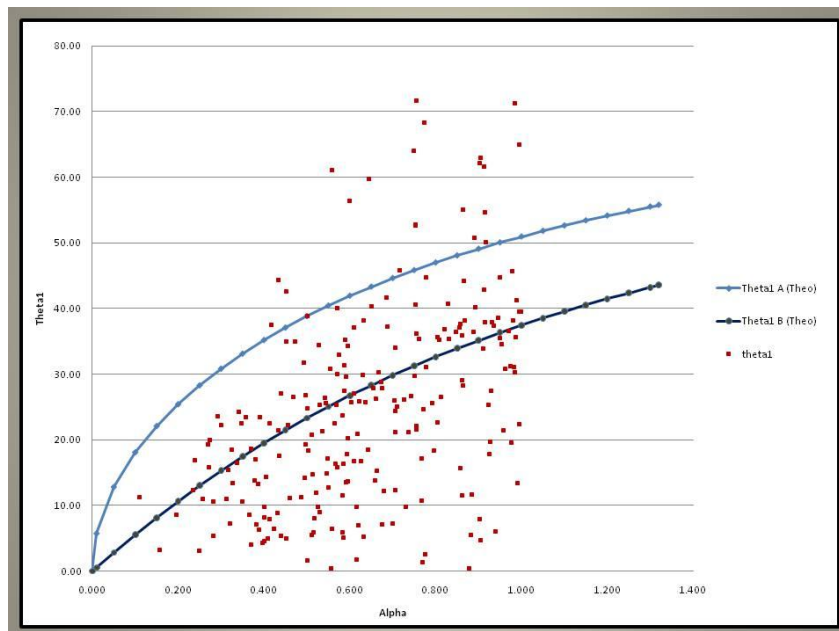
Figure 5.6: Measurements of θ_1 in relation to α. The solid curve line is based on theoretical predictions based on condition of minimum lumen surface and drag and minimum lumen volume and pumping power, while the scatter points represent our arteriolar normative data results.
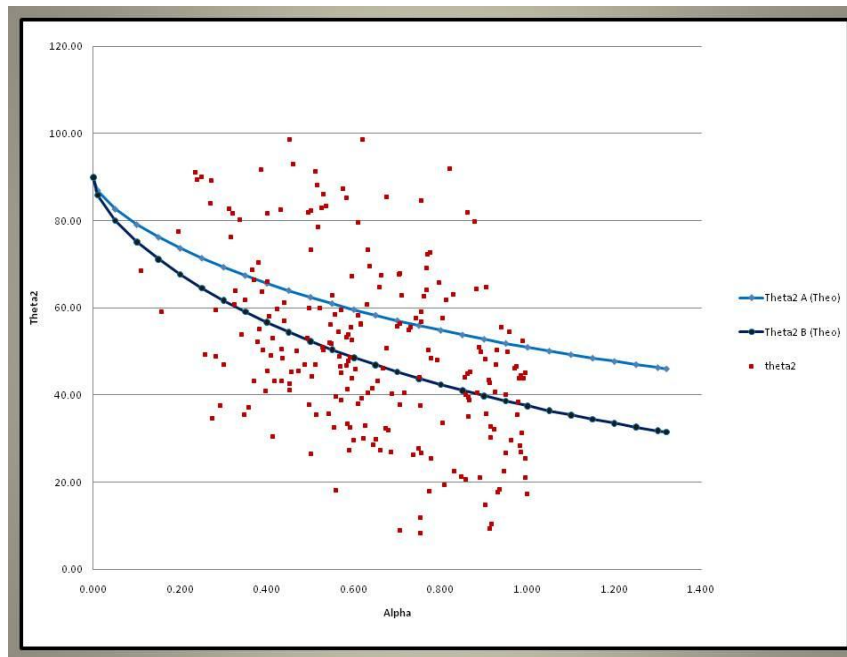
Figure 5.7: Measurements of θ_2 in relation to α. The solid curve line is based on theoretical predictions based on condition of minimum lumen surface and drag and minimum lumen volume and pumping power, while the scatter points represent our arteriolar normative data results.

Quantitatively, when bands of only +/- 10% deviation from each of the theoretical optimum curves in figures 5.3 – 5.7 were constructed, the amount of arteriolar normative data in our study that would be encompassed within this range was calculated and presented here in comparison to the previously reported arteriolar data from a 34 years old man by Zamir and co-workers [87] as shown in table 5.7 (in case of β parameter, the data scatter appeared to be exaggerated as the diameters were squared in the expression of ratio β, thus bands of +/-20% deviation was constructed in this case).

Feature	Manual (Zamir)	Manual (rectangle)
$\lambda 1$	64%	76%
$\lambda 2$	64%	77%
Θ	60%	64%
$\theta 1$	32%	43%
$\theta 2$	48%	41%
β (20%)	55%	77%

Table 5.7: A strip of +/- 10% deviation around theoretical curves covers the given percentages of the manual measurements obtained with the developed technique as compared to Zamir et al manual measurements.

The corresponding theoretical relationships for the retinal venular system were not previously analysed, thus we were unable to benchmark our venular normative data.

3. Assessment of the inter-eye stability of retinal vascular geometrical measurements in normal subjects

The temporal and nasal fundus image sets of both eyes of 5 normal volunteers were analysed for this study. The subjects aged 38 to 65 years old (Mean = 47.6) A total of 347 vascular bifurcations were analysed, 164 bifurcations in right eyes versus 183 in left eyes. 162 were arteriolar while 185 were venular bifurcations. 136 of these bifurcations were located in the nasal fundus image while 211 were located temporally.

Unpaired two sample T test was used to compare the overall results of the right eyes versus the left eyes for all the vascular geometrical parameters as shown in table 5.8

Two sample T test Right versus Left Normal Overall measurements				
	Mean difference	**95% Confidence Interval**		**p value**
PARENT VESSEL WIDTH	0.48	0.04	0.92	0.030
CHILD 1 VESSEL WIDTH	0.54	0.10	0.97	0.010
CHILD 2 VESSEL WIDTH	0.38	0.05	0.70	0.024
ALPHA	-0.01	-0.06	0.04	0.700
BETA	0.03	-0.04	0.09	0.460
LAMBDA	-0.01	-0.04	0.03	0.790
LAMBDA 1	0.01	-0.01	0.03	0.220
LAMBDA 2	0.01	-0.03	0.04	0.770
THETA ANGLE	3.70	0.60	6.70	0.010
THETA 1 ANGLE	-0.10	-3.70	3.60	0.970
THETA 2 ANGLE	2.90	-1.40	7.20	0.190
JUNCTION EXPONENT	0.44	-0.35	1.23	0.270
OPTIMALITY PARAMETER	-0.11	-0.25	0.01	0.060

Table 5.8: Results of the unpaired T test comparing Right versus Left overall geometrical data in healthy subjects

The results for the absolute vessel width measurements demonstrated a statistically significant difference between the two eyes, with the right vessels' widths measuring larger than their left counterparts. There was no statistical difference for the relative diameters and area ratios between both eyes. As for the bifurcating and branching angles estimates, there seemed to be a statistically significant, for the bifurcating angle (θ) between both eyes, with the right bifurcating angles marginally wider than the left angles. The same relationship was not maintained for either of the child vessels branching angles.

The right and left overall data was then subcategorised to arteriolar and venular sub-groups and the unpaired two sample T test was performed, the results of which are shown in tables 5.9 and 5.10

Two sample T test Right versus Left Normal arteriolar bifurcations				
	mean difference	95% Confidence Interval		p value
PARENT VESSEL WIDTH	0.68	0.12	1.24	0.018
CHILD 1 VESSEL WIDTH	0.73	0.14	1.32	0.015
CHILD 2 VESSEL WIDTH	0.38	-0.1	0.87	0.120
ALPHA	-0.05	-0.12	0.02	0.120
BETA	-0.01	-0.11	0.09	0.890
LAMBDA	-0.03	-0.08	0.01	0.140
LAMBDA 1	0.02	-0.02	0.05	0.380
LAMBDA 2	-0.02	-0.06	0.02	0.370
THETA ANGLE	5.80	1.00	10.60	0.017
THETA 1 ANGLE	-2.60	-8.50	3.30	0.390
THETA 2 ANGLE	8.40	1.80	15.0	0.012
JUNCTION EXPONENT	-0.08	-1.42	1.27	0.920
OPTIMALITY PARAMETER	-0.08	-0.26	0.10	0.390

Table 5.9: Results of the unpaired T test comparing Right versus Left arteriolar geometrical data in healthy subjects

Two sample T test Right versus Left Normal venular bifurcations				
	mean difference	95% Confidence Interval		p value
PARENT VESSEL WIDTH	0.28	-0.37	0.93	0.400
CHILD 1 VESSEL WIDTH	0.35	-0.28	0.99	0.270
CHILD 2 VESSEL WIDTH	0.37	-0.06	0.81	0.091
ALPHA	0.03	-0.04	0.10	0.410
BETA	0.06	-0.02	0.13	0.140
LAMBDA	0.02	-0.03	0.08	0.400
LAMBDA 1	0.02	-0.01	0.04	0.330
LAMBDA 2	0.03	-0.02	0.07	0.210
THETA ANGLE	1.90	-2.10	5.80	0.360
THETA 1 ANGLE	2.90	-1.50	7.30	0.190
THETA 2 ANGLE	-2.10	-7.80	3.60	0.470
JUNCTION EXPONENT	0.82	-0.12	1.76	0.086
OPTIMALITY PARAMETER	-0.16	-0.34	0.01	0.062

Table 5.10: Results of the unpaired T test comparing Right versus Left venular geometrical data in healthy subjects

On analysing the results, it was worthwhile to note that the absolute vessel width measurements' relationship demonstrated for the overall data was, in part, still evident for the arteriolar vessels' subgroup, however this was not clear for the venular subgroup. Similarly, there was a statistically significant difference noted for the bifurcating angle (θ) for the arteriolar bifurcations, with the right bifurcating angles estimates being wider than the corresponding left bifurcating angles. No similar clear trend or relationship was found for either of the child vessels branching angles. The bifurcating angle (θ) relationship between the right and left eyes was not maintained for the venular bifurcations. The results showed no other statistical significant difference for any of the relative diameter or area ratios parameters in the arteriolar or venular subgroups.

The overall data were then categorised to nasal and temporal subgroups to evaluate whether there were any topographic differences across the fundus for the inter-eye relationships in any of the analysed geometrical parameters. The results are shown in tables 5.11 and 5.12

Two sample T test Right versus Left Normal Nasal bifurcations				
	mean difference	95% Confidence Interval		p value
PARENT VESSEL WIDTH	-0.05	-0.68	0.59	0.880
CHILD 1 VESSEL WIDTH	0.15	-0.47	0.78	0.620
CHILD 2 VESSEL WIDTH	0.12	-0.33	0.55	0.610
ALPHA	0.01	-0.08	0.09	0.880
BETA	0.06	-0.05	0.17	0.260
LAMBDA	0.08	-0.05	0.07	0.790
LAMBDA 1	0.02	-0.01	0.06	0.130
LAMBDA 2	0.02	-0.03	0.08	0.410
THETA ANGLE	-0.60	-5.40	4.00	0.770
THETA 1 ANGLE	-2.90	-8.20	2.30	0.270
THETA 2 ANGLE	2.00	-5.30	9.30	0.590
JUNCTION EXPONENT	0.60	-0.85	2.04	0.420
OPTIMALITY PARAMETER	-0.24	-0.43	-0.03	0.019

Table 5.11: Results of the unpaired T test comparing Right versus Left nasal overall geometrical data in healthy subjects

Two sample T test Right versus Left Normal Temporal bifurcations				
	mean difference	95% Confidence Interval		p value
PARENT VESSEL WIDTH	0.81	0.22	1.41	0.007
CHILD 1 VESSEL WIDTH	0.78	0.18	1.38	0.010
CHILD 2 VESSEL WIDTH	0.54	0.09	0.98	0.020
ALPHA	-0.02	-0.08	0.04	0.500
BETA	0.00	-0.08	0.08	1.000
LAMBDA	-0.01	-0.06	0.03	0.520
LAMBDA 1	0.01	-0.02	0.03	0.680
LAMBDA 2	-0.01	-0.05	0.03	0.690
THETA ANGLE	6.40	2.50	10.4	0.001
THETA 1 ANGLE	2.60	-2.10	7.40	0.270
THETA 2 ANGLE	3.60	-1.80	9.00	0.190
JUNCTION EXPONENT	0.36	-0.57	1.28	0.450
OPTIMALITY PARAMETER	-0.04	-0.21	0.12	0.610

Table 5.12: Results of the unpaired T test comparing Right versus Left temporal overall geometrical data in healthy subjects

Interestingly, the absolute vessel widths measurements inter-eye relationship noted for the overall data appeared more obvious for the temporal vessels, with a statistical significant difference shown from the results with the right temporal vessels measuring wider than the left temporal vessels. In contrast, there was no statistical significant difference for the absolute vessel widths measurements between the right and left nasal vessels.

Similarly, the bifurcating angle (θ) inter-eye relationship shown for the overall data was more apparent for the temporal vessels with the results showing a strong statistical significant difference, with the right temporal bifurcating angles measuring wider than the left temporal angles, no relationship was found for the child vessels branching angles. The nasal bifurcating angle (θ) and the child vessels branching angles showed no inter-eye statistical difference. Otherwise, there were no statistical differences detected for any of the relative diameters or area ratios parameters in the temporal or nasal vascular bifurcations.

5.7 Discussion

The retinal vasculature provides an invaluable non-invasive window for the study of subtle small vessel changes. The properties of the retinal vascular network, including the branching pattern have been studied previously over the last decade. However, theoretical studies describing the physiological principles governing the retinal network have not been systematically compared with normative experimental data, and the influence of different systemic factors has not been established.

This study represented an attempt to provide a normative reference data for the retinal vascular geometrical measurements in a sample of adult healthy individuals. We have described the distribution of a variety of retinal geometrical parameters and their association with age, BMI and smoking. This data is important for interpretation of further results for the diabetic subjects analysed in this project. It could also have future potential clinical implications as being a benchmark for further studies of similar populations with corresponding demographics with different vascular risk factors.

1. Descriptive analysis of the distribution of normal vascular geometry measurements.

Previous published normative retinal vascular geometrical data has been sparse and patchy, mainly extracted from values of control groups analysed in comparison to other groups with systemic vascular disease. To our knowledge, to date, there are no published studies dedicated only to the analysis of normal retinal geometrical architecture in anything more than a few individuals. We compared our results to available data from the control group results in Stanton et al, King et al, Chapman et al, and Martinez-Perez et al. [88-92] This is shown in table 5.14

	Study Normative data			Stanton et al 1995	King et al 1996	Chapman et al 2000	Martinez-Perez et al 2002	Chapman et al 2002
	Overall Data	Arteriolar Data	Venular Data	Arteriolar	Arteriolar	Arteriolar	Arteriolar	Arteriolar
Bifurcating angle Theta (Mean) (Range) (SD)	77.19 (38.32 - 132.46) (15.5)	75.34 (38.32-128.8) (15.9)	78.54 (39.52-132.46) (15.08)	84 (70-103)	78	79.7 (74.9 - 84.5)	84.5	79 -- (11)
Junction Exponent (Mean) (Range) (SD)	3.69 (1.24 - 18.29) (2.11)	4.16 (1.48 - 17.47) (2.16)	3.35 (1.24 - 18.92) (2.01)	2.65	---	3.87 (3.14 - 4.59)	---	---

Table 5.13: Overall, arteriolar and venular normative results as derived from healthy subjects compared to previously published data.

When our normative data is compared to other published studies, there is an obvious variation in the mean and range of measurements for the bifurcating angle and the junction exponent. These variations however could perhaps be expected and meaningful comparisons are difficult. The methodology and measurement techniques used for the studies, together with variations in the type and resolution of retinal images, the size of the population examined, the inclusion and exclusion criteria for subject selection and the type and size of the bifurcations analysed will all add variation to the results. This is also compounded by the innate hypersensitivity of the junction exponent to subtle variations in vessel width measurements as previously discussed.

The results of sub-analysis of our data revealed a tendency for larger retinal venular calibre as compared to their arteriolar counterparts, a finding that could be related to the different function of the arteriolar and venular vascular systems. The results seemed also to suggest the prevalence of larger bifurcating angles in the venular system, as well as changes in the other geometrical ratios and parameters as compared to the arteriolar system, the significance of such observations is not clear, however, one could interpret that the difference of geometrical features between the

retinal arteriolar and the venular systems might at some stage reflect the variable susceptibility and response of both vascular systems to different systemic vascular conditions or inflammatory stimuli. [170] Consequently, changes in the retinal venular geometrical features may in itself act as specific markers of systemic or cerebral vascular diseases in contrast to other conditions signalled by alterations of the retinal arteriolar network. For example, the Beaver Dam Eye Study demonstrated that subjects with highest levels of inflammatory and endothelial dysfunction markers tend to have larger venular calibre. [173] Similarly, experimental animal studies had shown that intravitreal injection of lipid hydro-peroxide affected the size of the venular caliber, but not the arteriolar vessels. [174] It was previously postulated that retinal venular dilatation could mark the presence of diffuse retinal ischaemia, and by proxy cerebral ischaemia, thus larger venular diameters were found to be associated with marked progression of peri-ventricular and sub-cortical white matter lesions and more incident lacunar infarcts. [175]

Further topographic analysis of the normative data suggested the prevalence of larger temporal retinal vessels as compared to nasal vessels, which was not associated with differences in the other geometrical parameters. Changes in the vascular width between the nasal and temporal retinal vessels might be related to regional distribution or preference of certain diabetic retinopathic features across the retina. A related - yet not similar - observation was previously noted; for example, it is widely accepted that diabetic retinopathy lesions start temporally from the fovea, and become most pronounced later in this area, it was also suggested by Bek and Helgesen that regional distribution of diabetic retinopathy lesions may be caused by changes in retinal vasomotion; nevertheless further studies are needed to explore such relationship. [171]

In contrary to previous published results [88], further analysis of our normative data showed no association of age with any changes in retinal vascular widths or bifurcating angles estimates. However, in this study, the analysis was performed for the overall data, unlike previous studies that focused mainly on the retinal arteriolar network. Similarly, our results demonstrated no effect of smoking or BMI on the different retinal geometrical features.

At this stage, it is worth mentioning that in some of the unpaired T tests calculated earlier to assess the differences between subcategories of data; the resultant "mean difference" values for the various geometrical parameters were, in some cases, lower than the corresponding calculated intra-observer "within-subject" measurement errors previously estimated. However, such observation should have no detrimental effect on the presented results. That is explained by the random occurrence of such measurement error around the "true" values of any measured geometrical parameter in any subcategory, in other words, there is no logical assumption that the measurement error would consistently occur in one direction rather than the other for certain subcategories of data to skew the results. This measurement error could thus neutralise its own effect when comparisons are made at "group" level as presented earlier. On the other hand, the calculated measurement errors would set the limitations for data comparative analysis should this be done at the "isolated bifurcation level" in which case, the difference between geometrical parameters of two individual bifurcations would need to exceed the "within-subject" measurement error to be deemed clinically significant.

2. Assessment of optimality of the normative geometrical data.

The retinal vascular network, far from being a totally random network, has a tendency to conform to some "optimal" principles, in order to minimise physical properties such as shear stress and work across the network. [70-72, 80] The branching vessels at a vascular bifurcation follow certain patterns that achieve a compromise between the requirements for minimum lumen surface and volume and minimum pumping power for driving blood through a branch, also satisfying the requirement for a minimum drag force applied on the endothelial surface. As a consequence, it has been found that the optimum bifurcation angles depend on the flow in, as well as the radii of the vessels involved. These optimality principles were derived mainly from theoretical considerations of the cardiovascular system as a fluid conducting network and were based on theoretical models of arterial junctions.

Previous research by Zamir et al [87] found that the human retina exhibits a relatively high degree of optimality in terms of its vascular branching characteristics,

consistent with the fact that the within the retina, the vessels are not under any other physiological or anatomical constraints, and are therefore free to branch in an optimum way. These results must be interpreted with caution however as they were derived from the arteriolar vascular tree of a single healthy 34-year old male.

As presented earlier, in our study, only an average of 50% of the normative data coincided within the calculated optimal range for the bifurcating angle θ, and the area ratio, β. This appeared to be true for both the arteriolar and venular bifurcations. Nevertheless, there seemed to be a slight tendency of the venular system to abide better with the optimality values and ranges as compared to the arteriolar system. A possible explanation might be due to the measurement technique. Veins are generally darker in retinal images with clearer edges and are thus easier to measure. This might have led to less measurement error and increased accuracy of estimating the angles and ratios resulting in the slight difference noted in the results. No significant difference was detected between the proximal and the distal bifurcations.

The overall mean value for area ratio β was close to the optimal calculation; however some deviation could be noticed when the means were calculated for the arteriolar or venular subgroups. The results demonstrated also that in this study, the qualitative relationship between the branching angles of the two child vessels was maintained in an average of 80% of the bifurcations. The relationship between the parent, larger child and smaller child vessels was also true in an average of 95% of cases.

As previously suggested, the measurements of branching angles and vascular diameters can never be expected to line up neatly along any curve or a straight line without scatter. [87] In fact, as previously shown, a band of +/- 10 % deviation from theoretical curves seemed to include a higher proportion of arteriolar geometrical data from our normative data in this study as compared to Zamir et al data derived from a single healthy male as in (table 5.7).

Nevertheless, the amount of variability noticed in this study between the experimentally measured normative geometrical features and the theoretical predictions could be related to different factors. Firstly, the number of subjects included for this study with a wide age range group and the large total amount of

analysed vascular bifurcations as compared to previous studies could have resulted in a wider normal biological scatter. Secondly, the large variation could be related to the multi-fractal pattern as previously suggested in that the main bulk of the scatter could be due to vascular design and pattern variability within the retinal vascular tree. [176] The large variability could also be related to measurement and other experimental inaccuracies although our measurement technique was considered as repeatable as other previously used methods.

It has been suggested that the ultimate test of the degree of optimality of a vascular network is not the mere difference between the experimentally measured and the optimum branching values, but the "cost" of that difference. The "cost" is defined as the increase in value of the physiological entity, which is minimised when the branching geometry is optimum. [82] Interestingly, Zamir and Bigelow [177] demonstrated in their experiment that there could be a considerable variation or departure of the branching angles values in the cardiovascular system from the optimum values, yet this corresponds to a very low penalty in the cost to the network system as a whole. In the constructed junction boxes round an optimum bifurcation value, there was a wide range of possible variations in branching angles within a 2% cost penalty contour. In fact, the range of scatter of physiological data in their study was significantly close to that observed with possible variations within the 2% penalty. As a consequence, the experimentally measured geometrical data can be still considered − in terms of cost − highly consistent with the theoretical optimality principles.

3. Assessment of inter-eye stability

In this section, we compared the geometrical features between both eyes in 5 normal volunteers. The overall results showed no significant difference in most of the examined features such as the relative diameters ratios or the area ratios. However, an interesting observation could be extracted from the data suggesting that the right arteriolar vessels seemed wider in diameter than the left arteriolar vessels, and that the right temporal vessels were wider than their left counterparts. This was also associated with a statistically significant wider bifurcating angles in the right

arteriolar bifurcations as compared to the left arteriolar bifurcations, and in the right temporal bifurcations as compared to the left temporal ones.

This observation of topographic geometrical inter-eye differences has not been examined or reported in detail in the literature before, and the clinical significance of such observation is not yet clear. It could be related to the way the human vascular network is designed and the way the arterial branching occurs from the main neck arteries and beyond, yet no further conclusions can be drawn until validated by further experiments. Previous analysis from the Rotterdam Scan Study reported no statistically significant differences between right and left eyes for the arteriolar and venular diameters in older patients' cohort, [175] furthermore, the correlation of retinal arteriolar and venular calibres within twins in the Australian Twins Eye Study was high. [178] On the other hand, another study demonstrated that the mean right central retinal artery equivalent was consistently larger than mean left central retinal artery equivalent in community-based older population, such observation might be related – in a way – to our findings. [179] However, it is important to point out that the patients groups age and other characteristics were different in these studies so results cannot be directly compared.

We also acknowledge that such observations might be unfounded and could be the result of the use of certain statistical tests that would inevitably cluster the data analysed, thus further detailed statistical analysis might be needed before any conclusions are reached.

5.8 Conclusion

In conclusion, this study attempted to present a comprehensive normative reference data that is considered of paramount importance for interpretation of further results obtained from similar population cohorts with different stages of diabetic retinopathy in this study. It can also be regarded as a benchmark reference for retinal vascular analysis in future clinical studies on similar age-matched population groups. However it is worth observing that due to the numerous systemic and environmental factors that affect retinal arteriolar and venular measurements, it might be difficult to

determine uniformly standard normative values across different population groups. [170]

The results presented here reflected measurements obtained from a sample of healthy Caucasians population of certain demographic features, thus caution would be advised when the resultant data are used for future comparisons. It could only be used to bench mark other patients cohorts of same demographic characteristics and with retinal images of same properties using the semi-manual tool.

The study also presented the actual distribution of the normative data along the theoretical calculated predictions of the different geometrical parameters, and determined the degree of scatter. Our results revealed an acceptable degree of adherence to the theoretical calculations considering the large sample size and variability of the analysed data. Our results included further information on the geometrical features of the retinal venular system that has not been explored before. Finally, the inter-eye topographic architectural and geometrical differences presented here are interesting and suggestive of a possible pattern of regional predilection for certain vascular geometrical relationships. Such findings warrant further analysis in future studies.

Chapter 6: Cross-sectional Comparative Analysis of Retinal Vascular Geometry in Diabetic Subjects

6.1 Overview

In the previous chapters, we described the details of developing a computer-assisted semi-manual technique for retinal geometrical vascular analysis. The precision and repeatability of the obtained measurements with the developed technique were analysed and the results compared favourably to other used vascular analysis techniques. The custom-designed technique was then utilised to evaluate in detail the normative geometrical data from healthy normal volunteers. These normative results set a benchmark for future vascular analysis of similar population cohorts with systemic or cerebral vascular diseases.

In this chapter, we arrive at the main research question for this thesis regarding the geometrical vascular changes in diabetes. The chapter discusses the descriptive analysis of the retinal geometrical vascular features in age-matched population cohorts of diabetic subjects with different stages of diabetic retinopathy. These results are compared to the normative data presented earlier. The associations of changes in different geometrical features with advancing retinopathic stages are evaluated in detail, to explore whether such changes − if found − could act as markers of advanced diabetic retinopathy. The effect of other demographic and clinical factors on any founded relationship is also assessed. The findings of this study thus determine the value of retinal geometrical analysis as a novel feature in the context of diabetic retinopathy grading assessment.

6.2 Introduction

Diabetic retinopathy remains a significant cause of acquired visual loss in working age adults worldwide. The medical, social and financial impact of the disease is substantial.

The DRS, ETDRS, DCCT, and UKPDS as well as other influential studies provided the scientific basis for the care of diabetic patients to preserve vision. In caring for patients with diabetic retinopathy and in the evaluation of the eye for treatment, it is fundamental to determine the level of non-proliferative and proliferative diabetic retinopathy and diabetic macular oedema, the presence of associated systemic conditions, and to initiate ocular treatment and follow-up evaluation based on the clinical findings.

The EDTRS clarified the natural history of diabetic retinopathy and the risk of progression to PDR and high risk PDR. Retinal lesions such as haemorrhages, microaneurysms, venous beading and intraretinal microvascular abnormalities were determined to be associated with risk of progression to PDR. These risks of progression based on baseline level of retinopathy provide the current foundations for recommended disease management and follow-up evaluation. [51, 53]

However, accurate grading of diabetic retinopathy from the retinal photographs is not always easy, and detailed identification of different retinopathy features proved to be difficult in some cases, specially the identification of early disc or retinal neovascular proliferations. The presence of extensive retinal haemorrhages, IRMAs, venous beading suggests rapidly progressive closure of the retinal capillary bed and severe retinal ischaemia. New vessels on the surface of the disc or on the surface of the retinal nerve fiber layer are usually present in such eyes but may be relatively unimpressive and easily overlooked especially when viewed in non-stereoscopic photographs. [47]

In addition, it seemed that in some eyes, there is an obvious mismatch between the level of retinal ischaemia and the characteristic retinal features described before. For example, in the presence of severe or significant retinal non-perfusion, the level of

NPDR may not appear too advanced and thus the grading of the retinal images of these eyes may not reflect the actual advanced stage of the retinal pathology, which in turn, would delay determining the need and timeliness of laser treatment. [180] Indeed, it has been speculated that the transient nature of some of these characteristic intraretinal lesions might explain its absence when early new vessels are first recognised, but it seems likely that at least some of these eyes might not have had previous severe NPDR. [47]

This study was conducted to assess the diagnostic value of a variety of different retinal vascular geometrical features in association with the progression of diabetic retinopathy, as a novel marker in determining the level of retinal ischaemia. We have described in previous chapters the association of changes in these geometrical features with other different systemic diseases such as hypertension and peripheral vascular disease. The possible association between retinal vascular geometry and dysfunctional vascular endothelium resulting from retinal ischaemia has also been described. If proven, such an association of retinal geometrical vascular features with progressive diabetic retinopathy could act as a new marker that could be measured with future computerised tools for quantitative analysis of diabetic retinopathy, and potentially improve clinical decisions in disease.

6.3 Objectives

Having established the normative range of retinal vascular geometry in a cohort of healthy individuals, the objectives of this study were:

1. To describe the distribution of retinal vascular geometrical features in diabetic patients with different grades of diabetic retinopathy.

2. To compare the geometrical measurements between the different groups with different grades of diabetic retinopathy, and detect any correlation of geometrical parameters with progression of diabetic retinopathy severity.

3. To assess the relationships of certain demographic and clinical risk factors such as age, sex, type and duration of diabetes, hypertension, and hypercholesterolaemia with RVG changes in this diabetic population.

6.4 Subjects and Methods

The study was based on images from the database at Sunderland eye infirmary and the south of the Tyne and Wear (SOTW) diabetic retinopathy-screening programme. Four categories of retinal images with different grades of diabetic retinopathy were collected; "No diabetic retinopathy", "mild non-proliferative diabetic retinopathy", "severe non-proliferative diabetic retinopathy", and "proliferative diabetic retinopathy".

Patients attending the diabetic clinic at the eye infirmary had temporal and nasal 50 degrees fundus images for each eye as part of their routine clinical care. The temporal retinal images were centered on the fovea, and the nasal images were captured with the optic disc positioned one to two disc diameters from the image edge similar to the imaging protocol adopted by the study in previous experiments, and using the same fundus camera. Retinal images of those diabetic patients were randomly selected from the image database and broadly classified into three categories of different diabetic retinopathy stages; namely mild and severe non-

proliferative diabetic retinopathy, and proliferative diabetic retinopathy. Random sampling within each group occurred through generating a sequence of random digits utilising a net-based research randomiser programme (by Geoffrey C. Urbaniak and Scott Plous).

The "No diabetic retinopathy" group of images were obtained from the SOTW diabetic retinopathy screening programme image database as patients with no diabetic retinopathy are not routinely referred to the hospital diabetic clinic. The screening programme adopts two-field digital retinal photography for screening, captured with fundus cameras of similar field and image resolution to those used in the hospital. The retinal images were randomly selected from the database of images previously graded to have no retinopathy (R0, M0) using the National Screening Committee NSC screening classification. Randomisation was performed with the same net-based research randomiser.

Retinal images of patients aged 65 years or younger were considered for inclusion in the study. Within each category, the image quality was graded for field positioning and image clarity for all the retinal images and only those classified to have "good" quality - using the NSC standards for diabetic retinopathy screening image quality grading - were collected for the study. Retinal images which showed evidence of laser scars treatment, obvious concurrent retinal pathology or gross suspicious glaucomatous optic disc cupping were excluded.

The patients' medical data relating to the images collected from the diabetic clinic image database were extracted from the hospital clinical notes. The information recorded included duration, type of diabetes, history of hypertension and hypercholesterolaemia on treatment. Co-current history of other microvascular complications such as diabetic neuropathy or diabetic foot ulcer, and / or nephropathy or proteinuria, and previous history of cerebral vascular stroke, ischaemic heart disease, or transient ischaemic attacks were also noted, thus reflecting the severity of diabetic microvascular end organ damage. Smoking history was also recorded. The subject's refractive history was also noted, and retinal images of subjects with refraction beyond +/-3 dioptres were excluded. However, for the

"No retinopathy" group of images, detailed medical information was not available from the screening database at that stage.

All images were anonymised and coded according to the study protocol. The images were all grouped together and presented randomly to a certified tertiary diabetic retinopathy grader. The nasal and temporal retinal images were graded according to the modified system of 45-degrees field grading standards for the assessment of diabetic retinopathy developed for the EURODIAB IDDM complication study and an overall diabetic retinopathy grade was assigned for each eye. [55] The grader was masked of any patient's clinical information related to the images specially the age, type or duration of diabetes. The four groups of images with different diabetic retinopathy grades were thus refined and accurately categorised into four levels; level 0 (No retinopathy), level 1 (Minimal NPDR), level 3 (Severe NPDR), and level 5 (Proliferative retinopathy). Retinal images graded level 2 (Moderate NPDR) were excluded from the study, to ascertain that the 4 included categories are clearly distinct from each other, and thus meaningful comparisons between them can be made.

Temporal and nasal retinal images of ten to fifteen eyes were randomly selected from each of the 4 subgroups of diabetic retinopathy levels to be included for analysis in the study using a net-based research randomiser. The corresponding patients' demographic and clinical data were also saved and tabulated for further analysis. In the "Proliferative retinopathy" subgroup, more eyes were included, as it was noted that the number of identifiable bifurcations per image is less being more commonly masked by large areas of retinal or pre-retinal haemorrhages, together with the fact that these eyes tend to dilate poorly thus slightly degrading the image quality.

The selected included image sets were then again grouped together and randomly presented to the investigator for image analysis of the retinal vascular geometrical features. The definite grade of the images was masked; however it was impossible to mask the retinopathic features of the image completely whilst vascular analysis was performed.

All retinal images were analysed by one investigator with the custom-designed semi-manual computer algorithm to assess different retinal vascular geometry parameters. Images were initially labelled to select arteriolar and venular bifurcations to be analysed. Ten to 20 identifiable vascular bifurcations were labelled in each image for further analysis. Care was taken to select a variable sample of bifurcations within each image, including arterial and venous, large and small, central and peripheral, above and below the image horizontal meridian, whenever possible.

The labelled bifurcations were then marked - as previously described in the methodology chapter - and the absolute vessel widths measurements, bifurcating and branching angle, and the other relative diameter ratios, area ratios and asymmetry ratio were estimated.

The extracted geometrical features were described in terms of

1. Absolute vessel width measurements in pixels (parent vessel width, larger child (child 1) vessel width, and smaller child (child 2) vessel width). The diameters of the parent vessel, larger child branch, and the smaller child branch are expressed as d_0, d_1, and d_2 respectively.

2. Bifurcating angles in degrees (θ, θ_1, and θ_2). The bifurcation angle (θ) is the bifurcating angle between the two children vessels, while angle (θ_1) is the branching angle between the first (larger) child segment and the parent direction, while angle (θ_2) is the branching angle between the second (smaller) child and the parent direction.

3. Relative diameter ratios, such as (λ, λ_1, λ_2) and area ratio (β), the asymmetry ratio (α), the junction exponent and the optimality parameter.

The resultant calculated absolute vessel width measurements, bifurcating angles measurements, and other parameters and ratios estimates were extracted and tabulated. The images' grading was then revealed, and the corresponding results were subdivided back into the 4 categories of diabetic retinopathy levels, together with the related demographic and clinical data.

6.5 Statistical analysis

Statistical analysis was performed using Minitab 16 statistical software. Descriptive statistical analysis is initially presented for the overall data, and the arteriolar and venular subcategories for the four categories of diabetic retinopathy levels. Values presented were the mean, median, minimum, maximum, 1st and 3rd quartiles, and standard deviation.

Chi Square test X^2 was used to detect differences between baseline characteristics. One-way ANOVA was performed to compare between the subgroups of diabetic cohorts with different grades of diabetic retinopathy. A (p) value ≤ 0.05 was considered significant. In cases with significant (p) values, the Fisher-protected least significant difference FLSD ad-hoc test was used. The results were also sub analysed for arteriolar and venular subgroups.

Multiple linear regression analysis was then used to determine the effect of different demographic and clinical risk factors on the RVG parameters in the diabetic population with or without established retinopathy. Tested features included the continuous variables; age, duration of diabetes and categorical variables; sex, type of diabetes, history of hypertension, and history of hypercholesterolemia. We constructed three models; model 1 included age and sex, model 2 additionally included the diabetes type and history of hypertension, model 3 additionally included diabetes duration and history of hypercholesterolemia.

Furthermore, due to the limited number of previous studies on retinal geometrical analysis, it was difficult to determine the vascular widths and bifurcating angles "clinically important difference" (d) as suggested by Goodall et al.[181] However, on observing the spread and variations of our data, an assumption was made to consider approximate 0.5 pixel difference of absolute vessel width and 5 degrees difference in bifurcating angle estimation between compared categories to be a meaningful "clinically important difference" (d). This value together with the standard deviation of our geometrical data was used to determine the study power.

6.6 Results

A total of 1518 arteriolar and venular bifurcations were marked and analysed for this experiment for the different diabetic categories. The number and subdivision of the analysed vascular bifurcations per category is shown in table 6.1

Numbers of analysed bifurcations			
	Total	**Arteriolar**	**Venular**
No diabetic retinopathy	242	117	125
Minimal NPDR	310	136	174
Severe NPDR	372	139	233
Proliferative diabetic retinopathy	594	231	363

Table 6.1: Numbers of analysed bifurcations in the 4 categories of diabetic eyes.

Power calculation: Following Goodall et al. calculations, if the average standard deviations *(s)* for absolute vessel widths and angular bifurcations presented below are considered, together with the assumed meaningful "clinically important difference" *(d)*, then for a *(s/d)* ratio of 2.50 the included numbers for the overall analysed bifurcations in all categories and sub-categories would result in an average of 80% to 90% study power in most cases. [181]

The demographic and clinical data of the included diabetic subjects in the 4 categories were collated and compared as shown in table 6.2

Demographic and Clinical Baseline Characteristics of Diabetic subjects					
	No Retinopathy group	Minimal NPDR group	Severe NPDR group	PDR group	P value
Subjects (Eyes)	10 Subjects (10 eyes)	10 Subjects (10 eyes)	12 Subjects (12 eyes)	19 Subjects (27 eyes)	
Age: Mean (SD) (Range)	55.5 (8.9) (43 - 65)	56.6 (9.5) (37 - 65)	53 (9.0) (41 – 65)	50 (12.5) (26 - 65)	0.92
Female	60%	50%	42%	58%	0.21
Type II Diabetes	70%	80%	83%	73%	0.70
Duration of DM in months: Mean (SD) (Range)	118 (65) (24 - 144)	148 (74) (37 - 240)	128 (93) (12 - 300)	211 (124) (2 - 456)	**<0.05**
Hypertension		70%	67%	48%	0.74
High Cholesterol		70%	34%	57%	0.16
Associated microvascular complications					
NONE		70%	59%	63%	
IHD, CVA, TIA		20%	0%	5%	
Neuropathy, Foot Ulcer		10%	25%	10%	0.44
,Nephropathy		0%	17%	21%	
Smoking		30%	17%	21%	0.8

Table 6.2: Demographic and clinical data of the diabetic subjects with different grades of diabetic retinopathy

As shown, the groups were reasonably age matched, an equivalent number of right versus left eyes were analysed. There was higher percentage of type II diabetics as compared to type I. Unsurprisingly, the duration of diabetes was longer in the "proliferative retinopathy" group as compared to the other groups, reflecting an established risk factor for progression of diabetic retinopathy. However, unexpectedly, the minimal NPDR group had higher prevalence of hypertensive and hypercholesterolaemic subjects. Most of the diabetic subjects in all groups had no

associated microvascular complications, yet there was higher prevalence of ischaemic heart disease and cerebrovascular accidents in subjects with minimal NPDR that might be related to the high prevalence of type II diabetes, while a higher prevalence of kidney end organ disease was noted in subjects with proliferative diabetic retinopathy.

1. Descriptive analysis of the distribution of the geometrical vascular parameters in 4 categories of diabetic subjects with no diabetic retinopathy, minimal, severe and proliferative diabetic retinopathy

Results of the vascular bifurcations analysis for the diabetic subjects were calculated for the various geometrical parameters. The mean, medium, standard deviation, minimum and maximum, the first and the third quartile were estimated for each parameter in each category. The results are presented together with the normative results derived from the age-matched healthy non-diabetic population for benchmarking as shown in table 6.3

	Non-diabetic group	No Retinopathy group	Mild NPDR group	Severe NPDR group	PDR group
Parent vessel d_0					
Min	3.47	3.81	3.96	4.15	4.22
Max	14.83	11.82	14.67	17.38	18.05
Mean	8.06	6.97	8.39	8.56	8.98
Median	8.03	6.85	8.08	8.29	8.78
Standard Deviation	2.34	1.61	2.37	2.39	2.63
1st quartile	6.14	5.94	6.48	6.59	6.74
3rd quartile	9.80	7.77	9.95	10.11	10.64
Child 1 vessel d_1					
Min	3.05	2.93	3.13	3.38	3.33
Max	14.18	11.23	14.15	16.41	18.06
Mean	7.25	6.17	7.44	7.56	8.01
Median	7.21	6.03	7.25	7.17	7.72
Standard deviation	2.26	1.56	2.30	2.34	2.52
1st quartile	5.37	5.08	5.51	5.67	5.91
3rd quartile	8.73	7.07	8.99	9.07	9.63
Child 2 vessel d_2					
Min	2.43	2.82	3.13	3.11	2.91
Max	12.31	7.82	11.52	10.68	13.80
Mean	5.22	4.66	5.47	5.51	5.76
Median	4.87	4.50	5.09	5.20	5.34
Standard Deviation	1.57	1.04	1.53	1.44	1.70
1st quartile	4.06	3.90	4.40	4.46	4.55
3rd quartile	6.18	5.28	6.19	6.24	6.68
Theta angle θ					
Min	38.32	40.32	40.53	40.25	38.27
Max	132.46	119.02	133.99	137.28	161.53
Mean	77.19	77.04	79.85	80.02	83.23
Median	77.72	76.69	79.97	79.53	81.67
Standard Deviation	15.50	15.60	17.39	17.76	18.91
1st quartile	66.25	64.39	66.61	67.47	70.44
3rd quartile	87.74	88.00	91.73	90.95	93.78

Theta 1 angle θ_1					
Min	0.04	0.51	0.23	0.07	0.00
Max	71.66	81.24	85.51	72.89	113.73
Mean	24.57	25.14	25.12	25.82	25.05
Median	22.36	23.61	23.14	23.58	22.02
Standard Deviation	21.08	14.03	15.78	15.23	16.75
1st quartile	12.16	14.40	12.42	13.77	11.72
3rd quartile	33.31	33.95	34.62	35.33	34.05
Theta 2 angle θ_2					
Min	8.00	2.02	4.33	2.64	3.09
Max	106.99	103.97	120.19	124.65	132.87
Mean	53.40	51.97	55.01	54.84	58.57
Median	51.70	49.14	52.30	53.26	56.73
Standard Deviation	19.68	19.26	21.19	21.69	23.67
1st quartile	39.35	37.59	39.14	38.54	42.25
3rd quartile	67.36	65.52	71.40	68.84	74.87
Lambda λ					
Min	0.29	0.46	0.32	0.29	0.31
Max	1.00	1.00	1.00	1.00	1.00
Mean	0.75	0.77	0.76	0.75	0.74
Median	0.76	0.80	0.80	0.77	0.76
Standard Deviation	0.16	0.14	0.16	0.15	0.16
1st quartile	0.64	0.66	0.64	0.65	0.62
3rd quartile	0.88	0.90	0.91	0.88	0.89
Lambda 1 λ_1					
Min	0.64	0.69	0.69	0.62	0.53
Max	1.10	1.32	1.01	1.11	1.11
Mean	0.90	0.88	0.87	0.88	0.88
Median	0.91	0.88	0.89	0.89	0.90
Standard Deviation	0.08	0.06	0.06	0.07	0.07
1st quartile	0.85	0.85	0.84	0.83	0.84
3rd quartile	0.95	0.92	0.93	0.94	0.95

Lambda 2 λ_2					
Min	0.29	0.42	0.31	0.27	0.28
Max	1.05	0.88	0.95	0.93	0.92
Mean	0.66	0.68	0.66	0.66	0.65
Median	0.67	0.68	0.69	0.67	0.67
Standard Deviation	0.13	0.11	0.13	0.12	0.13
1st quartile	0.58	0.60	0.58	0.58	0.56
3rd quartile	0.75	0.76	0.76	0.74	0.76
Alpha α					
Min	0.09	0.21	0.10	0.08	0.09
Max	1.00	0.99	1.00	1.00	1.00
Mean	0.58	0.62	0.61	0.60	0.58
Median	0.57	0.64	0.64	0.60	0.57
Standard Deviation	0.23	0.21	0.24	0.22	0.23
1st quartile	0.40	0.43	0.41	0.42	0.38
3rd quartile	0.77	0.81	0.82	0.78	0.79
Beta β					
Min	0.66	0.88	0.89	0.67	0.53
Max	2.32	2.36	1.89	1.86	1.91
Mean	1.27	1.25	1.24	1.22	1.24
Median	1.25	1.24	1.22	1.22	1.22
Standard Deviation	0.21	0.18	0.16	0.18	0.19
1st quartile	1.13	1.13	1.14	1.09	1.11
3rd quartile	1.40	1.37	1.34	1.35	1.37
Junction exponent χ					
Min	1.24	1.62	1.66	1.24	1.05
Max	18.92	8.42	18.82	14.16	16.44
Mean	3.69	3.33	3.34	3.30	3.55
Median	3.12	3.09	2.98	2.98	3.04
Standard Deviation	2.11	3.24	3.17	3.13	3.32
1st quartile	2.48	2.50	2.56	2.37	2.44
3rd quartile	4.20	3.86	3.66	3.75	4.20

Optimality parameter ρ					
Min	-1.15	-1.21	-0.94	-0.93	-0.97
Max	0.89	0.75	0.74	0.85	0.90
Mean	-0.11	-0.05	-0.02	-0.01	-0.04
Median	-0.34	-0.27	0.13	-0.03	-0.20
Standard Deviation	0.54	0.52	0.49	0.52	0.53
1st quartile	-0.58	-0.53	-0.50	-0.51	-0.57
3rd quartile	0.45	0.48	0.45	0.50	0.49

Table 6.3: The descriptive statistical analysis of the overall data for retinal vascular geometrical parameters in the four subcategories of diabetic subjects together with the corresponding normative data.

The overall data were then subdivided into arteriolar and venular bifurcations, and the different descriptive statistical measurements and estimates were calculated for each of the analysed geometrical parameters together with the normative data as shown in tables 6.4 (a) and (b).

Arteriolar Data					
	Non-diabetic group	No Retinopathy group	Mild NPDR group	Severe NPDR group	PDR group
Parent vessel d_0					
Min	3.54	3.95	3.96	4.15	4.30
Max	13.54	9.80	12.39	12.92	12.85
Mean	7.45	6.47	7.54	7.58	8.06
Median	7.55	6.47	7.46	7.29	7.92
Standard Deviation	1.75	1.08	1.68	1.65	1.84
1st quartile	6.14	5.73	6.27	6.34	6.51
3rd quartile	8.53	7.27	8.66	8.71	9.34
Child 1 vessel d_1					
Min	3.10	3.29	3.72	3.38	3.33
Max	14.18	9.25	11.28	13.51	12.21
Mean	6.76	5.78	6.65	6.73	7.23
Median	6.68	5.69	6.25	6.44	7.02
Standard deviation	1.73	1.10	1.62	1.66	1.80
1st quartile	5.47	5.07	5.42	5.59	5.80
3rd quartile	7.97	6.43	7.77	7.68	8.47

Child 2 vessel d₂					
Min	2.50	2.83	3.42	3.22	3.11
Max	12.31	7.82	9.27	9.99	11.13
Mean	5.25	4.60	5.42	5.43	5.62
Median	4.87	4.47	5.17	5.21	5.36
Standard Deviation	1.58	0.99	1.37	1.33	1.43
1st quartile	4.07	3.90	4.39	4.58	4.59
3rd quartile	6.24	5.21	6.45	5.94	6.54
Theta angle θ					
Min	38.32	40.32	45.42	43.44	49.11
Max	128.85	115.84	133.99	134.58	161.53
Mean	75.34	76.13	79.14	78.78	84.33
Median	75.56	74.69	77.41	75.73	82.95
Standard Deviation	15.90	15.84	17.98	18.43	18.56
1st quartile	62.47	62.95	65.21	66.87	71.60
3rd quartile	86.30	87.57	89.14	87.59	95.03
Theta 1 angle θ₁					
Min	0.40	1.58	0.23	2.96	0.40
Max	71.66	68.88	85.51	72.89	87.90
Mean	24.83	25.77	27.32	28.33	27.44
Median	23.51	22.47	25.46	25.76	24.71
Standard Deviation	15.34	15.19	16.66	15.40	16.44
1st quartile	12.35	13.93	13.23	16.18	15.24
3rd quartile	35.31	36.04	35.35	39.04	35.52
Theta 2 angle θ₂					
Min	8.38	2.02	4.33	11.85	8.54
Max	98.64	103.97	120.19	117.85	132.87
Mean	50.63	50.36	51.99	50.45	56.88
Median	48.73	47.30	48.61	50.53	55.41
Standard Deviation	19.77	20.29	21.31	20.31	22.89
1st quartile	37.68	37.14	38.22	35.78	40.11
3rd quartile	62.76	64.40	66.95	62.26	72.19

Lambda λ					
Min	0.33	0.51	0.45	0.46	0.44
Max	1.00	1.00	1.00	1.00	1.00
Mean	0.79	0.80	0.82	0.81	0.79
Median	0.79	0.83	0.85	0.83	0.81
Standard Deviation	0.14	0.12	0.12	0.11	0.13
1st quartile	0.70	0.70	0.76	0.73	0.69
3rd quartile	0.90	0.91	0.93	0.92	0.91
Lambda 1 λ_1					
Min	0.72	0.73	0.69	0.64	0.67
Max	1.10	1.32	1.01	1.06	1.09
Mean	0.91	0.88	0.89	0.89	0.88
Median	0.91	0.89	0.89	0.89	0.91
Standard Deviation	0.07	0.07	0.06	0.07	0.07
1st quartile	0.86	0.86	0.84	0.85	0.85
3rd quartile	0.95	0.93	0.92	0.94	0.95
Lambda 2 λ_2					
Min	0.32	0.45	0.42	0.49	0.44
Max	1.05	0.87	0.95	0.93	0.92
Mean	0.71	0.71	0.72	0.71	0.70
Median	0.72	0.73	0.74	0.72	0.71
Standard Deviation	0.11	0.09	0.10	0.08	0.10
1st quartile	0.62	0.64	0.66	0.66	0.63
3rd quartile	0.79	0.79	0.79	0.79	0.79
Alpha α					
Min	0.11	0.26	0.20	0.22	0.20
Max	1.00	0.99	0.99	1.00	0.99
Mean	0.62	0.66	0.69	0.68	0.64
Median		0.70	0.72	0.68	0.66
Standard Deviation	0.21	0.19	0.19	0.18	0.20
1st quartile	0.49	0.48	0.57	0.53	0.48
3rd quartile	0.82	0.83	0.86	0.85	0.83

Beta β					
Min	0.80	0.97	0.89	0.80	0.85
Max	2.32	2.36	1.89	1.86	1.79
Mean	1.37	1.32	1.31	1.31	1.31
median	1.33	1.30	1.29	1.32	1.31
Standard Deviation	0.21	0.19	0.17	0.18	0.19
1st quartile	1.20	1.20	1.19	1.21	1.17
3rd quartile	1.45	1.42	1.42	1.43	1.45
Junction exponent χ					
Min	1.48	1.90	1.72	1.52	1.63
Max	17.47	8.42	18.82	14.16	16.44
Mean	4.16	3.70	3.80	3.92	4.15
Median	3.64	3.46	3.23	3.51	3.59
Standard Deviation	2.16	1.27	2.00	1.85	2.25
1st quartile	2.77	2.82	2.75	2.81	2.69
3rd quartile	4.75	4.35	4.23	4.25	4.69
Optimality parameter ρ					
Min	-1.15	-1.21	-0.94	-0.93	-0.91
Max	0.78	0.66	0.74	0.79	0.76
Mean	-0.28	-0.22	-0.17	-0.23	-0.21
Median	-0.49	-0.43	-0.39	-0.45	-0.45
Standard Deviation	0.51	0.49	0.50	0.50	0.52
1st quartile	-0.65	-0.60	-0.60	-0.59	-0.62
3rd quartile	0.28	0.35	0.37	0.33	0.40

Table 6.4 (a): The descriptive statistical analysis of the arteriolar data for retinal vascular geometrical parameters in the four subcategories of diabetic subjects together with the corresponding normative data.

Venular Data					
	Non-diabetic group	**No Retinopathy group**	**Mild NPDR group**	**Severe NPDR group**	**PDR group**
Parent vessel d_0					
Min	3.47	3.81	4.02	4.37	4.22
Max	14.83	11.82	14.67	17.38	18.05
Mean	8.50	7.42	9.04	9.13	9.55
Median	8.62	7.30	9.13	9.13	9.54
Standard Deviation	2.60	1.87	2.62	2.56	2.88
1st quartile	6.18	6.18	6.69	6.83	6.98
3rd quartile	10.63	8.49	11.01	11.24	11.57
Child 1 vessel d_1					
Min	3.05	2.93	3.31	3.77	3.72
Max	13.85	11.23	14.15	16.41	18.06
Mean	7.60	6.51	8.04	8.05	8.50
Median	7.67	6.41	8.22	8.03	8.52
Standard deviation	2.51	1.83	2.55	2.54	2.79
1st quartile	5.31	5.05	5.71	5.73	5.98
3rd quartile	9.62	7.61	9.79	9.90	10.59
Child 2 vessel d_2					
Min	2.43	2.82	3.13	3.11	2.91
Max	11.28	7.66	11.52	10.68	13.80
Mean	5.18	4.72	5.51	5.55	5.82
Median	4.90	4.53	5.05	5.17	5.26
Standard Deviation	1.57	1.08	1.64	1.47	1.85
1st quartile	4.03	3.91	4.40	4.43	4.46
3rd quartile	6.08	5.36	6.09	6.47	6.77
Theta angle θ					
Min	39.52	43.95	40.53	40.25	38.27
Max	132.46	119.02	121.18	137.28	147.71
Mean	78.54	77.68	80.40	80.75	82.53
Median	79.02	77.53	81.73	81.08	80.01
Standard Deviation	15.08	15.12	16.96	17.36	19.13
1st quartile	68.10	67.34	67.47	68.18	69.93
3rd quartile	88.50	88.10	93.81	91.78	93.37

Theta 1 angle θ_1					
Min	0.04	0.51	0.27	0.07	0.00
Max	70.83	81.24	66.85	70.06	113.73
Mean	24.39	24.81	23.43	24.34	23.53
Median	21.81	24.94	20.91	22.68	20.05
Standard Deviation	24.46	12.90	14.90	14.97	16.79
1st quartile	11.74	15.30	11.03	12.57	10.72
3rd quartile	31.70	33.15	32.96	33.80	32.47
Theta 2 angle θ_2					
Min	8.00	8.01	6.58	2.64	3.09
Max	106.89	92.46	112.93	124.65	129.48
Mean	55.42	53.00	57.34	57.43	59.65
Median	55.38	49.81	54.97	57.77	57.77
Standard Deviation	19.38	17.92	20.85	22.10	23.63
1st quartile	40.41	37.79	40.19	40.17	43.27
3rd quartile	68.90	69.10	74.27	70.90	75.95
Lambda λ					
Min	0.29	0.46	0.32	0.29	0.31
Max	1.00	0.99	1.00	1.00	1.00
Mean	0.72	0.75	0.72	0.72	0.72
Median	0.72	0.76	0.71	0.73	0.73
Standard Deviation	0.17	0.15	0.17	0.17	0.17
1st quartile	0.59	0.63	0.58	0.60	0.59
3rd quartile	0.85	0.87	0.88	0.87	0.87
Lambda 1 λ_1					
Min	0.64	0.69	0.73	0.62	0.53
Max	1.06	0.98	1.00	1.11	1.11
Mean	0.89	0.87	0.88	0.87	0.88
Median	0.90	0.88	0.89	0.88	0.90
Standard Deviation	0.08	0.05	0.06	0.07	0.08
1st quartile	0.84	0.83	0.84	0.83	0.83
3rd quartile	0.94	0.92	0.94	0.93	0.94

Lambda 2 λ_2					
Min	0.29	0.42	0.31	0.27	0.28
Max	0.96	0.88	0.85	0.92	0.90
Mean	0.63	0.65	0.63	0.63	0.63
Median	0.63	0.65	0.64	0.63	0.63
Standard Deviation	0.12	0.11	0.13	0.12	0.13
1st quartile	0.54	0.57	0.53	0.54	0.54
3rd quartile	0.72	0.73	0.74	0.72	0.73
Alpha α					
Min	0.09	0.21	0.10	0.08	0.09
Max	0.99	0.98	1.00	1.00	1.00
Mean	0.54	0.59	0.55	0.55	0.55
Median	0.52	0.56	0.51	0.52	0.53
Standard Deviation	0.23	0.22	0.25	0.24	0.24
1st quartile	0.34	0.40	0.34	0.36	0.35
3rd quartile	0.72	0.77	0.77	0.75	0.76
Beta β					
Min	0.66	0.88	0.89	0.67	0.53
Max	1.86	1.61	1.63	1.72	1.91
Mean	1.21	1.20	1.19	1.18	1.20
Median	1.20	1.19	1.18	1.17	1.18
Standard Deviation	0.18	0.15	0.14	0.16	0.18
1st quartile	1.08	1.10	1.09	1.06	1.08
3rd quartile	1.32	1.30	1.28	1.28	1.30
Junction exponent χ					
Min	1.24	1.62	1.66	1.24	1.05
Max	18.92	6.39	7.43	9.21	16.04
Mean	3.35	3.02	2.99	2.94	3.18
Median	2.89	2.83	2.84	2.80	2.82
Standard Deviation	2.01	0.96	0.88	0.99	1.46
1st quartile	2.32	2.36	2.43	2.21	2.32
3rd quartile	3.63	3.39	3.39	3.40	3.64

Optimality parameter ρ					
Min	-0.93	-0.76	-0.78	-0.84	-0.97
Max	0.85	0.75	0.70	0.85	0.90
Mean	0.02	0.09	0.09	0.12	0.06
Median	0.21	0.30	0.29	0.33	0.31
Standard Deviation	0.52	0.48	0.46	0.49	0.51
1st quartile	-0.49	-0.38	-0.41	-0.41	-0.46
3rd quartile	0.50	0.53	0.49	0.56	0.53

Table 6.4 (b): The descriptive statistical analysis of the venular data for retinal vascular geometrical parameters in the four subcategories of diabetic subjects together with the corresponding normative data.

On evaluating the overall data for the different geometrical parameters, a noticeable trend was evident for absolute vessel width measurements (parent vessel, child 1 vessel, and child 2 vessel), where a gradual increase in the vessel diameters was associated with increase severity of diabetic retinopathy grade. This relationship was true for the all 3 vessels at a bifurcation; parent vessel and the two daughter vessels' diameters. This same trend was maintained for the 3 vessels width measurements in the arteriolar and venular subgroups. An average 25% increase in the vascular diameters of the arteriolar and venular retinal networks was estimated in eyes with proliferative diabetic retinopathy as compared to those with no retinopathy.

Similarly, on assessing the bifurcating angles measurements in the overall data, there was a clear tendency for the total bifurcating angle (θ) to gradually increase in value with progression of diabetic retinopathy grading. The arteriolar and venular bifurcations demonstrated the same relationship, with the bifurcating angle (θ) measuring an average of 7° wider in the proliferative retinopathy group as compared to eyes with no retinopathy. This appeared to be related to a similar trend noted in the branching angles for the smaller child vessel (θ_2) which also gradually increased in width with increased severity of retinopathy grading, which was clearly observed in the overall data, as well as the arteriolar, and venular subgroups. The (θ_2) angle values were in average 6.5° wider in proliferative retinopathy as compared to the no

215

retinopathy diabetic groups. The branching angle for the larger child vessel (θ_1) did not show a similar trend, in relation to the progression of the retinopathy grading.

Otherwise, no fixed or clear trend could be noticed for either of the relative diameter ratios (λ, λ_1 and λ_2) in relation to the progression of diabetic retinopathy grading. The area ratio (β), the asymmetry ratio (α), and the optimality parameter ratio estimates also showed no obvious trend or change in values between the different grades of diabetic retinopathy. The junction exponent (χ) estimates demonstrated a slight gradual increase in value with progression of diabetic retinopathy severity, which seemed generally true for the overall and the arteriolar data only. However, considering the wide variability of junction exponent estimation as explained in previous chapters, the significance of this change will be further evaluated in the next section.

In general, the data presented above showed a broad overlap in ranges of measurements and estimates for all the geometrical parameters between subgroups of different diabetic retinopathy grades, and thus no definite values can identify certain parameter in any specific retinopathy grade.

2. Comparison of the geometrical parameters measurements between sub-groups of different grades of diabetic retinopathy

For the comparative analysis between the diabetic subjects with different grades of diabetic retinopathy, the distribution of the overall analysed geometrical measurements and estimates were compared using the ANOVA test. The results of the overall measurements are presented in table 6.5. Results for the arteriolar and venular bifurcations subgroups are presented in tables 6.6 A and B respectively. The overall significance of the ANOVA test is shown, along with the significant differences in-between the subgroups as determined by the FLSD test.

Retinal Parameter Mean ± (STD)	No Retinopathy Group (242 bifurcations)	Mild NPDR Group (310 bifurcations)	Severe NPDR Group (372 bifurcations)	PDR Group (594 bifurcations)	p value
OVERALL DATA					
Parent Vessel Diameter d_0 (pixels)	$6.97 \pm (1.61)*$	$8.39 \pm (2.37)$ †	$8.56 \pm (2.39)$†	$8.98 \pm (2.63)$‡	**0.000**
Large Child Diameter d_1 (pixels)	$6.17 \pm (1.56)*$	$7.44 \pm (2.30)$†	$7.56 \pm (2.34)$†	$8.01 \pm (2.52)$‡	**0.000**
Smaller Child Diameter d_2 (pixels)	$4.66 \pm (1.04)*$	$5.47 \pm (1.53)$†	$5.51 \pm (1.44)$†	$5.76 \pm (1.70)$‡	**0.000**
Bifurcating Angle θ (Degrees)	$77.04 \pm (15.6)*$	$79.85 \pm (17.4)*$†	$80.02 \pm (17.8)$†	$83.23 \pm (18.9)$‡	**0.000**
Branching Angle θ_1 (Degrees)	$25.14 \pm (14.1)$	$25.12 \pm (15.8)$	$25.82 \pm (15.2)$	$25.05 \pm (16.7)$	0.941
Branching Angle θ_2 (Degrees)	$51.97 \pm (19.3)*$	$55.01 \pm (21.2)*$	$54.84 \pm (21.7)*$†	$58.57 \pm (23.7)$†	**0.027**
Bifurcation Index λ	$0.77 \pm (0.14)$	$0.76 \pm (0.16)$	$0.75 \pm (0.15)$	$0.74 \pm (0.16)$	0.088
Larger child diameter ratio λ_1	$0.88 \pm (0.06)$	$0.87 \pm (0.06)$	$0.88 \pm (0.07)$	$0.88 \pm (0.07)$	0.168
Smaller child diameter ratio λ_2	$0.68 \pm (0.11)$	$0.66 \pm (0.13)$	$0.66 \pm (0.12)$	$0.65 \pm (0.13)$	0.070
Asymmetry Ratio α	$0.62 \pm (0.21)$	$0.61 \pm (0.24)$	$0.60 \pm (0.22)$	$0.58 \pm (0.23)$	0.129
Area Ratio β	$1.25 \pm (0.18)$	$1.24 \pm (0.16)$	$1.22 \pm (0.18)$	$1.24 \pm (0.19)$	0.253
Junction Exponent χ	$3.33 \pm (3.24)*$†	$3.34 \pm (3.17)*$†	$3.30 \pm (3.13)$†	$3.55 \pm (3.32)*$	**0.050**
Optimality Parameter $\mathcal{P}$	$-0.05 \pm (0.52)$	$-0.02 \pm (0.49)$	$-0.01 \pm (0.52)$	$-0.04 \pm (0.53)$	0.652

Table 6.5: The distribution of the overall geometrical measurements in the diabetic subgroups. The p-value of ANOVA test is shown with the significant differences between the subgroups as determined by the FLSD test. (Means that do not share a symbol are significantly different)

ARTERIOLAR DATA

Retinal Parameter Mean ± (STD)	No Retinopathy Group (117 bifurcations)	Mild NPDR Group (136 bifurcations)	Severe NPDR Group (139 bifurcations)	PDR Group (231 bifurcations)	p value
Parent Vessel Diameter d_0 (pixels)	6.47 ± (1.08)*	7.54 ± (1.68)†	7.58 ± (1.65)†	8.06 ± (1.84)‡	**0.000**
Large Child Diameter d_1 (pixels)	5.78 ± (1.10)*	6.65 ± (1.62)†	6.73 ± (1.66)†	7.23 ± (1.80)‡	**0.000**
Smaller Child Diameter d_2 (pixels)	4.60 ± (0.99)*	5.42 ± (1.37)†	5.43 ± (1.33)†	5.62 ± (1.43)†	**0.000**
Bifurcating Angle θ (Degrees)	76.13 ± (15.8)*	79.14 ± (17.9)*	78.78 ± (18.4)*	84.33 ± (18.6)†	**0.000**
Branching Angle θ_1 (Degrees)	25.77 ± (15.2)	27.32 ± (16.6)	28.33 ± (15.4)	27.44 ± (16.4)	0.560
Branching Angle θ_2 (Degrees)	50.36 ± (20.3)*	51.99 ± (21.3)*	50.45 ± (20.3)*	56.88 ± (22.9)†	**0.014**
Junction Exponent χ	3.70 ± (1.27)	3.80 ± (2.00)	3.92 ± (1.85)	4.15 ± (2.25)	0.161

Table 6.6A

VENULAR DATA

Retinal Parameter Mean ± (STD)	No Retinopathy Group (125 bifurcations)	Mild NPDR Group (174 bifurcations)	Severe NPDR Group (233 bifurcations)	PDR Group (363 bifurcations)	p value
Parent Vessel Diameter d_0 (pixels)	7.42 ± (1.87)*	9.04 ± (2.62)†	9.13 ± (2.56)†‡	9.55 ± (2.88)‡	**0.000**
Large Child Diameter d_1 (pixels)	6.51 ± (1.83)*	8.04 ± (2.55)†‡	8.05 ± (2.54)†	8.50 ± (2.79)‡	**0.000**
Smaller Child Diameter d_2 (pixels)	4.72 ± (1.08)*	5.51 ± (1.64)†	5.55 ± (1.47)†	5.82 ± (1.85)‡	**0.000**
Bifurcating Angle θ (Degrees)	77.68 ± (15.1)	80.40 ± (16.9)	80.75 ± (17.4)	82.53 ± (19.1)	0.062
Branching Angle θ_1 (Degrees)	24.81 ± (12.9)	23.43 ± (14.9)	24.34 ± (15.0)	23.53 ± (16.8)	0.921
Branching Angle θ_2 (Degrees)	53.00 ± (17.9)	57.34 ± (20.9)	57.43 ± (22.1)	59.65 ± (23.7)	0.504
Junction Exponent χ	3.02 ± (0.96)	2.99 ± (0.88)	2.94 ± (0.99)	3.18 ± (1.46)	0.07

Table 6.6B

Table 6.6: The distribution of the arteriolar (A) and venular (B) geometrical measurements in the diabetic subgroups. The p-value of ANOVA test is shown with the significant differences between the subgroups as determined by the FLSD test. (Means that do not share a symbol are significantly different)

The results of the ANOVA test shows that increased DR severity was associated with an overall significant steady and gradual dilatation of the vascular segments width that reached maximum with established PDR (p=0.000). These relationships were also maintained for the arteriolar and venular bifurcations subgroups (p=0.000).

The results of the overall data also revealed a significant gradual widening of the total bifurcation angle (θ) with increased severity of DR and development of proliferative retinopathy (p=0.000). This widening reflected specifically an associated steady increase in the branching angle of the smaller-child vessel segment (θ_2) with DR progression (p=0.027), with no similar change occurring in the larger-child vessel segment branching angle (θ_1). Such relationships for (θ) and (θ_2) angles were maintained also for the arteriolar bifurcations (p=0.000, p=0.014 respectively), however in the venular bifurcations, the same trend of angular widening was apparent yet did not reach a statistically significant levels (p=0.062, p=0.504 respectively).

The rest of the analysed geometrical parameters showed no definite relationships with different DR grades in the overall and arteriolar or venular subgroups apart from a significant relationship observed for the χ (p=0.050) nevertheless with no clearly defined trend between the different diabetic subgroups. In the arteriolar subgroup, there was a noted gradual increase in χ with increased DR severity yet this did not reach a statistical significant level. The same relationship was not observed in the venular subgroup.

3. Comparison of geometrical parameters between normal non-diabetic subjects and diabetic subjects with no detectable diabetic retinopathy

The results presented in the previous section described the relationship of changes in geometrical measurements and estimates in eyes of diabetic subjects with either no detectable retinopathy or different grades of retinopathy. The results demonstrated the steady and gradual increase in absolute vessel width measurements and the widening of the bifurcating angle θ subtended between the large and small child vascular segments at a bifurcation, and the branching angle of the small child θ_2 that was associated with the progressive worsening of the diabetic retinopathy grade and development of proliferative changes. In this section, we investigated whether these changes actually preceded the development of detectable diabetic retinopathy in subjects diagnosed with diabetes as a sign of early microvascular damage. These geometrical retinal parameters were thus compared between the cohort of normal non diabetic subjects of a similar population – previously analysed for benchmarking and its data described in detail in the previous chapter – with the group of diabetic subjects with no clinical detectable retinopathy. Unpaired two sample T test was performed and the results are shown in table 6.7

Two sample T test Normal group versus No Retinopathy group (Overall Data)				
	mean difference	95% Confidence Interval		p value
PARENT VESSEL WIDTH d_0	1.09	0.81	1.37	0.000
CHILD 1 VESSEL WIDTH d_1	1.08	0.80	1.35	0.000
CHILD 2 VESSEL WIDTH d_2	0.56	0.37	0.74	0.000
THETA ANGLE θ	0.20	-2.22	2.50	0.900
THETA 1 ANGLE θ_1	-1.20	-3.39	0.94	0.270
THETA 2 ANGLE θ_2	-0.10	-3.95	3.80	0.980

Table 6.7: Unpaired T test results for overall data between eyes of normal non-diabetic subjects and the diabetic subjects with no-retinopathy group.

The results revealed a statistically significant difference for the absolute vessel width measurements of the parent, larger child, and smaller child vascular segments, in eyes of diabetic subjects with no retinopathy (p=0.000). The vessels widths were smaller in the

diabetic subjects as compared to the normal non diabetic eyes. There were no detectable differences in any of the bifurcating and branching angles measurements between the two groups.

It could thus be concluded from the above observations that the absolute retinal vascular widths had a tendency to constrict with the development of diabetes; however this tendency is reversed with the development of clinically detectable diabetic retinopathy and continues thereafter. Conversely, for the bifurcating and branching angles, there was no evidence of any changes preceding the development of clinically detectable retinopathy, and it seemed that the changes and differences previously described developed with other signs of early retinal microvascular damage manifested in the minimal NPDR group and progressed gradually subsequently.

4. Evaluation of the effect demographic and associated clinical factors on the observed changes in retinal geometrical parameters in the diabetic subgroups.

In this section, we evaluated the effect of various demographic and clinical risk factors such as age, sex, duration and type of diabetes and history of systemic hypertension or hypercholesterolemia on the observed geometrical and architectural changes in retinal vascular network associated with worsening of diabetic retinopathy grade.

The relationship between the different demographic and clinical risk factors for disease progression and the various RVG features was demonstrated with the multiple regression analysis as shown in Table 6.8 for the overall measurements and Table 6.9 for the sub-analysed arteriolar and venular subgroups. Three models are presented; model 1 included age and sex, model 2 additionally included the diabetes type and history of hypertension, model 3 additionally included diabetes duration and history of hypercholesterolemia.

	OVERALL					
	MODEL 1		MODEL 2		MODEL 3	
AGE	Coefficient	P value	Coefficient	P value	Coefficient	P value
d_0	**-0.0226**	**0.000**	**-0.025**	**.000**	**-0.029**	**.000**
d_1	**-0.0224**	**0.000**	**-0.0275**	**.000**	**-0.031**	**.000**
d_2	**-0.0152**	**0.000**	**-0.0201**	**.000**	**-0.0223**	**.000**
α	0.001	0.291	.000	0.97	0.0001	0.807
β	**-0.001**	**0.035**	**-0.001**	**0.004**	**-0.001**	**0.008**
Θ	-0.052	0.236	-0.07	0.139	-0.07	0.165
θ_1	0.0161	0.719	-0.034	0.512	-0.041	0.436
θ_2	-0.07	0.24	-0.015	0.824	-0.005	0.944
X	**-0.0149**	**.000**	**-0.0204**	**.000**	**-0.019**	**.000**
$\mathcal{P}$	**0.003**	**0.009**	**0.004**	**0.004**	**0.004**	**0.006**
FEMALE						
d_0	**-0.305**	**0.023**	**-0.26**	**0.05**	**-0.327**	**0.017**
d_1	**-0.345**	**0.008**	**-0.298**	**0.025**	**-0.358**	**0.007**
d_2	-0.0769	0.363	-0.053	0.539	-0.083	0.333
α	0.0235	0.065	0.022	0.08	0.025	0.053
β	-0.007	0.474	-0.005	0.627	-0.003	0.768
Θ	-1.77	0.23	-0.675	0.501	-0.796	0.428
θ_1	0.068	0.945	0.553	0.586	0.481	0.637
θ_2	-1.73	0.202	-1.61	0.244	-1.67	0.229
X	**-0.244**	**0.006**	**-0.22**	**0.015**	**-0.213**	**0.019**
$\mathcal{P}$	**0.057**	**0.045**	0.0526	0.071	0.049	0.094
TYPE 2 DM						
d_0			0.021	0.9	**0.686**	**0.001**
d_1			0.001	0.993	**0.598**	**0.003**
d_2			0.196	0.063	**0.495**	**.000**
α			0.036	0.023	0.011	0.571
β			0.0261	0.038	0.006	0.691
Θ			-0.486	0.692	0.991	0.519
θ_1			1.08	0.382	1.726	0.269
θ_2			**-3.655**	**0.031**	-2.7	0.203
X			**0.234**	**0.034**	0.1608	0.249
$\mathcal{P}$			-0.045	0.203	-0.007	0.866

HYPERTENSION					
d_0		0.198	0.175	0.1209	0.419
d_1		0.217	0.122	0.147	0.309
d_2		0.031	0.732	0.015	0.872
α		-0.017	0.198	-0.014	0.316
β		-0.0001	0.982	0.002	0.821
Θ		2.53	0.018	1.689	0.127
θ_1		1.82	0.091	1.93	0.083
θ_2		1.98	0.176	0.978	0.521
X		0.009	0.919	0.012	0.904
$\mathcal{P}$		-0.002	0.941	-0.011	0.714
DURATION					
d_0				**0.004**	**.000**
d_1				**0.003**	**.000**
d_2				**0.001**	**.000**
α				**-0.0001**	**0.024**
β				**-0.0001**	**0.023**
Θ				**0.0113**	**0.04**
θ_1				0.003	0.514
θ_2				0.0085	0.268
X				-0.0004	0.346
$\mathcal{P}$				0.0001	0.109
CHOLESTEROL					
d_0				**0.298**	**0.028**
d_1				**0.272**	**0.037**
d_2				0.071	0.405
α				-0.012	0.318
β				-0.0106	0.301
Θ				**2.957**	**0.003**
θ_1				-0.358	0.723
θ_2				**3.47**	**0.012**
X				-0.014	0.873
$\mathcal{P}$				0.034	0.239

Table 6.8: Results of multiple regression analysis for different risk factors with overall data. The Coefficient and p values are shown for model 1 (age and sex), model 2 (age, sex, diabetes type, history of hypertension), model 3 (age, sex, diabetes type, history of hypertension, duration of diabetes, and history of high cholesterol)

223

	ARTERIOLAR						VENULAR					
	MODEL 1		MODEL 2		MODEL 3		MODEL 1		MODEL 2		MODEL 3	
AGE	Coeff	P	Coeff	P	Coeff	P	Coeff	P	Coeff	P	Coeff	p
d_0	**-0.0271**	**0.000**	**-0.0278**	**0.000**	**-0.0301**	**0.000**	**-0.02**	**0.021**	**-0.0228**	**0.026**	**-0.03**	**0.004**
d_1	**-0.0299**	**0.000**	**-0.0299**	**0.000**	**-0.0329**	**0.000**	**-0.021**	**0.011**	**-0.024**	**0.015**	**-0.03**	**0.003**
d_2	**-0.0211**	**0.000**	**-0.026**	**0.000**	**-0.0272**	**0.000**	**-0.011**	**0.039**	**-0.013**	**0.035**	**-0.017**	**0.008**
α	0.0001	0.623	-0.0005	0.537	-0.001	0.722	0.001	0.26	0.001	0.517	0.0006	0.522
β	**-0.002**	**0.01**	**-0.002**	**0.005**	**-0.002**	**0.004**	-0.0003	0.49	-0.0006	0.269	-0.001	0.351
Θ	-0.103	0.137	-0.115	0.165	-0.094	0.268	-0.0194	0.736	-0.046	0.487	-0.064	0.357
θ_1	0.0651	0.288	0.024	0.74	0.0138	0.855	-0.018	0.768	-0.07	0.289	-0.092	0.226
θ_2	-0.173	0.037	-0.142	0.152	-0.111	0.274	-0.003	0.965	0.075	0.45	0.075	0.467
X	**-0.029**	**0.000**	**-0.037**	**0.000**	**-0.0369**	**0.000**	-0.004	0.265	-0.005	0.2	-0.005	0.211
$\mathcal{P}$	**0.004**	**0.014**	**0.004**	**0.033**	**0.005**	**0.023**	0.002	0.148	0.003	0.099	0.002	0.149
FEMALE												
d_0	0.1295	0.369	0.109	0.465	0.0096	0.948	**-0.48**	**0.015**	-0.39	0.051	**-0.489**	**0.015**
d_1	0.0674	0.631	0.0492	0.736	-0.0462	0.751	**-0.552**	**0.004**	**-0.456**	**0.019**	**-0.541**	**0.006**
d_2	0.0203	0.858	0.0368	0.756	-0.005	0.962	-0.129	0.286	-0.104	0.398	-0.151	0.225
α	-0.003	0.859	0.003	0.839	0.011	0.533	**0.037**	**0.034**	0.0302	0.091	0.031	0.086
β	-0.0262	0.098	-0.019	0.234	-0.014	0.367	-0.012	0.282	-0.0135	0.267	-0.0118	0.339
Θ	-0.518	0.735	0.241	0.88	-0.272	0.865	-1.866	0.151	-1.42	0.28	-1.73	0.191
θ_1	-0.904	0.503	-0.314	0.822	-0.423	0.766	0.366	0.795	0.688	0.632	0.503	0.729
θ_2	0.47	0.797	0.627	0.741	0.228	0.905	-2.91	0.132	-2.47	0.208	-2.58	0.194
X	**-0.42**	**0.011**	**-0.36**	**0.036**	**-0.345**	**0.048**	**-0.19**	**0.029**	**-0.197**	**0.027**	**-0.194**	**0.03**
$\mathcal{P}$	0.0801	0.061	0.08	0.071	0.071	0.113	**0.076**	**0.034**	**0.073**	**0.046**	0.068	0.064
TYPE 2 DM												
d_0			**0.115**	**0.544**	**0.632**	**0.007**			-0.182	0.442	0.494	0.113
d_1			**0.0657**	**0.723**	**0.594**	**0.009**			-0.199	0.387	0.378	0.213
d_2			**0.255**	**0.135**	**0.458**	**0.014**			0.017	0.905	0.349	0.071
α			0.0321	0.151	-0.009	0.738			0.0379	0.074	0.0336	0.232
β			0.012	0.565	-0.001	0.944			0.0174	0.229	0.006	0.74
Θ			-1.99	0.323	-0.721	0.772			-0.213	0.892	1.77	0.392
θ_1			0.281	0.875	1.181	0.592			1.683	0.323	2.96	0.191
θ_2			-2.34	0.332	-1.969	0.508			**-5.23**	**0.025**	-4.69	0.129
X			0.254	0.246	0.155	0.565			0.095	0.365	0.088	0.528
$\mathcal{P}$			-0.012	0.822	0.006	0.927			-0.026	0.545	0.003	0.953

	Coeff.	p	Coeff.	p	Coeff.	p	Coeff.	p
HYPERTENSION								
d_0	-0.123	0.453	-0.118	0.48	**0.494**	**0.016**	**0.456**	**0.032**
d_1	-0.096	0.547	-0.072	0.659	**0.528**	**0.008**	**0.49**	**0.018**
d_2	-0.0246	0.85	-0.0152	0.909	0.128	0.312	0.15	0.256
α	0.013	0.498	0.0111	0.574	**-0.042**	**0.022**	**-0.039**	**0.042**
β	0.0214	0.237	0.0267	0.151	-0.005	0.649	-0.002	0.863
Θ	3.755	0.032	2.997	0.096	2.33	0.087	1.834	0.194
θ_1	2.198	0.155	2.396	0.133	1.468	0.321	1.434	0.353
θ_2	1.538	0.461	0.598	0.781	2.982	0.14	2.443	0.246
X	0.123	0.513	0.114	0.558	-0.049	0.587	-0.034	0.717
P	0.0062	0.899	-0.009	0.852	-0.012	0.736	-0.017	0.665
DURATION								
d_0			**0.003**	**0.000**			**0.003**	**0.001**
d_1			**0.003**	**0.000**			**0.0032**	**0.003**
d_2			**0.001**	**0.002**			**0.001**	**0.008**
α			**-0.001**	**0.006**			-0.0001	0.778
β			-0.001	0.2			-0.001	0.333
Θ			0.0125	0.172			0.0117	0.112
θ_1			0.005	0.515			0.007	0.374
θ_2			0.0071	0.515			0.0037	0.733
X			-0.0006	0.522			-0.001	0.892
P			0.001	0.418			0.001	0.405
CHOLESTEROL								
d_0			0.103	0.477			0.236	0.221
d_1			0.031	0.826			0.221	0.239
d_2			0.0193	0.868			-0.021	0.855
α			-0.002	0.89			-0.011	0.498
β			-0.023	0.137			-0.013	0.25
Θ			**3.23**	**0.038**			2.026	0.115
θ_1			-0.551	0.689			0.32	0.819
θ_2			**3.722**	**0.046**			1.94	0.309
X			0.0138	0.935			-0.056	0.517
P			0.064	0.137			0.0194	0.585

Table 6.9: Results of multiple regression analysis for different risk factors with arteriolar and venular data. The Coefficient and p values are shown for model 1 (age and sex), model 2 (age, sex, diabetes type, history of hypertension), model 3 (age, sex, diabetes type, history of hypertension, duration of diabetes, and history of high cholesterol)

In the results presented above, increased age was associated with significant decreased arteriolar and venular vascular width (p=<0.01), together with reduction in the arteriolar area ratio β (p=<0.01) and χ (p=<0.01) estimates and an increase in the arteriolar optimality parameter P (p= <0.05).

Female sex was associated with decreased venular vascular width (p=<0.05) (apart from the diameter of the smaller-child vessel segment), as well as reduction in the arteriolar and venular χ (p=<0.05).

Type 2 diabetes was associated with increased arteriolar vascular width (p=<0.05) while the increased duration of diabetes was associated with increased arteriolar and venular vascular width (p= <0.01).

History of hypertension was associated with increased venular vascular width (p=<0.05) (excluding the small-child vessel segment), while history of high cholesterol was associated with increased both the arteriolar bifurcation angle (θ) (p=<0.05) and the smaller-child branching angle (θ_2) (p=<0.05).

There were no other significant associations noted between the examined variables and the rest of the RVG features (data not shown).

6.7 Discussion

Over the past three decades, various methods to treat diabetic retinopathy and macular oedema had been validated by several multicenter clinical trials in an effort to preserve patients' vision.

In 1968, at the Airlie House Convention, a collection of retinal images with diabetic retinopathy were endorsed as "Standard photographs" to illustrate both the appearance and degree of the various lesions of diabetic retinopathy. The Airlie House classification was subsequently modified by the DRS, and extended by the EDTRS. Current standard methods for grading diabetic retinopathy are based on semi-quantitative grading of the

severity of retinopathy by comparison with this set of standard images showing various retinopathic features. [53, 55]

It is well established now that severe vision loss from diabetes primarily results from intraocular angiogenesis (proliferative diabetic retinopathy), and moderate visual loss principally occurs from leakage of the retinal vessels (diabetic macular oedema). The risk of severe visual loss from PDR is approximately 40% after 6 years if not treated. [61]

The clinical trials such as DRS, ETDRS, DCCT, UKPDS and the DRVS had ascertained the ability of pan-retinal scatter laser photocoagulation and other surgical methods such as pars plana vitrectomy to reduce the risk of severe vision loss from PDR to less than 2%, and the risk of moderate visual loss from clinically significant macular oedema by 50%. [51, 53, 182] Today, blindness from diabetic retinopathy is largely preventable with timely detection and appropriate interventional therapy. The current challenge is thus to identify and access all diabetic persons for accurate evaluation and treatment to preserve vision, and to apply systemic standards of care previously validated.

- Limitations of current methods of classification of diabetic retinopathy

However, until now the debate about indications and timing for treatment of diabetic patients with variable features of NPDR and PDR is far from settled. For example, the EDTRS recommended scatter laser treatment to be delayed till eyes with NPDR approach the high-risk PDR stage. With the knowledge that eyes with severe NPDR have a 52% risk of developing PDR within one year, and a 60% risk of developing high risk PDR within 5 years [64], a policy of continued observation would be expected to spare a minority of eyes from the risks of treatment, while increasing the risk of rapid progression that might occur between follow-up visits, with patients presenting late with large vitreous haemorrhages, making plans of satisfactory treatment difficult. Other local and systemic factors – not considered with initial EDTRS recommendations – would be taken into account in choosing between prompt treatment and deferral such as patients' age, type of diabetes and their commitment to careful follow up, level of arteriosclerosis, and presence or absence of renal or hypertensive retinopathy. If deferral of treatment is opted, these patients require follow-up evaluation on 4 – 6 months basis.

In general, the EDTRS results and clinical impression suggested that for older patients with type II diabetes who have very severe NPDR or early PDR, prompt photocoagulation is safer than deferral, while in younger patients with type I diabetes, there is little to lose from deferring scatter photocoagulation until high risk PDR develops. The EDTRS did not consider the coexisting level of NPDR in the presence of PDR, nevertheless the clinical practice of some eye specialists suggested that based on risk of progression to high risk PDR for baseline levels of NPDR, the level of NPDR and macular oedema and the medical status may be deciding factors in determining follow-up and timing of laser treatment for patients with PDR who are not at the high risk stage.

It is thus clear that there is still a need in clinical practice for further methods and novel markers for stratification of eyes with different grades of diabetic retinopathy, and identification of eyes with signs of progression and at risk of visual loss. However, it is important to understand that diabetic eye disease is an end organ response to a generalised metabolic disease, and that present strategies for dealing with diabetic retinopathy address only the retinal signs of established vascular damage.

- Retinal vascular calibre analysis

Various research groups have investigated the associations and clinical significance of early retinal vascular calibre changes in individuals with diabetes and pre-diabetes, in an attempt to clarify their role in identifying subtle changes in the retinal microvasculature, which might offer new approaches to screening and prevention of retinopathy. This has been helped by recent advances in digital retinal imaging technology and improvements in computer image analysis software. [135, 157]

Prospective data from population-based cohorts have shown that changes in retinal vascular calibre may predict the development of diabetes [123], and impaired fasting glucose. [127] In middle-aged persons without diabetes, retinal arterioles were significantly narrower in persons who subsequently developed diabetes during the ensuing 3.5 years as compared with those who did not. [123] Moreover, the WESDR reported that persons with type II diabetes without retinopathy had smaller mean arteriolar and venular diameters than persons without diabetes. The differences were independent of age, mean arterial blood pressure or smoking. [183]   Retinal arteriolar

narrowing was considered a marker of microvascular damage from inflammation and other processes, and reflected the intimal thickening, medial hyperplasia, hyalinization, and sclerosis seen histopathologically. [184] These findings were recently supported by Mandecka et al. In their study, they demonstrated that in a group of type 1 diabetic patients without retinopathy, with relatively good glycaemic control, there was reduced retinal arterial and venous vasodilatation after a flickering light stimulus, which they hypothesised to denote a state of endothelial dysfunction and disturbance of retinal autoregulation, that might play a role in the early stage of the development of microvascular disorders before the development of morphological signs of diabetic retinopathy. [185]

Further studies evaluated the associations of vascular calibre changes with developing signs of diabetic retinopathy. The WESDR reported that in persons with younger onset diabetes, larger arteriolar and venular calibre, independent of retinopathy severity level, was related to the progression of retinopathy, and larger venular calibre was associated with the 4 year incidence of proliferative retinopathy. However, large calibre of retinal vessels was not associated with incident retinopathy. [186] Alibrahim et al demonstrated in their study in children and adolescents with type I diabetes, that large arteriolar calibre was significantly associated with the onset of mild NPDR, independent of age, gender, diabetes duration, glucose control, blood pressure and BMI. [187] Similarly, in a cross-sectional analysis of the Blue Mountain Eye Study, Kifley et al confirmed an association of wider retinal arteriolar calibre with milder levels of diabetic retinopathy, and increasing severity of the retinopathy was associated with widening of venular calibre. [188] The usefulness of venular calibre as a surrogate marker of diabetic microvascular complications has been supported by many studies. It has been speculated that retinal venular widening might be the result of increased blood flow associated with hyperglycaemia, and retinal hypoxia, and it might also occur as result of an inflammatory process. [189, 190]

Most of the previous epidemiological studies adopted the technique developed by Parr, Hubbard, and colleagues to measure retinal vascular calibres from photographs and summarised these as the arterio-venous ratios. This technique proved to have substantial reproducibility; however the conclusions drawn from these studies reflected results from only a limited retinal area surrounding the disc in which the vessels were measured. [135]

On comparing with the above mentioned population-studies, the results of our study appear consistent with their findings and the suggested theories. Our study demonstrated a clinical and statistical narrowing of both the arteriolar and venular vessels associated with the diabetic subjects with no clinical detectable retinopathy as compared with an age matched population of non diabetic subjects. This association reverses with the development of early sign of diabetic retinopathy in the subgroup of diabetic subjects with minimal non proliferative diabetic retinopathy, and continues thereafter in a gradual yet steady manner with worsening of the retinopathy severity grade in the subgroup of subjects with severe non proliferative diabetic retinopathy, and peaks in association with the established proliferative retinopathy. These relationships were largely maintained in both the arteriolar and venular retinal vascular networks.

As previously speculated, the retinal vascular dilatation associated with worsening of diabetic retinopathy presented here could reflect the increased blood flow associated with hyperglycaemia [189], and retinal hypoxia [191], brought on by altered retinal autoregulation. [185] Alternatively, it could also represent an inflammatory process implicated in the pathogenesis of impaired glucose metabolism. [190]

Unlike the findings of previously mentioned studies, the results of this study represent a collective analysis of a wide variety of arteriolar and venular vascular segments of different sizes, and orientations across the entire nasal and temporal retinal fields at variable distances from the optic disc, thus could arguably represent more the retinal microvascular state in diabetic retinopathy.

- Retinal vascular architecture analysis

The development of recent image analysis computer software has allowed the measurement and detailed study of other architectural and geometrical changes in the retinal microvasculature. As previously discussed, ageing and hypertension have been associated with reduced branching angles at arteriolar bifurcations, together with reduced microvascular density. [88, 89] Suboptimal arteriolar bifurcations have also been associated with peripheral vascular disease in the form of altered junction exponent ratios

and optimality parameters, but with no significant change detected in the bifurcation angles. [91] Results from the Beaver Dam Eye Study demonstrated an increase risk of IHD death associated with suboptimal relationship of arteriolar diameters at bifurcation, with decreased arteriolar tortuosity. [101]

In this study, detailed geometrical analysis of the arteriolar and venular bifurcations was performed. The association of the geometrical features with the level of diabetic retinopathy was evaluated and comparisons were made between the different subgroups of diabetic subjects.

Unlike previous reports on arteriolar bifurcation narrowing with hypertension, the results of our study revealed a gradual yet significant widening of both the arteriolar and venular bifurcating angles with increased severity of the diabetic retinopathy grade. This association started to develop in subjects with minimal background non proliferative diabetic retinopathy, and gradually increased in subjects with severe non proliferative retinopathy, and reached its relative maximum width in subjects with proliferative retinopathy. This association was found to be in conjunction with a similar relationship of the branching angle of the smaller child vessel segment at a bifurcation, which also markedly increased in width with increased severity of the diabetic retinopathy grade in both arteriolar and venular bifurcations. Diabetic subjects with no detectable clinical diabetic retinopathy showed no difference in their bifurcating angles when compared with non diabetic subjects. No change was noticed in the branching angle of the larger child vessel with any level of diabetic retinopathy.

Considering the growing evidence in literature about the impact of endothelial cells dysfunction and its role in the pathogenesis of hypertensive and diabetic retinopathy [164, 192, 193], one would expect similar changes in vascular bifurcating angles in both retinopathies. On the contrary, the results are contradictory to those previously described. However, this might not be surprising bearing in mind the different impact of hypertension and diabetes on retinal vessels. In a distinct contrast to the association of hyperglycaemia with retinal vascular calibre dilatation as previously explained, it has been long known that generalised retinal arteriolar narrowing is an early characteristic sign of hypertensive retinopathy [194, 195], with recent studies demonstrating a graded association of narrowed retinal arterioles with increasing blood pressure in different

populations of various ethnic and age groups. [168, 196] Indeed, previous authors have speculated that the narrowed bifurcation angles associated with hypertension, might be related to the higher degree of vasoconstriction and enhanced resting tone of the retinal vessels, although the mechanism by which vasoconstriction might alter the bifurcating angles remained unclear. [96]

Similarly, it could well be that what we are describing here of gradual and continuous widening of bifurcating angles with increased severity of diabetic retinopathy is actually a reflection of increased work-load and energy loss sustained by a compromised retinal vascular network with progressive worsening of retinopathy. This retinopathy progression in turn reflects increased retinal ischaemia resulting in alterations in blood flow,[197] endothelial dysfunction, [198] and attenuation in oxygen concentration, [90] all of which have previously been shown to affect vascular branching angles. The results of this study are in keeping and correspond to the recent findings of Sasongko and colleagues showing larger arteriolar branching angles in association with longer diabetes duration. [199]

The data results of our study for the rest of the geometrical features especially the junction exponent and the optimality parameter did not reveal a consistent clinically or statistically significant change in association with the increased severity of diabetic retinopathy. This, together with the maintenance of comparable values of the asymmetrical ratio, area ratio, and the relative vascular diameters between the different subgroups of subjects with different grades of diabetic retinopathy shows that despite changes in vascular calibres, the vessel segments retain similar relationships at the bifurcation and implies that the retinal vessels attempt to maintain the a co-ordinated regulation of vascular tone at the bifurcating points as previously suggested [90], and retain its optimality in response to different stimuli. On the other hand, we acknowledge that the wide range of variability in measurements found with some parameters such as the junction exponent as previously discussed might have diluted any existing relationships.

- Relation of retinal vascular geometrical and architectural changes with various demographic and clinical risk factors.

The study evaluated the association of RVG alterations with increased severity of DR in age-matched cohorts of adult type 1 and 2 diabetics with established DR ranging from minimal NPDR to PDR.

Age was associated with reduced arteriolar and venular vascular widths, corresponding to earlier work by Klein et al on type 1 and type 2 diabetics.[166] [183] The reduced JER noted with age in diabetics is also consistent with similar results reported with age progression in non-diabetic subjects. [88] Our results suggest that female diabetic patients might have relatively compromised retinal vascular networks, reflected in reduced JER, as compared to their male compatriots. This observation supports previous reports that female type 1 diabetic patients could be at greater risk for diabetic microvascular complications as compared with age-matched male patients. [200, 201]

Longer duration of diabetes was associated with arteriolar and venular dilatation. Proposed mechanisms underlying this relationship are multifactorial and relate to ongoing retinal hypoxia, inflammation and endothelial dysfunction. There was no effect noted on branching angles as previously reported. [199] The increased arteriolar bifurcating angles noted here with high cholesterol levels supports the evolving evidence in previous studies of the role of lipids on the retinal microvasculature. [202]

It is worth noting here that these observed alterations in RVG associated with the various risk factors would have not affected our previous comparative results of diabetic subjects with different grades of retinopathy, as the study diabetic subgroups were evenly matched in most of their demographic and clinical data as presented in table 6.2

- Interpretation of results

Several important points needed to be observed in interpreting the findings in this study.

1. In this study, we did not control for variations in pulsatility associated with the cardiac cycle. This was previously estimated to cause up to 6% in variation for arteriole and venule absolute width diameters. [203] However, assuming that the photographs were taken at random during the cardiac cycle, we think this would have resulted only in minor attenuation of our findings. Furthermore this would have no effect on the other geometrical features analysed, and together with the fact that in this study, the vascular segments within 1 disc diameter around the optic disc were excluded, to reduce the effect of the cardiac pulse on the large retinal vessels at the optic disc, the detrimental effect of pulsatility variations would thus be minimal.

2. Being a retrospective cross sectional study, the clinical data collected for analysis were obtained from hospital clinical notes; however clinical details may not have been accurate. This might have affected accurate stratification of our subjects with regard to their associated clinical data such as hypertension, and high cholesterol levels and smoking history. In addition, the lack of clinical details of subjects with no detectable diabetic retinopathy hindered our chance for assessing the distribution of associated clinical factors to compare with the other groups.

3. The results and findings of this study, like other large population studies, are cross sectional associations between groups of subjects with different grades of diabetic retinopathy. As shown in our data, there was a wide overlap between ranges of measurements for the different analysed parameters, thus no fixed value would be possible to define a certain parameter for a specific grade of diabetic retinopathy. We believe that the relationships and associations described in this study cannot be primarily attributed to an observer measurement error, as any measurement variability would occur at random within all the subgroups, and mostly neutralise each other. This was previously reflected by the calculated low mean differences of the inter-visit individual study as previously described in section 4.6.2.

However, it remains unclear whether these calculated differences between the different diabetic groups and the associations described are sufficiently large to differentiate patients at an individual subject level, or even at the bifurcation level taking into consideration that at such level of comparisons, the calculated intra-observer within-subject measurement errors would need to be taken into account to define clinical significance, which in turn would – to a degree - hamper the ability to categorise patients in accordance to their retinal geometrical features.

6.8 Conclusion

In this chapter, the results of cross sectional analysis of cohorts of diabetic subjects with different grades of diabetic retinopathy demonstrated the association of retinal vascular architectural and geometrical changes with the worsening of diabetic retinopathic stages and development of proliferative disease. These changes represent novel vascular markers of advancing diabetic retinopathy, which have not been described before. In this era of developing technology for automated detection of diabetic retinopathy, we believe that the implementation of geometrical vascular analysis can thus offer new means and provide additional information to identify diabetic subjects with advanced retinopathy, especially when other retinopathic features are unclear or absent.

Chapter 7: Retrospective Analysis of Retinal Vascular Geometry in Longitudinal Data of Diabetic Subjects

7.1: Overview

This chapter evaluates the role of retinal geometrical analysis on the individual level in providing clues for progression of diabetic retinopathy, and establishment of proliferative retinopathy. Having described the cross-sectional comparative associations of geometrical changes with advancing diabetic retinopathy between cohorts of diabetic subjects, this study explores if similar changes can be detected in subjects with progressing retinopathy, and whether such geometrical markers would precede the development of proliferative retinopathy. The study also assesses the predictive value of geometrical analysis in identifying patients at risk of developing future proliferative retinopathy.

7.2 Introduction

In the previous chapter, we were able to demonstrate that there are changes in certain retinal vascular geometrical measurements with increased severity of diabetic retinopathy as compared with age matched non diabetic controls. These findings were the result of cross sectional comparative analysis, and thus the ability to determine the predictive value of these changes was limited.

Furthermore, analysis of the data revealed a significantly wide range of measurements within each subgroup with a considerable amount of overlap of these ranges between these subgroups. It was thus unclear whether these changes in geometrical measurements could be detected on an individual basis.

This study was thus designed to evaluate the relationship of changes in retinal geometry with progression of diabetic retinopathy in a sample of diabetic patients attending diabetic retinopathy screening and who demonstrated progression to proliferative diabetic retinopathy "Progressors". These relationships were compared to an age matched sample of diabetic patients who had been followed up for a corresponding period of time and showed no signs of diabetic retinopathy progression "Non-progressors". The study assessed whether any detectable RVG changes could be noticed in the final screening images – with confirmed proliferative diabetic retinopathy - when comparisons are made against the baseline screening images and the penultimate visit – irrespective of its diabetic retinopathy grading - before the establishment of proliferative changes in the progressors group, and in the corresponding images of the non-progressors group. If verified, RVG changes could have an important clinical role as useful novel features utilised in anticipating the imminent development of proliferative diabetic changes and thus flagging up those patients at risk once they reached this critical stage of progression during their screening process.

Finally the study also attempted to explore whether the retinal vascular network of subjects who progressed to proliferative diabetic retinopathy exhibited any structural changes at baseline that might distinguish them from those who did not show any signs of progression. If proven, this could potentially identify individual retinal vascular networks that were at higher risk of developing future retinovascular complications, which in turn could lead to modifications and adjustments of the diabetic retinopathy screening plan for such subjects.

7.3 Objectives

1. To assess the differences in retinal architectural and geometrical features between the baseline, penultimate and final screening fundus images for the age-matched progressors and non-progressors groups after the same period of follow-up.

2. To evaluate the predictive value of the various retinal vascular architectural and geometrical features in diabetic subjects at base-line for subsequent development of proliferative retinopathy.

7.4 Subjects and Methods

The study was designed as a pilot predictive study for analysis of retrospective data obtained from retinal images of diabetic subjects who had been followed up for an average period of 6 years. Retinal screening images collected from the image database of the South of the Tyne and Wear (SOTW) diabetic retinopathy screening programme were used.

Patients who were graded as having proliferative diabetic retinopathy (NCS grade, R3) during the year 2009 were identified. All these patients had been referred to the diabetic retinopathy clinics at Sunderland Eye Infirmary and cases which had a confirmed clinical diagnosis of proliferative diabetic retinopathy were noted from the hospital clinic letters. Amongst these cases, subjects who were 65 years of age or less, with a preceding screening follow-up period of 6 years or more were chosen.

For these patients, the baseline screening images at initial presentation, the final screening images and the screening images captured at the penultimate visits were extracted. The baseline screening retinal images were captured with a Zeiss FF 450 Plus fundus camera fitted with a JVC KY-F70B 3CCD digital camera with a resolution of 1360 X 1024 pixels, similar to the camera system based at Sunderland Eye Infirmary utilised for the rest of the study, however the penultimate and final visit screening images were mostly captured with upgraded camera systems with a resolution of 2544 X 1696 pixels, and 3504 X 2336 pixels.

The retinal images were graded for field position and image quality according to the national screening committee for diabetic retinopathy screening guidelines. Only subjects with retinal images graded as "good" were considered for the study. Cases in which the retinal images showed any evidence of concurrent retinal or optic nerve pathology such as retinal vascular occlusions, or advanced glaucomatous optic disc cupping were then excluded. The included cases with relatively long follow-up screening period, and who showed recent progression to definite clinically proven proliferative diabetic retinopathy constituted "the progressors group".

An age-matched sample of diabetic subjects who attended the same diabetic retinopathy screening programme, and were followed up for a corresponding period of time, and their retinal screening images showed no evidence of progression of diabetic retinopathy grade were then selected. The same inclusion and exclusion criteria were considered. The retinal screening images of these subjects captured at baseline during initial presentation, the penultimate and final visit screening images were extracted. These subjects represented a control group for comparison and constituted "the non-progressors group".

The retinal screening images for both the progressors and non-progressors groups were formally graded by certified primary and / or arbitration diabetic retinopathy graders as part of the screening programme protocol. The National Screening Committee grading for each subject's screening visit were recorded. The retinal images of all subjects in both groups were anonymised and coded according to the study protocol.

Image labelling and marking

Ten to 15 identifiable arteriolar and venular vascular bifurcations were labelled for each baseline nasal and temporal retinal image for the selected eyes of subjects in both groups. Equivalent numbers of right and left eyes were chosen for both groups. Care was taken to select bifurcations of variable size and orientation across the central and peripheral image fields. For each subject, the same vascular bifurcations were then nominated in the corresponding penultimate and final retinal screening images.

The labelled images of all visits for all subjects in both groups were grouped together and randomly presented to one observer for the vascular bifurcations' marking utilizing the custom-built semi-manual observer-driven technique designed and adopted for this thesis. The random sequence of image digits was determined using a net-based research randomiser. The observer was masked to the image order of each subject, the marking results of the corresponding images, and the diabetic retinopathy grading for each image, however it was impossible to mask the other retinopathic features.

As previously described in the methodology chapter, for each vascular bifurcation, the absolute vessel widths measurements for the parent vessel, large and small child vessels were calculated. The total bifurcating angle subtended between the two child vessels, together with the branching angles of each child vessel segments were also measured, and the other relative diameter ratios, area ratios and asymmetry ratio were then estimated. The resultant data were tabulated and those of corresponding vascular bifurcations in each image set of visits were linked together to facilitate like for like comparisons to be made.

7.5 Statistical analysis

One-way ANOVA was used to compare the RVG features between baseline, penultimate and final visits' images for both the progressors and non-progressors groups, and FLSD ad-hoc test was performed for significant relations only where the (p) value was ≤ 0.05.

Binary logistic regression analysis was used to determine the odd ratios for retinopathy progression based on baseline RVG features measurements of both the progressors and non-progressors groups with the binary variables being "progress" and "non-progress" with the RVG features being the dependable variables at baseline.

7.6 Results

The progressors group included 5 eyes of 5 subjects with an age range 50 – 65 years (mean = 57 years). There were 3 right eyes and 2 left eyes. A total of 121vascular bifurcations were analysed for per screening visit (55 arteriolar and 66 venular bifurcations). The NCS diabetic retinopathy grading for these eyes is described in table 7.1

NSC diabetic retinopathy grading for progressors group					
	Patient 1	**Patient 2**	**Patient 3**	**Patient 4**	**Patient 5**
Baseline at presentation	R 1	R 0	R 0	R 0	R 1
Penultimate visit	R 1	R 1	R 1	R 1	R 1
Final visit	R 3	R 3	R 3	R 3	R 3

Table7.1: NSC grading for the progressors group

The non-progressors control group consisted of 5 eyes of 5 subjects with an age range 47 – 65 years (mean = 59 years). There were 3 left and 2 right eyes. A total of 97 bifurcations were analysed per screening visit (51 arteriolar and 46 venular bifurcations). The NSC diabetic retinopathy grading was (R 0) for all eyes in all screening visits.

The total follow up screening period was 6 years for the subjects in both the progressors and non-progressors groups. There was an average of 1 year interval between the penultimate and final screening visits.

Power calculation: Following Goodall et al. calculations, considering the previously calculated average standard deviations *(s)* for absolute vessel widths and angular bifurcations, together with the assumed meaningful "clinically important difference" *(d)*, then for a *(s/d)* ratio of 2.50 the included numbers for the overall analysed bifurcations for the "progressors" and "non-progressors" would result in an average of 80% to 90% study power, however this dropped significantly to 50% power for the arteriolar and venular subcategories analysis. [181]

1. Evaluation of retinal vascular geometrical features distribution in the baseline, penultimate and final screening fundus images for the "progressors" and "non-progressors".

The differences in the geometrical measurements were compared between the baseline retinal screening images captured at presentation, the penultimate images and the final screening images for each group. Absolute vascular width comparisons were excluded from the analysis due to significant difference in the used camera systems over the follow-up period with difference in image resolution that could hamper comparisons made in terms of absolute pixel size. The rest of the geometrical measurements, being non-dimensional, thus unaffected by image resolution, are presented using the ANOVA test for the overall data as shown in tables 7.2 and 7.3 for the "progressors" and "non-progressors" groups respectively.

PROGRESSORS OVERALL DATA				
Retinal Parameter Mean ± (STD)	Baseline Visit (No or minimal NPDR)	Penultimate Visit (No or minimal NPDR)	Final Visit (PDR)	p value
Bifurcating Angle θ (Degrees)	78.43 ± (15.5)	78.48 ± (14.8)	80.33 ± (13.0)	0.54
Branching Angle θ_1 (Degrees)	26.47 ± (14.9)	28.49 ± (15.3)	26.26 ± (13.9)	0.501
Branching Angle θ_2 (Degrees)	51.98 ± (20.5)	49.98 ± (21.0)	54.07 ± (17.6)	0.334
Bifurcation Index λ	0.773 ± (0.14)	0.804 ± (0.20)	0.797 ± (0.23)	0.476
Larger child diameter ratio λ_1	0.868 ± (0.06)	0.854 ± (0.08)	0.858 ± (0.08)	0.406
Smaller child diameter ratio λ_2	0.665 ± (0.10)	0.672 ± (0.11)	0.668 ± (0.13)	0.921
Asymmetry Ratio α	0.619 ± (0.22)	0.691 ± (0.37)	0.691 ± (0.44)	0.237
Area Ratio β	1.213 ± (0.15)	1.203 ± (0.14)	1.211 ± (0.17)	0.892
Junction Exponent χ	3.102 ± (1.02)	3.01 ± (0.83)	3.104 ± (1.08)	0.721
Optimality Parameter $\mathcal{P}$	0.047 ± (0.52)	0.068 ± (0.49)	0.025 ± (0.50)	0.233

Table 7.2: Means and Standard deviations for the geometrical features in the progressors group baseline, penultimate and final visits for the overall data. P value for ANOVA test is shown

NON-PROGRESSORS OVERALL DATA				
Retinal Parameter **Mean ± (STD)**	**Baseline Visit** **(No Retinopathy)**	**Penultimate Visit** **(No Retinopathy)**	**Final Visit** **(No Retinopathy)**	**p value**
Bifurcating Angle θ (Degrees)	75.0 ± (16.3)	75.6 ± (16.4)	77.5 ± (14.1)	0.49
Branching Angle θ_1 (Degrees)	26.8 ± (14.8)	26.4 ± (14.8)	27.9 ± (15.1)	0.78
Branching Angle θ_2 (Degrees)	48.1 ± (18.2)	49.1 ± (17.6)	49.6 ± (16.6)	0.83
Bifurcation Index λ	0.83 ± (0.11)	0.82 ± (0.14)	0.83 ± (0.19)	0.87
Larger child diameter ratio λ_1	0.86 ± (0.06)	0.85 ± (0.07)	0.85 ± (0.08)	0.62
Smaller child diameter ratio λ_2	0.71 ± (0.09)	0.70 ± (0.13)	0.70 ± (0.09)	0.63
Asymmetry Ratio α	0.71 ± (0.18)	0.71 ± (0.20)	0.74 ± (0.34)	0.55
Area Ratio β	1.27 ± (0.18)	1.23 ± (0.17)	1.25 ± (0.21)	0.44
Junction Exponent χ	3.51 ± (2.02)	3.34 ± (1.57)	3.61 ± (2.48)	0.65
Optimality Parameter $\mathcal{P}$	-0.04 ± (0.52)	0.03 ± (0.52)	-0.03 ± (0.56)	0.48

Table 7.3: Means and Standard deviations for the geometrical features in the non-progressors group baseline, penultimate and final visits for the overall data. P value for ANOVA test is shown

There was no statistically significant difference noted in any of the analysed RVG features in the progressive group between the three screening visits, however; there was a noted widening of the vascular bifurcating angle (θ) together with a corresponding widening of the smaller-child vessel branching angle (θ_2) in the final visit with development of PDR – a trend similar to that observed in the cross-sectional comparative study. Such trend was maintained for the arteriolar and venular subgroup analysis. (Table 7.4)

For the non-progressors group, no statistically significant difference was noted for any of the analysed RVG parameters between the three screening visits, and no obvious trend in angular width changes could be observed similar to the progressors group. The FLSD ad-hoc test was not performed for any of the analysed features in either groups as the results did not reach the set significant p-value for the ANOVA test.

PROGRESSORS ARTERIOLAR DATA				
Retinal Parameter Mean ± (STD)	**Baseline Visit**	**Penultimate Visit**	**Final Visit**	**p value**
Bifurcating Angle θ (Degrees)	79.46 ± (18.8)	80.24 ± (15.8)	82.58 ± (15.7)	0.628
Branching Angle θ_1 (Degrees)	24.94 ± (14.0)	25.77 ± (11.6)	24.71 ± (11.9)	0.924
Branching Angle θ_2 (Degrees)	54.58 ± (22.8)	54.47 ± (22.1)	57.87 ± (18.7)	0.675

PROGRESSORS VENULAR DATA				
Retinal Parameter Mean ± (STD)	**Baseline Visit**	**Penultimate Visit**	**Final Visit**	**p value**
Bifurcating Angle θ (Degrees)	77.59 ± (12.3)	75.15 ± (10.6)	78.57 ± (10.8)	0.302
Branching Angle θ_1 (Degrees)	27.72 ± (15.7)	27.72 ± (15.4)	27.47 ± (15.2)	0.995
Branching Angle θ_2 (Degrees)	49.87 ± (18.4)	47.43 ± (17.7)	51.10 ± (16.2)	0.561

Table 7.4: Means and Standard deviations for the geometrical features in the progressors group baseline, penultimate and final visits for the arteriolar and venular data. P value for ANOVA test is shown

The RVG analysis was then repeated for the "progressors" and "non-progressors" subjects at the individual level to evaluate whether any significant changes or trends could be identified for any of the examined features. No statistically significant RVG changes could be detected for any subject; however the trend of widening of the total bifurcating angle (θ) together with widening of smaller-child vessel branching angle (θ_2) could still be noted in most of the "progressors" subjects. Such trend wasn't clearly identified in the "non-progressors" subjects.

2. Comparison of the retinal vascular geometrical features at the base-line visit between the progressors and non-progressors group.

Binary logistic regression was performed to determine the predictive value of the different retinal vascular architectural and geometrical measurements at baseline for future progression to PDR, as calculated from the initial images captured at presentation for the progressors and non-progressors group. As these images were obtained approximately within the period between 2004 and 2005, they were all captured by the same screening camera system which was adopted at that time. All images were thus of the same size and resolution. Consequently, this made it appropriate for analysis to be performed for the absolute vessel width measurements as well as the relative diameter ratios, area and asymmetry ratios, together with the bifurcating angle measurements. The analysis was done initially for the overall data, then sub-analysed for the arteriolar and venular data. The results are shown in table 7.5

BINARY LOGISTIC REGRESSION ANALYSIS										
	OVERALL			**ARTERIOLAR**			**VENULAR**		
Retinal Parameter	**Coeff**	**OR (95% CI)**	**p value**	**Coeff**	**OR (95% CI)**	**p value**	**Coeff**	**OR (95% CI)**	**p value**
Parent Vessel Diameter d_0	-0.025	0.97(0.84 - 1.14)	0.742	-0.145	0.86(0.64 - 1.18)	0.352	-0.021	0.98(0.81 - 1.18)	0.831
Large Child Diameter d_1	-0.007	0.99 (0.84 - 1.17)	0.93	-0.178	0.84(0.61 - 1.16)	0.279	0.031	1.03(0.84 - 1.27)	0.768
Smaller Child Diameter d_2	**-0.318**	**0.73 (0.58 - 0.92)**	**0.007**	**-0.358**	**0.70(0.49 - 1.00)**	**0.05**	**-0.301**	**0.74(0.55 - 1.00)**	**0.05**
Bifurcating Angle θ	0.013	1.01 (1.00 - 1.03)	0.121	0.015	1.02(0.99 - 1.04)	0.177	0.011	1.01(0.98 - 1.04)	0.418
Branching Angle θ_1	-0.001	1.00 (0.98 - 1.02)	0.844	-0.007	0.99(0.97 - 1.02)	0.574	0.002	1.00(0.98 - 1.03)	0.858
Branching Angle θ_2	0.011	1.01 (1.00 - 1.02)	0.154	0.014	1.01(1.00 - 1.03)	0.125	0.005	1.01(0.98 - 1.03)	0.632
Bifurcation Index λ	**-3.281**	**0.04 (0.00 - 0.31)**	**0.002**	-2.397	0.09(0.00 -2.39)	0.151	**-3.715**	**0.02(0.00 - 0.42)**	**0.01**
Larger child ratio λ_1	1.079	2.94 (0.04 - 213)	0.621	-2.459	0.09(0.00 - 44.5)	0.441	5.689	298(0.53 - 168)	0.07
Smaller child ratio λ_2	**-4.845**	**0.01 (0.00 - 0.13)**	**0.001**	**-4.327**	**0.01(0.00 - 0.82)**	**0.04**	**-5.284**	**0.01(0.00 - 0.34)**	**0.014**
Asymmetry Ratio α	**-2.023**	**0.13 (0.03 - 0.51)**	**0.003**	-1.481	0.23(0.03 - 1.81)	0.162	**-2.293**	**0.10(0.02 - 0.64)**	**0.015**
Area Ratio β	**-2.025**	**0.13 (0.03 - 0.68)**	**0.015**	**-2.288**	**0.10(0.01 - 0.94)**	**0.044**	-1.297	0.27(0.01 - 5.15)	0.386
Junction Exponent χ	-0.118	0.83 (0.68 - 1.01)	0.069	-0.181	0.83(0.66 - 1.06)	0.131	-0.099	0.90(0.54 - 1.53)	0.709
Optimality Parameter $\mathcal{P}$	0.347	1.42(0.82 - 2.46)	0.217	0.357	1.01(0.78 - 2.39)	0.311	0.221	1.41(0.91 - 2.11)	0.201

Table 7.5: Results of binary logistic regression analysis for the overall data, arteriolar and venular subgroups. The coefficient, odds ratios, 95% confidence intervals, and p values are shown.

The most striking result was that reduced overall, arteriolar and venular smaller-child vessel width (d_2) at baseline significantly predicted future progression to PDR (OR=0.73(95% CI 0.58-0.92)). This was also reflected on the vascular width ratio estimates; reduced overall, arteriolar as well as venular smaller-vessel ratios (λ_2) were significantly predictive for future progression. This was also true for the overall and venular bifurcation index (λ). Reduced asymmetry ratio (α) and area ratio (β) estimates at baseline were also predictive of future progression. [(OR=0.13 (95% CI 0.03-0.51)) and (OR=0.13(95% CI 0.03-0.68)) respectively] The results reached statistical significance in the venular subgroup analysis for the asymmetry ratio (α) and the arteriolar analysis for the area ratio (β). No significant relationships were detected for the other analysed geometrical features.

It is worth mentioning here that despite that the retinopathy grading of the baseline images was slightly varied - the non-progressors all had a grading of R0 whilst the grading of the progressors group included R0 and R1 levels, it is unlikely that these differences in baseline grading between the two groups would have confounded the predictive results in any way. Previous results presented in tables 6.3 – 6.6 had all shown that smaller-child vessel width (d_2) is wider in the mild NPDR group R1 as compared to the No-retinopathy group R0, yet the results of the binary logistic regression test reveals that it is a "narrower" (d_2) in the "progressors" group at baseline which predicts the future progression to PDR.

7.7 Discussion

Over the past decade, the results of several major population studies have been published demonstrating the value of retinal image analysis as a non-invasive measure of early changes in the vasculature that would not be detectable on routine clinical examination and that might aid in identification of individuals at risk of certain systemic vascular diseases. For example, the ARIC data suggested that retinal microvascular abnormalities such as microaneurysms, soft exudates, blot and flame-shaped haemorrhages were related to and predictive of stroke. [98] Meanwhile, changes in retinal vascular calibre were associated with various conditions such as carotid artery diseases, MRI detected lacunar infarcts, clinical strokes and incidence of coronary heart disease. [175, 204, 205] Moreover, changes in retinal vascular geometry have been shown to be associated with increased cardiovascular risk. [101]

Importantly changes in retinal vascular calibre were also shown to predict the development of type II diabetes, as well as being a preclinical marker of hypertension risk. [123, 124, 206]

The findings of these studies - supported with the development of robust retinal image analysis techniques - might allow physicians to identify individuals at risk, and optimise the management of those with established diabetes and/or hypertension as well as monitor the severity of their subclinical microvascular damage. However, the results of these studies were based on cross-sectional analysis of data obtained from different population groups and thus the accuracy and precision of the results of these studies "on the individual level" need to be confirmed and resolved before adopting retinal vascular imaging analysis in clinical practice.

The results of our previous cross sectional comparative study demonstrated a graded and continuous association of retinal vascular architectural and geometrical changes with increased severity of diabetic retinopathy grade. The significance of such associations however on an individual level was not clear. In this pilot longitudinal predictive study, we attempted to establish the clinical relevance of such findings on an individual level by comparing geometrical features in the retinal vasculature in diabetic subjects with clinically confirmed retinopathic progression before and after the development of proliferative retinopathy. We also tried to evaluate the predictive value of any differences in these geometrical features in identifying the individuals who are at risk of future progression.

- Evaluation of differences in retinal architectural and geometrical measurements between the baseline screening images and the penultimate and final screening images

Our results for the progressors group revealed no statistically significant difference in the analysed RVG features within the baseline, penultimate and final screening images. Nevertheless, a noticeable trend of widening of the bifurcating angle (θ) together with the smaller-child branching angle (θ_2) measurements was demonstrated specifically in the final screening images with established PDR. These alterations in angular measurements were consistent with the corresponding cross-sectional comparative relationships previously established with increased severity of diabetic retinopathy grading. Such trends of angular widening were maintained for the sub-analysed arteriolar and venular data. The angular widening changes in final screening images with established PDR could also be noted in most but not all the progressors' subjects. The limited number of analysed bifurcations for each subject made it unlikely for these relationships to reach any statistical significant values.

In other words, for most diabetic patients who progressed to proliferative retinopathy in this group, the changes in the angle measurements were suggestive of the establishment of the proliferative changes distinguishing that final screening image from the previous screening visits. Nevertheless, the geometrical changes in angle measurements could not be detected prior to the development of proliferative diabetic changes to highlight the risk of progression in these subjects.

Furthermore, the unnoticeable changes in the angular measurements especially for (θ) and (θ_2) between the baseline and penultimate screening images are in keeping with the previously presented cross-sectional comparative analysis between subjects with no retinopathy and those with minimal NPDR, as all the penultimate images were graded as (R1) for the progressors' group. It wasn't feasible to assess geometrical changes in subjects when the penultimate screening images are graded as (R2) with severe NPDR subsequent to progression to established PDR. This bias occurred as patients identified on screening with moderate and severe NPDR (routinely graded according to the NSC as R2), are referred to the hospital

diabetic clinic for follow up at that stage and thus subsequently were not identifiable in our selection process.

As for the non-progressors' group, the results of longitudinal data analysis showed no significant relationships for RVG changes within the baseline, penultimate and screening images, yet a trend of angular widening for the bifurcating angle (θ) and the smaller-vessel branching angle (θ_2) in the final screening images was also noticed. These angular changes were similar – though weaker – than those demonstrated in the progressors group. These differences were not maintained at the individual level for all subjects. It could be detected in only two out of the five non progressors.

The differences in angle measurements presented in the non-progressors' group which were noticeable in the final screening images, with no detectable retinopathy, might be explained by two assumptions. First, the change in retinal geometrical angle measurements between the baseline and the later final screening images could reflect a progression of peripheral retinal ischaemia that might have developed in these subjects' retinae over time despite the lack of presence of clinically detectable diabetic retinopathic features. Such a mismatch is increasingly recognised in diabetic subjects with the use of the ultra wide field viewing utilising the Optos P200 scanning laser ophthalmoscope. This observation is supported by previous reports of a significant increase in the mean number of sectors containing retinal ischemia with the use of this technique as compared to conventional digital fundal imaging in patients with pre-proliferative diabetic retinopathy. [207] This peripheral ischaemia, if present in our non progressors, might have resulted in the angular measurement changes as occurred in the patients with pre-proliferative and proliferative retinopathy. Examples of significant peripheral retinal ischemia associated with mild - moderate NPDR as captured by the Optos SLO are shown in figure 7.1 and 7.2
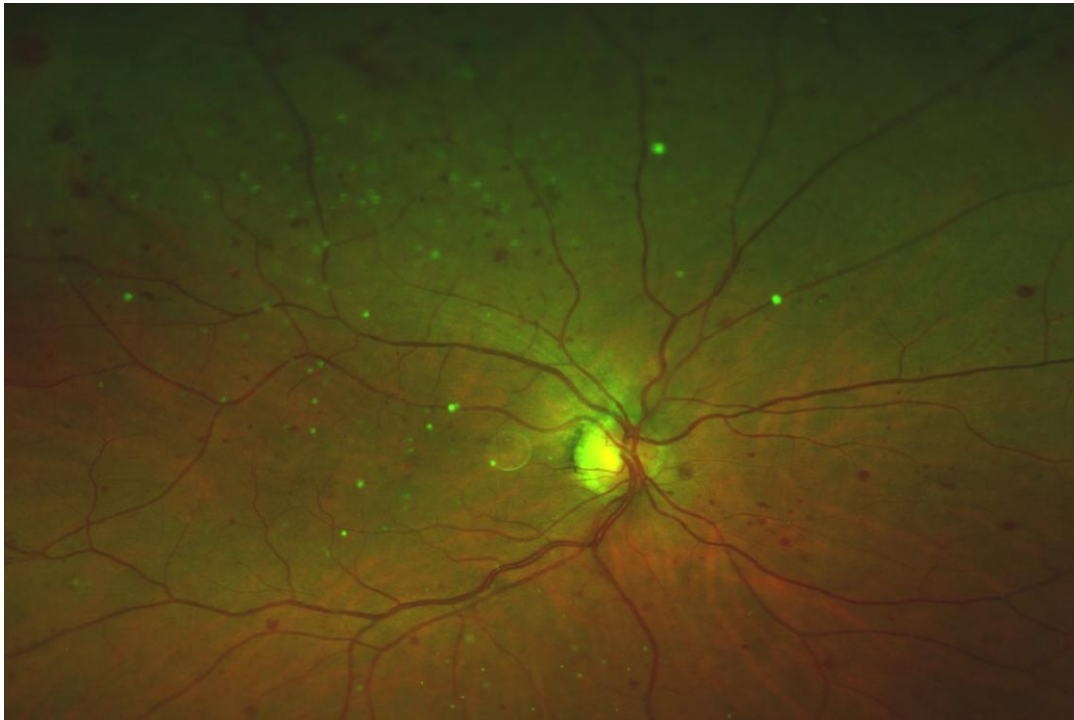
Figure 7.1: An example of an Optos SLO image of a diabetic subject with mild-moderate NPDR changes
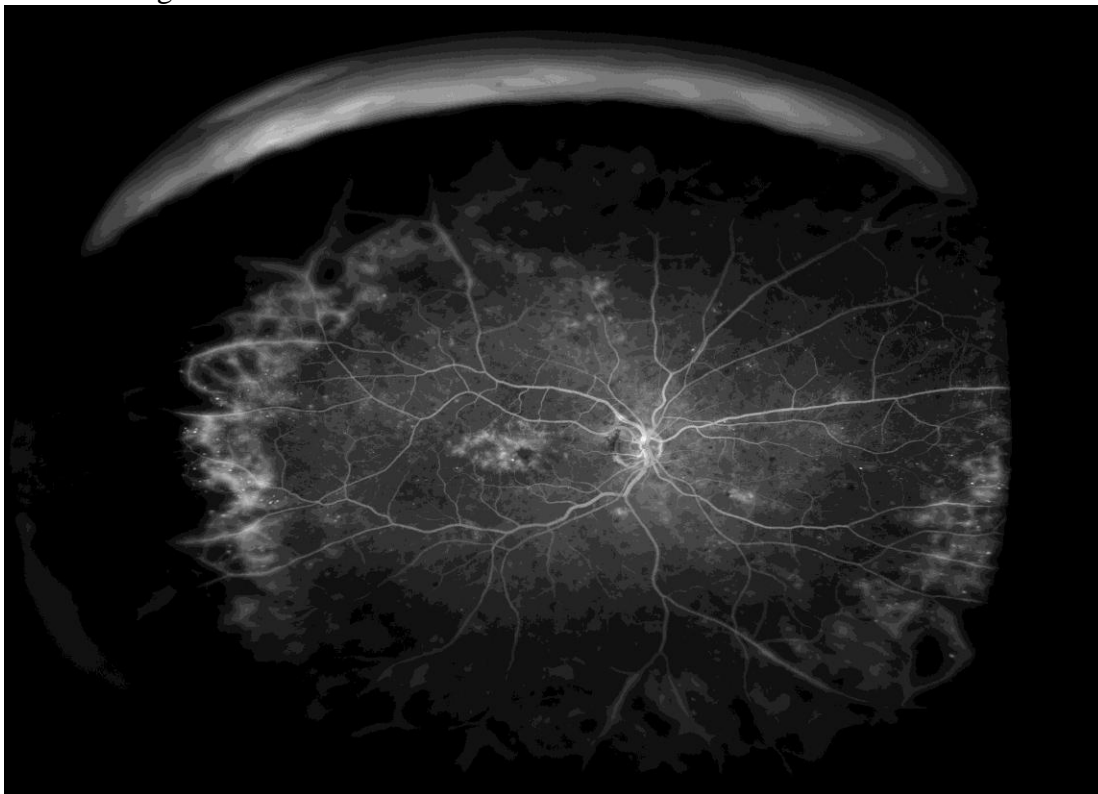

Figure 7.2: An example of an Optos SLO image of a fluorescein angiogram of the same diabetic subject with mild – moderate NPDR changes, showing marked peripheral capillary shut-down.

Second, despite the care that we took to adapt our custom-designed labelling and marking algorithm to analyse the retinal images of differing size and resolutions for the longitudinal data, it is still possible that the differences noted in angle measurements between the baseline and the final retinal images in the progressors and non-progressors' groups were, at least partly, resulting from measurement error that came about by the different camera systems utilised.

- Comparison of the geometrical features of the retinal vascular network at the baseline visit between the progressors and non-progressors.

The development of proliferative diabetic retinopathy remains a leading cause of blindness, which cannot be totally prevented by optimising metabolic control, and which has only been conclusively proven to respond to retinal photocoagulation. [208] Over the years, many large-scale epidemiological studies have sought to identify a variety of risk factors for the development of PDR and thus identify targets for treatment. The background of intra-retinal lesions against which proliferative retinal lesions arise is variable. In 1978, the Diabetic Retinopathy Study reported that the risk for proliferative diabetic retinopathy is greatest in eyes with severe NPDR characterised by the presence of cotton wool spots, intra-retinal microvascular abnormalities, venous beading, and extensive retinal haemorrhages or microaneurysms. About 50% of such eyes assigned to the untreated control group had developed PDR within 15 months. [56] The DRS definitions were proposed only for the severe stage of non-proliferative diabetic retinopathy. Later, the Early Treatment Diabetic Retinopathy Study EDTRS research group adopted and modified the DRS definitions to set a wider retinopathy severity scale which divided diabetic retinopathy into 13 levels ranging from the absence of retinopathy to severe vitreous haemorrhage. [51]

The EDTRS examined the power of various retinal photographic risk factors and combinations of abnormalities to predict the progression to proliferative retinopathy over 5 year follow up visits. The results of this work set the standards for future treatment and the development of screening guidelines for diabetic retinopathy, upon which our current clinical practice is largely based. They concluded that one year progression rates increased fourfold or more with increasing severity of haemorrhages and/or microaneurysms, IRMAs and venous beading and doubled with increasing severity of cotton wool spots. There was little or no relationship found between the severity of hard exudates and risk of PDR. The presence of venous beading was a

more powerful predictor of the subsequent development of PDR than was the presence of any other abnormality.

The EDTRS however acknowledged in their report that few eyes were included in their analysis that had minimal or no retinopathy, thus the definitions regarding the lower range of NPDR could not be examined, and indeed the risk of progression to PDR by baseline retinopathy severity included only eyes with retinopathy severity scale 35 (Mild NPDR) or above. Furthermore, results from the EURODIAB prospective complication study demonstrated that 4% of their subjects without diabetic retinopathy at baseline were associated with progression to PDR after a mean follow-up period of 7.3 years, this was compared to 17% of those with minimal NPDR, 40% of those with moderate NPDR, and 79% of those with severe NPDR. [208]

In this section of the study, we attempted to evaluate the predictive value of different geometrical features in the development of PDR, by comparing these features between the baseline visits of the progressors and the non-progressors. The baseline images for the subjects included in both groups in our study had no or minimal diabetic retinopathic features, thus the implication of determining the predictive values of these geometrical features – if found – is high in identifying the risk of progression to PDR in these subjects who are considered at a subclinical level or early stages of diabetic retinopathy. If achieved, the predictive values of these features would, in its part, complement and add to the aforementioned results of the previous large studies.

The predictive study results have shown that in adult diabetics with initially no or minimally clinically detectable retinopathy, alterations in RVG at baseline in the form of narrower arteriolar and venular small-child vessel segment absolute vessel width and relative diameter ratio at a bifurcation together with a reduced asymmetry and area ratio values can predict future progression to PDR.

The exact pathophysiology behind this predictive value of reduced smaller-child segment vessel width and its related altered relative diameter ratio at baseline is unclear; nevertheless it could be interesting to hypothesize that it might be related in a way or another to the future change in the smaller-child branching angle (θ_2) demonstrated with severe non proliferative and proliferative diabetic retinopathy which is in itself related to the same vessel segment.

It is worth mentioning that the calculated low odds ratios for the relevant structural and geometrical parameters might reflect the small sample size analysed for this study. A larger study is needed to clarify this.

The results of this study are highly suggestive that diabetic subjects with no retinopathy or early minimal non proliferative diabetic retinopathy with altered relationship of vessel segment widths at the vascular bifurcations and low area ratio β, and asymmetry ratio α could be at higher risk of future development of proliferative retinopathy. The results of this study echo the earlier attempts by Fanucci et al. in 1990 who suggested that architectural changes in the arterial bifurcations of human vascular networks in the form of narrow branching angles and normal area ratios, or wide angles and lower area ratios might be prone to vascular disease. [79]

We acknowledge that our results are far from being conclusive for various reasons that will be discussed below, however if proven, it could lead in the future to early identification of diabetic subjects at risk of future progression utilising these newly described geometrical changes and alter their retinopathy screening plans and management strategies.

- Interpretation of results

This retrospective study has revealed several observations that may help in identifying those at risk of future complications. However, caution should be taken in interpreting these results as the study is limited by several factors, some of which had been discussed already

1. Being retrospective, the photographic methods and systems used could not be standardised, and thus retinal screening images of different sizes and properties were included for analysis. Such variation in image quality might have – in a way – contributed to the results shown. The definite extent of error – if present – could not be determined at this level of analysis.

2. The demographic data and retinal images used for this study were collected from the local diabetic retinopathy screening service; however, the clinical data related to the included subjects were not accessible and consequently, several previously known risk factors for progression of diabetic retinopathy were not accounted for, such as the duration of diabetes, and its metabolic control, diastolic blood pressure, albumin

excretion rate, cholesterol and triglycerides levels amongst others. [208] Thus, the independence of the predictable value of the geometrical features represented above cannot be confirmed at this stage.

7.8 Conclusion

In conclusion, this study demonstrated that certain retinal vascular geometrical features could act as a novel marker of the development and establishment of proliferative diabetic retinopathy on an individual level. The study also revealed the effective value of these features in early identification of diabetic individuals with no or minimal non proliferative diabetic retinopathy at risk of future progression to proliferative retinopathy. The implications of these results are great for future care development of the diabetic patients, yet at this stage these results are mainly highly suggestive and thus further prospective studies with detailed analysis of these findings would be recommended to evaluate its usefulness before being adopted in clinical practice.

Chapter 8: General Discussion and Conclusions

8.1 Introduction

Diabetic retinopathy is considered one of the most common causes of preventable blindness in the working age group in the United Kingdom. Numerous studies have shown that there is a rising incidence of diabetes and its complications in all age groups, both in the UK and worldwide. In 2006, the International Diabetes Federation (IDF) published data showed that diabetes now affects 246 million people worldwide, with 46% of all those affected in the 40 – 59 age group. A recent review by Gonzalez et al, estimated that the prevalence of diabetes in the UK from 2.8% in 1996 to 4.3% in 2005. The incidence of diabetes in the UK increased from 2.71/1000 persons-year in 1996 to 4.42/1000 persons-year in 2005, with the incidence of type 1 diabetes remaining relatively constant however the incidence of type 2 diabetes was rising steeply. [209] Over the years, many studies have reported on the natural history and prevalence of diabetic retinopathy and of sight threatening diabetic retinopathy in different populations.

Diabetic retinopathy is classified into 2 stages: non-proliferative and proliferative. The earliest clinically visible signs in non-proliferative DR are microaneurysms and retinal haemorrhages. Progressive capillary non-perfusion is accompanied by the development of cotton wool spots, venous beading and intra-retinal microvascular abnormalities. Proliferative DR occurs with further retinal ischaemia and is marked by the growth of new blood vessels on the surface of the retina or the optic disc. Diabetic macular oedema, which can occur at any stage of DR, is characterised by increased vascular permeability and the deposition of hard exudates in the macular area. The major risk factors for diabetic retinopathy have been established from major epidemiological studies.

The development of diabetic retinopathy screening in Europe was first encouraged by the St Vincent declaration which in 1992 set a target for reduction of new blindness by one third in the following 5 years. [210] In 2002, the National Service Framework for diabetes announced the introduction of a national screening programme for sight threatening diabetic retinopathy in England offering screening for early detection and treatment if necessary of diabetic retinopathy as part of a systematic programme targeting 100% coverage of those at risk by the end of 2007. Screening for diabetic retinopathy has been shown to be cost-effective in health

economic terms [59] and based on evidence of early treatment efficacy of sight threatening diabetic retinopathy as presented by the large treatment trials. [56] Indeed, the beneficial long-term impact of systematic retinal screening is now being shown; in Newcastle district, where consistent and systematic annual screening of diabetic retinopathy has been adopted since 1986, a recent survey showed that, unlike the national UK data, diabetic retinopathy was the second commonest cause of blindness and partial sight registration in the working age population. [211]

In the last two decades, researchers and scientists have made significant progress in exploring the pathophysiology of diabetes and diabetic retinopathy. However, despite the advances in understanding the distribution, causes, and severity of diabetic retinopathy, the scientific evidence is ever changing and requires continuous monitoring. This is currently considered of paramount importance because of the increasing burden of diabetes on the population and the medical systems providing care to them. [212] In fact, diabetic eye disease is considered an end organ response to a generalised metabolic disorder; nevertheless, the present strategies for dealing with diabetic retinopathy do not capture early changes and still address retinopathy that is already established. Various individual retinal lesions are used to identify the risk of progression of retinopathy and visual loss, such as microaneurysms which are saccular out-pouchings of retinal capillaries, ruptured microaneurysms, leaking capillaries, as well as intra-retinal microvascular abnormalities resulting in intra-retinal haemorrhages which mark severe stages of non-proliferative retinopathy. Proliferative retinopathy is marked by proliferating endothelial cell tubules, with variable rate of growth.

Recent research has thus focused on the need for innovative methods to identify patients with early risk of development or progression of diabetic retinopathy. The availability and establishment of such approaches may result in a shift of emphasis toward monitoring and treating earlier stages of diabetic retinopathy. Several studies have described the associations and clinical significance of early retinal arteriolar and venular vascular caliber changes in individuals with pre-diabetes, diabetes and its complications. Prospective data have shown that retinal vascular caliber changes may predict the development of type 2 diabetes [123, 124], and arteriolar narrowing preceded the development of diabetic retinopathy, whilst dilated arteriolar and venular calibers marked the progression of retinopathy stage. However, the assessment of retinal vascular caliber represents only a sole parameter of the retinal vascular geometry and does not convey information regarding the detailed complexity of the retinal vascular branching

pattern [213], thus other studies have explored the role of other architectural retinal changes, such as arteriolar length to diameter ratios, increased tortuosity, branching angles changes, and reduced microvascular density with other vascular diseases. Some of these retinal changes for example have been shown to be associated with increased age, hypertension, and increased cardiovascular risk.

This study attempted to evaluate the association and clinical significance of architectural and geometrical retinal vascular changes with different stages of diabetic retinopathy and its predictive role in early identification of diabetic subjects at risk of future progression of their retinopathy stage.

For that purpose we developed a semi-manual technique that is capable of determining and estimating these vascular changes. The development process went through different phases until we arrived at the adopted version of the algorithm used for the study. This utilised technique addressed all the pitfalls of the early attempts and tried to overcome the drawbacks of other semi-manual vascular measurement techniques such as one-point cross sectional profiles for vascular width estimations.

8.2 Repeatability assessment and technique comparison

This study evaluated the repeatability and precision of the custom designed algorithm for retinal vascular geometrical analysis utilised for this thesis. Sources of variability were identified to be either:

1) Subjective measurement errors by the grader (Grader variability)

2) Photographic acquisition technique variability.

3) Short term changes in geometric estimates and measurements related to the individual' metabolic control (Individual Variability).

The techniques precision was compared to those of other available semi-manual techniques for vascular width measurement. In keeping with previous studies, our results showed that the individual variability is generally larger than the grader variability. However, our estimated

ranges for the intra-grader and the individual intra-visit coefficient of variation for vessel width measurements compared favourably to corresponding results for other published semi-manual techniques. In addition, the inter-visit variability across images captured two weeks apart had minimal effect on the overall individual variability, although the range of angular measurements change was wider in subjects with poor metabolic control, as reflected by large variation in blood pressure and blood glucose levels between visits, as compared to subjects with good metabolic control. Importantly however this change occurred in both directions thus not affecting the overall mean difference of measurements between the two visits.

In practical terms, the coefficient of variation results calculated for the intra-grader variability and the individual intra-visit variability set the limits for the overall vascular measurements precision or reproducibility. The extent of this variability, which could also be expressed in terms of measurement error values, determined the minimum appreciable difference that could be detected between two different individuals or conditions (for example normal versus disease) if comparisons were made at a "single vascular bifurcation level". Nevertheless, as this variability occurred in random for the measurements obtained, it did not affect comparisons made at the "group level", where large numbers of bifurcations were compared for different subjects or conditions. This was reflected in the small mean difference values calculated for the individual inter-visit variability.

When compared with other available semi-manual techniques for vessel width analysis, the performance of the custom-designed rectangle technique appeared more precise in estimating the measured geometrical ratios and parameters. This was expressed as lower coefficient of variations values, mean values which adhered more to the corresponding calculated theoretical optimal values, and a lower frequency of "failure events". The improvement of the designed technique performance could be attributed to the averaging of the vessel segment width estimation along the rectangle length as compared to the one-point cross-sectional vessel width profiles adopted by other techniques, as well as the improved perpendicular alignment of the rectangle width estimation in relation to the axis of the chosen vascular segment.

In general, the reproducibility and precision of this custom-designed technique compared favourably to other techniques especially with the relatively low image resolution used in this thesis, and was thus considered acceptable to be utilised for the whole research project.

8.3 Normality study

This study was devised to establish normative reference data for the geometrical features derived from a population of self-assessed normal subjects. The study evaluated the effect of different factors such as age, smoking, BMI on the resultant data. Furthermore, the study assessed the extent of optimality of these normative data by comparing it to the calculated theoretical optimal values. In addition, inter-eye comparisons of the different geometrical features were made in a sample of subjects to estimate the degree of stability of measurements between both eyes in healthy normal subjects.

Comprehensive descriptive data concerning the different retinal structural and geometrical features, with sub-analysis for the arteriolar and venular vascular networks was presented. Comparisons of this data to previously published results were difficult due to the lack of standardisation of the inclusion criteria and methodological techniques used in the previous studies, together with the sparse analysis in these studies. The resulting mean values for the different features were in general comparable to other published results, albeit with a wider range of confidence interval that might reflect the larger sample size included in this study. The sub-analysis of the data revealed an expected increased width of the retinal venules as compared to the arterioles, however, the results also showed a tendency of widening of venular bifurcating angles as compared to its arteriolar counterparts. Topographically, temporal and proximal retinal vessels were generally larger than nasal and distal vessels respectively. No difference in angular measurements was noted across the different retinal quadrants.

Unlike previous studies, there was no effect of age detected on the bifurcating angle (θ) subtended between the two child vessels, yet the results were suggestive of an opposite effect in the branching angles of each of the two child vessels, with an increase in the large child branching angle and the decrease in the small child branching angle. These opposing effects tended to neutralise each other and hence the total bifurcating angle (θ) remained unchanged with age. Otherwise, no other effect of age, BMI, or smoking history could be noted on any of the other geometrical features analysed.

On evaluating the degree of optimality of our normative data, the results demonstrated a moderate degree of consistency, with an average of 50% of our results confined within the

theoretical optimal ranges. "Qualitatively", the analysed retinal networks seemed to adhere to the expected and previously described optimal relationships concerning the vessel widths and angular measurements between the vessel segments at the arteriolar vascular bifurcations, and "quantitative" assessment of the extent of included data within a 10% range band around these relationships' curves compared favourably with previous studies. The noted considerable extent of deviation of our results in relation to the theoretical laws of optimality could be related to an expected biological scatter of the geometrical values in normal healthy individuals or variability of vascular designs within a normal retinal vascular network. This deviation might also be explained by the difference in measurement technique adopted in this study as well as the inclusion of large numbers of symmetrical and asymmetrical vascular bifurcations of different sizes across the whole fundus image, in a larger scale as compared to previously published work.

Finally, the study evaluated the stability of the structural and geometrical features between both eyes in a sample of healthy individuals. The results demonstrated a tendency for the right arteriolar bifurcations to have wider vascular segments widths, and larger total bifurcating angles (θ) than the left arteriolar bifurcations. The same relationship was noticeable for the right temporal bifurcations as compared to the left temporal bifurcations. Such relationships were not obvious for the corresponding venular or nasal bifurcations. Interestingly, these results correlated well with similar observation previously reported in older healthy subjects who showed larger right than left central retinal arterial equivalent. [179] However, the results were contradicted by other studies findings. The exact factors related to such observed variations are still unclear, as one would assume that the left common carotid artery and its branches would be larger than those on the right side as they arise directly from the aortic arch whereas the right common carotid artery arises from the brachiocephalic trunk.

Although previous reports concluded that random eye selection for computer-assisted vascular analysis would adequately represent the retinal vessel diameters for these subjects, nevertheless, in our study, effort was made to include corresponding numbers of right and left eyes in the selected cohorts of diabetic subjects analysed for further steps of this work to rule out the confounding factor of eye laterality in our subsequent data analysis.

In general, the results of this study provided a valuable bench mark of normative data of the retinal vascular network in healthy subjects with detailed topographic sub-analysis of these

features across the retinal image. This data was thus used for reference for the further analysis performed for the diabetic studies in this thesis. This data could also be utilised as a "Control normative sample" data for future studies of computer-assisted retinal vascular analysis in other systemic or cerebral vascular disorders in similar population cohorts with comparative demographic features. It is prudent to note that the results presented here would depend in a way or another on the utilised images properties and resolution, especially that absolute vascular widths were measured in terms of pixel size. Therefore, the resultant data could be comparable to other data extracted from images sets of similar properties and analysed using the same semi-manual tool.

8.4 Diabetic cross-sectional study

Based on previous studies which described changes in retinal geometrical measurements with systemic vascular disorders such as hypertension and atherosclerosis, this study was designed to evaluate if there were any changes in retinal vascular geometry with increased severity of diabetic retinopathy in age-matched population cohorts, and to assess the effect of other possible confounding demographic and clinical factors on any detected association.

The results of the study revealed a graded increase in the absolute arteriolar and venular vessel segments width measurements with increased severity of diabetic retinopathy, which was also associated with a gradual but continuous increase in the total bifurcating angle and the smaller child vessel branching angle measurements. These changes reached their maximum with proliferative diabetic retinopathy. Analysis of the data suggested that these graded changes in vessel width and angular measurements accompanied, yet did not precede, the development of clinically detectable diabetic retinopathy. In fact, the results showed a reverse relationship of the absolute vascular segments width between non diabetics and diabetics with no detectable retinopathy; hence it seemed that early narrowing of the retinal blood vessels could occur in diabetic subjects and precede the development of diabetic retinopathy. On the other hand, it is important to note that these changes were detectable not only with the establishment of proliferative diabetic retinopathy, but also preceded the development of such changes. It is also worth mentioning that the changes described here in retinal vessels width measurements with increased retinopathic severity occurred uniformly around the vascular bifurcations, and thus there was no obvious difference in the relative diameter ratios or the asymmetry and area ratios detected between the different diabetic cohorts.

Despite considering the common pivotal role played by the vascular wall endothelial cells in the pathophysiology of systemic vascular disorders on retinal vessels, in contrast to the previously reported retinal geometry changes associated with the increased vascular tone in hypertension, the results described here might actually reflect reduced vascular tone with the development of diabetic retinopathy together with altered auto regulation that has been described. [185]

Similarly, previous studies concluded that the "acute" bifurcating angles of older and hypertensive subjects could reflect an altered space-filling branching pattern and "reduced" microvascular density [88], and indeed we built our own theory for the study based on similar findings obtained with regional fractal analysis in diabetic subjects. [129] However, in fact our unexpected study findings revealing "wider" bifurcating angles with diabetes can be well supported by emerging reports of "increased" fractal dimensions of the retinal vasculature associated with the development of diabetic retinopathy, reflecting increased geometrical complexity of the retinal vascular branching pattern, which occur independently – and not as a result – of proliferative retinal changes. [213] The results of this study echoed the recent emerging results by Sasongko and colleagues demonstrating larger arteriolar branching angles in association with longer diabetes duration. [199]

The implications of these study findings are important in identifying novel retinal markers and features for defining advancing diabetic retinopathy. To our knowledge, these markers have not been described before, and if confirmed in larger prospective studies and adopted in clinical practice, it would advance our understanding and potentially allow the earlier detection of the development of severe non proliferative or proliferative retinopathy. This could prove to be a valuable clinical tool to identify those patients approaching PDR especially when other retinopathic features are absent or not clear.

However, there are still many issues that need to be resolved before retinal geometrical analysis can be utilised in clinical practice. It is important to identify the exact relationship between these described changes and the progressive capillary non-perfusion and retinal ischaemia in the advanced stages of diabetic retinopathy as identified with fluorescein angiograms. It is also essential to clarify the correlation of these vascular changes with the other established retinopathic features defining severe non proliferative or proliferative retinopathy. As a

consequence, the independent diagnostic value of these novel vascular markers could be then established.

8.5 Diabetic longitudinal study

Previous population-based studies have reported a variety of changes in vascular caliber or geometrical architecture with various systemic disorders; however the practical usability of these findings on an individual level remains to be determined. The aim of this study was to assess the clinical and predictive value of the previously described associations of retinal vascular structural and geometrical changes with advanced severity of diabetic retinopathy on the individual level. As demonstrated in the results of our cross-sectional study, there is a significant overlap in the ranges and means of the measurements between the population cohorts with different grades of diabetic retinopathy. This is compounded by the observed variations in the corresponding geometrical measurements of the normal population cohort. As a result, normal and diabetic subjects with different grades of diabetic retinopathy cannot be categorised or defined in terms of their specific mean values for any of the retinal structural and geometrical features.

Consequently, in view of this observed range of variability in normal and diabetic subjects, it seems rational, that it is the "change" in the measurements for each individual over certain period of time that could be of practical value in predicting or defining progression of retinopathy, rather than the absolute measurements' mean values. In this study, comparisons were thus made between baseline screening retinal images and penultimate and final retinal screening images for a sample of diabetic subjects who progressed to proliferative retinopathy over a period of approximately 6 years. The analysis was done on the group and individual level and the results were compared to a control sample of diabetic subjects who did not demonstrate any clinical evidence of progression of their diabetic retinopathy over the same period of time. The study also aimed at comparing the geometrical features in the initial screening retinal images of the two groups to evaluate the predictive value of these features at baseline for future progression of diabetic retinopathy.

In the predictive study, we attempted to establish the clinical relevance of the comparative study' findings on an individual level. The results showed the same trend, previously

demonstrated in the comparative study, of bifurcation angular widening with progression of retinopathy and reaching the maximum with established PDR after an average of 6 years follow up. These changes were rather clearer in the arteriolar vascular system than the venular system, yet did not reach statistical significance, which might be related to the small number of recruited subjects. Further comparative analysis between the baseline and final screening visits regarding the absolute vascular width measurements was hampered by the difference in retinal image properties between the two visits brought about with the adoption of updated retinal fundus camera systems by the screening programmes over the years.

The predictive study results have also shown that in adult diabetics with initially no clinically detectable retinopathy, alterations in RVG at baseline in the form of narrower arteriolar and venular small-child vessel segment diameter at a bifurcation and a reduced asymmetry and area ratio values can predict future progression to PDR. The exact pathophysiology behind these baseline changes in diabetic subjects with future progressive retinopathy is unclear; nevertheless, it could be interesting to hypothesize that it might be related in one way or another to the future widening of the related branching angle of the same vascular segment with development of severe retinal ischaemia and eventually PDR. Such an early altered relationship between the vascular segments at a bifurcation noted at baseline screening images might be considered as an indicator of compromised vascular networks prone to disease – which in itself might reflect a primary genetic characteristic – and consequently a predictive feature of future risk of retinopathic progression.

The findings of this pilot study are compromised by the small sample size, together with the lack of standardisation of photographic techniques, in addition to the lack of available relevant clinical data. Thus it is difficult to draw firm conclusions; nevertheless the implications of the study findings, which could still be detected despite these limitations, would justify larger prospective studies.

8.6 Limitations of the study

1. The study adopted a custom-designed semi-manual computer-assisted tool for vascular analysis which was by default observer-driven and dependant on subjective interpretation of defining the vessel edge by negotiating changes on the pixel grey scale. The technique performance was proven to be more precise than other alternative available semi-manual tools for vascular width estimation which relied on computer-generated cross-sectional intensity profiles. However, despite using an initial training images set to familiarise the observers with the technique used before starting the analysis of the study images, there was a noticeable slow and gradual subjective change in the approaches used to determine the vessel width when dealing with vessels of different sizes and varying levels of contrast as the study progressed. This long-term modification of the observers' performance with the vessel marking tool over time might have had a confounding effect on the analysed results.

2. In spite of its precision and user-friendly technique, the marking technique was also time-consuming with several tasks needing to be accomplished for each included bifurcation for analysis. Furthermore, unsurprisingly, the time needed for marking and analysing small or hazy bifurcations with low background contrast was significantly longer. Hence, in view of the time constraint for this project, fewer bifurcations could be analysed per image and a limited number of subjects and images could be included for each undertaken study, nevertheless, every effort was made to include sufficient numbers of subjects, images and analysed bifurcations for all the proposed studies to an extent not to compromise the studies' outcomes.

3. The observer and individual reproducibility of the utilised technique was shown to be comparable to and surpass those of other available semi-manual techniques; in practical terms the estimated intra-visit repeatability measures for vessel width measurement and angular width estimations were larger than the intra-observer corresponding measures which supports the fact that variability in image capturing constitute the main source of measurement variability. This estimated measurement variability occurred randomly, thus its impact on the data analysis was largely neutralised when comparisons were

made on the group level, yet it constituted a significant background "noise" that hampered analysis at the bifurcation level. Further refinements are thus needed in analysis techniques to improve the accuracy as well as to increase the reproducibility and speed of these methods to develop techniques that are precise and efficient enough for clinical use and to be adopted for large-scale population studies. Similarly, improvements of retinal image capturing and registering techniques should be adopted in the future in a way that could align a sequence of retinal images automatically by registering common landmarks of interest in these images. This would further reduce the photographic source of variability and enhance the technique's precision. On the other hand, the variability study results revealed a significant inter-observer difference and bias in vascular measurements especially the absolute vascular width estimations. Such difference constitutes an important limitation factor for the practical application of the use of the designed semi-manual tool in clinical settings as measurements extracted by different observers might not be comparable and conclusions cannot be drawn then. Such limitation would not affect the rest of the thesis results being obtained by one observer only, yet caution is needed if the same technique is used elsewhere for further studies to ensure that single observer measurements are needed for meaningful results to be reached.

4. The study utilised retinal fundus images collected from the image data set at Sunderland Eye Infirmary, and from the local South of the Tyne diabetic retinopathy screening service. The decision was made at the launch of the project to use these retinal images to be of similar properties and size to those adopted in clinical practice, and thus improve the credibility and practical implications of its findings. The moderate size and resolution of the used images has definitely limited the capability of the study to identify and analyse small peripheral or para-macular vascular bifurcations at a reliable level, thus these very small bifurcations had to be excluded from the image analysis. In fact, the resolution of the utilised images in this study was lower than that used in most of previous vascular analysis studies which relied mostly on digitalisation of high-quality scanned retinal images. Since the time of the study launch, there has been a considerable upgrading of the retinal fundus camera systems implemented by the diabetic retinopathy screening service, with resultant improvement in the images resolution and clarity. The use of these images of higher resolution in future similar

research has the potential to expand our knowledge with further detailed geometrical analysis of the retinal vascular network.

5. The impact of the relatively lower resolution of retinal fundus images used for this study was also confounded by the actual image quality. The overall photographic quality of the included images for the study was judged to be "good" following the image quality guidelines set by the diabetic retinopathy screening guidelines, however such grading of image quality did not seem to be sensitive enough to detect subtle measures of image quality such as the level of contrast and mild peripheral image blur, which might have had an influence on our vascular measurements and estimations specially for the relatively smaller and peripheral bifurcations. In contrast, the selective inclusion of images of "good" quality only meant that the adopted technique reliability and repeatability were not tested on "raw" images' sample representative of a diabetic screening community settings including subjects with significant cataract and other media opacities which would degrade the image quality which would in turn definitely adversely affects the technique reliability indices. The decision of inclusion of "good" images only was made at the setting of the research project in an attempt to single out the tested sources of variability (observer and image capturing variability) and reduce other confounding factors. Careful interpretation of the repeatability results is thus recommended and should be taken in consideration if the same semi-manual tool is to be used in clinical settings to expect that the reliability of the technique would suffer further from that confounding factor.

6. The study has followed in the footsteps of the early pioneering work by Zamir and his co-workers in defining the vascular bifurcating angle subtended between the two child vessels at a bifurcation as the angle measured between the two tangential lines to the slopes of curvature of the child vessel segments, and the branching angle for each of the child vessels as the angle between the tangential line to the slope of curvature for that child vessel and the continuation of the parent vessel segment central axis. Such definition proved to be applicable in most of the analysed vascular bifurcations. However, in practical terms, the retinal vascular network in normal and diabetic subjects appeared to express a wide variety of branching designs in between them, and

it wasn't uncommon to experience difficulty in subjectively deciding the angle width in many cases by applying the above definition. This was mainly true in certain bifurcations where the child vessel adopts a rather sharp bend in its course shortly after its initial deflection out from the main parent vessel segment. In such cases, the tangential line to the slope of curvature did not seem to actually represent the course of the child vessel segment at the vicinity of the bifurcation and subsequently the subjective estimation of the branching angle for such child vessel segments was difficult to call.

In fact, at this stage of research in retinal vascular geometry, there is no clear universal consensus on the best methods for estimating bifurcating angles to be adopted for analysis. Furthermore, the impact of variations in the vascular volumetric flow, velocity of flow, cross-sectional area and alterations of vessel-wall shear force on the local retinal vascular bifurcation geometry in pathological situations is still unknown, together with the actual influence of these variations on the vessel-wall endothelial cells at the vicinity of the bifurcations. It is thus not unreasonable to speculate that these altered optimality principles associated with pathological vascular states might influence the vessel segments "within" the bifurcation region rather than "after" the bifurcation apex in a concept similar to that described earlier by Fanucci and co-workers. As a consequence, it is unclear whether these variations would thus be reflected principally by changes in the overall curvature of the vascular segments at the bifurcations – which would be detected by applying the tangential line to the curvature slope – or on the other hand it may lead mainly to alterations in the initial deflections of these vascular segments. Further research is needed to explore the local geometrical features at retinal vascular bifurcations in normal and pathological conditions and to ascertain the best parameter for angular width estimation that would reflect the changes in the vascular network brought along by the vascular disorders and would ideally be capable of differentiating between normal and disease conditions.

7. Being a retrospective study, the project has relied mainly on hospital clinic notes to extract the relevant clinical data for the diabetic subjects included in the different studies. In most case, the available recorded clinical data was incomplete and patchy. This was compounded by the lack of available clinical data for the diabetic subjects relating to the retinal images collated from the local diabetic retinopathy screening

service. Such compromise in the accuracy of the collected data could have had an effect on the analysis of the confounding factors on vascular geometrical changes described in this thesis. Moreover, detailed analysis for some of the clinical factors is still to be determined; for example further in-depth examination of the effect of duration, severity, and level of control of hypertension and hypercholesterolemia is important to be assessed in future studies.

8.7 Future work

1. Evaluation of new technologies

In an ideal world, with more available resources and less time and financial constraints, several aspects of this thesis project could be modified and expanded to overcome the limitations and build on the work completed, and validate the resulting findings.

The original aim for this project was to develop a reliable computer-assisted tool to be used for the retinal geometrical analysis, and to utilise it to evaluate the retinal vascular network geometrical features in normal and diabetic subjects.

The performance of the developed semi-manual technique achieved a relatively acceptable reliability and precision. However, being subjective and in view of its calculated range of human measurement error, as expressed by the repeatability measures, together with its time-consuming nature, it became obvious that there is a need for a more robust automated technique capable of determining the retinal geometrical features with high levels of performance if retinal geometrical analysis is to be adopted in large population studies. Such development would constitute a vital step should geometrical vascular analysis proceed beyond purely scientific interest and become implemented in future automated diabetic retinopathy screening processes. A fully automated vascular identification system is required and needs to be capable of segmenting and labelling all retinal blood vessels and to automate extraction of the different geometrical measurements from the vascular network.

A. Evaluation of fully automated vascular analysis system

Over the past few years, and in conjunction with the current thesis, we have been involved with our computer science research collaborators in developing a fully automated system for vascular analysis. We are developing a robust algorithm utilising a novel diameter-sensitive exploratory model to extract most of the vascular network, with a junction forming algorithm which can deal with overlaps, closely parallel vessels, crossings and overlapping lesions. Initial evaluations have shown that the algorithm can accurately locate the vessel edges under difficult conditions and yield precise vessel width measurements with sub-pixel average width errors. The developed technique has been evaluated against a number of ground truth data sets for vessel widths, and has demonstrated significant improvements as compared to the performance of the benchmark methods. [161]

Further research is still required to validate this newly developed automated algorithm using the dataset of images of normal and diabetic subjects with different grades of diabetic retinopathy as utilised in this study and bench-marking the results against our results for bifurcation geometry presented here with the adopted semi-manual technique.

The vascular measurements obtained with such an automated system would have the advantage of not being subject to operator errors, including intra and inter observer variability. However, it will be important to evaluate the extent and range of the individual variability with the automated technique using the individual repeatability study dataset of images. We also need to assess the feasibility of utilising image analysis techniques in the future to align a sequence of retinal images automatically in real time during the process of image capture in an attempt to reduce the photographic source of individual variability.

Having established the accuracy and reliability of the automated system measurements, we then need to evaluate whether the differences in retinal geometrical features between images of different grades of diabetic retinopathy as demonstrated in this study could be detected using the new system. It is important to assess the findings of this comparative study and evaluate whether the cross sectional associations demonstrated with the semi-manual technique would be accentuated with the automated system after exclusion of the background "noise" of measurement variability.

Furthermore, the ability of the automated system to detect "change" in a sequence of retinal images will be examined utilising the image dataset for the longitudinal diabetic study for the progressors and non-progressors groups.

Once established, the use of the automated vascular analysis system would facilitate large scale population studies to be undertaken, with further analysis of increased number of bifurcations for each image, thus enhancing our current understanding of retinal vascular geometry in normal and disease states.

B. Evaluation of Optomap non-mydriatic fundus imaging

Recently, a novel non-mydriatic fundus imaging device, the Optomap Panoramic200 (Optos PLC, Dunfermline, Fife, Scotland. UK) has become available. The system allows non mydriatic imaging that extends beyond the equator to cover 180 - 200°. This is made possible by the special optical design of the scanning laser ophthalmoscope, which also has the advantage of being much less susceptible to any media opacities such as cataracts. Utilising this ultra-wide field retinal images in future studies could shed more light on peripheral geometrical changes that might be associated with peripheral retinal ischaemia in diabetic retinopathy, which is difficult to evaluate with conventional fundus imaging.

However, there are different issues that need to be addressed before adopting this new technology. First we need to assess whether the developed automated system could be adapted to be used with the new imaging system. Second, there are still concerns regarding the lower resolution of the currently available Optomap as compared to high quality fundus cameras. Third, it will be important to evaluate the potential effect of peripheral image distortion on the analysis of peripheral vascular bifurcations; however such distortion would be expected to be less significant owing to the scanning laser technology as compared to the conventional methods of retinal imaging. [214]

2. Future prospective diabetic studies

        A. Prospective cross-sectional and fluorescein diabetic study

A prospective cross-sectional diabetic study is proposed. The aim of this study would be to evaluate geometrical retinal vascular changes with advancing stages of diabetic retinopathy and assess the independence of these relationships in relation to other demographic and clinical factors. Being prospective this study would address the limitations of our thesis study and expand our current knowledge on geometrical features in diabetes. This could be achieved through recruiting diabetic subjects with various grades of diabetic retinopathy – including those with no clinically detectable retinopathy. Detailed medical data would be collected. All subjects will have their retinal images captured with an advanced high-resolution fundus camera system. Geometrical analysis would be performed with the developed automated vascular analysis technique for all the images. Comparative analysis of the geometrical features would then be estimated between the different diabetic groups and the relationships with the other demographic and clinical factors would be evaluated. Moreover, analysis of the topographic distribution of the different geometrical features within the retinal images in subjects with different grades of diabetic retinopathy is needed.

In a subgroup of diabetic subjects having fundus fluorescein angiography as part of routine clinical practice for assessment of macular oedema, severe NPDR or PDR, further topographic geometrical analysis could be carried out to explore the differential changes in geometry within a retinal image in relation to areas of retinal capillary shut down. Such analysis would elucidate the global versus local response of the retinal vascular network to retinal ischaemia. If founded, these differential changes of the retinal geometrical features within the retinal image could in the future act as markers of localised retinal ischaemia and guide modified pan-retinal laser treatments plans for these subjects without the necessity for angiography.

B. Prospective longitudinal diabetic study

At this stage it would seem important to conduct a prospective longitudinal diabetic study. The study would aim at determining the value and clinical usability of geometrical vascular analysis in the screening of diabetic retinopathy and the independence of the predictive value of the retinal geometrical changes in differentiating risk of retinopathic progression at an individual level. A purpose designed study could be used but would have to be large and would require long follow up to gain adequate numbers of patients with progressive retinopathy. Alternatively images from a completed study such as the UKPDS or DCCT could be used although this would have the disadvantages of using digitised slides and non-optimally designed image acquisition.

The overall results of these proposed prospective diabetic studies would provide further information regarding retinal geometrical vascular analysis that could add to the existing risk prediction models of diabetes, as supported by the needed developed automated technology. Consequently, this could set the path for the implementation of such analysis in diabetic screening programmes, which in turn could improve our early detection and clinical care for the diabetic patients.

8.8 Conclusion

This research has presented a new reliable semi-manual technique for analysis of the retinal vascular geometrical features in normal and disease states. Normative retinal vascular geometrical data that could be the benchmark gold standard for future vascular analysis studies has been presented. The association of changes in retinal geometric features with advancing stages of diabetic retinopathy has been investigated. Novel retinal vascular geometrical markers indicative of the establishment of severe non-proliferative or proliferative diabetic retinopathy have been discovered and the results are suggestive that these markers may allow quantitative assessment of diabetic microvascular damage and have predictive role in determining the risk of future progression to proliferative diabetic retinopathy.

This work could be considered as an initial step that sets the path for further detailed studies that would explore and examine these findings to expand our knowledge of the structure and geometry of the retinal vascular networks in diabetes.

Analysis of retinal vascular geometry may advance our understanding of the early pathophysiological pathways of diabetes, and potentially could improve our clinical care for patients with diabetic retinopathy.

Bibliography

1. Federman JL, G.P., Schubert H, et al *Systemic diseases*, in *Retina and Vitreous: Textbook of Ophthalmology*, Y.M. Podos SM, Editor. 1994. p. 7-24.
2. Benson WE, T.W., Duane TD, *Diabetes mellitus and the eye*, in *Duane's Clinical Ophthalmology*. 1994.
3. Organisation, W.H., *The World Health Report*, 2002.
4. Nabarro, J.D., *Diabetes in the United Kingdom: some facts and figures.* Diabet Med, 1988. **5**(9): p. 816-22.
5. Simmons, D., D.R. Williams, and M.J. Powell, *The Coventry Diabetes Study: prevalence of diabetes and impaired glucose tolerance in Europids and Asians.* Q J Med, 1991. **81**(296): p. 1021-30.
6. Bunce, C. and R. Wormald, *Leading causes of certification for blindness and partial sight in England & Wales.* BMC Public Health, 2006. **6**: p. 58.
7. Klein, R., et al., *Incidence of retinopathy and associated risk factors from time of diagnosis of insulin-dependent diabetes.* Arch Ophthalmol, 1997. **115**(3): p. 351-6.
8. Wirta, O.R., et al., *Occurrence of late specific complications in type II (non-insulin-dependent) diabetes mellitus.* J Diabetes Complications, 1995. **9**(3): p. 177-85.
9. Ramachandran, A., et al., *Diabetic retinopathy at the time of diagnosis of NIDDM in south Indian subjects.* Diabetes Res Clin Pract, 1996. **32**(1-2): p. 111-4.
10. *Tight blood pressure control and risk of macrovascular and microvascular complications in type 2 diabetes: UKPDS 38. UK Prospective Diabetes Study Group.* Bmj, 1998. **317**(7160): p. 703-13.
11. Morgan, C.L., et al., *The prevalence of multiple diabetes-related complications.* Diabet Med, 2000. **17**(2): p. 146-51.
12. Klein, R., et al., *The Wisconsin epidemiologic study of diabetic retinopathy. II. Prevalence and risk of diabetic retinopathy when age at diagnosis is less than 30 years.* Arch Ophthalmol, 1984. **102**(4): p. 520-6.
13. Klein, R., et al., *The Wisconsin epidemiologic study of diabetic retinopathy. III. Prevalence and risk of diabetic retinopathy when age at diagnosis is 30 or more years.* Arch Ophthalmol, 1984. **102**(4): p. 527-32.
14. Klein, R., B.E. Klein, and S.E. Moss, *The Wisconsin epidemiologic study of diabetic retinopathy: an update.* Aust N Z J Ophthalmol, 1990. **18**(1): p. 19-22.
15. Stratton, I.M., et al., *UKPDS 50: risk factors for incidence and progression of retinopathy in Type II diabetes over 6 years from diagnosis.* Diabetologia, 2001. **44**(2): p. 156-63.
16. Klein, R., et al., *The Wisconsin Epidemiologic Study of Diabetic Retinopathy: XXII the twenty-five-year progression of retinopathy in persons with type 1 diabetes.* Ophthalmology, 2008. **115**(11): p. 1859-68.
17. Klein, R., et al., *The Wisconsin Epidemiologic Study of Diabetic Retinopathy XXIII: the twenty-five-year incidence of macular edema in persons with type 1 diabetes.* Ophthalmology, 2009. **116**(3): p. 497-503.
18. Klein, R., B.E. Klein, and S.E. Moss, *Visual impairment in diabetes.* Ophthalmology, 1984. **91**(1): p. 1-9.
19. Moss, S.E., R. Klein, and B.E. Klein, *Ten-year incidence of visual loss in a diabetic population.* Ophthalmology, 1994. **101**(6): p. 1061-70.
20. Klein R, K.B., Moss SE, *The epidemiology of ocular problems in diabetes mellitus*, in *Ocular problems in Diabetes Mellitus*, F. SS, Editor. 1992, Blackwell: Bostn. p. 1-53.

21. *The relationship of glycemic exposure (HbA1c) to the risk of development and progression of retinopathy in the diabetes control and complications trial.* Diabetes, 1995. **44**(8): p. 968-83.

22. Younis, N., et al., *Prevalence of diabetic eye disease in patients entering a systematic primary care-based eye screening programme.* Diabet Med, 2002. **19**(12): p. 1014-21.

23. Younis, N., et al., *Incidence of sight-threatening retinopathy in Type 1 diabetes in a systematic screening programme.* Diabet Med, 2003. **20**(9): p. 758-65.

24. Klein, R., et al., *Relationship of hyperglycemia to the long-term incidence and progression of diabetic retinopathy.* Arch Intern Med, 1994. **154**(19): p. 2169-78.

25. Klein, R., et al., *Glycosylated hemoglobin predicts the incidence and progression of diabetic retinopathy.* Jama, 1988. **260**(19): p. 2864-71.

26. *The effect of intensive treatment of diabetes on the development and progression of long-term complications in insulin-dependent diabetes mellitus. The Diabetes Control and Complications Trial Research Group.* N Engl J Med, 1993. **329**(14): p. 977-86.

27. Stevens, R.J., I.M. Stratton, and R.R. Holman, *UKPDS58--modeling glucose exposure as a risk factor for photocoagulation in type 2 diabetes.* J Diabetes Complications, 2002. **16**(6): p. 371-6.

28. *Intensive blood-glucose control with sulphonylureas or insulin compared with conventional treatment and risk of complications in patients with type 2 diabetes (UKPDS 33). UK Prospective Diabetes Study (UKPDS) Group.* Lancet, 1998. **352**(9131): p. 837-53.

29. Wang, P.H., J. Lau, and T.C. Chalmers, *Meta-analysis of effects of intensive blood-glucose control on late complications of type I diabetes.* Lancet, 1993. **341**(8856): p. 1306-9.

30. Klein, R., et al., *The Wisconsin Epidemiologic Study of Diabetic Retinopathy: XVII. The 14-year incidence and progression of diabetic retinopathy and associated risk factors in type 1 diabetes.* Ophthalmology, 1998. **105**(10): p. 1801-15.

31. Chaturvedi, N., et al., *Effect of lisinopril on progression of retinopathy in normotensive people with type 1 diabetes. The EUCLID Study Group. EURODIAB Controlled Trial of Lisinopril in Insulin-Dependent Diabetes Mellitus.* Lancet, 1998. **351**(9095): p. 28-31.

32. West, K.M., L.J. Erdreich, and J.A. Stober, *A detailed study of risk factors for retinopathy and nephropathy in diabetes.* Diabetes, 1980. **29**(7): p. 501-8.

33. Skyler, J.S., *Microvascular complications. Retinopathy and nephropathy.* Endocrinol Metab Clin North Am, 2001. **30**(4): p. 833-56.

34. Ward, K.M., *Renal function (microalbuminuria).* Anal Chem, 1995. **67**(12): p. 383R-391R.

35. Parving, H.H., et al., *Prevalence of microalbuminuria, arterial hypertension, retinopathy and neuropathy in patients with insulin dependent diabetes.* Br Med J (Clin Res Ed), 1988. **296**(6616): p. 156-60.

36. Gall, M.A., et al., *Prevalence of micro- and macroalbuminuria, arterial hypertension, retinopathy and large vessel disease in European type 2 (non-insulin-dependent) diabetic patients.* Diabetologia, 1991. **34**(9): p. 655-61.

37. Rodman HM, S.L., Aiello LM, Merkatz IR, *Diabetic retinopathy and its relationship to pregnancy*, in *The Diabetic Pregnancy: A Perinatal Perspective*, A.P. Merkatz IR, Editor. 1979, Grune and Stratton: New York. p. 73-91.

38. Chew, E.Y., et al., *Metabolic control and progression of retinopathy. The Diabetes in Early Pregnancy Study. National Institute of Child Health and Human Development Diabetes in Early Pregnancy Study.* Diabetes Care, 1995. **18**(5): p. 631-7.

39.	Klein, B.E., et al., *The Wisconsin Epidemiologic Study of Diabetic Retinopathy. XIII. Relationship of serum cholesterol to retinopathy and hard exudate.* Ophthalmology, 1991. **98**(8): p. 1261-5.

40.	Chew, E.Y., et al., *Association of elevated serum lipid levels with retinal hard exudate in diabetic retinopathy. Early Treatment Diabetic Retinopathy Study (ETDRS) Report 22.* Arch Ophthalmol, 1996. **114**(9): p. 1079-84.

41.	Chen, H.-C., *Pathogenesis of Diabetic Retinopathy*, in *Vascular complications of Diabetes*, R. Donnelly, Editor. 2002, Blackwell: Oxford. p. 109-117.

42.	Greene, D.A., S.A. Lattimer, and A.A. Sima, *Sorbitol, phosphoinositides, and sodium-potassium-ATPase in the pathogenesis of diabetic complications.* N Engl J Med, 1987. **316**(10): p. 599-606.

43.	Aiello, L.P., et al., *Vascular endothelial growth factor-induced retinal permeability is mediated by protein kinase C in vivo and suppressed by an orally effective beta-isoform-selective inhibitor.* Diabetes, 1997. **46**(9): p. 1473-80.

44.	Ditzel, J., *Haemorheological factors in the development of diabetic microangiopathy.* Br J Ophthalmol, 1967. **51**(12): p. 793-803.

45.	Williamson, J.R., et al., *Hyperglycemic pseudohypoxia and diabetic complications.* Diabetes, 1993. **42**(6): p. 801-13.

46.	Mathews, M.K., et al., *Vascular endothelial growth factor and vascular permeability changes in human diabetic retinopathy.* Invest Ophthalmol Vis Sci, 1997. **38**(13): p. 2729-41.

47.	Davis MD, B.B., *Proliferative Diabetic Retinopathy*, in *Retina*, S.J. Ryan, Editor. 2001, Mosby. p. 1309-1349.

48.	Dowler, J., *Clinical features of diabetic retinopathy*, in *DiabeticRetinopathy*, O.P.V. Bijsterveld, Editor. 2000, Martin Dunitz: The Netherlands. p. 1 - 16.

49.	Yannof, M., *Ocular pathology: A text and atlas.* 1975, Hagerstown: Harper and Row. 397.

50.	Roy, M.S., et al., *Retinal cotton-wool spots: an early finding in diabetic retinopathy?* Br J Ophthalmol, 1986. **70**(10): p. 772-8.

51.	*Fundus photographic risk factors for progression of diabetic retinopathy. ETDRS report number 12. Early Treatment Diabetic Retinopathy Study Research Group.* Ophthalmology, 1991. **98**(5 Suppl): p. 823-33.

52.	Wilkinson, C.P., et al., *Proposed international clinical diabetic retinopathy and diabetic macular edema disease severity scales.* Ophthalmology, 2003. **110**(9): p. 1677-82.

53.	*Grading diabetic retinopathy from stereoscopic color fundus photographs--an extension of the modified Airlie House classification. ETDRS report number 10. Early Treatment Diabetic Retinopathy Study Research Group.* Ophthalmology, 1991. **98**(5 Suppl): p. 786-806.

54.	Harding, S., et al., *Grading and disease management in national screening for diabetic retinopathy in England and Wales.* Diabet Med, 2003. **20**(12): p. 965-71.

55.	Aldington, S.J., et al., *Methodology for retinal photography and assessment of diabetic retinopathy: the EURODIAB IDDM complications study.* Diabetologia, 1995. **38**(4): p. 437-44.

56.	*Photocoagulation treatment of proliferative diabetic retinopathy: the second report of diabetic retinopathy study findings.* Ophthalmology, 1978. **85**(1): p. 82-106.

57.	Wilson, J.M. and Y.G. Jungner, *[Principles and practice of mass screening for disease].* Bol Oficina Sanit Panam, 1968. **65**(4): p. 281-393.

58.	NICE, *Management of type 2 diabetes. Retinopathy - screening and early management*, 2002.

59. Dasbach, E.J., et al., *Cost-effectiveness of strategies for detecting diabetic retinopathy.* Med Care, 1991. **29**(1): p. 20-39.

60. *Photocoagulation for proliferative diabetic retinopathy: a randomised controlled clinical trial using the xenon-arc.* Diabetologia, 1984. **26**(2): p. 109-15.

61. *Photocoagulation treatment of proliferative diabetic retinopathy. Clinical application of Diabetic Retinopathy Study (DRS) findings, DRS Report Number 8. The Diabetic Retinopathy Study Research Group.* Ophthalmology, 1981. **88**(7): p. 583-600.

62. Ferris, F., *Early photocoagulation in patients with either type I or type II diabetes.* Trans Am Ophthalmol Soc, 1996. **94**: p. 505-37.

63. *Photocoagulation for diabetic maculopathy. A randomized controlled clinical trial using the xenon arc. British Multicentre Study Group.* Diabetes, 1983. **32**(11): p. 1010-6.

64. *Early photocoagulation for diabetic retinopathy. ETDRS report number 9. Early Treatment Diabetic Retinopathy Study Research Group.* Ophthalmology, 1991. **98**(5 Suppl): p. 766-85.

65. *Photocoagulation for diabetic macular edema. Early Treatment Diabetic Retinopathy Study report number 1. Early Treatment Diabetic Retinopathy Study research group.* Arch Ophthalmol, 1985. **103**(12): p. 1796-806.

66. *Focal photocoagulation treatment of diabetic macular edema. Relationship of treatment effect to fluorescein angiographic and other retinal characteristics at baseline: ETDRS report no. 19. Early Treatment Diabetic Retinopathy Study Research Group.* Arch Ophthalmol, 1995. **113**(9): p. 1144-55.

67. Arun, C.S., et al., *Effectiveness of screening in preventing blindness due to diabetic retinopathy.* Diabet Med, 2003. **20**(3): p. 186-90.

68. *The effect of intensive diabetes treatment on the progression of diabetic retinopathy in insulin-dependent diabetes mellitus. The Diabetes Control and Complications Trial.* Arch Ophthalmol, 1995. **113**(1): p. 36-51.

69. Masters, B.R., *Fractal analysis of the vascular tree in the human retina.* Annu Rev Biomed Eng, 2004. **6**: p. 427-52.

70. Murray, C.D., *The Physiological Principle of Minimum Work Applied to the Angle of Branching of Arteries.* J Gen Physiol, 1926. **9**(6): p. 835-841.

71. Murray, C.D., *The Physiological Principle of Minimum Work: I. The Vascular System and the Cost of Blood Volume.* Proc Natl Acad Sci U S A, 1926. **12**(3): p. 207-14.

72. Zamir, M., *Optimality principles in arterial branching.* J Theor Biol, 1976. **62**(1): p. 227-51.

73. Hogan MJ, A.J., Weddel JE., *Histology of the Human Eye.* 1971, Philadelphia, PA: Saunders.

74. Ozanics V, J.F., *Prenatal development of the eye and its adnexa*, in *Ocular Anatomy, Embryology and Teratology*, F. Jakobiec Editor. 1982, Harper Row: Philadelphia, PA. p. 11- 96.

75. Maxwell, P.H. and P.J. Ratcliffe, *Oxygen sensors and angiogenesis.* Semin Cell Dev Biol, 2002. **13**(1): p. 29-37.

76. Phelps, D.L., *Oxygen and developmental retinal capillary remodeling in the kitten.* Invest Ophthalmol Vis Sci, 1990. **31**(10): p. 2194-200.

77. Taarnhoj, N.C., et al., *Heritability of retinal vessel diameters and blood pressure: a twin study.* Invest Ophthalmol Vis Sci, 2006. **47**(8): p. 3539-44.

78. Lee, K.E., et al., *Familial aggregation of retinal vessel caliber in the beaver dam eye study.* Invest Ophthalmol Vis Sci, 2004. **45**(11): p. 3929-33.

79. Fanucci, E., et al., *Optimal branching of human arterial bifurcations.* Invest Radiol, 1990. **25**(1): p. 62-6.

80.   Sherman, T.F., *On connecting large vessels to small. The meaning of Murray's law.* J Gen Physiol, 1981. **78**(4): p. 431-53.

81.   Zamir, M., *Nonsymmetrical bifurcations in arterial branching.* J Gen Physio, 1978. **72**(6): p. 837-45.

82.   Zamir, M. and H. Chee, *Branching characteristics of human coronary arteries.* Can J Physiol Pharmacol, 1986. **64**(6): p. 661-8.

83.   Zamir, M. and J.A. Medeiros, *Arterial branching in man and monkey.* J Gen Physiol, 1982. **79**(3): p. 353-60.

84.   Zamir, M. and N. Brown, *Arterial branching in various parts of the cardiovascular system.* Am J Anat, 1982. **163**(4): p. 295-307.

85.   Fanucci, E., A. Orlacchio, and M. Pocek, *The vascular geometry of human arterial bifurcations.* Invest Radiol, 1988. **23**(10): p. 713-8.

86.   Fleming, A.D., et al., *Automatic detection of retinal anatomy to assist diabetic retinopathy screening.* Phys Med Biol, 2007. **52**(2): p. 331-45.

87.   Zamir, M., J.A. Medeiros, and T.K. Cunningham, *Arterial bifurcations in the human retina.* J Gen Physiol, 1979. **74**(4): p. 537-48.

88.   Stanton, A.V., et al., *Vascular network changes in the retina with age and hypertension.* J Hypertens, 1995. **13**(12 Pt 2): p. 1724-8.

89.   King, L.A., et al., *Arteriolar length-diameter (L:D) ratio: a geometric parameter of the retinal vasculature diagnostic of hypertension.* J Hum Hypertens, 1996. **10**(6): p. 417-8.

90.   Chapman, N., et al., *Acute effects of oxygen and carbon dioxide on retinal vascular network geometry in hypertensive and normotensive subjects.* Clin Sci (Lond), 2000. **99**(6): p. 483-8.

91.   Chapman, N., et al., *Peripheral vascular disease is associated with abnormal arteriolar diameter relationships at bifurcations in the human retina.* Clin Sci (Lond), 2002. **103**(2): p. 111-6.

92.   Martinez-Perez, M.E., et al., *Retinal vascular tree morphology: a semi-automatic quantification.* IEEE Trans Biomed Eng, 2002. **49**(8): p. 912-7.

93.   Rose, G., *Familial Patterns in Ischaemic Heart Disease.* Br J Prev Soc Med, 1964. **18**: p. 75-80.

94.   Chapman, N., et al., *Retinal vascular network architecture in low-birth-weight men.* J Hypertens, 1997. **15**(12 Pt 1): p. 1449-53.

95.   Klein, R., et al., *Are retinal arteriolar abnormalities related to atherosclerosis?: The Atherosclerosis Risk in Communities Study.* Arterioscler Thromb Vasc Biol, 2000. **20**(6): p. 1644-50.

96.   Chapman, N., Baharudin, S., King, L., Thom, S., Hughes, A., Stanton, A., *Acute effects of L-NMMA on retinal arteriolar network topography in normotensive man (Abstract).* J. Hum. Hypertens., 2000(14): p. 841 - 842.

97.   Ingebrigtsen, T., et al., *Bifurcation geometry and the presence of cerebral artery aneurysms.* J Neurosurg, 2004. **101**(1): p. 108-13.

98.   Wong, T.Y., et al., *Retinal microvascular abnormalities and incident stroke: the Atherosclerosis Risk in Communities Study.* Lancet, 2001. **358**(9288): p. 1134-40.

99.   Wong, T.Y., et al., *Retinal arteriolar narrowing and risk of coronary heart disease in men and women. The Atherosclerosis Risk in Communities Study.* Jama, 2002. **287**(9): p. 1153-9.

100.   Wong, T.Y., et al., *Retinal microvascular abnormalities and 10-year cardiovascular mortality: a population-based case-control study.* Ophthalmology, 2003. **110**(5): p. 933-40.

101.   Witt, N., et al., *Abnormalities of retinal microvascular structure and risk of mortality from ischemic heart disease and stroke.* Hypertension, 2006. **47**(5): p. 975-81.

102. Risau, W., *Mechanisms of angiogenesis.* Nature, 1997. **386**(6626): p. 671-4.

103. Betz, A.L., P.D. Bowman, and G.W. Goldstein, *Hexose transport in microvascular endothelial cells cultured from bovine retina.* Exp Eye Res, 1983. **36**(2): p. 269-77.

104. Bradbury, M.W., *The blood-brain barrier. Transport across the cerebral endothelium.* Circ Res, 1985. **57**(2): p. 213-22.

105. Robinson, F., et al., *Retinal blood flow autoregulation in response to an acute increase in blood pressure.* Invest Ophthalmol Vis Sci, 1986. **27**(5): p. 722-6.

106. Patton, N., et al., *Retinal vascular image analysis as a potential screening tool for cerebrovascular disease: a rationale based on homology between cerebral and retinal microvasculatures.* J Anat, 2005. **206**(4): p. 319-48.

107. Mielke, R. and W.D. Heiss, *Positron emission tomography for diagnosis of Alzheimer's disease and vascular dementia.* J Neural Transm Suppl, 1998. **53**: p. 237-50.

108. Kwa, V.I., et al., *Retinal arterial changes correlate with cerebral small-vessel disease.* Neurology, 2002. **59**(10): p. 1536-40.

109. Wong, T.Y., et al., *Retinal microvascular abnormalities and cognitive impairment in middle-aged persons: the Atherosclerosis Risk in Communities Study.* Stroke, 2002. **33**(6): p. 1487-92.

110. Baker, M.L., et al., *Retinal microvascular signs, cognitive function, and dementia in older persons: the Cardiovascular Health Study.* Stroke, 2007. **38**(7): p. 2041-7.

111. Patton, N., et al., *The association between retinal vascular network geometry and cognitive ability in an elderly population.* Invest Ophthalmol Vis Sci, 2007. **48**(5): p. 1995-2000.

112. Patton, N., et al., *Asymmetry of retinal arteriolar branch widths at junctions affects ability of formulae to predict trunk arteriolar widths.* Invest Ophthalmol Vis Sci, 2006. **47**(4): p. 1329-33.

113. Nguyen, T.T., J.J. Wang, and T.Y. Wong, *Retinal vascular changes in pre-diabetes and prehypertension: new findings and their research and clinical implications.* Diabetes Care, 2007. **30**(10): p. 2708-15.

114. Keech, A., et al., *Effects of long-term fenofibrate therapy on cardiovascular events in 9795 people with type 2 diabetes mellitus (the FIELD study): randomised controlled trial.* Lancet, 2005. **366**(9500): p. 1849-61.

115. Klein, R., B.E. Klein, and S.E. Moss, *The relation of systemic hypertension to changes in the retinal vasculature: the Beaver Dam Eye Study.* Trans Am Ophthalmol Soc, 1997. **95**: p. 329-48; discussion 348-50.

116. Cugati, S., et al., *Five-year incidence and progression of vascular retinopathy in persons without diabetes: the Blue Mountains Eye Study.* Eye (Lond), 2006. **20**(11): p. 1239-45.

117. Wong, T.Y., et al., *Three-year incidence and cumulative prevalence of retinopathy: the atherosclerosis risk in communities study.* Am J Ophthalmol, 2007. **143**(6): p. 970-6.

118. Klein, R., et al., *Hypertension and retinopathy, arteriolar narrowing, and arteriovenous nicking in a population.* Arch Ophthalmol, 1994. **112**(1): p. 92-8.

119. Wong, T.Y. and P. Mitchell, *Hypertensive retinopathy.* N Engl J Med, 2004. **351**(22): p. 2310-7.

120. *The prevalence of retinopathy in impaired glucose tolerance and recent-onset diabetes in the Diabetes Prevention Program.* Diabet Med, 2007. **24**(2): p. 137-44.

121. Klein, R., et al., *The relationship of retinopathy in persons without diabetes to the 15-year incidence of diabetes and hypertension: Beaver Dam Eye Study.* Trans Am Ophthalmol Soc, 2006. **104**: p. 98-107.

122. Wong, T.Y., et al., *Do retinopathy signs in non-diabetic individuals predict the subsequent risk of diabetes?* Br J Ophthalmol, 2006. **90**(3): p. 301-3.

123. Wong, T.Y., et al., *Retinal arteriolar narrowing and risk of diabetes mellitus in middle-aged persons.* Jama, 2002. **287**(19): p. 2528-33.

124. Wong, T.Y., et al., *Retinal arteriolar narrowing, hypertension, and subsequent risk of diabetes mellitus.* Arch Intern Med, 2005. **165**(9): p. 1060-5.

125. de Rekeneire, N., et al., *Diabetes, hyperglycemia, and inflammation in older individuals: the health, aging and body composition study.* Diabetes Care, 2006. **29**(8): p. 1902-8.

126. Ling, P.R., et al., *Hyperglycemia induced by glucose infusion causes hepatic oxidative stress and systemic inflammation, but not STAT3 or MAP kinase activation in liver in rats.* Metabolism, 2003. **52**(7): p. 868-74.

127. Ikram, M.K., et al., *Retinal vessel diameters and risk of impaired fasting glucose or diabetes: the Rotterdam study.* Diabetes, 2006. **55**(2): p. 506-10.

128. Hughes, A.D., et al., *Quantification of topological changes in retinal vascular architecture in essential and malignant hypertension.* J Hypertens, 2006. **24**(5): p. 889-94.

129. Avakian, A., et al., *Fractal analysis of region-based vascular change in the normal and non-proliferative diabetic retina.* Curr Eye Res, 2002. **24**(4): p. 274-80.

130. Remky, A., O. Arend, and S. Hendricks, *Short-wavelength automated perimetry and capillary density in early diabetic maculopathy.* Invest Ophthalmol Vis Sci, 2000. **41**(1): p. 274-81.

131. Wolf, S., et al., *Retinal capillary blood flow measurement with a scanning laser ophthalmoscope. Preliminary results.* Ophthalmology, 1991. **98**(6): p. 996-1000.

132. Woldenberg, M.J. and K. Horsfield, *Relation of branching angles to optimality for four cost principles.* J Theor Biol, 1986. **122**(2): p. 187-204.

133. Kiani, M.F. and A.G. Hudetz, *Computer simulation of growth of anastomosing microvascular networks.* J Theor Biol, 1991. **150**(4): p. 547-60.

134. Brinchmann-Hansen, O., *The light reflex on retinal arteries and veins. A theoretical study and a new technique for measuring width and intensity profiles across retinal vessels.* Acta Ophthalmol Suppl, 1986. **179**: p. 1-53.

135. Hubbard, L.D., et al., *Methods for evaluation of retinal microvascular abnormalities associated with hypertension/sclerosis in the Atherosclerosis Risk in Communities Study.* Ophthalmology, 1999. **106**(12): p. 2269-80.

136. Brinchmann-Hansen, O., Engvold, O., *Microphotometry of the blood column and the light streak on retinal vessels in fundus photographs.* Acta Ophthalmol Scand, 1986. **Supplement 179**: p. 9 - 19.

137. Gregson, P.H., et al., *Automated grading of venous beading.* Comput Biomed Res, 1995. **28**(4): p. 291-304.

138. Rassam, S.M., et al., *Accurate vessel width measurement from fundus photographs: a new concept.* Br J Ophthalmol, 1994. **78**(1): p. 24-9.

139. Zhou, L., et al., *The detection and quantification of retinopathy using digital angiograms.* IEEE Trans Med Imaging, 1994. **13**(4): p. 619-26.

140. Gao, X.W., et al., *Quantification and characterisation of arteries in retinal images.* Comput Methods Programs Biomed, 2000. **63**(2): p. 133-46.

141. Chapman, N., et al., *Computer algorithms for the automated measurement of retinal arteriolar diameters.* Br J Ophthalmol, 2001. **85**(1): p. 74-9.

142. Lowell, J., et al., *Measurement of retinal vessel widths from fundus images based on 2-D modeling.* IEEE Trans Med Imaging, 2004. **23**(10): p. 1196-204.

143. Zamir, M. and N. Brown, *Internal geometry of arterial bifurcations.* J Biomech, 1983. **16**(10): p. 857-63.

144. Al-Diri, B., et al., *Manual measurement of retinal bifurcation features.* Conf Proc IEEE Eng Med Biol Soc, 2010. **2010**: p. 4760-4.

145. Karch, R., et al., *Staged growth of optimized arterial model trees.* Ann Biomed Eng, 2000. **28**(5): p. 495-511.

146. Patton, N., et al., *Retinal image analysis: concepts, applications and potential.* Prog Retin Eye Res, 2006. **25**(1): p. 99-127.

147. Shimada, N., et al., *Reduction of retinal blood flow in high myopia.* Graefes Arch Clin Exp Ophthalmol, 2004. **242**(4): p. 284-8.

148. Patton, N., et al., *Effect of axial length on retinal vascular network geometry.* Am J Ophthalmol, 2005. **140**(4): p. 648-53.

149. Wong, T.Y., et al., *Does refractive error influence the association of blood pressure and retinal vessel diameters? The Blue Mountains Eye Study.* Am J Ophthalmol, 2004. **137**(6): p. 1050-5.

150. Amerasinghe, N., et al., *Evidence of retinal vascular narrowing in glaucomatous eyes in an Asian population.* Invest Ophthalmol Vis Sci, 2008. **49**(12): p. 5397-402.

151. Mitchell, P., et al., *Retinal vessel diameter and open-angle glaucoma: the Blue Mountains Eye Study.* Ophthalmology, 2005. **112**(2): p. 245-50.

152. Scanlon, P., *Definition of acceptable image quality*, in *National Screening Programme for Diabetic Retinopathy* 2006.

153. Ikram, M.K., et al., *Retinal vessel diameters and risk of stroke: the Rotterdam Study.* Neurology, 2006. **66**(9): p. 1339-43.

154. Bland, J.M. and D.G. Altman, *Measurement error.* Bmj, 1996. **313**(7059): p. 744.

155. Bland, J.M. and D.G. Altman, *Measurement error proportional to the mean.* Bmj, 1996. **313**(7049): p. 106.

156. Sharrett, A.R., et al., *Retinal arteriolar diameters and elevated blood pressure: the Atherosclerosis Risk in Communities Study.* Am J Epidemiol, 1999. **150**(3): p. 263-70.

157. Couper, D.J., et al., *Reliability of retinal photography in the assessment of retinal microvascular characteristics: the Atherosclerosis Risk in Communities Study.* Am J Ophthalmol, 2002. **133**(1): p. 78-88.

158. Chen, H.C., et al., *Vessel diameter changes during the cardiac cycle.* Eye, 1994. **8 (Pt 1)**: p. 97-103.

159. Knudtson, M.D., et al., *Variation associated with measurement of retinal vessel diameters at different points in the pulse cycle.* Br J Ophthalmol, 2004. **88**(1): p. 57-61.

160. Newsom, R.S., et al., *Retinal vessel measurement: comparison between observer and computer driven methods.* Graefes Arch Clin Exp Ophthalmol, 1992. **230**(3): p. 221-5.

161. Al-Diri, B., et al., *Automated analysis of retinal vascular network connectivity.* Comput Med Imaging Graph, 2010 (Epub ahead of print).

162. Atherton, A., et al., *The effect of acute hyperglycaemia on the retinal circulation of the normal cat.* Diabetologia, 1980. **18**(3): p. 233-7.

163. Frame, M.D. and I.H. Sarelius, *Arteriolar bifurcation angles vary with position and when flow is changed.* Microvasc Res, 1993. **46**(2): p. 190-205.

164. Xing, C., et al., *Genome-wide linkage study of retinal vessel diameters in the Beaver Dam Eye Study.* Hypertension, 2006. **47**(4): p. 797-802.

165. Wong, T.Y., et al., *Associations between the metabolic syndrome and retinal microvascular signs: the Atherosclerosis Risk In Communities study.* Invest Ophthalmol Vis Sci, 2004. **45**(9): p. 2949-54.

166. Klein, R., et al., *Retinal vascular abnormalities in persons with type 1 diabetes: the Wisconsin Epidemiologic Study of Diabetic Retinopathy: XVIII.* Ophthalmology, 2003. **110**(11): p. 2118-25.

167.   Wong, T.Y., et al., *Retinal vessel diameters and their associations with age and blood pressure.* Invest Ophthalmol Vis Sci, 2003. **44**(11): p. 4644-50.

168.   Leung, H., et al., *Relationships between age, blood pressure, and retinal vessel diameters in an older population.* Invest Ophthalmol Vis Sci, 2003. **44**(7): p. 2900-4.

169.   Cooper, L.S., et al., *Retinal microvascular abnormalities and MRI-defined subclinical cerebral infarction: the Atherosclerosis Risk in Communities Study.* Stroke, 2006. **37**(1): p. 82-6.

170.   Sun, C., et al., *Retinal vascular caliber: systemic, environmental, and genetic associations.* Surv Ophthalmol, 2009. **54**(1): p. 74-95.

171.   Bek, T. and A. Helgesen, *The regional distribution of diabetic retinopathy lesions may reflect risk factors for progression of the disease.* Acta Ophthalmol Scand, 2001. **79**(5): p. 501-5.

172.   Skov Jensen, P., P. Jeppesen, and T. Bek, *Differential diameter responses in macular and peripheral retinal arterioles may contribute to the regional distribution of diabetic retinopathy lesions.* Graefes Arch Clin Exp Ophthalmol, 2011. **249**(3): p. 407-12.

173.   Klein, R., et al., *Are inflammatory factors related to retinal vessel caliber? The Beaver Dam Eye Study.* Arch Ophthalmol, 2006. **124**(1): p. 87-94.

174.   Tamai, K., Matsubara, A., Tomida, K., et al. , *Lipid hydroproxide stimulates leukocyte-endotheluim interaction in the retinal microcirculation.* Exp Eye Res, 2002. **75**(1): p. 69-75.

175.   Ikram, M.K., et al., *Retinal vessel diameters and cerebral small vessel disease: the Rotterdam Scan Study.* Brain, 2006. **129**(Pt 1): p. 182-8.

176.   Zamir, M., *Fractal dimensions and multifractility in vascular branching.* J Theor Biol, 2001. **212**(2): p. 183-90.

177.   Zamir, M. and D.C. Bigelow, *Cost of departure from optimality in arterial branching.* J Theor Biol, 1984. **109**(3): p. 401-9.

178.   Sun, C., Zhu, G., Wong, T.Y., et al *Quantitative Genetic Analysis of the retinal vascular caliber. The Australian Twins Eye Study.* Hypertension, 2009. **54**: p. 788-795.

179.   Leung, H., et al., *Computer-assisted retinal vessel measurement in an older population: correlation between right and left eyes.* Clin Experiment Ophthalmol, 2003. **31**(4): p. 326-30.

180.   Aiello, L., *Perspectives on Diabetic Retinopathy.* Am J Ophthalmol, 2003. **136**: p. 122 - 135.

181.   Goodall, E.A., J. Moore, and T. Moore, *The estimation of approximate sample size requirements necessary for clinical and epidemiological studies in vision sciences.* Eye (Lond), 2009. **23**(7): p. 1589-97.

182.   *Two-year course of visual acuity in severe proliferative diabetic retinopathy with conventional management. Diabetic Retinopathy Vitrectomy Study (DRVS) report #1.* Ophthalmology, 1985. **92**(4): p. 492-502.

183.   Klein, R., et al., *Retinal vascular caliber in persons with type 2 diabetes: the Wisconsin Epidemiological Study of Diabetic Retinopathy: XX.* Ophthalmology, 2006. **113**(9): p. 1488-98.

184.   Wong, T.Y., et al., *Retinal microvascular abnormalities and their relationship with hypertension, cardiovascular disease, and mortality.* Surv Ophthalmol, 2001. **46**(1): p. 59-80.

185.   Mandecka, A., et al., *Abnormal retinal autoregulation is detected by provoked stimulation with flicker light in well-controlled patients with type 1 diabetes without retinopathy.* Diabetes Res Clin Pract, 2009. **86**(1): p. 51-5.

186. Klein, R., et al., *The relation of retinal vessel caliber to the incidence and progression of diabetic retinopathy: XIX: the Wisconsin Epidemiologic Study of Diabetic Retinopathy.* Arch Ophthalmol, 2004. **122**(1): p. 76-83.

187. Alibrahim, E., et al., *Retinal vascular caliber and risk of retinopathy in young patients with type 1 diabetes.* Ophthalmology, 2006. **113**(9): p. 1499-503.

188. Kifley, A., et al., *Retinal vascular caliber, diabetes, and retinopathy.* Am J Ophthalmol, 2007. **143**(6): p. 1024-6.

189. Grunwald, J.E., et al., *Total retinal volumetric blood flow rate in diabetic patients with poor glycemic control.* Invest Ophthalmol Vis Sci, 1992. **33**(2): p. 356-63.

190. Caballero, A.E., *Metabolic and vascular abnormalities in subjects at risk for type 2 diabetes: the early start of a dangerous situation.* Arch Med Res, 2005. **36**(3): p. 241-9.

191. Saldivar, E., et al., *Microcirculatory changes during chronic adaptation to hypoxia.* Am J Physiol Heart Circ Physiol, 2003. **285**(5): p. H2064-71.

192. van Hecke, M.V., et al., *Inflammation and endothelial dysfunction are associated with retinopathy: the Hoorn Study.* Diabetologia, 2005. **48**(7): p. 1300-6.

193. Lip, P.L., et al., *Plasma VEGF and soluble VEGF receptor FLT-1 in proliferative retinopathy: relationship to endothelial dysfunction and laser treatment.* Invest Ophthalmol Vis Sci, 2000. **41**(8): p. 2115-9.

194. Tso, M.O. and L.M. Jampol, *Pathophysiology of hypertensive retinopathy.* Ophthalmology, 1982. **89**(10): p. 1132-45.

195. Walsh, J.B., *Hypertensive retinopathy. Description, classification, and prognosis.* Ophthalmology, 1982. **89**(10): p. 1127-31.

196. Wong, T.Y., et al., *Retinal microvascular abnormalities and blood pressure in older people: the Cardiovascular Health Study.* Br J Ophthalmol, 2002. **86**(9): p. 1007-13.

197. Bursell, S.E., et al., *Retinal blood flow changes in patients with insulin-dependent diabetes mellitus and no diabetic retinopathy.* Invest Ophthalmol Vis Sci, 1996. **37**(5): p. 886-97.

198. Jarvisalo, M.J., et al., *Endothelial dysfunction and increased arterial intima-media thickness in children with type 1 diabetes.* Circulation, 2004. **109**(14): p. 1750-5.

199. Sasongko, M.B., et al., *Alterations in retinal microvascular geometry in young type 1 diabetes.* Diabetes Care, 2010. **33**(6): p. 1331-6.

200. Cheung, N., et al., *Retinal arteriolar dilation predicts retinopathy in adolescents with type 1 diabetes.* Diabetes Care, 2008. **31**(9): p. 1842-6.

201. Mohsin, F., et al., *Discordant trends in microvascular complications in adolescents with type 1 diabetes from 1990 to 2002.* Diabetes Care, 2005. **28**(8): p. 1974-80.

202. Leung, H., et al., *Dyslipidaemia and microvascular disease in the retina.* Eye (Lond), 2005. **19**(8): p. 861-8.

203. George, G.S., M.L. Wolbarsht, and M.B. Landers, 3rd, *Reproducible estimation of retinal vessel width by computerized microdensitometry.* Int Ophthalmol, 1990. **14**(2): p. 89-95.

204. Ikram, M.K., et al., *Are retinal arteriolar or venular diameters associated with markers for cardiovascular disorders? The Rotterdam Study.* Invest Ophthalmol Vis Sci, 2004. **45**(7): p. 2129-34.

205. Wong, T.Y., et al., *Quantitative retinal venular caliber and risk of cardiovascular disease in older persons: the cardiovascular health study.* Arch Intern Med, 2006. **166**(21): p. 2388-94.

206. Wong, T.Y., et al., *Prospective cohort study of retinal vessel diameters and risk of hypertension.* Bmj, 2004. **329**(7457): p. 79.

207. Huang, L., Friberg, T.R., Eller, A.W., *Ultra Wide Angle Fluorescein Angiography (Optos Panoramic200A) Compared to 7–Field Fluorescein Angiographic Imaging of*

Pre–Proliferative Diabetic Retinopathy Invest Ophthalmol Vis Sci, 2005. **46**(E-abstract): p. 369.

208. Porta, M., et al., *Risk factors for progression to proliferative diabetic retinopathy in the EURODIAB Prospective Complications Study.* Diabetologia, 2001. **44**(12): p. 2203-9.

209. Gonzalez, E.L., et al., *Trends in the prevalence and incidence of diabetes in the UK: 1996-2005.* J Epidemiol Community Health, 2009. **63**(4): p. 332-6.

210. *St Vincent Joint Task Force of Diabetes. Report of the visual impairment subgroup*, 1994, British Diabetic Association / Department of Health.

211. Arun, C.S., et al., *Long-term impact of retinal screening on significant diabetes-related visual impairment in the working age population.* Diabet Med, 2009. **26**(5): p. 489-92.

212. Klein, B.E., *Overview of epidemiologic studies of diabetic retinopathy.* Ophthalmic Epidemiol, 2007. **14**(4): p. 179-83.

213. Cheung, N., et al., *Quantitative assessment of early diabetic retinopathy using fractal analysis.* Diabetes Care, 2009. **32**(1): p. 106-10.

214. Neubauer, A.S., et al., *Nonmydriatic screening for diabetic retinopathy by ultra-widefield scanning laser ophthalmoscopy (Optomap).* Graefes Arch Clin Exp Ophthalmol, 2008. **246**(2): p. 229-35.

National Research Ethics Service

Sunderland Research Ethics Committee

Room 002
TEDCO Business Centre
Viking Industrial Park
Jarrow
Tyne & Wear NE32 3DT

Telephone 0191 4283563 or 4283545   Fax 0191 4283432

Helen Wilson (Co-ordinator) e-mail: helen.wilson@suntpct.nhs.uk

Our Ref: CW/WH/SJR

23rd September 2003

Mr M S Habib
Retinal Research Fellow
Sunderland Eye Infirmary
Queen Alexandra Road
Sunderland
SR2 9HP

Dear Mr Habib

Assessment of the retinal vascular geometry in normal and diabetic eyes

Your application for ethical approval was considered by the Sunderland Local Research Ethics Committee on 22nd September 2003. Members noted that the application form needed to be signed and perhaps you could address this in due course.

The design of the study was found to be acceptable and I am pleased to confirm that your study was approved.

Yours sincerely

Rev C Worsfold
Vice Chairman
Sunderland Local Research Ethics Committee

Copy to: Mr D H Steel, Consultant Ophthalmologist, Sunderland Eye Infirmary

This Research Ethics Committee is an advisory committee to the North East Strategic Health Authority
*The National Research Ethics Service (NRES) represents the NRES Directorate within
the National Patient Safety Agency and Research Ethics Committees in England*

287

Posters

Habib M, Al Diri B, Lowell J, Hunter A, Steel DHW Constancy of retinal vascular bifurcation geometry across the normal fundus and between venous to arterial bifurcations
Invest. Ophthalmol. Vis. Sci. 2006 47: E- Abstract 2784

Steel DHW Habib M, Al Diri B, Lowell J, Hunter A, Assessment of accuracy and repeatability of semi-automated analysis of retinal vascular geometry in Normal and Diabetic subjects
Invest. Ophthalmol. Vis. Sci. 2006 47: E- Abstract 2792

Patient Information Sheet

Research study of the retinal vascular bifurcation angles in normal and diabetic eyes.

You are being invited to take part in a research study. Before you decide, it is important for you to understand why the research is being done and what it will involve. Please take time to read the following information carefully and discuss it with friends, relatives and your GP if you wish. Ask us if there is anything that is not clear or if you would like more information. Take time to decide whether or not you wish to take part.

Thank you for reading this.

Aim of the study

We are doing this research project to study the blood vessels at the back of your eye on your retina (The retina acts as the photographic film of the eye). We are looking at these blood vessels in patients with diabetes as well as in other people without diabetes. We want to know if measurements made of these blood vessels are stable over short periods of time.

Other studies have shown that these blood vessels are affected by diseases such as high blood pressure and we want to see if they are affected in a similar way in people with diabetes. We believe that early, but detectable changes, in the blood vessels may be an important sign in predicting which people with diabetes go on to get damage to the retina. This can occur from leaking blood vessels or burst blood vessels causing bleeding into the eye requiring laser treatment and occasionally blindness. Potentially these early signs could be of great help in the early detection and treatment of patients at risk.

As the first part of a larger study we need to know that any measurements we make do not vary widely over minutes or a few days.

Why have I been chosen?

We are recruiting 20 normal subjects and 20 diabetic subjects with different grades of diabetic retinopathy.

Do I have to take part?

It is up to you to decide whether or not to take part. If you to decide to take part you will be given this information sheet to keep and asked to sign a consent form. If you decide to take part, you are still free to withdraw at any time and without giving a reason. This will not affect the standard of care you receive.

What will happen to me if I take part?

If you decide to take part of the study, we will first check your blood pressure and take a list of your current medications. We will dilate both pupils with eye drops. This takes about 20 minutes and you will be seated in a dimly lit room whilst they are starting to work. Two photographs of the back of each of your eyes will be taken. This will be repeated three times at 10 minutes intervals. You will be seated in the darkened room during the intervals.
You will be then asked to return back to the unit after one week to be dilated for another single set of photographs.
There is no particular need to inform your GP as the dilating drops used for the study are the drops used routinely in the outpatient clinics for looking at your eyes. There are no harmful side effects from the retinal photographs or drops.

What do I have to do?

After being dilated, you should not drive for around 6 hours until your vision returns back to normal with wearing off of the effect of the dilating drops.

What are the side effects of taking part?

Following pupil dilatation, your vision will be temporarily blurred. You might notice increased glare in bright light till the effect of drops wear off (usually about 4 hours but is some people it can be longer for up to 10 hours).
You may also notice temporary difficulty in reading and close work.

What are the possible benefits of taking part?

There is no direct intended benefit that you will notice for taking part in this study.
However we hope that the information we get from this study will help us in early detection and management of diabetic patients under risk of developing diabetes affecting the retina. This may eventually help in preventing loss of vision secondary to diabetes.

Will my taking part in this study be kept confidential?

All information and the retinal photographs that are collected during the course of the study will be kept strictly confidential. Any information about you, which leaves the hospital (such as research publications), will have your name, address, date of birth and hospital number removed so that you cannot be identified from it. The research investigators will only have access to your data and/or retinal photographs through a hospital password. All data will be handled according to the NHS policy of patients' confidentiality.

Contact for further Information.

If you would like more information about the study, you can contact:

Mr M Habib   Retinal Research Fellow
Mr D H Steel   Consultant Ophthalmologist

through Mr Steel's secretary at Sunderland Eye Infirmary.
Tel No: - 0191 5656256 ext: 49065

Many thanks for taking part in this study.

FORM SLREC 4

SUNDERLAND LOCAL RESEARCH ETHICS COMMITTEE

ETHICS COMMITTEE CONSENT FORM
..Sunderland   Eye   Infirmary

I...

of..

....

hereby give the consent of myself to be a subject in the study entitled:-

Assessment of Retinal Vascular Geometry in Normal and Diabetic Eyes....

....

the nature of which has been explained to me by
Mr D Steel / Mr M Habib....(delete as appropriate)...
who are in charge of the project.

Every care will be taken to avoid any undue harm or discomfort to you from this trial. However, if you suffer any adverse effect, the Medical Staff, the Hospital Trust, the Primary Care Trust and the Drug Manufacturer will not be legally responsible unless you can prove negligence or breach of duty.

I give this permission under the expressed understanding that *myself/son/daughter could be withdrawn from the study at any time, either on my own volition of on medical advice of the Consultant in charge of the Project.

Date.. Signed...
                                          Patient

I confirm that I have explained the nature, purpose and implications of the above study to the person who signed the above form of consent.

Date.. Signed...
                                          Doctor in Charge
                                          of Project

293